

Synthesis of glycomimetics of the natural Siglec-8 ligand and their pharmacodynamic characterization

Inauguraldissertation

zur
Erlangung der Würde eines Doktors der Philosophie
vorgelegt der
Philosophisch-Naturwissenschaftlichen Fakultät
der Universität Basel
und der Universität Utrecht

von

Gabriele Conti

Basel, 2023

Genehmigt von der Philosophisch-Naturwissenschaftlichen Fakultät auf Antrag von:

First Supervisor: Prof. Dr. Daniel Ricklin, *Departement Pharmazeutische Wissenschaften, Universität Basel*

First Supervisor: Prof. em. Dr. Beat Ernst, *Departement Pharmazeutische Wissenschaften, Universität Basel*

First Supervisor: Prof. Dr. Roland Pieters, *Departement Farmaceutische Wetenschappen, Universiteit Utrecht*

Second Supervisor: PD Dr. Martin Smiesko, *Departement Pharmazeutische Wissenschaften, Universität Basel*

External Expert: Prof. Dr. Karl-Heinz Altmann, *Departement Chemie und Angewandte Biowissenschaften, ETH Zürich*

Additional Expert: Prof. Dr. Geert-Jan Boons, *Departement Farmaceutische Wetenschappen, Universiteit Utrecht*

Basel, 21.09.2021

Prof. Dr. Marcel Mayor

Dean of Faculty

“Everything that drowns me makes me wanna fly”

Table of content

Table of content	4
Abstract	6
Abbreviations	8
Introduction	10
1. <i>Carbohydrates and immune system</i>	10
2. <i>Siglecs</i>	12
2.1. A new class of I-type lectins	12
2.2. Siglecs are single-pass transmembrane proteins	13
2.3. Siglecs recognize differently linked sialosides.....	15
2.4. Siglecs are regulators of immune cell signalling.....	17
2.4.1. Conserved siglecs.....	18
2.4.2. CD33-related siglecs.....	20
3. <i>Siglec-8</i>	24
3.1. Siglec-8 is a CD33-related Siglec specific for 6'-sulfo-sLe ^x	24
3.2. Siglec-8 is an inhibitory regulator of eosinophils and mast cells.....	26
3.3. Siglec-F – the mouse paralogue	28
3.4. New promising pharmacological target for eosinophil- and mast cell-related disorders.....	29
3.5. On the chemistry of Siglec-8 ligands	30
4. <i>Aim of the project</i>	32
5. <i>References</i>	33
Identification of the lead molecule	46
<i>Paper 1: A Potent Mimetic of the Siglec-8 Ligand 6'-Sulfo-Sialyl Lewis^x</i>	46
Oligo- and Multivalent presentation of Siglec-8 ligand	62
<i>Manuscript 1: Targeting Siglec-8 with Oligo- and Multivalent Ligands modulates immune cell activation</i>	62
Abstract.....	63
Introduction	64
Results and discussion	65
Conclusion.....	76
Experimental Part	77
References	80
Supporting Information	85
1. Synthesis	85
2. Determination of polymer 33 loading	105
3. Differential Scanning Fluorimetry	106
4. Isothermal Titration Calorimetry	106
5. NMR and MS identification of target compounds.....	112
6. References	134
2nd Generation of Siglec-8 ligands	135
<i>Manuscript 2: 2nd Generation Siglec-8 Ligands: Effects of Bioisosteric Modification at C-4 and C-9</i>	135
Abstract.....	136
Introduction	136
Results and discussion	137
Conclusion.....	151

Experimental part	152
References	189
Summary and outlook	192
Acknowledgements	193
Curriculum Vitae.....	196

Abstract

Glycans are an important class of natural products, since all living cells are covered by different types of carbohydrates forming the glycocalyx. Therefore, any cell-cell recognition process is based on the ability of one cell to recognize the specific glycan pattern which is presented on the other cell surface. This is particularly important for the activation of the immune system, which needs to selectively recognize and kill invading pathogens while not damaging self cells. However, sometimes this delicate equilibrium shifts towards unwanted pathological conditions where the immune system is not able anymore to distinguish between self and non-self cells, causing autoimmune diseases. Additionally, undesired overexpression of immune cells can also lead to medical conditions, like allergic inflammation. Therefore, it is fundamental to rely on specific mechanisms to control immune system homeostasis and avoid abnormal up-regulation of these cells. For this reason, immune cells display inhibitory receptors which suppress their activation via different mechanisms, such as inducing cell death.

One type of inhibitory proteins expressed on immune cells are siglecs, a class of I-type transmembrane proteins which selectively recognize sialic acid-containing structures. Siglecs possess multifarious functions, according to the structure and cell type expressing them, but the majority of them acts as inhibitory receptor thanks to the presence of ITIM and ITIM-like motifs in their intracellular domain. One member of this family is Siglec-8, which is expressed only on eosinophils, mast cells, and to some extent on basophils. It exerts its inhibitory function by promoting eosinophils apoptosis and inhibition of mast cells degranulation, representing therefore an interesting pharmacological target for the treatment of diseases in which these cell types are overexpressed, among which asthma and allergic inflammations.

This thesis describes a medicinal chemistry approach for the development of high-affinity Siglec-8 ligands to identify potential drug candidates for the treatment of eosinophil- and mast cell-associated diseases. This drug discovery process started from the known structure of the preferred natural Siglec-8 ligand identified via a glycan array approach, the tetrasaccharide 6'-sulfo-sialyl Lewis^x (6'-sulfo-sLe^x). The complex chemical structure of this compound neither allows an easy and straightforward synthesis of derivatives, nor do its chemical properties meet the requirements for drug-like molecules.

First, the minimal binding epitope of 6'-sulfo-sLe^x was identified in the corresponding Neu5Ac- α 2-3-Gal6S disaccharide. Although it has a simplified chemical structure, the affinity was reduced only by a factor 2 (Paper 1). In-depth analysis of the pharmacophores, with the aid of computational

studies, allowed the development of a glycomimetic analogue, where the galactose moiety was replaced by a carbocyclic structure. Affinity was improved thanks to a reduced desolvation penalty by removing non-interacting hydroxyl groups. When finally the C-9 hydroxyl group of the sialic acid was transferred into an aromatic sulfonamide, affinity was further improved almost 20-fold.

Generally, carbohydrate-binding proteins are characterized by weak affinities in the low millimolar range towards their ligands due to shallow and solvent-exposed binding sites. One way to deal with this problem is to design multivalent structures to achieve huge affinity improvements. Even in the case of a protein with a single binding site like Siglec-8, multivalency can enhance affinity through statistical rebinding, which relies on the increased local concentration of binding moiety. Thus, once the bound ligand dissociates, another one is in close proximity and immediately replaces it. To study this statistical rebinding effect in Siglec-8, different oligovalent ligands were synthesised and tested (Manuscript 1). Thermodynamic analysis showed that each binding epitope contributed enthalpically to the same extent as in the monovalent interaction, while entropic penalties were observed. Dissection of the entropic term in its components for some compounds revealed that greatly favourable solvation entropies were counterbalanced by bigger conformation entropy penalties. Additionally, to take the multivalent presentation concept to its extreme, a glycopolymer was synthesized and tested in cell-based bioassays to demonstrate the binding to Siglec-8. On the other hand, the biological outcome obtained with the best monovalent sulphonamide glycomimetic was much smaller. However, this assay proved the potential of the developed glycomimetic structures, and provided additional proof of the potential pharmacological applications that compounds with improved affinity could have.

To further improve the affinity of our glycomimetic Siglec-8 ligands, different strategies were explored (Manuscript 2). Firstly, bioisosteres of the carboxylic acid and sulfate group led to a complete loss of activity towards Siglec-8, confirming the crucial role for these two functionalities. Secondly, the previously unexplored C-4 position of the sialic acid was modified leading to amide derivatives with improved affinity. Finally, second generation sulphonamides were synthesized. While changing the electronic properties of the naphthalene moiety did not influence affinity, the extended aromatic system proved to be more important for having high-affinity compounds.

Abbreviations

6'-Sulfo-sLe ^x	6'-Sulfo-sialyl Lewis ^x
Aq.	Aqueous
Calcd.	Calculated
CD22	Cluster of differentiation-22
CD33rSiglecs	CD33 related siglecs
CRD	Carbohydrate recognition domain
DBU	1,8-Diazabicyclo[5.4.0]undec-7-ene
DCM	Dichloromethane
DIBAL-H	Diisobutylaluminum hydride
DIPEA	<i>N,N</i> -Diisopropylethylamine
DMAP	4-Dimethylamino-pyridine
DMF	<i>N,N</i> -dimethylformamide
DMSO	Dimethyl sulfoxide
DTT	Dithiothreitol
ELSD	Evaporative light scattering detector
ESI	Electrospray ionization
HEPES	4-(2-Hydroxyethyl)piperazine-1-ethanesulfonic acid
HPLC	High-performance Liquid Chromatography
Ig	Immunoglobulin
IL	Interleukin
IPTG	Isopropyl- β -D-1-thiogalactoside
ITAM	Immunoreceptor tyrosine-based activation motif
ITC	Isothermal titration calorimetry
ITIM	Immunoreceptor tyrosine-based inhibitory motif
MS	Mass spectrometry

Abbreviations

Neu5Ac	<i>N</i> -Acetylneuraminic acid
Neu5Gc	<i>N</i> -Glycolylneuraminic acid
NiNTA	Nickel-nitrilotriacetic acid
NIS	<i>N</i> -Iodosuccinimide
NMR	Nuclear magnetic resonance
PE	Petroleum ether
Py	Pyridine
Quant.	Quantitative
ROS	Reactive oxygen species
rt	Room temperature
Satd.	Saturated
SH2	Src Homology 2
Siglec	Sialic acid immunoglobuline-like lectin
TBDPSCI	<i>tert</i> -Butyl(chloro)diphenylsilane
TBTA	Tris((1-benzyl-4-triazolyl)methyl)amine
Tf	Trifluoroacetyl
THF	Tetrahydrofuran
TLC	Thin-layer chromatography
TMSN ₃	Azidotrimethylsilane
Ts	<i>para</i> -Toluenesulfonyl

Introduction

1. Carbohydrates and immune system

All living species have developed defensive systems to protect themselves against threats posed by various pathogens, including viruses, bacteria, fungi, or more generally every disease causing agent. When a pathogen overcomes the physical barriers of a host and enters an organism, the first immune response is provided by the innate immune system. However, because this response is neither specific nor long-lasting, vertebrates and other species have evolved a second layer of defence, the adaptive or acquired immune system. It is triggered by the generic immune response by the innate system to pathogen invasion, generating a specific immunological memory and thus creating a tailor-made and long-lasting protection of the host.^{1,2}

To trigger the immune response, the pathogen has to be recognized by the host. Considering that all living cells are covered by a complex glycan layer, the so-called glycocalyx,³ a crucial factor in pathogen recognition is the ability of the host to distinguish specific glycan patterns expressed on the surface of the pathogen. Additionally, the host's immune system has to discern between the foreign invading cells (nonself) and its own cells (self), in order to selectively kill harmful pathogens. If the immune system does not distinguish between self and nonself as in case of autoimmune disorders, exaggerated immune responses damage the healthy tissues. Therefore, to prevent the overstimulation of the immune system, immune cells present inhibitory receptors that, upon binding to specific ligands, downregulate the immune response, restoring the physiological condition.⁴

The role of the omnipresent glycocalyx is not limited to pathogen recognition, but also comprise numerous additional relevant biological processes, such as cell adhesion, migration, activation and inhibition events.⁵ The human glycome – the combination of all sugars present in an organism – is mainly composed of only nine monosaccharides (Figure 1).⁶ Despite the enormous number of possible combinations, the variability is limited by the available carbohydrate processing enzymes. As a result, a limited number of glycans are present, distinguishable according to the core of the glycan structure, and the termini, which are specifically recognized by carbohydrate-binding proteins (lectins).⁶

Among the monosaccharides composing the human glycome, sialic acid has a special status. The term sialic acid actually refers to a family of more than fifty related sugars. In mammals, their number is limited primarily to Neu5Ac and N-glycolylneuraminic acid (Neu5Gc), together with some minor differently acetylated derivatives. Neu5Gc is synthesised from Neu5Ac through an enzymatic

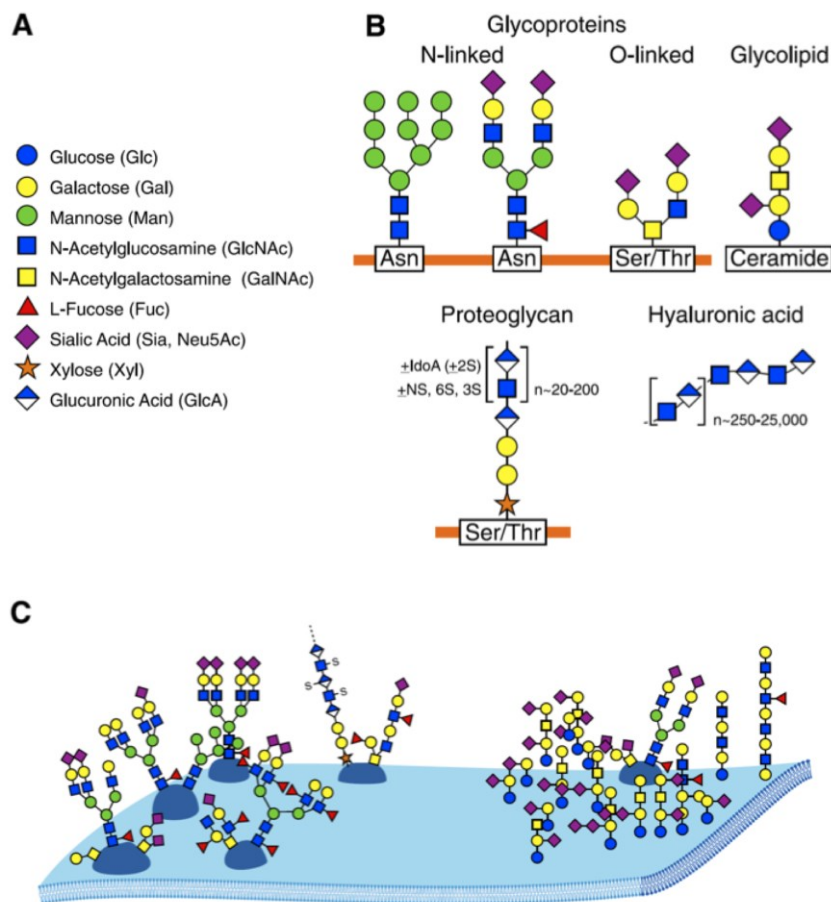


Figure 1. Human glycome. A) List of the nine most common monosaccharides present in humans, with their symbolic representations. B) Classification of human glycans. Almost all proteins are glycosylated and, depending on the amino acid residue involved in the linkage, it can be through either by N-linked or O-linked glycosylation. Huge variability of glycan structures arises from the different regio- and stereochemistry of glycosidic bonds. C) Schematic cell surface representation (figure taken from [6]).

hydroxylation by Cmah (cytidine monophosphate-*N*-acetylneuraminic acid hydroxylases). Due to an irreversible mutation in the *CMAH* gene, humans are not able to synthesise Neu5Gc, leaving Neu5Ac as the predominant form. Different sialyltransferases are responsible for the attachment of Neu5Ac at the termini of oligosaccharide chains by α 2-3, α 2-6 or α 2-8 linkages.⁶⁻¹⁰ Being mostly found at the terminal part of the glycans of almost all cell types, sialic acid has great importance in the interactions between glycan-binding proteins and these sialoglycans.

2. Siglecs

The biological roles of sialoglycans in human health are manifold.^{8,11,12} Thanks to their negative charge and polarity, they are involved in structural and physical roles such as neural plasticity, glomerular filtration and blood cell charge repulsion. They can be exploited by pathogens as ligands for their receptors, like in influenza virus infections, where the first crucial step is the binding of the sialylated sugars on the surface of epithelial cells by the virus protein hemagglutinin. Additionally, pathogens exploit sialic acids in molecular mimicry developing the ability to express sialoglycans on their surfaces, mimicking host cells and evading immune activation. Finally, sialic acids can be exploited by the host as ligands for intrinsic proteins such as factor H, selectins and siglecs. *Factor H* binds sialic acids on cell surfaces, downregulating activation of the complement system, thus promoting cell survival. *Selectins* are transmembrane proteins that initiate leukocyte rolling on endothelial surfaces, which is the first step in the inflammatory cascade.¹³ *Siglecs* are predominantly expressed by immune cells in a cell type-restricted manner and promote inhibition or activation of the immune response. Considering their multiple roles in regulating immune functions, and their distinct expression on different types of cells, siglecs represent promising targets for the pharmacological treatment of various diseases.^{5-7,9,14-18}

2.1. A new class of I-type lectins

The first clue of this new class of proteins dates back to 1990, when sequence analysis of the B cell receptor CD22 cDNA showed that its extracellular portion is composed of five immunoglobulin-like domains, with similarities to the known myelin-associated glycoprotein MAG, a neuronal cell mediator of cell-cell contacts during myelogenesis.¹⁹ One year later, CD22 was proved to bind two sialylated glycoproteins,²⁰ and the macrophage receptor Sialoadhesin was purified and characterized. Its name reflects its ability to bind sialoglycoconjugates, and mediate cellular interactions.²¹ Three years later, in 1994, Sialoadhesin was demonstrated to be composed of seventeen immunoglobulin-like domains, showing similarities with CD22 and MAG. Due to those structural resemblances and their ability to recognize sialoglycans, Sialoadhesin, CD22 and MAG were initially classified in a new family of proteins called the Sialoadhesin family.²² This nomenclature was first modified to I-type lectin²³ and finally to the consensus name Siglec in 1998, which stands for sialic acid-binding immunoglobulin-like lectins. Proteins of this family must have the ability to bind sialylated glycans and share sequence similarities with the other proteins of the group, *i.e.* having extracellular *N*-

terminal V-set immunoglobulin-like domains, followed by a variable number of C2-set Ig-like domains.²⁴

Over the past years, many other siglecs have been discovered, and now this subfamily of the immunoglobulin superfamily consists of fifteen different proteins in humans, and some others have also been discovered in other animals (Figure 2).²⁵ Human siglecs are named by increasing numbers according to their discovery, while siglecs in mice are denoted by letters.

2.2. Siglecs are single-pass transmembrane proteins

Siglecs are type I single-pass transmembrane proteins, extracellularly presenting an *N*-terminal V-set domain with resemblances to the variable domain of antibodies, followed by a varying number of C2-set Ig-like domains, similar to the constant region of immunoglobulins. The transmembrane part of the protein is followed by a cytosolic tail, which may contain signalling motifs (Figure 2A).

The V-set Ig-like domain consists of nine β -strands, forming a sandwich of two β -sheets. This domain contains a conserved arginine residue that is crucial for sialic acid recognition by forming a salt bridge with the carboxylic group Neu5Ac moiety. In addition, two aromatic residues are also commonly present to participate in glycan recognition (Figure 2B). Furthermore, a loop between two β -strands seems to be highly conserved playing an important role in binding, which can lead to a conformational adaption.^{5,7} The *N*-terminal V-set domain is followed by variable numbers of C2-set Ig-like domains, in most of the siglecs from one to four (except for CD22 (6 CS-domain) and Sialoadhesin (16 CS domains)). Similarly to V-set domains, C2-set domains consist of two β -sheets of antiparallel β -strands, but the number of strands is reduced to seven.^{5,7} Interestingly, the V-set and the first C2-set domains possess extra cysteine residues that form an interdomain disulphide bridge and an intra- β -strand disulphide bond, which both are supposed to participate in binding.

In their cytosolic part, most siglecs present immunoreceptor tyrosine-based inhibition motifs (ITIM and ITIM-like motifs) with which they exert their biological functions. ITIM motifs are peptide motifs with the consensus sequence of I/V/L/SxYxxL/V, whereas the consensus sequence for ITIM-like motifs is D/ExYxEV/IK/R. Ligand binding from the *N*-terminal V-set domain results in a higher accessibility of the tyrosines of these motifs, which are then phosphorylated by kinases of the Src family. This phosphorylation creates high-affinity docking sites for cytoplasmic tyrosine phosphatases such as SHP-1 (Src homology region 2 domain-containing phosphatase-1), SHP-2 or SOCS3 (suppressor of cytokine signalling 3), which are triggering a cascade of intracellular events.

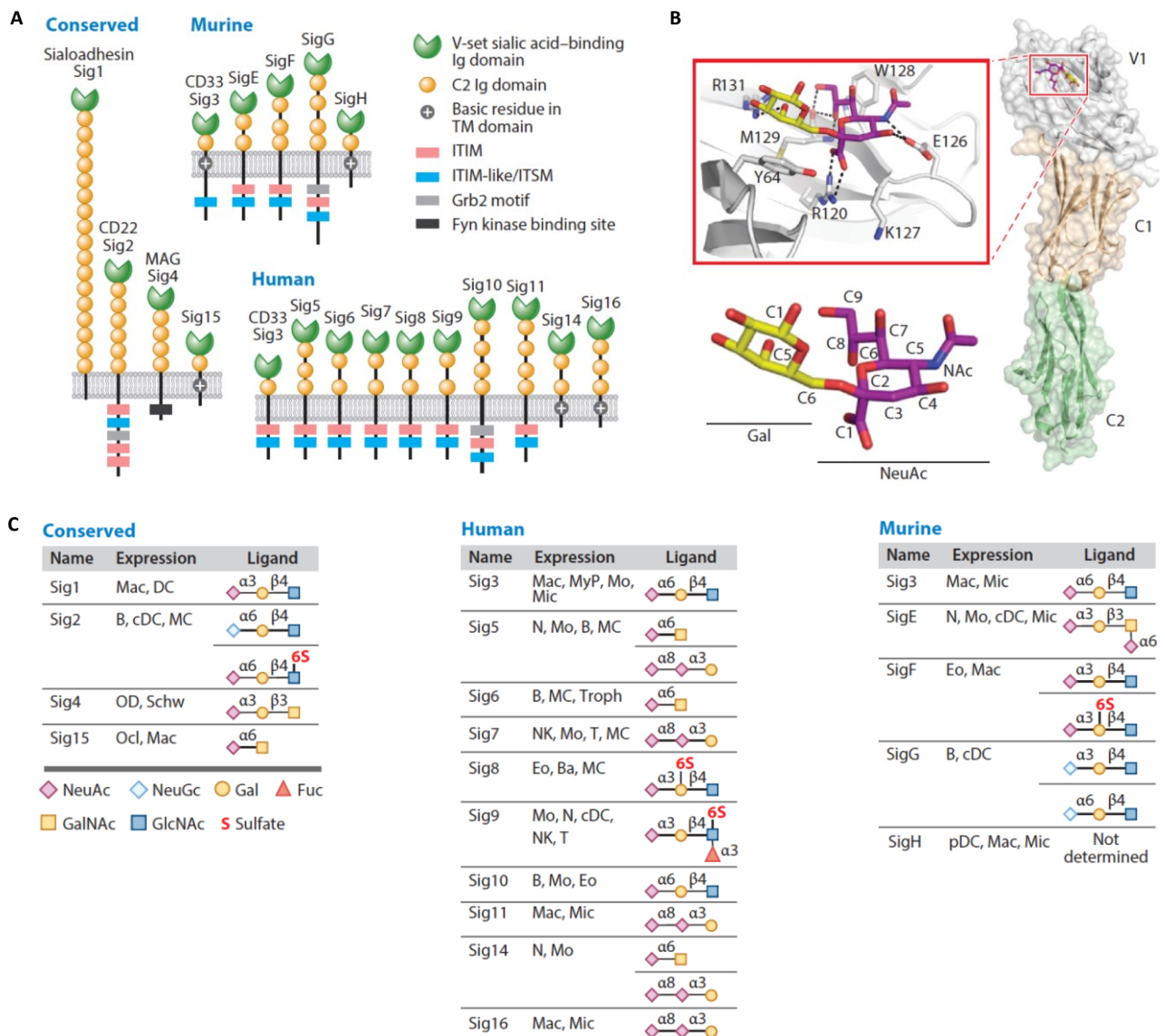


Figure 2. Human and murine Siglecs. A) Structures of the various siglecs. B) Typical binding interaction between Neu5Ac and lectin domain of siglecs, with the typical salt bridge between the carboxyl group and the conserved Arg residue. C) Cell type expression pattern and preferred natural ligand of each Siglecs (B: B cells; Ba: basophils; cDC and pDC: conventional and plasmacytoid dendritic cells; Eo: eosinophils, Mac: macrophages; MC: mast cells; Mic: microglia; Mo: monocytes; NK: natural killer cells; N: neutrophils; Ocl: osteoclasts; OD: oligodendrocytes; Schw: Schwann cells; T: T cells; Troph: placental trophoblasts) (figure taken from [26]).

SHP-1 and SHP-2 are known to be involved in cell development, growth and survival, as well as tissue inflammation and cellular chemotaxis²⁷, while SOCS3 can compete with the first two of them and additionally functions as a negative regulator of cytokine signalling.⁷ ITIM activity seems to outpace ITIM-like one, but both are required to fully exert the biological functions of siglecs.^{28,29}

Some siglecs (Siglec-14, -15 and -16) do not possess any ITIM motifs in the cytoplasmic tail, but present a positively charged amino acid, lysine or arginine, in the transmembrane region. This allows them to recruit the negatively charged aspartic acid residues of activator adaptor proteins DAP12 and

DAP10.^{5,7} DAP12 is a transmembrane protein with a short extracellular part with no binding activity, and an intracellular immunoreceptor tyrosine-based activation motif (ITAM). ITAM motifs are peptide chains with the consensus sequence of D/ExxYxxL/Ix[x]₆₋₈YxxL/I. After tyrosine phosphorylation upon ligand binding, ITAM recruits tyrosine kinases of the spleen tyrosine (Syk) family, initiating a series of events that finally lead to cellular activation.³⁰ DAP10 possess a transmembrane region similar to DAP12, but its cytosolic part is composed of a short peptide sequence YINM. In this case, tyrosine phosphorylation leads to the recruitment of phosphatidylinositol-3 kinase P13K, initiating intracellular activating signalling.³⁰

A last category of siglecs, namely Sialoadhesin, has neither ITIM nor ITIM-like motifs, nor associates with ITAM-containing proteins. This protein differs from the other siglecs also because of its long extracellular region of sixteen C2-set domains and a V-set domain, making it the longest extracellular domain of all siglecs by far, and suggesting a primary role in cell-cell interactions, rather than cellular activation or inhibition.

Human siglecs are usually divided into two groups according to their sequence homology. One group consists of the conserved siglecs, Sialoadhesin (Siglec-1), CD22 (Siglec-2), MAG (Siglec-4), and Siglec-15 with roughly a 20 – 30 % sequence identity. They are conserved across mammals, where clear orthologues can be found. The second group is the CD33 (Siglec-3)-related siglecs, CD33, Siglec-5, -6, -7, -8, -9, -10, -11, -12, -14, and -16. CD33 Siglecs share higher sequence identity, from 50 to 99 %, and are rapidly evolving. This may be driven by the necessity of the host to adapt to the evolving sialome of pathogens, as a consequence of the Red Queen effect. “It takes all the running you can do, to keep in the same place”. These words from the Red Queen to Alice, in Lewis Carroll’s novel *Through the Looking Glass*, provide a figurative image for the evolutionary race between competing species, such as pathogens that evolve to have better chances to invade the host, which has to adapt to those changes for maintaining an adequate immune response.³¹ Due to the rapid evolution of siglecs of this group, it is difficult to find orthologues in other species.^{7,25}

2.3. Siglecs recognize differently linked sialosides

The main feature of siglecs is their ability to specifically recognize glycosylated structures that present sialic acids at their termini (Figure 2C). Commonly, human siglecs bind with low affinity to sialylated structures, which display Neu5Ac α 2-3 or α 2-6 linked to galactose or Neu5Ac α 2-6 linked to *N*-acetylgalactosamine. Few siglecs show preferences for α 2-8 disialylated glycans (Siglec-5, -7, -11, -14, -16).

Despite these common aspects of sialic acid recognition, each siglec has developed a characteristic specificity towards different sialosides, by extending their minimal binding motifs to extended termini, as well as functionalization such as sulfation at different positions (Figure 2C).^{7,26} Glycan arrays provided a key contribution in the identification of these specificities. However, the endogenous ligands are often still unknown.

It has been recently calculated that the local concentration of sialic acids within the glycocalyx can reach more than 100 mM.³² As a result, siglec binding sites are usually “masked” by so-called *cis* interactions with molecules on the same cell surface. These interactions are characterized by low affinity and are driven only by the massive concentration of ligands nearby, but do not preclude *trans* interactions, *i.e.* binding to sialosides that are displayed by different cells (Figure 3). In fact, siglec binding to *cis* or *trans* ligands is a dynamic equilibrium, driven by the relative affinity of the species and their concentration near the binding site. *Cis* interactions are believed to set a signalling baseline for the maintenance of homeostasis, while *trans* interactions may activate and increase siglec signalling. Nevertheless, it is not clear how *cis* and *trans* ligands can bind the protein at the same binding site, leading to different outcomes. Further studies are necessary to elucidate this cooperation, especially because the nature of the endogenous ligands for siglecs is often unknown.

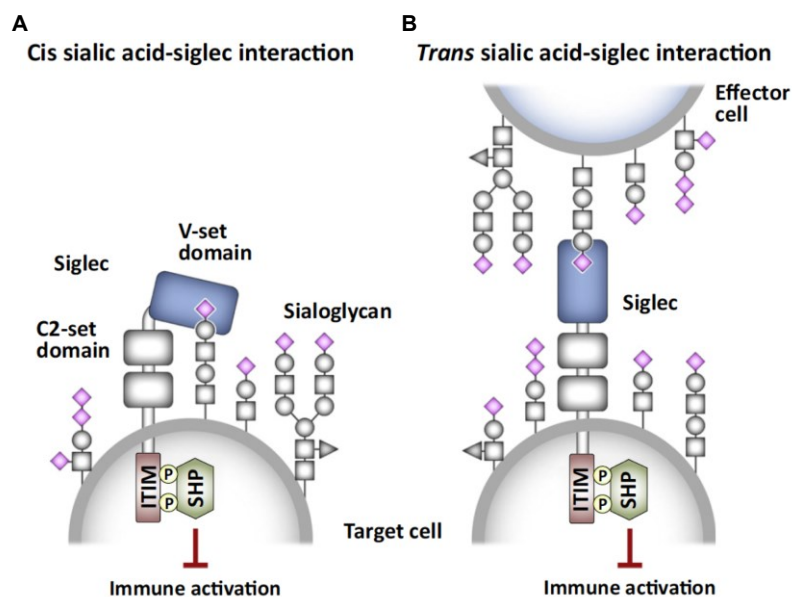


Figure 3. Cis vs trans interactions. A) Interaction with sialosides on the same cell surface prevent lectin binding with *trans* ligands. B) High-affinity *trans* ligands replace *cis* interactions (figure taken from [16]).

Interactions between carbohydrate-binding proteins and their sugar ligands are usually weak. The low affinity is mainly due to shallow and broad binding sites, which generally accounts for K_D values in the range of 0.5 to 3 mM.⁷ To increase affinity, nature often exploits multiple interactions. Many lectins aggregate to form oligomeric structures that can establish multivalent interactions with glycan

ligands simultaneously. Through multivalency, an increase in binding affinity can be achieved by different mechanisms (Figure 4).³³ Through chelation (Figure 4A), *i.e.* the concurrent binding of two or more binding sites of a protein with a multivalent ligand, affinity enhancement is obtained as a result of reduced translational/rotational entropy costs, since these entropy costs are paid only for the first binding event. When binding involves ligation of a secondary, different from the primary binding site, it is called subsite binding. When dealing with a single binding site, an increase in affinity can still be achieved with multivalent ligands through statistical rebinding (Figure 4C). In this case, the increased local concentration of the ligand allows a fast rebinding upon dissociation, decreasing the off-rate and therefore increasing the affinity. Finally, it is possible that a multivalent ligand binds to binding sites of distinct proteins, forming aggregates (Figure 4D).

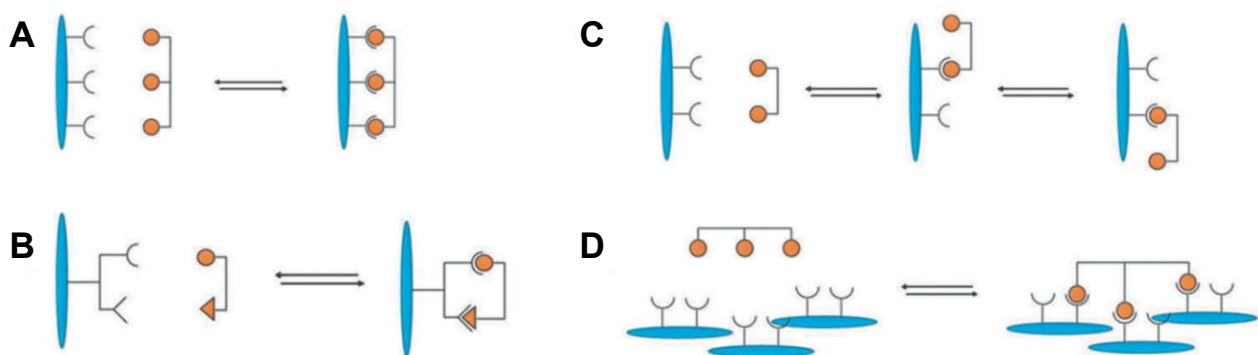


Figure 4. Multivalency mechanisms. A) Chelation. B) Subsite binding. C) Statistical rebinding. D) Aggregation (figure taken from [33]).

2.4. Siglecs are regulators of immune cell signalling

An interesting peculiarity of siglecs is their distinct and cell-specific expression on cells of the immune system, with just a few exceptions. Some siglecs are mainly restricted to a single cell type, while others show a broader expression pattern.¹⁴ Nevertheless, it is clear that the biological roles of each siglec depend on the cell type displaying it.

Another crucial aspect in siglec signalling is the cytosolic domain, namely whether the protein has ITIM motifs in the cytoplasmic tail, associates with ITAM-containing proteins, or presents no signalling functions. Additionally, the binding with *cis* ligands or *trans* ligands leads to different biological outcomes. All these factors account for the distinct roles of each siglec, ranging from pathogen recognition, signal attenuation, apoptosis to inhibition of cell activation.⁵

2.4.1. Conserved siglecs

The group of conserved siglecs consists of Sialoadhesin, CD22, MAG and Siglec-15. They exhibit low sequence similarity, but are conserved across mammalian species. Their different structures and biological functions make them unique within the siglec family.

Sialoadhesin (Siglec-1). Sialoadhesin is also known as Siglec-1 or CD169. It is mainly expressed on tissue-resident macrophages and dendritic cells (DCs), with an immunostimulatory function in the former and immunosuppressive in the latter.^{7,34,35} The unusually long extracellular domain and the lack of intracellular signalling motifs suggest a role in cell-cell interactions, rather than cell signalling.⁷

CD169⁺ macrophages, the lymphoid tissue-resident macrophages, constitutively show high levels of Sialoadhesin. It takes part in pathogen uptake, as it can recognize and bind to exosomes and specific pathogens, among them HIV. The sialylated structures on the viral envelop allow its binding with the carbohydrate-recognition domain (CRD) of Sialoadhesin, which is also responsible for HIV presentation to dendritic cells. Moreover, CD169⁺ are able to interact with DCs precisely because of the binding of Sialoadhesin to DC sialosides.³⁶ An additional role as endocytic receptor has been described with pathogens, such as *Trypanosoma cruzi*, *Neisseria meningitidis* and *Campylobacter jejuni*.^{10,37} Sialoadhesin-mediated endocytosis has been shown to proceed in a clathrin-dependent fashion, and this ability has been linked to the uptake and dissemination of several enveloped viruses like HIV.^{38–41}

CD22 (Siglec-2). One of the most extensively studied siglec is the B-cell receptor Siglec-2, also called CD22.^{19,26} Its atypical intracellular domain is composed of six tyrosine-based signalling motifs, four ITIMs and two potential ITAMs,^{7,10,37,42} responsible for its role as a regulator of function and survival by maintaining a threshold for B-cell activation.⁴³ Cross-linking of CD22 results in ITIM phosphorylation by Lyn tyrosine kinase, which is followed by SHP-1 recruitment and inhibition of BCR signalling. However, this inhibitory pathway does not exhaust the biological role of CD22, since it can also establish activating signalling through interaction with activating molecules such as Grb2 (growth factor receptor-bound protein 2).⁴²

Similarly to Sialoadhesin, CD22 also shows clathrin-dependent endocytic properties. CD22 ligation with antibodies or multivalent ligands results in internalization of the complex, with subsequent recycling of the siglec to the cell surface. In the more acidic environment of the endosomes, the multivalent ligands are released, CD22 can move back to the cell surface and exert its endocytic ability again. In contrast, antibodies are not accumulated intracellularly, but are recycled back to the cell surface together with CD22. Thus, instead of triggering endocytosis, antibody ligation

may influence the constitutive equilibrium between the cell surface and the intracellular region. An important role in CD22-mediated endocytosis is played by its intracellular motifs, thus suggesting a different mechanism compared to Sialoadhesin, which lacks cytosolic domains.^{26,44}

Myelin-associated glycoprotein MAG (Siglec-4). MAG is expressed on myelinated cells of the nervous system; oligodendrocytes in the CNS and Schwann cells of the PNS. Its cytosolic region does not contain an inhibition motif (ITIM or ITIM-like), nor associates with ITAM-containing protein, but presents a Fyn kinase phosphorylation site. MAG is expressed on the periaxonal myelin membrane, close to the axon, to stabilize the myelin-axon interactions through binding to the axon gangliosides GD1a and GT1b. Additionally, it is involved in regulating axon regeneration and myelin formation. Indeed, MAG-deficient mice and mice lacking GD1a and GT1b gangliosides show axon degeneration, both central and peripheral, resulting in hampered motor functions. Furthermore, mucin-1 (MUC1), a heavily glycosylated protein overexpressed in many types of cancer, has been reported to bind MAG and promote tumour spread.^{10,37}

The mechanism of action of MAG is not completely understood, but it is known that ligation with antibodies induces a rapid increase in Fyn kinase activity. Additionally, it has been reported that MAG forms dimeric structures via association of the two membrane-proximal C2-set domains. This *cis* process, together with the *trans* interactions with gangliosides, is important for the biological activity of MAG, as demonstrated by point mutations preventing dimerization and resulting in loss of function.⁴⁵ Lastly, similarly to Sialoadhesin and CD22, MAG undergoes endocytosis by a clathrin-dependent pathway.⁴⁶

Siglec-15. Siglec-15 is the shortest siglecs, having only two Ig-like domains and a really short cytoplasmic tail with no signalling motifs, but it associates with DAP12. Siglec-15 is expressed on macrophages and dendritic cells, but it is mostly found in osteoclasts, with regulator functions in their differentiation. Indeed, Siglec-15-deficient mice show osteoporosis and compromised osteoclast differentiation. A similar result is obtained with Siglec-15 mutants that are no longer able to bind sialic acid. Therefore, Siglec-15 represents an interesting therapeutic target for osteoclast-related diseases. Besides this, new interesting functions of Siglec-15 in tumour immunity and infectious diseases are recently reported.⁴⁷ These roles appear to be correlated to the ability of Siglec-15 to interact and reduce T cell response, which is important in regulating tumour growth and microbial infections.

2.4.2. CD33-related siglecs

The discovery and characterization of Siglec-5 and Siglec-6 started to point out some interesting differences among siglecs.^{48,49} Whereas these two siglecs showed remarkable similarities with CD33 (the amino acid identities among these three proteins are more than 55 %), major differences were found with Sialoadhesin, CD22 and MAG. Therefore, Siglec-5 and Siglec-6, together with CD33, were classified as members of the siglec subclass of CD33-related siglecs. Over the years, many other siglecs were identified and classified as part of this subgroup, and at the same time, new additional features shared by these proteins were discovered.^{50–52} The high sequence similarity among this class seem to be caused by rapid genetic evolutions from the CD33 gene, probably to keep the pace of the evolving pathogens exploiting sialic acids for host invasion or in molecular mimicry mechanisms. Hence, it is quite difficult to find clear orthologues species other than humans, as opposed to the conserved siglecs.

CD33 (Siglec-3). CD33 is expressed on human myeloid progenitor and leukemic cells, but it can also be found in mature monocytes and macrophages,⁵³ Antibody ligation causes inhibition of myeloid progenitor and leukemic cells proliferation and induction of apoptosis in chronic (CML) and acute myeloid leukaemia (AML).^{54,55} Thus, CD33 has received attention as a target for the treatment of AML, and a monoclonal antibody coupled with the antitumor calicheamicin (Gemtuzumab ozogamicin) was exploited for its treatment. CD33 is also gaining attention in relation to Alzheimer's disease (AD) since it is also expressed on microglia, which contribute significantly to amyloid-beta peptide (A β) clearance. CD33-deficient mice showed increased clearance and reduced accumulation of A β , without altering the normal physiology of healthy mice.⁵⁶ Therefore, targeting CD33 may represent a good strategy for the treatment of AD. Finally, CD33 has also demonstrated endocytic properties, mostly regulated by the ITIMs. Tyrosine phosphorylation by Src kinases promotes internalization, while SHP-1 and SHP-2 phosphatases may catalyse dephosphorylation and affect endocytosis.⁵⁷

Siglec-5 & Siglec-14. Within the siglec family, Siglec-5 and Siglec-14 are the first example of pair receptors. Siglec-5 is a classic inhibitory siglec with ITIM and ITIM-like motifs, expressed on neutrophils, monocytes, basophils and mast cells,⁴⁸ while Siglec-14 is present on neutrophils and monocytes and lacks any signalling motifs.^{58,59} Their *N*-terminal V-set domain and the first C2-set domain are practically identical, thus they both recognize sialylated structures equally. While Siglec-5 acts as an inhibitory receptor via recruitment of SHP-1 and SHP-2, hampering Fc γ RI-mediated calcium flux, Siglec-14 promotes immunity and inflammatory responses through regulation of protein kinase B (Akt) and p38 mitogen-activated protein kinase (p38 MAPK) pathways.

A fine example of this dual activity has been shown in group B *Streptococcus* infections. This class of bacteria display sialic acids as terminal residues of the glycocalyx as a molecular mimicry tool, enabling them to bind Siglec-5 and trigger inhibition of the immune system to promote their survival. In contrast, Siglec-14 is also able to recognize the bacteria's sialylated structures, therefore restoring the immune response. Indeed, Siglec-14 deficiency has been linked to increased microbial survival and decreased immune activation.⁵⁹ Similarly to other siglecs, Siglec-5 has also demonstrated endocytic properties as defence mechanisms, and it is also possible that some pathogens may exploit this capacity to spread the infections.³⁷

Siglec-6. Siglec-6 is a classic CD33rSiglec having three Ig-like domains and two ITIM motifs, thus operating as an inhibitory receptor. Besides being weakly expressed on basophils and B cells, it is predominantly present on mast cells, where its biological roles are not fully understood. However, Siglec-6 reduces mast cells degranulation and there seems to be a correlation between this lectin and colorectal cancer, where the presence of Siglec-6 ligands may help the proliferation of cancer cells by inhibiting mast cells immune response.⁶⁰

Siglec-7. The main siglec expressed on NK cells is Siglec-7,⁶¹ one of the few siglecs that shows binding preference towards α 2-8 linked disialylated glycans. In addition, some binding activity was also detected for sulfated versions of the tetrasaccharide sialyl Lewis^x (sulfo-sLe^x), both 6-sulfo- and 6'-sulfo-sLe^x.⁷

The cytosolic region of this protein suggests a sialic acid-dependent inhibitory function, a role which is exploited by tumour cells for suppressing immune system activation, thus Siglec-7 has been studied as potential target for anticancer therapies. Siglec-7 seems to be involved also in many other pathologies, as indicated by studies showing reduced expression in HIV positive patients or patients with hepatitis C virus infections.⁶¹ New insights into the mechanism of action of this protein have been recently elucidated by Yamakawa and coworkers, who discovered the presence of a second binding region able to recognize α 2-8 linked di- and tri-sialosides in a competitive or non-competitive manner. This interesting discovery suggests a dualistic action on the recognition of ligands by this protein with a flexible loop regulating the two sites activity.⁶¹ Further studies are necessary to properly understand all the aspects of this allosteric mechanism, but this new discovery raises some interesting questions regarding the function of Siglec-7, and furthermore, on whether other siglecs display the same feature.

Siglec-8. Being the principal biological target of this thesis, a more detailed discussion on Siglec-8 will follow in Chapter 3.

Siglec-9. One of the highest sequence similarity among CD33-related Siglecs has been discovered between Siglec-7 and Siglec-9, which share almost 98 % identity in their sequence.⁶² Siglec-7 is expressed on NK cells, monocytes, macrophages and DCs, whereas Siglec-9 is mostly present on the surface of neutrophils, with a primary role as inhibitory protein.⁶² The two proteins differ also in their ligand specificity: Siglec-9's main ligands are α 2-3-linked sialosides, with the sulfonated 6-sulfo-sLe^x as the preferred ligand identified by glycan arrays. The position of the sulfate group is obviously crucial for specificity: the isomer 6'-sulfo-sLe^x has no activity towards Siglec-9 but actually is the main ligand of Siglec-8 instead.^{7,62}

As previously discussed with regards to Siglec-7, also Siglec-9 seems to be important in tumour evasion.^{10,16} Similarly, the inhibitory function of Siglec-9 has been exploited by Group B *Streptococcus*, which can dampen immune activation of neutrophils by presenting host sialosides on their surfaces.^{16,63}

Siglec-10. Compared to CD33-related Siglecs, Siglec-10 exhibits structural differences. Besides the slightly longer extracellular domain, the cytosolic region is peculiar for the presence of a membrane-proximal Grb2 motif, in addition to the classic ITIM and ITIM-like motifs.^{26,64} Regarding its cellular expression, Siglec-10 has been found on B cells, monocytes and eosinophils, where it acts as an immune suppressor after ligand recognition.^{6,16,26,64} It mainly recognizes α 2-3 and α 2-6-linked Neu5Ac, with some activity also towards the Neu5Gc variant.^{14,64}

Similarly to other Siglecs, a correlation between Siglec-10 activation and immune evasion by tumour cells has been described. Indeed, by overexpression of CD24, a glycosylated protein linked to proliferation and survival of T cells, tumour cells can improve their survival chance in different ways, among others by activation of Siglec-10.⁶⁵

Siglec-11 & Siglec-16. These siglecs are the second example of pair receptors, with the former acting as inhibitory and the latter as activatory receptor. These two proteins share more than 99 % identity in their extracellular region, thus not surprisingly show the same selectivity towards α 2-8-linked polysialylated glycans. They are both expressed on macrophages and microglia.^{10,26}

Siglec-12, -13 and -17. These three siglecs are not present in Figure 2, each for a specific reason. Siglec-12 in humans has lost the ability to bind sialic acids due to a mutation of the critical arginine in the binding site. In order to distinguish the human protein from its ortholog, the chimpanzee Siglec-12, which maintains the conserved arginine and so the ability to bind sialosides, is usually referred to as Siglec-XII.³⁷ Siglec-13 is an ITAM-associated protein present in chimpanzees but absent in humans, due to deletion of the gene from the human genome. Indeed, the Siglec-13 gene is not present due to an *Alu*-mediated deletion, while it can be found on chimpanzee monocytes. Siglec-17, finally,

is found in primates but has been inactivated by a frameshift mutation during human evolution. However, the Siglec-17P pseudogene is still expressed at high levels in NK mRNA. Interestingly, it was discovered that restoring the expression of either Siglec in innate immune cells can alter inflammatory cytokine secretion in response to Toll-like receptor-4 stimulation. This suggests that these genetic eliminations represent infectious and/or other inflammatory selective processes.⁶⁶

3. Siglec-8

3.1. Siglec-8 is a CD33-related Siglec specific for 6'-sulfo-sLe^x

Siglec-8, an immunoglobulin-type lectin, was first discovered in 2000.^{67,68} It is solely expressed on eosinophils and mast cells, and to a weak extent on basophils.⁶⁹ Since many pathological conditions are associated with altered functions and/or expressions of these cells, among which allergic inflammation and asthma, it is not surprising that researchers have focused their attention on this protein.

From a structural point of view, Siglec-8 is a classic member of the CD33-related family, with an extracellular domain composed of an *N*-terminal V-set domain and two C2-set domains, and the cytosolic inhibitory motifs ITIM and ITIM-like.^{67,68,70} The Siglec-8 initially discovered had only a short cytoplasmic tail with no tyrosine-based motifs, but shortly after, a variant possessing extracellular domains and intracellular inhibitory motifs was identified and named Siglec-8L. Further experiments showed that both versions are expressed in human eosinophils, and Siglec-8L was found in higher quantity than Siglec-8. However, the reasons for the presence of these two variants, and their biological functions are still not clear.⁷⁰

Siglecs of the CD33-related family usually share high sequence similarity. For Siglec-8, the highest sequence overlap is with Siglec-7 and Siglec-9, with 71 % and 68 % similarity, respectively in the extracellular domain (Figure 5).⁶⁷ The folding topology of the Siglec lectin domain is represented by a β -sandwich of two antiparallel β -sheets (ABED and C'CFGG'), which is similar to the V-set Ig-domain. Additionally, three cysteine residues are responsible for two disulfide bonds, one within the V-set domain and one with the next C2-set domain in an inter-domain fashion.⁷¹

Despite the nature of the endogenous ligands of Siglec-8 is still unknown, insights into the glycan specificity were obtained by a glycan array approach, which pointed out a peculiar activity towards sulfated Neu5ac- α 2-3-Gal6S structures, with the tetrasaccharide 6'-sulfo-sLe^x representing the highest activity. The site of the sulfate modification is crucial for both activity and specificity. Binding of Siglec-8 is completely abolished if the sulfate group is missing or in a different position than the 6-position of the Gal moiety. In contrast, the regioisomer 6-sulfo-sLe^x (sulfate in the 6-position of the GlcNAc moiety) is the preferred ligand for Siglec-9.^{6,72}

In 2016, Pröpster *et al* published the NMR solution structure of the Siglec-8 CRD alone and in complex with the main ligand 6'-sulfo-sLe^x.⁴ Their research pointed out important features of the

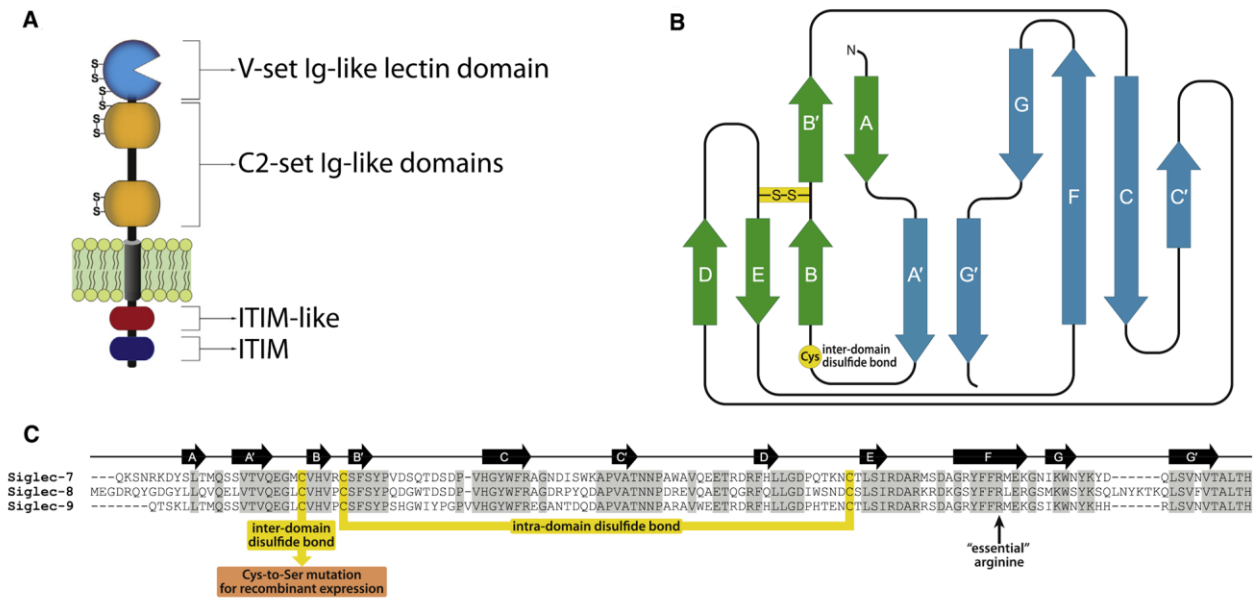


Figure 5. Siglec-8 structure. A) Schematic representation of the extracellular, transmembrane and intracellular domains of Siglec-8. B) Fold topology of a typical Siglec N-terminal V-set Ig-like domain. C) Sequence alignment with human Siglec-7 and -9 (figure taken from [71]).

protein structure and of the molecular interactions at the basis of the recognition of the tetrasaccharide (Figure 6). The main characteristics of the lectin domain, the β -sandwich fold of two antiparallel β -sheets with an intra-domain disulfide bond, the presence of the conserved arginine Arg109 and the extended GG' loop, were confirmed.

The principal interactions between protein and ligand are the essential salt bridge between the carboxylic acid of the sialic acid and the essential Arg109, a second salt bridge between the sulfate group and Arg56 and Glu59, and a complex H-bond network established by the glycerol side chain of the sialic acid. On the other hand, only few interactions were found with the GlcNAc and Fuc moieties. All these interactions accounted for an affinity of $279 \pm 6 \mu\text{M}$ (K_D measured by ITC).⁴

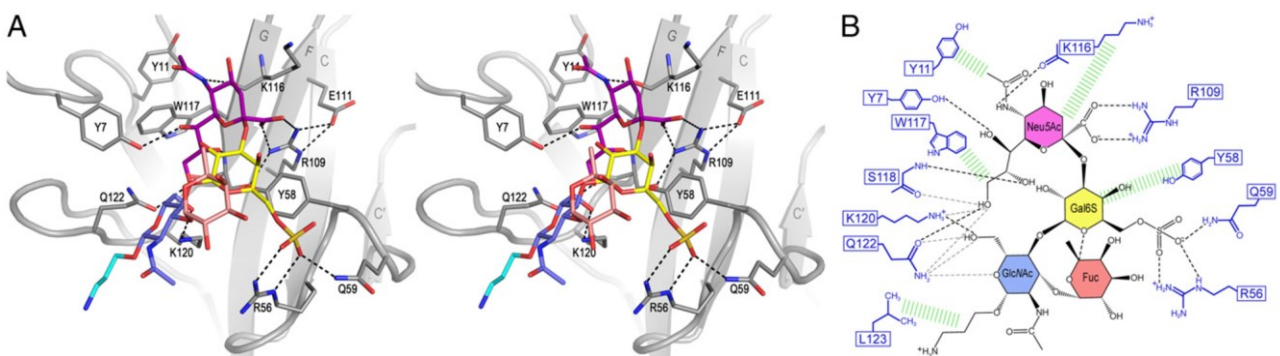


Figure 6. Binding interactions between Siglec-8 and 6'-sulfo-sLe^x. A) View of the binding interface between Siglec-8 and its preferred ligand. B) Schematic representation of intermolecular binding interactions. PDB ID: 2N7B (figure taken from [4]).

3.2. Siglec-8 is an inhibitory regulator of eosinophils and mast cells

The intracellular domain of Siglec-8 consists of two inhibitory motifs, a membrane-proximal ITIM motif and a membrane-distal ITIM-like motif. Therefore, this protein is mainly an inhibitory regulator to maintain homeostasis and avoid overexpression of the cells in which it is expressed.⁶⁸ However, the mechanisms of action by which this inhibitory function is achieved differ between eosinophils and mast cells.

Initially, it was found that Siglec-8 ligation with antibodies induces cellular apoptosis, but only with the presence of a secondary cross-linking antibody or with cytokine priming.⁷³ This apoptotic process is mediated by the production of reactive oxygen species (ROS), leading to subsequent mitochondrial dysfunction, and activation of caspase-3, caspase-8 and caspase-9, enzymes responsible for programmed cell death. Interestingly, pre-treatment of eosinophils with the survival-promoting cytokine interleukin-5 (IL-5) failed to inhibit apoptosis, but instead, reduced the amount of the cross-linking antibody needed to achieve cell death.⁷⁴ The reason for this is still unknown, but may be related to a different colocalization of Siglec-8 and other cell surface receptors after cytokine priming. Such priming often takes place in patients affected by asthma or other diseases in which eosinophils are dysregulated, suggesting a promising role as therapeutic agents against Siglec-8.⁷⁵ Some years later, also a synthetic glycopolymer bearing the tetrasaccharide 6'-sulfo-sLe^x as binding moiety, was discovered to induce eosinophil apoptosis, raising hopes for successful use of synthetic glycans for targeting Siglec-8.⁷⁶

Finally, excellent insights into the signalling pathway in case of eosinophils were obtained by Carroll *et al* (Figure 7).⁷⁷ After ligation with antibodies or sialosides, apoptosis of eosinophils is triggered in an NADPH oxidase-mediated fashion. Especially interesting was the finding that eosinophil adhesion and spreading via increased CD11b/CD18 integrin surface expression are a necessary prerequisite for the apoptosis to take place, but only in case eosinophils are pretreated with IL-5. Interleukin-5 is a mediator of eosinophil activation, and according to the authors, IL-5 priming may be necessary for a proper arrangement of both the integrins CD11b/CD18 closer to Siglec-8, allowing for the signalling cascade to proceed.⁷⁷⁻⁷⁹ This signalling pathway involves increased phosphorylation of Akt, a kinase crucial for cell proliferation, but that can also promote ROS production which eventually leads to apoptosis. Additionally, the roles of p38 and JNK1 were better elucidated, as they were found to be downstream and that their inhibition prevents apoptosis.

Whereas numerous studies were done to elucidate the cellular mechanism of eosinophil apoptosis, far less is known about the inhibitory activity of Siglec-8 on mast cells. Most importantly, Siglec-8

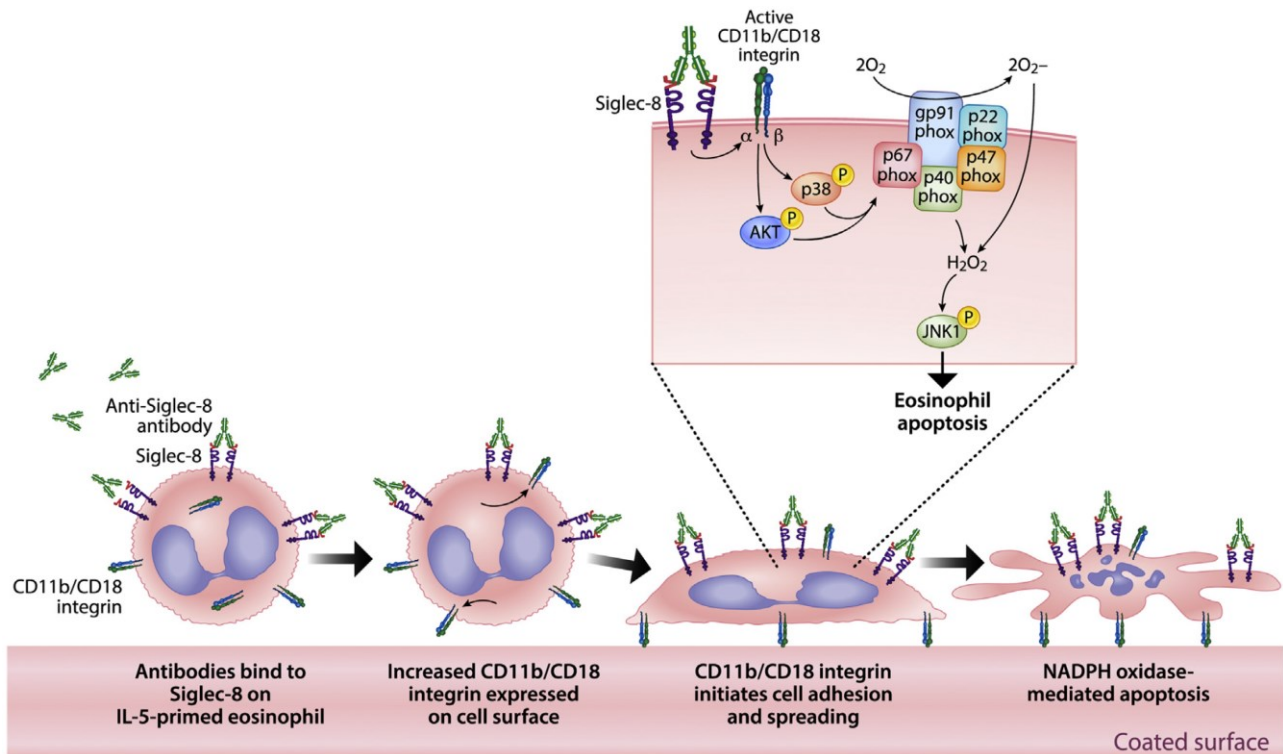


Figure 7. Siglec-8-induced eosinophil apoptosis signalling pathway. Binding of Siglec-8 in IL-5-primed eosinophils increase CD11b/CD18 expression, which in turns mediate cellular adhesion and spreading, leading to ROS accumulation and eventually to apoptosis (figure taken from [77]).

ligation on mast cells does not induce apoptosis. The downregulation of these cells is achieved via inhibition of FcεRI-mediated Ca^{2+} flux and release of histamine and PGD_2 , which consequent impediment of cell degranulation.⁸⁰

One other characteristic of Siglec-8 is the ability to be internalized, a phenomenon which has been seen for other siglecs as well, both in the conserved and CD33-related subgroups.²⁶ This endocytic activity can be clathrin/dynamin-dependent or lipid raft/caveolae-mediated, but in both ways, it relies on actin rearrangement and functioning of tyrosine kinases and PKC (Figure 8). Under physiological conditions, Siglec-8 is masked by *cis* sialosides, but after interaction with *trans* ligands, a complex molecular machinery is activated: cytosolic endocytic clathrins are recruited and start to cluster on the inner part of Siglec-8 in a highly ordered fashion, inducing membrane bending by actin filaments, which eventually leads to the formation of a clathrin-coated pit. Scission of this pit by the GTPase dynamin results in the formation of a vesicle.^{81,82} If the process is lipid raft-mediated, the protein responsible for the vesicle formation is caveolins, thanks to its oligomerization ability. Interestingly, only the membrane-proximal ITIM motif plays a role in Siglec-8 endocytosis, as the mutation of its tyrosine drastically diminishes it, while no changes are observed in the case of ITIM-like tyrosine mutation.⁸¹

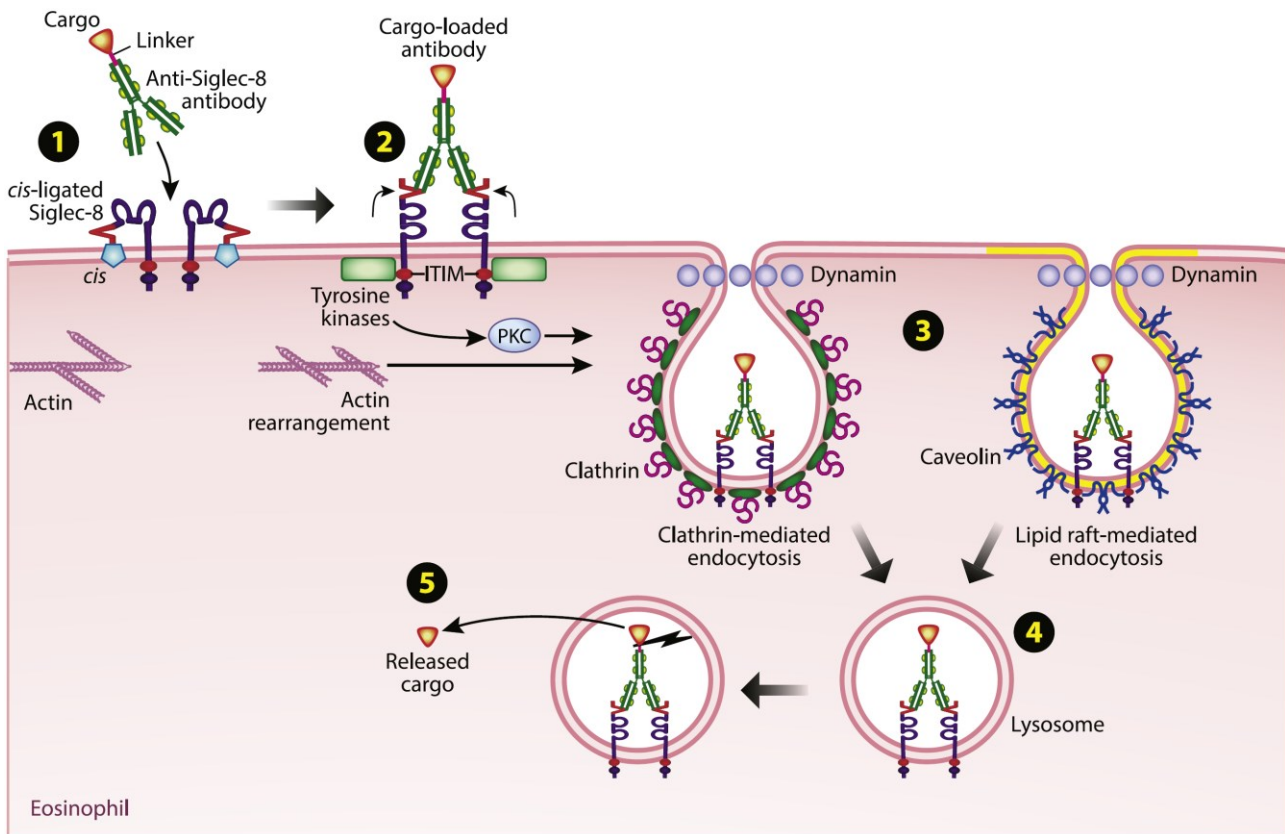


Figure 8. Siglec-8 endocytic pathway. Siglec-8 internalization can proceed via either clathrin-mediated or lipid raft-mediated pathways. After engagement with ligands, the intracellular ITIM induces rearrangement and activation of both tyrosine kinases and PKC. Both pathways end in Siglec-8 internalization in lysosomes. This process can be exploited for the delivery of toxic payload into eosinophils (figure taken from [81]).

3.3. Siglec-F – the mouse paralogue

Despite no clear murine orthologue of Siglec-8 has been identified yet, some similarities with the mouse Siglec-F suggest to consider them as functional paralogues. Siglec-F is a typical CD33-related Siglec, with one additional Ig-like domain: its extracellular region is composed of three C2-set domains and one N-terminal V-set domain, and a cytoplasmic tail with membrane-proximal ITIM and membrane-distal ITIM-like motifs.^{83–85} Siglec-F was at first considered an orthologue for human Siglec-5, based on gene structure, gene maps and phylogenetic analysis.^{86,87} However, further evidence suggested a closer similarity to Siglec-8 as functional convergent paralogues. These include pattern expression, Siglec-F is mainly expressed on eosinophils, and ligand specificity, the sulfated tetrasaccharide 6'-sulfo-sLe^x is the principal ligand for both proteins.⁸³ Yet, major differences between the two proteins exist. Unlike Siglec-8, Siglec-F is also expressed on alveolar macrophages and at low levels on T cells and neutrophils, but it has never been found on mast cells. Also, the ligand specificity is not exactly the same, since Siglec-F recognizes also some sialosides lacking the sulfate

group which is crucial for Siglec-8 binding.⁸⁸ Besides, the signalling pathways by which the two proteins exert their function is significantly different: Siglec-F induced apoptosis does not require NADPH oxidase activity, SHP-1 or Src kinases, but it is dependent on caspase activation.⁸⁹ Also, the endocytic mechanisms are different, since Siglec-F induced endocytosis is clathrin, dynamin and caveolin independent, but depends on ARF6. ARF6 is a GTPase regulator of endosome movement between the plasma membrane and an endosomal compartment that is not clathrin-driven. Bound Siglec-F is sorted to ARF6-positive endosomes, which fuse with clathrin-cargo derived endosomes prior to final sorting to endosomes and lysosomes.⁹⁰

Therefore, although Siglec-F is considered a paralogue of Siglec-8, it can not be used as an animal model to study the effect of Siglec-8 ligation in pathologies such as asthma or allergic diseases, due to the above-mentioned differences. For this purpose, new transgenic mouse strains expressing the human Siglec-8 in eosinophils and/or mast cells have been developed to better mimic the *in vivo* effect of Siglec-8 binding in humans.^{81,91,92}

3.4. New promising pharmacological target for eosinophil- and mast cell-related disorders

A number of pathologies are associated with a dysregulation in the number and activity of eosinophils and mast cells. Asthma is a chronic lung disease affecting hundreds of millions of people, and it has been estimated to be the cause of more than 400.000 deaths globally in 2016.⁹³ Despite the symptoms can be managed by short-term medication during asthma attacks or by avoiding triggers, no cures are available to date. This disease is characterized by airways obstruction and inflammation and hyperresponsiveness of the bronchi after the encounter with inhaled allergens, leading to breathlessness, wheezing and coughing. Eosinophils and mast cells play a crucial role in asthma, the former through an increase in their number and their release of cytotoxic mediators, and the latter through the release of various bronchoconstrictors.^{94,95} Therefore, thanks to its ability to induce eosinophils apoptosis and inhibit mast cell degranulation, Siglec-8 could be a promising therapeutic target for the treatment of asthma. For the same reason, various eosinophilic disorders associated with high levels of eosinophils may benefit from induction of their apoptosis through Siglec-8 binding. This includes eosinophilic esophagitis (EoE), gastritis (EG), duodenitis (EoD), gastroenteritis (EGE), colitis (EC), hypereosinophilic syndrome (HES) and others.^{96,97} On the other hand, abnormal proliferation and accumulation of mast cells are the cause of pathologies such as mastocytosis, mast cell activation syndrome (MCAS), and Hereditary Alpha Trypsinemia (HAT).^{98–100}

In support of the pharmacological relevance and attractiveness of Siglec-8 to treat these diseases, Allakos Inc. developed Lirentelimab (AK002), a humanized non-fucosylated monoclonal antibody

specific for Siglec-8, which has already shown promising results in clinical trials with reduced eosinophil count and symptoms in patients affected by EG and EGE. Symptoms improvement was also observed in phase II clinical trial for chronic urticaria and phase I clinical trial for severe allergic conjunctivitis and indolent systemic mastocytosis. Lirentelimab is currently under investigation in phase II and III clinical trials for the treatment of EG/EoD and EoE.^{101,102}

3.5. On the chemistry of Siglec-8 ligands

Due to their shallow binding sites and the generally low affinities of their natural ligands,⁵ carbohydrate-binding proteins have always been considered as difficult targets regarding the development of small molecule ligands. Moreover, the structures of carbohydrates pose numerous synthetic challenges, ranging from a huge variability regarding regio- and stereochemistry of carbohydrates, often requiring different protecting group strategies and often additional structural modifications. As a result, the synthetic routes for carbohydrates are often long and tedious. Furthermore, the high number of hydroxyl groups leads to poor pharmacokinetic properties.¹⁰³ Consequently, it comes as no surprise that carbohydrates have not been extensively studied as therapeutic agents, and Siglec-8 is no exception. However, recent technological developments in glycan synthesis and analysis, and an in-depth understanding of the structural details of glycan recognition has increased the interest in this class of compounds.¹⁰⁴

Considering the great variability of carbohydrates, drug discovery processes in glycoscience usually begin with microarrays for determining binding specificity. With this high-throughput technology, a large number of different glycans attached to a solid support are simultaneously screened for their binding to the target protein. Despite many challenges still remain, among which the fact that only a small portion of glycan diversity is covered, glycan arrays represent a potent tool.¹⁰⁵ Indeed, Siglec-8 specificity towards the sulfated 6'-sulfo-sLe^x was first discovered by a glycan array approach in 2005, when the activities for 172 different carbohydrates were screened. The high specificity of Siglec-8 was confirmed by the fact that no binding to the closely related isomer 6S-sLe^x was detected, and no other proteins were previously known to bind 6'-sulfo-sLe^x.⁷²

Despite the discovery of the preferred ligand, the lack of structural information on the binding mode of the tetrasaccharide to Siglec-8 posed serious issues for drug development processes. Only after the publication of the NMR solution structure of the 6'-sulfo-sLe^x/Siglec-8 complex and therefore the elucidation of the binding details, a proper medicinal chemistry research could be started. However, the above-mentioned problems associated with carbohydrate-binding protein still discouraged any big efforts for the development of small molecules targeting Siglec-8. It took another

three years to see the first and only research on modified carbohydrates showing improved binding to this lectin.¹⁰⁶ After gathering evidence of higher binding towards modified sialosides bearing sulfonamide modifications at the C-9, Nycholat and coworkers screened Siglec-8 versus 156 glycans in a microarray fashion, and found interesting results with some aromatic sulfonamides. Then, they chose the 2-naphthalenesulfonamide as preferred modification and synthesised a liposome displaying the corresponding modified trisaccharide of 6-sulfo-Neu5Aca(2-3)Gal β (1-4)GlcNAc and proved its binding to Siglec-8 and Siglec-F in cell-based and *in vivo* assays. However, this work did not address many important factors, such as the binding affinity towards the protein, or the thermodynamic profile of the interaction, which are key information for a proper understanding of the binding mechanism and the future development of small molecules for Siglec-8.

4. Aim of the project

The pharmacological relevance of Siglec-8 for the treatment of various eosinophilic and mast cell-related pathologies has already been discussed. However, no small molecules targeting Siglec-8 are available to date.

Due to the nature of the shallow and extended binding pockets of lectins, interactions with ligands are usually weak (0.5 to 3 mM).⁷ Besides, the chemical structure of carbohydrates poses complex challenges in their synthesis due to the various substituents disposition, regio- and stereochemistry of glycosidic bonds, ring sizes, and further modifications are often required. Nonetheless, several strategies have been utilized to develop effective therapeutics for lectins.^{16,104,107}

In this context, this thesis aims to develop high-affinity small molecule ligands targeting Siglec-8, which may potentially represent a novel therapeutic treatment for eosinophilic and mast cell-related diseases, as well as a tool to better elucidate the cellular pathways of Siglec-8 signalling.

The structural information of the binding between Siglec-8 and its preferred ligand 6'-sulfo-sLe^x has been used as a starting point for the identification of the minimal binding epitope that can still be recognized by the protein. This would allow reducing the synthetic complexity of the molecules while retaining the activity. Then, different strategies have been applied to increase the affinity of the compounds. This includes removal of hydrophilic substituents not primarily involved in binding, bioisosteric replacement of the carboxylate and sulfate groups, functionalization of the C-9 and C-4 of the sialic acid, as well as oligo- and multivalent presentation.

5. References

- 1 D. Male, R. Stokes Peebles Jr., V. Male, *Immunology*, Elsevier, **2020**.
- 2 J. Rimer, I. R. Cohen, N. Friedman, Do all creatures possess an acquired immune system of some sort?, *BioEssays* **2014**, *36*, 273–281.
- 3 A. Varki, Evolutionary forces shaping the Golgi glycosylation machinery: Why cell surface glycans are universal to living cells, *Cold Spring Harb. Perspect. Biol.* **2011**, *3*, 1–14.
- 4 J. M. Pröpster, F. Yang, S. Rabbani, B. Ernst, F. H. T. Allain, M. Schubert, Structural basis for sulfation-dependent self-glycan recognition by the human immune-inhibitory receptor Siglec-8, *Proc. Natl. Acad. Sci. U. S. A.* **2016**, *113*, E4170–E4179.
- 5 S. Pillai, I. A. Netravali, A. Cariappa, H. Mattoo, Siglecs and Immune Regulation, *Annu. Rev. Immunol.* **2012**, *30*, 357–392.
- 6 R. L. Schnaar, Glycobiology simplified: diverse roles of glycan recognition in inflammation, *J. Leukoc. Biol.* **2016**, *99*, 825–838.
- 7 P. R. Crocker, J. C. Paulson, A. Varki, Siglecs and their roles in the immune system, *Nat. Rev. Immunol.* **2007**, *7*, 255–266.
- 8 A. Varki, Sialic acids in human health and disease, *Trends Mol. Med.* **2008**, *14*, 351–360.
- 9 T. Angata, C. M. Nycholat, M. S. Macauley, Therapeutic Targeting of Siglecs using Antibody- and Glycan-Based Approaches, *Trends Pharmacol. Sci.* **2015**, *36*, 645–660.
- 10 A. Varki, R. D. Cummings, J. D. Esko, P. Stanley, G. W. Hart, M. Aebi, A. G. Darvill, T. Kinoshita, N. H. Packer, J. H. Prestegard, R. L. Schnaar, P. H. Seeberger, *Essentials of Glycobiology*, Cold Spring Harbor Laboratory Press, **2017**.
- 11 A. Varki, P. Gagneux, Multifarious roles of sialic acids in immunity, *Ann. N. Y. Acad. Sci.* **2012**, *1253*, 16–36.
- 12 A. Varki, Are humans prone to autoimmunity? Implications from evolutionary changes in hominin sialic acid biology, *J. Autoimmun.* **2017**, *83*, 134–142.
- 13 R. P. McEver, Selectins: Initiators of leucocyte adhesion and signalling at the vascular wall, *Cardiovasc. Res.* **2015**, *107*, 331–339.
- 14 M. S. Macauley, P. R. Crocker, J. C. Paulson, Siglec-mediated regulation of immune cell function in disease, *Nat. Rev. Immunol.* **2014**, *14*, 653–666.
- 15 B. S. Bochner, N. Zimmermann, Role of siglecs and related glycan-binding proteins in immune responses and immunoregulation, *J. Allergy Clin. Immunol.* **2015**, *135*, 598–608.
- 16 C. Büll, T. Heise, G. J. Adema, T. J. Boltje, Sialic Acid Mimetics to Target the Sialic Acid-Siglec Axis, *Trends Biochem. Sci.* **2016**, 519–531.

- 17 R. P. Schleimer, R. L. Schnaar, B. S. Bochner, Regulation of airway inflammation by Siglec-8 and Siglec-9 sialoglycan ligand expression, *Curr. Opin. Allergy Clin. Immunol.* **2016**, *16*, 24–30.
- 18 J. A. O’Sullivan, D. J. Carroll, B. S. Bochner, Glycobiology of Eosinophilic Inflammation: Contributions of Siglecs, Glycans, and Other Glycan-Binding Proteins, *Front. Med.* **2017**, *4*, 116.
- 19 I. Stamenkovic, B. Seed, The B-cell antigen CD22 mediates monocyte and erythrocyte adhesion, *Nature* **1990**, *345*, 74–77.
- 20 I. Stamenkovic, D. Sgroi, A. Aruffo, M. S. Sy, T. Anderson, The B lymphocyte adhesion molecule CD22 interacts with leukocyte common antigen CD45RO on T cells and α 2-6 sialyltransferase, CD75, on B cells, *Cell* **1991**, *66*, 1133–1144.
- 21 P. R. Crocker, S. Kelm, C. Dubois, B. Martin, A. S. McWilliam, D. M. Shotton, J. C. Paulson, S. Gordon, Purification and properties of sialoadhesin, a sialic acid-binding receptor of murine tissue macrophages., *EMBO J.* **1991**, *10*, 1661–1669.
- 22 S. Kelm, A. Pelz, R. Schauer, M. T. Filbin, S. Tang, M. E. de Bellard, R. L. Schnaar, J. A. Mahoney, A. Hartnell, P. Bradfield, P. R. Crocker, Sialoadhesin, myelin-associated glycoprotein and CD22 define a new family of sialic acid-dependent adhesion molecules of the immunoglobulin superfamily, *Curr. Biol.* **1994**, *4*, 965–972.
- 23 L. D. Powell, A. Varki, I-type Lectins, *J. Biol. Chem.* **1995**, *270*, 14243–14246.
- 24 P. R. Crocker, E. A. Clark, M. Filbin, S. Gordon, Y. Jones, J. H. Kehrl, S. Kelm, N. Le Douarin, L. D. Powell, J. Roder, R. L. Schnaar, D. C. Sgroi, I. Stamenkovic, R. Schauer, M. Schachner, T. K. van den Berg, A. P. van der Merwe, S. M. Watt, A. Varki, Siglecs: a family of sialic-acid binding lectins, *Glycobiology* **1998**, *8*, v.
- 25 K. F. Bornhöfft, T. Goldammer, A. Rebl, S. P. Galuska, Siglecs: A journey through the evolution of sialic acid-binding immunoglobulin-type lectins, *Dev. Comp. Immunol.* **2018**, *86*, 219–231.
- 26 S. Duan, J. C. Paulson, Siglecs as Immune Cell Checkpoints in Disease, *Annu. Rev. Immunol.* **2020**, *38*, 365–395.
- 27 Z. Z. Chong, K. Maiese, The Src homology 2 domain tyrosine phosphatases SHP-1 and SHP-2: Diversified control of cell growth, inflammation, and injury, *Histol. Histopathol.* **2007**, *22*, 1251–1267.
- 28 A. D. Barrow, J. Trowsdale, You say ITAM and I say ITIM, let’s call the whole thing off: the ambiguity of immunoreceptor signalling, *Eur. J. Immunol.* **2006**, *36*, 1646–1653.
- 29 M. Daëron, S. Jaeger, L. Du Pasquier, E. Vivier, Immunoreceptor tyrosine-based inhibition

- motifs: a quest in the past and future, *Immunol. Rev.* **2008**, *224*, 11–43.
- 30 L. L. Lanier, DAP10- and DAP12-associated receptors in innate immunity, *Immunol. Rev.* **2009**, *227*, 150–160.
- 31 A. Varki, Nothing in Glycobiology Makes Sense, except in the Light of Evolution, *Cell* **2006**, *126*, 841–845.
- 32 B. E. Collins, O. Blixt, A. R. DeSieno, N. Bovin, J. D. Marth, J. C. Paulson, Masking of CD22 by cis ligands does not prevent redistribution of CD22 to sites of cell contact, *Proc. Natl. Acad. Sci. U. S. A.* **2004**, *101*, 6104–6109.
- 33 W. Lu, R. J. Pieters, Carbohydrate–protein interactions and multivalency: implications for the inhibition of influenza A virus infections, *Expert Opin. Drug Discov.* **2019**, *14*, 387–395.
- 34 P. R. Crocker, S. Gordon, Mouse macrophage hemagglutinin (sheep erythrocyte receptor) with specificity for sialylated glycoconjugates characterized by a monoclonal antibody, *J. Exp. Med.* **1989**, *169*, 1333–1346.
- 35 A. Hartnell, J. Steel, H. Turley, M. Jones, D. G. Jackson, P. R. Crocker, Characterization of human sialoadhesin, a sialic acid binding receptor expressed by resident and inflammatory macrophage populations, *Blood* **2001**, *97*, 288–296.
- 36 J. Grabowska, M. A. Lopez-Venegas, A. J. Affandi, J. M. M. Den Haan, CD169+ macrophages capture and dendritic cells instruct: The interplay of the gatekeeper and the general of the immune system, *Front. Immunol.* **2018**, *9*, 1–14.
- 37 S. Von Gunten, B. S. Bochner, Basic and clinical immunology of Siglecs, *Ann. N. Y. Acad. Sci.* **2008**, *1143*, 61–82.
- 38 N. Vanderheijden, P. L. Delputte, H. W. Favoreel, J. Vandekerckhove, J. Van Damme, P. A. van Woensel, H. J. Nauwynck, Involvement of Sialoadhesin in Entry of Porcine Reproductive and Respiratory Syndrome Virus into Porcine Alveolar Macrophages, *J. Virol.* **2003**, *77*, 8207–8215.
- 39 H. van Gorp, W. van Breedam, P. L. Delputte, H. J. Nauwynck, The porcine reproductive and respiratory syndrome virus requires trafficking through CD163-positive early endosomes, but not late endosomes, for productive infection, *Arch. Virol.* **2009**, *154*, 1939–1943.
- 40 P. D. Uchil, R. Pi, K. A. Haugh, M. S. Ladinsky, J. D. Ventura, B. S. Barrett, M. L. Santiago, P. J. Bjorkman, G. Kassiotis, X. Sewald, W. Mothes, A Protective Role for the Lectin CD169/Siglec-1 against a Pathogenic Murine Retrovirus, *Cell Host Microbe* **2019**, *25*, 87-100.e10.
- 41 D. Perez-Zsolt, J. Cantero-Pérez, I. Erkizia, S. Benet, M. Pino, C. Serra-Peinado, A.

- Hernández-Gallego, J. Castellví, G. Tapia, V. Arnau-Saz, J. Garrido, A. Tarrats, M. J. Buzón, J. Martinez-Picado, N. Izquierdo-Useros, M. Genescà, Dendritic Cells From the Cervical Mucosa Capture and Transfer HIV-1 via Siglec-1, *Front. Immunol.* **2019**, *10*, 825.
- 42 T. F. Tedder, J. C. Poe, K. M. Haas, CD22: A multifunctional receptor that regulates B lymphocyte survival and signal transduction, *Adv. Immunol.* **2005**, *88*, 1–50.
- 43 G. M. Doody, L. B. Justement, C. C. Delibrias, R. J. Matthews, J. Lin, M. L. Thomas, D. T. Fearon, A role in B cell activation for CD22 and the protein tyrosine phosphatase SHP, *Science* **1995**, *269*, 242–244.
- 44 M. K. O'Reilly, H. Tian, J. C. Paulson, CD22 Is a Recycling Receptor That Can Shuttle Cargo between the Cell Surface and Endosomal Compartments of B Cells, *J. Immunol.* **2011**, *186*, 1554–1563.
- 45 M. F. Pronker, S. Lemstra, J. Snijder, A. J. R. Heck, D. M. E. Thies-Weesie, R. J. Pasterkamp, B. J. C. Janssen, Structural basis of myelin-associated glycoprotein adhesion and signalling, *Nat. Commun.* **2016**, *7*, 1–13.
- 46 C. Winterstein, J. Trotter, E. M. Krämer-Albers, Distinct endocytic recycling of myelin proteins promotes oligodendroglial membrane remodeling, *J. Cell Sci.* **2008**, *121*, 834–842.
- 47 T. Angata, Siglec-15: a potential regulator of osteoporosis, cancer, and infectious diseases, *J. Biomed. Sci.* **2020**, *27*, 10.
- 48 A. L. Cornish, S. Freeman, G. Forbes, J. Ni, M. Zhang, M. Cepeda, R. Gentz, M. Augustus, K. C. Carter, P. R. Crocker, Characterization of siglec-5, a novel glycoprotein expressed on myeloid cells related to CD33, *Blood* **1998**, *92*, 2123–2132.
- 49 N. Patel, E. C. M. Brinkman-Van der Linden, S. W. Altmann, K. Gish, S. Balasubramanian, J. C. Timans, D. Peterson, M. P. Bell, J. F. Bazan, A. Varki, R. A. Kastelein, OB-BP1/Siglec-6, a leptin- and sialic acid-binding protein of the immunoglobulin superfamily, *J. Biol. Chem.* **1999**, *274*, 22729–22738.
- 50 T. Angata, E. H. Margulies, E. D. Green, A. Varki, Large-scale sequencing of the CD33-related Siglec gene cluster in five mammalian species reveals rapid evolution by multiple mechanisms, *Proc. Natl. Acad. Sci. U. S. A.* **2004**, *101*, 13251–13256.
- 51 H. Cao, P. R. Crocker, Evolution of CD33-related siglecs: regulating host immune functions and escaping pathogen exploitation?, *Immunology* **2011**, *132*, 18–26.
- 52 P. R. Crocker, S. J. McMillan, H. E. Richards, CD33-related siglecs as potential modulators of inflammatory responses, *Ann. N. Y. Acad. Sci.* **2012**, *1253*, 102–111.
- 53 V. C. Taylor, C. D. Buckley, M. Douglas, A. J. Cody, D. L. Simmons, S. D. Freeman, The Myeloid-specific Sialic Acid-binding Receptor, CD33, Associates with the Protein-tyrosine

- Phosphatases, SHP-1 and SHP-2 *, *J. Biol. Chem.* **1999**, *274*, 11505–11512.
- 54 C. Vitale, C. Romagnani, M. Falco, M. Ponte, M. Vitale, A. Moretta, A. Bacigalupo, L. Moretta, M. C. Mingari, Engagement of p75/AIRM1 or CD33 inhibits the proliferation of normal or leukemic myeloid cells, *Proc. Natl. Acad. Sci. U. S. A.* **1999**, *96*, 15091–15096.
- 55 C. Vitale, C. Romagnani, A. Puccetti, D. Olive, R. Costello, L. Chiossone, A. Pitto, A. Bacigalupo, L. Moretta, M. C. Mingari, Surface expression and function of p75/AIRM-1 or CD33 in acute myeloid leukemias: Engagement of CD33 induces apoptosis of leukemic cells, *Proc. Natl. Acad. Sci. U. S. A.* **2001**, *98*, 5764–5769.
- 56 T. Jiang, J. T. Yu, N. Hu, M. S. Tan, X. C. Zhu, L. Tan, CD33 in alzheimer's disease, *Mol. Neurobiol.* **2014**, *49*, 529–535.
- 57 R. B. Walter, B. W. Raden, R. Zeng, P. Häusermann, I. D. Bernstein, J. A. Cooper, ITIM-dependent endocytosis of CD33-related Siglecs: role of intracellular domain, tyrosine phosphorylation, and the tyrosine phosphatases, Shp1 and Shp2, *J. Leukoc. Biol.* **2008**, *83*, 200–211.
- 58 T. Angata, T. Hayakawa, M. Yamanaka, A. Varki, M. Nakamura, Discovery of Siglec-14, a novel sialic acid receptor undergoing concerted evolution with Siglec-5 in primates, *FASEB J.* **2006**, *20*, 1964–1973.
- 59 S. R. Ali, J. J. Fong, A. F. Carlin, T. D. Busch, R. Linden, T. Angata, T. Areschoug, M. Parast, N. Varki, J. Murray, V. Nizet, A. Varki, Siglec-5 and Siglec-14 are polymorphic paired receptors that modulate neutrophil and amnion signaling responses to group B Streptococcus, *J. Exp. Med.* **2014**, *211*, 1231–1242.
- 60 Y. Yu, B. R. J. Blokhuis, M. A. P. Diks, A. Keshavarzian, J. Garssen, F. A. Redegeld, Functional inhibitory siglec-6 is upregulated in human colorectal cancer-associated mast cells, *Front. Immunol.* **2018**, *9*, 1–11.
- 61 N. Yamakawa, Y. Yasuda, A. Yoshimura, A. Goshima, P. R. Crocker, G. Vergoten, Y. Nishiura, T. Takahashi, S. Hanashima, K. Matsumoto, Y. Yamaguchi, H. Tanaka, K. Kitajima, C. Sato, Discovery of a new sialic acid binding region that regulates Siglec-7, *Sci. Rep.* **2020**, *10*, 1–14.
- 62 Y. Zheng, X. Ma, D. Su, Y. Zhang, L. Yu, F. Jiang, X. Zhou, Y. Feng, F. Ma, The Roles of Siglec7 and Siglec9 on Natural Killer Cells in Virus Infection and Tumour Progression, *J. Immunol. Res.* **2020**, *2020*, DOI 10.1155/2020/6243819.
- 63 A. F. Carlin, S. Uchiyama, Y. C. Chang, A. L. Lewis, V. Nizet, A. Varki, Molecular mimicry of host sialylated glycans allows a bacterial pathogen to engage neutrophil Siglec-9 and dampen the innate immune response, *Blood* **2009**, *113*, 3333–3336.

- 64 R. E. Forgione, C. Di Carluccio, J. Guzmán-Caldentey, R. Gaglione, F. Battista, F. Chiodo, Y. Manabe, A. Arciello, P. Del Vecchio, K. Fukase, A. Molinaro, S. Martín-Santamaría, P. R. Crocker, R. Marchetti, A. Silipo, Unveiling Molecular Recognition of Sialoglycans by Human Siglec-10, *iScience* **2020**, *23*, 101231.
- 65 S. S. Yin, F. H. Gao, Molecular Mechanism of Tumor Cell Immune Escape Mediated by CD24/Siglec-10, *Front. Immunol.* **2020**, *11*, 1324.
- 66 X. Wang, N. Mitra, I. Secundino, K. Banda, P. Cruz, V. Padler-Karavani, A. Verhagen, C. Reid, M. Lari, E. Rizzi, C. Balsamo, G. Corti, G. De Bellis, L. Longo, W. Beggs, D. Caramelli, S. A. Tishkoff, T. Hayakawa, E. D. Green, J. C. Mullikin, V. Nizet, J. Bui, A. Varki, Specific inactivation of two immunomodulatory SIGLEC genes during human evolution, *Proc. Natl. Acad. Sci. U. S. A.* **2012**, *109*, 9935–9940.
- 67 H. Floyd, J. Ni, A. L. Cornish, Z. Zeng, D. Liu, K. C. Carter, J. Steel, P. R. Crocker, Siglec-8. A novel eosinophil-specific member of the immunoglobulin superfamily, *J. Biol. Chem.* **2000**, *275*, 861–866.
- 68 G. Foussias, G. M. Yoused, E. P. Diamandis, Molecular Characterization of a Siglec8 Variant Containing Cytoplasmic Tyrosine-Based Motifs, and Mapping of the Siglec8 Gene, *Biochem. Biophys. Res. Commun.* **2000**, *260*, 775–781.
- 69 J. A. O’Sullivan, A. T. Chang, B. A. Youngblood, B. S. Bochner, Eosinophil and mast cell Siglecs: From biology to drug target, *J. Leukoc. Biol.* **2020**, 1–9.
- 70 H. Aizawa, J. Plitt, B. S. Bochner, Human eosinophils express two Siglec-8 splice variants, *J. Allergy Clin. Immunol.* **2002**, *109*, 176.
- 71 J. M. Pröpster, F. Yang, B. Ernst, F. H. T. Allain, M. Schubert, Functional Siglec lectin domains from soluble expression in the cytoplasm of Escherichia coli, *Protein Expr. Purif.* **2015**, *109*, 14–22.
- 72 B. S. Bochner, R. A. Alvarez, P. Mehta, N. V. Bovin, O. Blixt, J. R. White, R. L. Schnaar, Glycan Array Screening Reveals a Candidate Ligand for Siglec-8, *J. Biol. Chem.* **2005**, *280*, 4307–4312.
- 73 E. Nutku, H. Aizawa, S. A. Hudson, B. S. Bochner, Ligation of Siglec-8: a selective mechanism for induction of human eosinophil apoptosis, *Blood* **2003**, *101*, 5014–5020.
- 74 E. Nutku, S. A. Hudson, B. S. Bochner, Mechanism of Siglec-8-induced human eosinophil apoptosis: Role of caspases and mitochondrial injury, *Biochem. Biophys. Res. Commun.* **2005**, *336*, 918–924.
- 75 E. Nutku-Bilir, S. A. Hudson, B. S. Bochner, Interleukin-5 Priming of Human Eosinophils Alters Siglec-8-Mediated Apoptosis Pathways, *Am. J. Respir. Cell Mol. Biol.* **2008**, *38*, 121–

- 124.
- 76 S. A. Hudson, N. V. Bovin, R. L. Schnaar, P. R. Crocker, B. S. Bochner, Eosinophil-selective binding and proapoptotic effect in vitro of a synthetic siglec-8 ligand, polymeric 6'-sulfated sialyl lewis X, *J. Pharmacol. Exp. Ther.* **2009**, *330*, 608–612.
- 77 D. J. Carroll, J. A. O'Sullivan, D. B. Nix, Y. Cao, M. Tiemeyer, B. S. Bochner, Sialic acid-binding immunoglobulin-like lectin 8 (Siglec-8) is an activating receptor mediating β 2-integrin-dependent function in human eosinophils, *J. Allergy Clin. Immunol.* **2018**, *141*, 2196–2207.
- 78 S. R. Barthel, M. W. Johansson, D. M. McNamee, D. F. Mosher, Roles of integrin activation in eosinophil function and the eosinophilic inflammation of asthma, *J. Leukoc. Biol.* **2008**, *83*, 1–12.
- 79 M. W. Johansson, K. A. Gunderson, E. A. B. Kelly, L. C. Denlinger, N. N. Jarjour, D. F. Mosher, Anti-IL-5 attenuates activation and surface density of β 2 -integrins on circulating eosinophils after segmental antigen challenge, *Clin. Exp. Allergy* **2013**, *43*, 292–303.
- 80 H. Yokoi, O. H. Choi, W. Hubbard, H. S. Lee, B. J. Canning, H. H. Lee, S. D. Ryu, S. von Gunten, C. A. Bickel, S. A. Hudson, D. W. MacGlashan, B. S. Bochner, Inhibition of Fc ϵ RI-dependent mediator release and calcium flux from human mast cells by sialic acid-binding immunoglobulin-like lectin 8 engagement, *J. Allergy Clin. Immunol.* **2008**, *121*, 499–506.
- 81 J. A. O'Sullivan, D. J. Carroll, Y. Cao, A. N. Salicru, B. S. Bochner, Leveraging Siglec-8 endocytic mechanisms to kill human eosinophils and malignant mast cells, *J. Allergy Clin. Immunol.* **2018**, *141*, 1774-1785.e7.
- 82 M. Kaksonen, A. Roux, Mechanisms of clathrin-mediated endocytosis, *Nat. Rev. Mol. Cell Biol.* **2018**, *19*, 313–326.
- 83 H. Tateno, P. R. Crocker, J. C. Paulson, Mouse Siglec-F and human Siglec-8 are functionally convergent paralogs that are selectively expressed on eosinophils and recognize 6'-sulfo-sialyl Lewis X as a preferred glycan ligand, *Glycobiology* **2005**, *15*, 1125–1135.
- 84 B. S. Bochner, Siglec-8 on human eosinophils and mast cells, and Siglec-F on murine eosinophils, are functionally related inhibitory receptors, *Clin. Exp. Allergy* **2009**, *39*, 317–324.
- 85 S. S. Farid, A. Mirshafiey, A. Razavi, Siglec-8 and Siglec-F, the new therapeutic targets in asthma, *Immunopharmacol. Immunotoxicol.* **2012**, *34*, 721–726.
- 86 T. Angata, R. Hingorani, N. M. Varki, A. Varki, Cloning and Characterization of a Novel Mouse Siglec, mSiglec-F: Differential evolution of the mouse and human (CD33) Siglec-3-related gene clusters, *J. Biol. Chem.* **2001**, *276*, 45128–45136.

- 87 H. Aizawa, N. Zimmermann, P. E. Carrigan, J. J. Lee, M. E. Rothenberg, B. S. Bochner, Molecular analysis of human Siglec-8 orthologs relevant to mouse eosinophils: Identification of mouse orthologs of Siglec-5 (mSiglec-F) and Siglec-10 (mSiglec-G), *Genomics* **2003**, *82*, 521–530.
- 88 T. Kiwamoto, T. Katoh, C. M. Evans, W. J. Janssen, M. E. Brummet, S. A. Hudson, Z. Zhu, M. Tiemeyer, B. S. Bochner, Endogenous airway mucins carry glycans that bind Siglec-F and induce eosinophil apoptosis, *J. Allergy Clin. Immunol.* **2015**, *135*, 1329-1340.e9.
- 89 H. Mao, G. Kano, S. A. Hudson, M. Brummet, N. Zimmermann, Z. Zhu, B. S. Bochner, Mechanisms of Siglec-F-Induced Eosinophil Apoptosis: A Role for Caspases but Not for SHP-1, Src Kinases, NADPH Oxidase or Reactive Oxygen, *PLoS One* **2013**, *8*, e68143.
- 90 H. Tateno, H. Li, M. J. Schur, N. Bovin, P. R. Crocker, W. W. Wakarchuk, J. C. Paulson, Distinct Endocytic Mechanisms of CD22 (Siglec-2) and Siglec-F Reflect Roles in Cell Signaling and Innate Immunity, *Mol. Cell. Biol.* **2007**, *27*, 5699–5710.
- 91 Y. Wei, K. Chhiba, F. Zhang, X. Ye, L. Wang, L. Zhang, P. Robida, L. Moreno-Vinasco, R. Schnaar, A. Roers, K. Hartmann, C.-M. Lee, D. Demers, T. Zheng, B. Bochner, Z. Zhu, Mast Cell-Specific Expression of Human Siglec-8 in Conditional Knock-in Mice, *Int. J. Mol. Sci.* **2018**, *20*, 19.
- 92 B. A. Youngblood, E. C. Brock, J. Leung, R. Falahati, B. S. Bochner, H. S. Rasmussen, K. Peterson, C. Bebbington, N. Tomasevic, Siglec-8 antibody reduces eosinophils and mast cells in a transgenic mouse model of eosinophilic gastroenteritis, *JCI Insight* **2019**, *4*, e126219.
- 93 T. Vos, A. A. Abajobir, C. Abbafati, K. M. Abbas, K. H. Abate, F. Abd-Allah, A. M. Abdulle, T. A. Abebo, S. F. Abera, V. Aboyans, L. J. Abu-Raddad, I. N. Ackerman, A. A. Adamu, O. Adetokunboh, M. Afarideh, A. Afshin, S. K. Agarwal, R. Aggarwal, A. Agrawal, S. Agrawal, A. Ahmad Kiadaliri, H. Ahmadi, M. B. Ahmed, A. N. Aichour, I. Aichour, M. T. E. Aichour, S. Aiyar, R. O. Akinyemi, N. Akseer, F. H. Al Lami, F. Alahdab, Z. Al-Aly, K. Alam, N. Alam, T. Alam, D. Alasfoor, K. A. Alene, R. Ali, R. Alizadeh-Navaei, A. Alkerwi, F. Alla, P. Allebeck, C. Allen, F. Al-Maskari, R. Al-Raddadi, U. Alsharif, S. Alsowaidi, K. A. Altirkawi, A. T. Amare, E. Amini, W. Ammar, Y. A. Amoako, H. H. Andersen, C. A. T. Antonio, P. Anwari, J. Ärnlöv, A. Artaman, K. K. Aryal, H. Asayesh, S. W. Asgedom, R. Assadi, T. M. Atey, N. T. Atnafo, S. R. Atre, L. Avila-Burgos, E. F. G. A. Avokpaho, A. Awasthi, B. P. Ayala Quintanilla, H. O. Ba Saleem, U. Bacha, A. Badawi, K. Balakrishnan, A. Banerjee, M. S. Bannick, A. Barac, R. M. Barber, S. L. Barker-Collo, T. Bärnighausen, S. Barquera, L. Barregard, L. H. Barrero, S. Basu, B. Battista, K. E. Battle, B.

T. Baune, S. Bazargan-Hejazi, J. Beardsley, N. Bedi, E. Beghi, Y. Béjot, B. B. Bekele, M. L. Bell, D. A. Bennett, I. M. Bensenor, J. Benson, A. Berhane, D. F. Berhe, E. Bernabé, B. D. Betsu, M. Beuran, A. S. Beyene, N. Bhala, A. Bhansali, S. Bhatt, Z. A. Bhutta, S. Biadgilign, K. Bienhoff, B. Bikbov, C. Birungi, S. Biryukov, D. Bisanzio, H. M. Bizuayehu, D. J. Boneya, S. Boufous, R. R. A. Bourne, A. Brazinova, T. S. Brugha, R. Buchbinder, L. N. B. Bulto, B. R. Bumgarner, Z. A. Butt, L. Cahuana-Hurtado, E. Cameron, M. Car, H. Carabin, J. R. Carapetis, R. Cárdenas, D. O. Carpenter, J. J. Carrero, A. Carter, F. Carvalho, D. C. Casey, V. Caso, C. A. Castañeda-Orjuela, C. D. Castle, F. Catalá-López, H. Y. Chang, J. C. Chang, F. J. Charlson, H. Chen, M. Chibalabala, C. E. Chibueze, V. H. Chisumpa, A. A. Chitheer, D. J. Christopher, L. G. Ciobanu, M. Cirillo, D. Colombara, C. Cooper, P. A. Cortesi, M. H. Criqui, J. A. Crump, A. F. Dadi, K. Dalal, L. Dandona, R. Dandona, J. Das Neves, D. V. Davitoiu, B. De Courten, D. De Leo, L. Degenhardt, S. Deiparine, R. P. Dellavalle, K. Deribe, D. C. Des Jarlais, S. Dey, S. D. Dharmaratne, P. K. Dhillon, D. Dicker, E. L. Ding, S. Djalalinia, H. P. Do, E. R. Dorsey, K. P. B. Dos Santos, D. Douwes-Schultz, K. E. Doyle, T. R. Driscoll, M. Dubey, B. B. Duncan, Z. Z. El-Khatib, J. Ellerstrand, A. Enayati, A. Y. Endries, S. P. Ermakov, H. E. Erskine, B. Eshrati, S. Eskandari, A. Esteghamati, K. Estep, F. B. B. Fanuel, C. S. E. S. Farinha, A. Faro, F. Farzadfar, M. S. Fazeli, V. L. Feigin, S. M. Fereshtehnejad, J. C. Fernandes, A. J. Ferrari, T. R. Feyissa, I. Filip, F. Fischer, C. Fitzmaurice, A. D. Flaxman, L. S. Flor, N. Foigt, K. J. Foreman, R. C. Franklin, N. Fullman, T. Fürst, J. M. Furtado, N. D. Futran, E. Gakidou, M. Ganji, A. L. Garcia-Basteiro, T. Gebre, T. T. Gebrehiwot, A. Geleto, B. L. Gemechu, H. A. Gesesew, P. W. Gething, A. Ghajar, K. B. Gibney, P. S. Gill, R. F. Gillum, I. A. M. Ginawi, A. Z. Giref, M. D. Gishu, G. Giussani, W. W. Godwin, A. L. Gold, E. M. Goldberg, P. N. Gona, A. Goodridge, S. V. Gopalani, A. Goto, A. C. Goulart, M. Griswold, H. C. Gughani, R. Gupta, R. Gupta, T. Gupta, V. Gupta, N. Hafezi-Nejad, A. D. Hailu, G. B. Hailu, R. R. Hamadeh, S. Hamidi, A. J. Handal, G. J. Hankey, Y. Hao, H. L. Harb, H. A. Hareri, J. M. Haro, J. Harvey, M. S. Hassanvand, R. Havmoeller, C. Hawley, R. J. Hay, S. I. Hay, N. J. Henry, I. B. Heredia-Pi, P. Heydarpour, H. W. Hoek, H. J. Hoffman, N. Horita, H. D. Hosgood, S. Hostiuc, P. J. Hotez, D. G. Hoy, A. S. Htet, G. Hu, H. Huang, C. Huynh, K. M. Iburg, E. U. Igumbor, C. Ikeda, C. M. S. Irvine, K. H. Jacobsen, N. Jahanmehr, M. B. Jakovljevic, S. K. Jassal, M. Javanbakht, S. P. Jayaraman, P. Jeemon, P. N. Jensen, V. Jha, G. Jiang, D. John, C. O. Johnson, S. C. Johnson, J. B. Jonas, M. Jürisson, Z. Kabir, R. Kadel, A. Kahsay, R. Kamal, H. Kan, N. E. Karam, A. Karch, C. K. Karema, A. Kasaeian, G. M. Kassa, N. A. Kassaw, N. J. Kassebaum, A. Kastor, S. V. Katikireddi, A. Kaul, N. Kawakami, P. N.

Keiyoro, A. P. Kengne, A. Keren, Y. S. Khader, I. A. Khalil, E. A. Khan, Y. H. Khang, A. Khosravi, J. Khubchandani, C. Kieling, D. Kim, P. Kim, Y. J. Kim, R. W. Kimokoti, Y. Kinfu, A. Kisa, K. A. Kissimova-Skarbek, M. Kivimaki, A. K. Knudsen, Y. Kokubo, D. Kolte, J. A. Kopec, S. Kosen, P. A. Koul, A. Koyanagi, M. Kravchenko, S. Krishnaswami, K. J. Krohn, B. Kuate Defo, B. Kucuk Bicer, G. A. Kumar, P. Kumar, S. Kumar, H. H. Kyu, D. K. Lal, R. Lalloo, N. Lambert, Q. Lan, A. Larsson, P. M. Lavados, J. L. Leasher, J. T. Lee, P. H. Lee, J. Leigh, C. T. Leshargie, J. Leung, R. Leung, M. Levi, Y. Li, Y. Li, D. Li Kappe, X. Liang, M. L. Liben, S. S. Lim, S. Linn, A. Liu, P. Y. Liu, S. Liu, Y. Liu, R. Lodha, G. Logroscino, S. J. London, K. J. Looker, A. D. Lopez, S. Lorkowski, P. A. Lotufo, N. Low, R. Lozano, T. C. D. Lucas, E. R. K. Macarayan, H. Magdy Abd El Razek, M. Magdy Abd El Razek, M. Mahdavi, M. Majdan, R. Majdzadeh, A. Majeed, R. Malekzadeh, R. Malhotra, D. C. Malta, A. A. Mamun, H. Manguerra, T. Manhertz, A. Mantilla, L. G. Mantovani, C. C. Mapoma, L. B. Marczak, J. Martinez-Raga, F. R. Martins-Melo, I. Martopullo, W. März, M. R. Mathur, M. Mazidi, C. McAlinden, M. McGaughey, J. J. McGrath, M. McKee, C. McNellan, S. Mehata, M. M. Mehndiratta, T. C. Mekonnen, P. Memiah, Z. A. Memish, W. Mendoza, M. A. Mengistie, D. T. Mengistu, G. A. Mensah, A. Meretoja, T. J. Meretoja, H. B. Mezgebe, R. Micha, A. Millear, T. R. Miller, E. J. Mills, M. Mirarefin, E. M. Mirrakhimov, A. Misganaw, S. R. Mishra, P. B. Mitchell, K. A. Mohammad, A. Mohammadi, K. E. Mohammed, S. Mohammed, S. K. Mohanty, A. H. Mokdad, S. K. Mollenkopf, L. Monasta, J. M. Hernandez, M. Montico, M. Moradi-Lakeh, P. Moraga, R. Mori, C. Morozoff, S. D. Morrison, M. Moses, C. Mountjoy-Venning, K. B. Mruts, U. O. Mueller, K. Muller, M. E. Murdoch, G. V. S. Murthy, K. I. Musa, J. B. Nacheга, G. Nagel, M. Naghavi, A. Naheed, K. S. Naidoo, L. Naldi, V. Nangia, G. Natarajan, D. E. Negasa, I. Negoi, R. I. Negoi, C. R. Newton, J. W. Ngunjiri, C. T. Nguyen, G. Nguyen, M. Nguyen, Q. Le Nguyen, T. H. Nguyen, E. Nichols, D. N. A. Ningrum, S. Nolte, V. M. Nong, B. Norrving, J. J. N. Noubiap, M. J. O'Donnell, F. A. Ogbo, I. H. Oh, A. Okoro, O. Oladimeji, A. T. Olagunju, T. O. Olagunju, H. E. Olsen, B. O. Olusanya, J. O. Olusanya, K. Ong, J. N. Opio, E. Oren, A. Ortiz, A. Osgood-Zimmerman, M. Osman, M. O. Owolabi, M. Pa, R. E. Pacella, A. Pana, B. K. Panda, C. Papachristou, E. K. Park, C. D. Parry, M. Parsaeian, S. B. Patten, G. C. Patton, K. Paulson, N. Pearce, D. M. Pereira, N. Perico, K. Pesudovs, C. B. Peterson, M. Petzold, M. R. Phillips, D. M. Pigott, J. D. Pillay, C. Pinho, D. Plass, M. A. Pletcher, S. Popova, R. G. Poulton, F. Pourmalek, D. Prabhakaran, N. Prasad, N. M. Prasad, C. Purcell, M. Qorbani, R. Quansah, R. H. S. Rabiee, A. Radfar, A. Rafay, K. Rahimi, A. Rahimi-Movaghar, V. Rahimi-Movaghar, M. Rahman, M. H. U.

Rahman, R. K. Rai, S. Rajsic, U. Ram, C. L. Ranabhat, Z. Rankin, P. V. Rao, P. C. Rao, S. Rawaf, S. E. Ray, R. C. Reiner, N. Reinig, M. B. Reitsma, G. Remuzzi, A. M. N. Renzaho, S. Resnikoff, S. Rezaei, A. L. Ribeiro, L. Ronfani, G. Roshandel, G. A. Roth, A. Roy, E. Rubagotti, G. M. Ruhago, S. Saadat, N. Sadat, M. Safdarian, S. Safi, S. Safiri, R. Sagar, R. Sahathevan, J. Salama, J. A. Salomon, S. S. Salvi, A. M. Samy, J. R. Sanabria, D. Santomauro, I. S. Santos, J. V. Santos, M. M. Santric Milicevic, B. Sartorius, M. Satpathy, M. Sawhney, S. Saxena, M. I. Schmidt, I. J. C. Schneider, B. Schöttker, D. C. Schwebel, F. Schwendicke, S. Seedat, S. G. Sepanlou, E. E. Servan-Mori, T. Setegn, K. A. Shackelford, A. Shaheen, M. A. Shaikh, M. Shamsipour, S. M. Shariful Islam, J. Sharma, R. Sharma, J. She, P. Shi, C. Shields, M. Shigematsu, Y. Shinohara, R. Shiri, R. Shirkoohi, S. Shirude, K. Shishani, M. G. Shrima, A. M. Sibai, I. D. Sigfusdottir, D. A. S. Silva, J. P. Silva, D. G. A. Silveira, J. A. Singh, N. P. Singh, D. N. Sinha, E. Skiadaresi, V. Skirbekk, E. L. Slepak, A. Sligar, D. L. Smith, M. Smith, B. H. A. Sobaih, E. Sobngwi, R. J. D. Sorensen, T. C. M. Sousa, L. A. Sposato, C. T. Sreeramareddy, V. Srinivasan, J. D. Stanaway, V. Stathopoulou, N. Steel, D. J. Stein, M. B. Stein, C. Steiner, T. J. Steiner, S. Steinke, M. A. Stokes, L. J. Stovner, B. Strub, M. Subart, M. B. Sufiyan, R. Suliankatchi Abdulkader, B. F. Sunguya, P. J. Sur, S. Swaminathan, B. L. Sykes, D. O. Sylte, R. Tabarés-Seisdedos, G. R. Taffere, J. S. Takala, N. Tandon, M. Tavakkoli, N. Taveira, H. R. Taylor, A. Tehrani-Banihashemi, T. Tekelab, G. Temam Shifa, A. S. Terkawi, D. J. Tesfaye, B. Tessema, O. Thamsuwan, K. E. Thomas, A. G. Thrift, T. Y. Tiruye, R. Tobe-Gai, M. C. Tollanes, M. Tonelli, R. Topor-Madry, M. Tortajada, M. Touvier, B. X. Tran, S. Tripathi, C. Troeger, T. Truelsen, D. Tsoi, K. B. Tuem, E. M. Tuzcu, S. Tyrovolas, K. N. Ukwaja, E. A. Undurraga, C. J. Uneke, R. Updike, O. A. Uthman, B. S. C. Uzochukwu, J. F. M. Van Boven, S. Varughese, T. Vasankari, S. Venkatesh, N. Venketasubramanian, R. Vidavalur, F. S. Violante, S. K. Vladimirov, V. V. Vlassov, S. E. Vollset, F. Wadilo, T. Wakayo, Y. P. Wang, M. Weaver, S. Weichenthal, E. Weiderpass, R. G. Weintraub, A. Werdecker, R. Westerman, H. A. Whiteford, T. Wijeratne, C. S. Wiysonge, C. D. A. Wolfe, R. Woodbrook, A. D. Woolf, A. Workicho, S. Wulf Hanson, D. Xavier, G. Xu, S. Yadgir, M. Yaghoubi, B. Yakob, L. L. Yan, Y. Yano, P. Ye, H. H. Yimam, P. Yip, N. Yonemoto, S. J. Yoon, M. Yotebieng, M. Z. Younis, Z. Zaidi, M. E. S. Zaki, E. A. Zegeye, Z. M. Zenebe, X. Zhang, M. Zhou, B. Zipkin, S. Zodpey, L. J. Zuhlke, C. J. L. Murray, Global, regional, and national incidence, prevalence, and years lived with disability for 328 diseases and injuries for 195 countries, 1990-2016: A systematic analysis for the Global Burden of Disease Study 2016, *Lancet* **2017**, *390*, 1211–1259.

- 94 P. J. Barnes, Immunology of asthma and chronic obstructive pulmonary disease, *Nat. Rev. Immunol.* **2008**, *8*, 183–192.
- 95 Y. Feng, H. Mao, Specific regulator of eosinophil apoptosis: Siglec-8 - new hope for bronchial asthma treatment, *Chin. Med. J. (Engl.)*. **2012**, *125*, 2048–2052.
- 96 M. E. Rothenberg, Eosinophilic gastrointestinal disorders (EGID), *J. Allergy Clin. Immunol.* **2004**, *113*, 11–28.
- 97 A. J. Lucendo, P. López-Sánchez, Targeted Therapies for Eosinophilic Gastrointestinal Disorders, *BioDrugs* **2020**, *34*, 477–493.
- 98 P. Valent, C. Akin, M. Arock, K. Brockow, J. H. Butterfield, M. C. Carter, M. Castells, L. Escribano, K. Hartmann, P. Lieberman, B. Nedoszytko, A. Orfao, L. B. Schwartz, K. Sotlar, W. R. Sperr, M. Triggiani, R. Valenta, H.-P. Horny, D. D. Metcalfe, Definitions, Criteria and Global Classification of Mast Cell Disorders with Special Reference to Mast Cell Activation Syndromes: A Consensus Proposal, *Int. Arch. Allergy Immunol.* **2012**, *157*, 215–225.
- 99 T. C. Theoharides, P. Valent, C. Akin, Mast Cells, Mastocytosis, and Related Disorders, *N. Engl. J. Med.* **2015**, *373*, 163–172.
- 100 J. Schanin, S. Gebremeskel, W. Korver, R. Falahati, M. Butuci, T. J. Haw, P. M. Nair, G. Liu, N. G. Hansbro, P. M. Hansbro, E. Evensen, E. C. Brock, A. Xu, A. Wong, J. Leung, C. Bebbington, N. Tomasevic, B. A. Youngblood, A monoclonal antibody to Siglec-8 suppresses non-allergic airway inflammation and inhibits IgE-independent mast cell activation, *Mucosal Immunol.* **2021**, *14*, 366–376.
- 101 B. A. H. Smith, C. R. Bertozzi, The clinical impact of glycobiology: targeting selectins, Siglecs and mammalian glycans, *Nat. Rev. Drug Discov.* **2021**, *20*, 217–243.
- 102 B. A. Youngblood, J. Leung, R. Falahati, J. Williams, J. Schanin, E. C. Brock, B. Singh, A. T. Chang, J. A. O’Sullivan, R. P. Schleimer, N. Tomasevic, C. R. Bebbington, B. S. Bochner, Discovery, Function, and Therapeutic Targeting of Siglec-8, *Cells* **2020**, *10*, 19.
- 103 V. C. Damalanka, A. Reddy Maddirala, J. W. Janetka, Novel approaches to glycomimetic design: development of small molecular weight lectin antagonists, *Expert Opin. Drug Discov.* **2021**, *16*, 513–536.
- 104 P. Valverde, A. Ardá, N. C. Reichardt, J. Jiménez-Barbero, A. Gimeno, Glycans in drug discovery, *Medchemcomm* **2019**, *10*, 1678–1691.
- 105 O. Oyelaran, J. C. Gildersleeve, Glycan arrays: recent advances and future challenges, *Curr. Opin. Chem. Biol.* **2009**, *13*, 406–413.
- 106 C. M. Nycholat, S. Duan, E. Knuplez, C. Worth, M. Elich, A. Yao, J. O’Sullivan, R. McBride, Y. Wei, S. M. Fernandes, Z. Zhu, R. L. Schnaar, B. S. Bochner, J. C. Paulson, A

Sulfonamide Sialoside Analogue for Targeting Siglec-8 and-F on Immune Cells, *J. Am. Chem. Soc.* **2019**, *141*, 14032–14037.

107 R. Hevey, Strategies for the Development of Glycomimetic Drug Candidates, *Pharmaceuticals* **2019**, *12*, 55.

Identification of the lead molecule

Paper 1: A Potent Mimetic of the Siglec-8 Ligand 6'-Sulfo-Sialyl Lewis^x

This publication describes the identification of the minimal binding epitope recognized by Siglec-8, namely the two terminal carbohydrate moieties of the tetrasaccharide 6'-Sulfo-sLe^x. It was selected as starting point for the identification of a glycomimetic with improved affinity. By closer examining the NMR structure for binding interactions between Siglec-8 CRD and 6'-sulfo-sLe^x, various strategies were explored eventually leading to a glycomimetic with 20-fold improved affinity.

Contribution to the project:

Gabriele Conti synthesised compounds **3**, **29**, **32**, **34**, **35**, **37**, **38**, **39**, **44**, **45**, **46**, **47**, **48**, **49**, **50**, and supervised Maja Kokot during her synthesis of compounds **40**, **41**, **42**, **43**. He expressed and purified Siglec-8 CRD, which he used to perform microscale thermophoresis and isothermal titration calorimetry assays. Additionally, he contributed to the writing of the manuscript and designed the graphic for the front cover of the journal issue.

This paper was published in *ChemMedChem* in 2020:

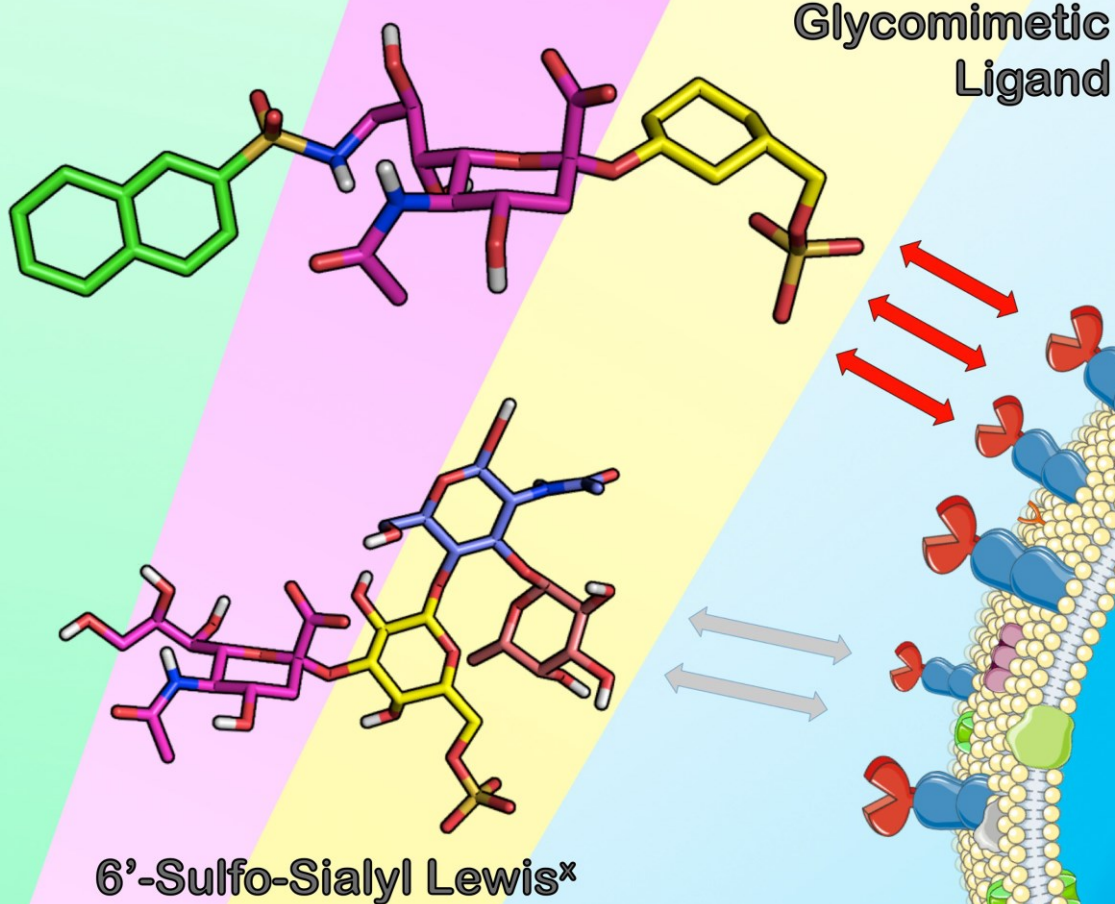
B. S. Kroezen, G. Conti, B. Girardi, J. Cramer, X. Jiang, S. Rabbani, J. Müller, M. Kokot, E. Luisoni, D. Ricklin, O. Schwardt, B. Ernst, A Potent Mimetic of the Siglec-8 Ligand 6'-Sulfo-Sialyl Lewis^x, *ChemMedChem* **2020**, *15*, 1706-1719.

© 2020 Wiley-VCH GmbH

ChemMedChem

**Chemistry
Europe**
European Chemical
Societies Publishing

Front Cover:
Beat Ernst et al.
A Potent Mimetic of the Siglec-8 Ligand 6'-Sulfo-Sialyl Lewis^x



18/2020

WILEY-VCH



A Potent Mimetic of the Siglec-8 Ligand 6'-Sulfo-Sialyl Lewis^x

Blijke S. Kroezen,^[a] Gabriele Conti,^[a] Benedetta Girardi,^[a] Jonathan Cramer,^[a] Xiaohua Jiang,^[a] Said Rabbani,^[a] Jennifer Müller,^[a] Maja Kokot,^[a] Enrico Luisoni,^[a] Daniel Ricklin,^[a] Oliver Schwardt,^[a] and Beat Ernst^{*[a]}

Siglecs are members of the immunoglobulin gene family containing sialic acid binding N-terminal domains. Among them, Siglec-8 is expressed on various cell types of the immune system such as eosinophils, mast cells and weakly on basophils. Cross-linking of Siglec-8 with monoclonal antibodies triggers apoptosis in eosinophils and inhibits degranulation of mast cells, making Siglec-8 a promising target for the treatment of eosinophil- and mast cell-associated diseases such as asthma. The tetrasaccharide 6'-sulfo-sialyl Lewis^x has been identified as a

specific Siglec-8 ligand in glycan array screening. Here, we describe an extended study enlightening the pharmacophores of 6'-sulfo-sialyl Lewis^x and the successful development of a high-affinity mimetic. Retaining the neuraminic acid core, the introduction of a carbocyclic mimetic of the Gal moiety and a sulfonamide substituent in the 9-position gave a 20-fold improved binding affinity. Finally, the residence time, which usually is the Achilles tendon of carbohydrate/lectin interactions, could be improved.

Introduction

Siglecs (sialic acid-binding immunoglobulin-type lectins) are cell surface proteins representing a subset of the I-type lectins located primarily on the surface of immune cells. They exhibit a sialic acid binding N-terminal domain, one or more C2-set immunoglobulin domains and a cytoplasmic tail.^[1–3] The cytoplasmic tail of most siglecs contains an immunoreceptor tyrosine-based inhibitory motif (ITIM), which participates in immunosuppressive cell signaling. Thus, ligand-binding induces phosphorylation of the tyrosine motif by an Src family kinase, resulting in the recruitment of the SH2 domain-containing phosphatases SH1, SH2 or SHIP-1.^[4] These phosphatases inhibit cellular processes through inactivation of essential kinases. Therefore, siglecs are inhibitory receptors, which can modulate crucial immune responses.^[5,6] In their resting state, most siglecs are engaged in *cis*-interactions with sialylated glycans expressed on the surface of the same cell.^[7] As a result, siglecs are essentially masked and can only interact with *trans*-ligands that display sufficient affinity or avidity to outcompete the *cis*-interactions.^[8]

Siglec-8 is a member of the CD33-related siglec family and is predominantly expressed on the cell-surface of eosinophils and mast cells and weakly on basophils.^[9,10] These cell types play a crucial role in the pathophysiology of asthma, a chronic

inflammatory disease characterized by a massive infiltration of eosinophils into the airways followed by degranulation of mast cells and the release of bronchoconstrictors.^[11,12] When Siglec-8 was cross-linked with antibodies, apoptosis of eosinophils^[13] and inhibition of the release of mediators from mast cells was observed.^[14] A promising alternative to target Siglec-8 with antibodies involves the multivalent display of siglec ligands on polymers and nanoparticles.^[15] Thus, it was shown that apoptosis can be initiated by treating eosinophils with a synthetic polyvalent Siglec-8 ligand^[16] and immunohistochemical analyses exhibited an up-regulation of Siglec-8 ligands in inflamed compared to healthy tissue.^[17] In addition, isolated eosinophils from the airways of allergen-challenged patients showed elevated susceptibility to Siglec-8-mediated apoptosis.^[18] Finally, variants in the Siglec-8 gene were associated with an increased susceptibility for asthma.^[19] In summary, Siglec-8 has been identified as a therapeutic target for the treatment of eosinophil and mast cell disorders.^[20–24]

Natural sialylated glycans generally exhibit only low monovalent affinities (0.5 to 3 mM), which, however, can be substantially improved by a multivalent presentation.^[25,26] The development of potent monovalent siglec ligands started from natural glycan ligands and successfully yielded high-affinity ligands for numerous siglecs: thus, high-affinity ligands for Siglec-1,^[27] Siglec-2,^[8,28–30] Siglec-4,^[31,32] Siglec-7^[33] and Siglec-8^[34] have been reported. The trisaccharide Neu5Ac α 2-3(6-O-sulfo)Gal β 1-4GlcNAc and the tetrasaccharide Neu5Ac α 2-3(6-O-sulfo)Gal β 1-4[Fuc α 1-3]GlcNAc [6'-sulfo-sLe^x (**1a**)] were identified in a glycan array screening as Siglec-8 ligands (Figure 1A).^[35–37] In this work, we describe the development of high-affinity Siglec-8 mimetics based on 6'-sulfo-sLe^x (**1a**).

[a] Dr. B. S. Kroezen, G. Conti, B. Girardi, Dr. J. Cramer, Dr. X. Jiang, Dr. S. Rabbani, J. Müller, M. Kokot, E. Luisoni, Prof. D. Ricklin, Dr. O. Schwardt, Prof. B. Ernst
Molecular Pharmacy Group
Department of Pharmaceutical Sciences
University of Basel
Klingelbergstrasse 50
4056 Basel (Switzerland)
E-mail: beat.ernst@unibas.ch

Supporting information for this article is available on the WWW under <https://doi.org/10.1002/cmdc.202000417>

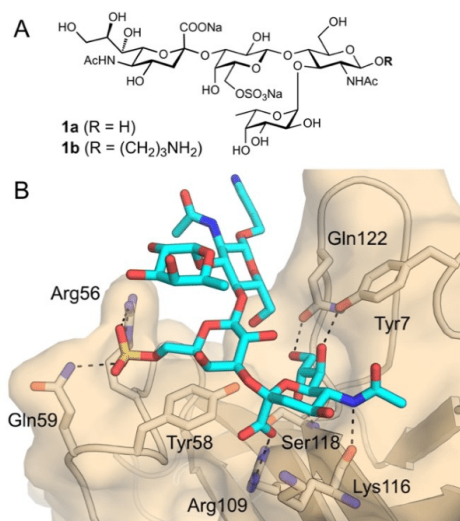


Figure 1. (A) 6'-sulfo-sLe^x (**1a**) and 3-aminopropyl 6'-sulfo-sLe^x (**1b**); (B) Binding mode of 3-aminopropyl 6'-sulfo-sLe^x (**1b**) in the carbohydrate-recognition domain (CRD) of Siglec-8 (PDB ID: 2N7B).^[38] The figure was generated using the software PyMOL.^[39] Color code: N: blue, O: red, S: yellow, protein backbone: beige, ligand C: light blue. Hydrogen bonds are depicted as dashed lines.

Results and Discussion

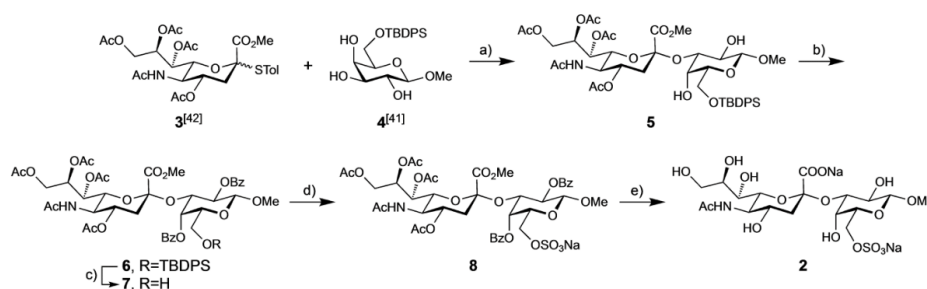
We recently published the NMR solution structures of the Siglec-8 lectin domain (PDB code: 2N7A) and its complex with 3-aminopropyl 6'-sulfo-sLe^x (**1b**) (PDB code: 2N7B).^[38] Using ¹H-¹⁵N HSQC titration and NOE experiments, both the affinity (295 μM), and the binding mode of Siglec-8 with tetrasaccharide **1b** (Figure 1B) have been determined.

Arg109, which is conserved in most siglecs,^[38] forms an essential salt bridge with the carboxylate of Neu5Ac. Moreover, the sulfate group in the 6'-position of the Gal moiety is engaged in another salt bridge with Arg56 and Gln59. This interaction proved to be crucial, as the binding affinity was drastically

reduced when the sulfate group in 3-aminopropyl 6'-sulfo-sLe^x (**1b**) was removed (28-fold loss of affinity) or moved to the D-GlcNAc moiety (9-fold loss in affinity).^[38] Essential hydrogen bonds are formed by the three hydroxyls of the glycerol side chain with Tyr7, Ser118 and Gln122, as well as by the *N*-acetyl group with the backbone of Lys116. Furthermore, various hydrophobic interactions, including *van der Waals* and sigma-π interactions with Tyr58 contribute to the binding affinity of tetrasaccharide **1b**. Surprisingly, the L-Fuc and D-GlcNAc moieties do not engage any interactions with the protein surface. Glycan arrays additionally showed that the fucose moiety does not significantly contribute to affinity.^[40] We therefore assumed that the disaccharide Neu5Acα2-3(6-*O*-sulfo)Gal (**2**, Scheme 1) represents the minimal binding epitope.

Synthesis and affinity of the minimal binding epitope. Sialylation of the galactose acceptor **4**^[41] with sialic acid donor **3**^[42] yielded disaccharide **5**. The highest yield and the best α-selectivity were obtained using NIS/TFOH as promoter, and MeCN/DCM as solvent. To avoid acetyl migration, the 2- and 4-OH of the Gal moiety were benzoylated (→**6**) before the silyl protection was selectively cleaved using HF-pyridine to afford disaccharide **7**. Next, the sulfate group was introduced using an excess of SO₃pyr in DMF (→**8**). Finally, acylate deprotection under Zemplén conditions and hydrolysis of the methyl ester with aq. NaOH yielded the test compound Neu5Acα2-3(6-*O*-sulfo)Gal (**2**, Scheme 1).

3-Aminopropyl 6'-sulfo-sLe^x (**1b**) has an affinity of 295 μM ± 26 μM (*K_D* by NMR) or 303 μM ± 11 μM (*IC*₅₀ in a competitive binding assay).^[38] Surprisingly, the *IC*₅₀ of the disaccharide Neu5Acα2-3(6-*O*-sulfo)Gal (**2**) is only by a factor 2 lower (733 μM, Table 1) than the *IC*₅₀ of lead tetrasaccharide **1b**. This result was quite encouraging, as the complexity of the epitope and the number of synthetic steps were significantly reduced, whilst the affinity was only modestly affected. For the determination of the *IC*₅₀'s, we applied a competitive binding assay^[43] with Siglec-8-CRD and streptavidin-peroxidase coupled to the biotinylated polyacrylamide glycopolymer 6'-sulfo-sLe^x-PAA as competitor. After incubation of the protein and the glycopolymer with a serial dilution of the tested ligand, the colorimetric reaction with the horseradish peroxidase substrate ABTS was measured to determine *IC*₅₀ values. We also applied



Scheme 1. a) NIS, TFOH, MeCN/DCM, -40 °C, 16 h (34%); b) Bz₂O, DMAP, pyridine, rt, 16 h (92%); c) HFpyr, pyridine, rt, 4 h (93%); d) SO₃pyr, DMF, 0 °C to rt, 4 h (93%); e) i. MeONa/MeOH, rt to 50 °C, 24 h; ii. NaOH (aq), rt, 1 h (81% over two steps).

Table 1. Binding affinity of 3-aminopropyl 6'-sulfo-sLe^x (**1b**)^[38] and derivatives thereof. IC₅₀ values were determined in a competitive binding assay.^[43] For the synthesis of monosaccharide **9** and disaccharides **11–13** with modified glycerol side chain see Supporting Information.

Compd.	Structure	IC ₅₀ [μM]	rIC ₅₀
1b ^[38]		303 ± 11	1
2		733 ± 163 ^[a]	2.2
9		n.a. ^[b]	–
10 ^[44]		n.a.	–
11		n.a.	–
12		n.a.	–
13		n.a.	–

[a] Average value over six measurements. [b] n.a.: not active up to 10 mM.

microscale thermophoresis (MST) for the determination of the K_D of binding.

The individual fragments, the galactose derivative **9** and the neuraminic acid derivative **10**,^[44] as well as the disaccharides **11–13** with modified glycerol side chains (for the synthesis see Supporting Information) did not show any affinity. The hydrogen bond network, the glycerol side chain is involved in (Figure 1B), obviously plays an important role in the binding process. Moreover, a ReliBase^[45] search shows that the 8-OH stabilizes the bioactive conformation of sialic acid in the bound conformation via an intramolecular hydrogen bond with the carboxylate. Overall, these results confirmed that the sulfated disaccharide **2** indeed represents the minimal carbohydrate epitope necessary for Siglec-8 binding.

Bioisosteres of the carboxylate and the sulfate group. To further improve the PK/PD profile of disaccharide **2**, the possibility of bioisosteric replacements of the carboxylate and the sulfate were explored, not only to improve affinity, but also to enhance selectivity and alter physical properties.^[46,47] The IC₅₀ measurements for the derivatives **14–24** (for their synthesis see Supporting Information) were conducted in the competitive binding assay (Table 2). For the reference compound **2**, an additional K_D value of 561 μM was obtained in the microscale thermophoresis (MST) assay, which is in good agreement with the competitive binding assay (733 μM) (entry 1). When the sulfate was modified while the carboxylate substituent was maintained (entries 2–8), reduced affinity was observed in four cases (entries 2, 3, 4 & 8) while all other modifications resulted

Table 2. Binding affinities for derivatives of lead structure **2**, bearing replacements for the sulfate and carboxylic acid functional groups. IC₅₀ values were determined in a competitive binding assay,^[43] while dissociation constants (K_D) were measured with MST. For the synthesis of the disaccharides **14–24** see Supporting Information.

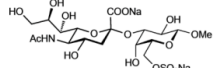
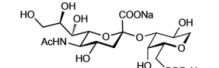
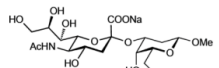
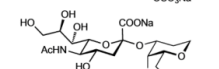
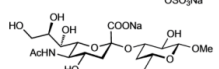
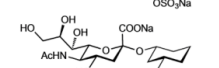
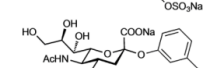
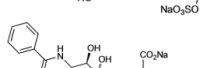
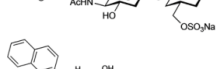
Entry	Compd.	R ¹	R ²	IC ₅₀ [μM]	K_D [μM]
Reference compound					
1	2	COONa	CH ₂ OSO ₃ Na	733 ^[a]	561
Sulfate bioisosteres					
2	14	COONa	COONa	1026	n.d. ^[b]
3	15	COONa	CH ₂ CH ₂ COONa	2199	n.d.
4	16	COONa	CH ₂ NH ₂	1393	n.d.
5	17	COONa	CH ₂ CH ₂ Ph	n.a. ^[c]	n.d.
6	18	COONa	CH ₂ N ₃	n.a.	n.d.
7	19	COONa	CH ₂ NHAc	n.a.	n.d.
8	20	COONa	CH ₂ OPO ₃ Na ₂	n.d.	2830
Carboxylic acid bioisosteres					
9	21	CONH ₂	CH ₂ OSO ₃ Na	1613	1011
10	22	CONHMe	CH ₂ OSO ₃ Na	n.d.	2850
11	23	CONHOH	CH ₂ OSO ₃ Na	n.d.	n.a.
12	24		CH ₂ OSO ₃ Na	n.d.	2836

[a] Average value over six measurements. [b] n.d.: not determined. [c] n.a.: not active up to 10 mM.

in inactive compounds. The carboxylate turned out to be the best replacement of the sulfate leading only to a moderate loss of affinity (1026 μM vs. 733 μM). Replacement of the carboxylate (entries 9–12) led to inactive or only moderately active ligands.

Modification of the galactose moiety. According to the structure of the complex of 3-aminopropyl 6'-sulfo-sLe^x (**1b**)/Siglec-8 obtained by NMR (Figure 1B) the 2- and the 4-OH of the galactose moiety do not significantly contribute to binding. In addition, the anomeric substituent points away from the protein surface and, when substituted with an OMe aglycone, cannot establish a contact with the protein surface. Therefore, a set of derivatives **25–30** where these three substituents were consecutively removed, was synthesized and evaluated regarding their binding to Siglec-8 with the competitive binding assay (Table 3). The syntheses of the test compounds **25–28** & **30** are available in the Supporting Information. For the enantioselective synthesis of disaccharide mimetic **29**, a racemic mixture of *cis* and *trans* isomers of ethyl 3-hydroxycyclohexane-1-carboxylate (**31**) turned out to be a feasible starting material (Scheme 2). The racemic *cis*-isomer **31** was obtained by chromatographic separation of the commercial *cis/trans* mixture. The enzymatic separation of the enantiomeric mixture *rac-cis*-**31** using the lipase Novozyme 435 and vinyl butyrate yielded the butyrate **32** in 35% yield.^[48,49] To determine its absolute configuration, ester **32** was hydrolyzed to acid **33**. Its optical rotation was in agreement with a literature value of the desired (1*S*,3*R*)-(+)-3-hydroxycyclohexane-1-carboxylate (**33**, $[\alpha]_D^{20} +10.3$ vs. $+10.7$ ^[50]). The synthesis of acceptor **35** was completed by reduction with DIBAL-*H* (**→34**), followed by the regioselective protection of the primary hydroxyl group with

Table 3. Biological evaluation of deoxygenated derivatives of lead structure **2**. IC₅₀ values were determined in a competitive binding assay,^[43] while dissociation constants (K_D) were measured with ITC. For the synthesis of the test compounds **25–28** & **30** with modified galactose moiety see Supporting Information.

Entry	Compd.	Structure	IC ₅₀ [μM]	K _D [μM]
1	2		733 ^[a]	574
2	25		381	n.d. ^[b]
3	26		674	n.d.
4	27		204	n.d.
5	28		271	n.d.
6	29		117	259
7	30		1246	n.d.
8	49		n.a. ^[c]	n.a.
9	50		n.d.	15

[a] Average value over six measurements. [b] n.d.: not determined. [c] n.a.: not active up to 10 mM.

TBDPSCI (\rightarrow **35**). The enantiomeric purity of the cyclohexanol derivative **35** (95% ee) was determined by conversion into the Mosher ester **36** and subsequent ¹⁹F NMR analysis (for details see Supporting Information). Then, acceptor **35** was glycosylated with donor **3** to yield the disaccharide mimic **37** in 81%. Finally, after removal of the silyl group with HF-pyr (\rightarrow **38**), the sulfate moiety was introduced using SO₃pyr in DMF to give sulfate **39**. Final deprotection with aqueous NaOH afforded the test compound **29**.

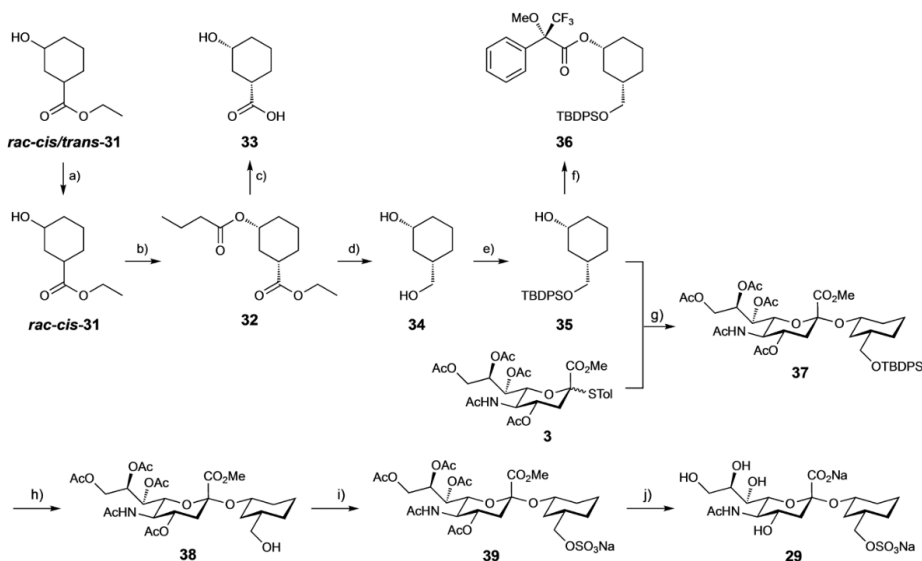
Almost the entire 2-fold affinity gain originated from deoxygenation at the anomeric center (\rightarrow **25**, Table 3, entry 2), rather than removal of the 2-OH group (\rightarrow **26**, entry 3). Noteworthy, these two modifications, i.e. removal of 1-OMe and 2-OH (\rightarrow **27**, entry 4), are positively cooperative, since the affinity for mimetic **27** (IC₅₀=204 μM) is more increased compared to the two individually deoxygenated compounds **25** (IC₅₀=381 μM) and **26** (IC₅₀=674 μM). Furthermore, deoxygenation in

the 4-position of the galactose moiety (\rightarrow **28**, entry 5) resulted in a three-fold improvement of affinity compared to the parent compound **2** (entry 1). Furthermore, with the cyclohexane derivative **29**, bearing only the CH₂OSO₃Na at the 5-position of the former galactose moiety, a further affinity enhancement could be realized, resulting in a six-fold higher potency for the cyclohexane derivative **29** (IC₅₀=117 μM) compared to disaccharide **2**. Finally, when the cyclohexane moiety of mimetic **29** was replaced by an aromatic aglycone (\rightarrow **30**, entry 7), the binding affinity was substantially reduced, probably because the directionality of the salt bridge formed by the sulfate is disturbed.

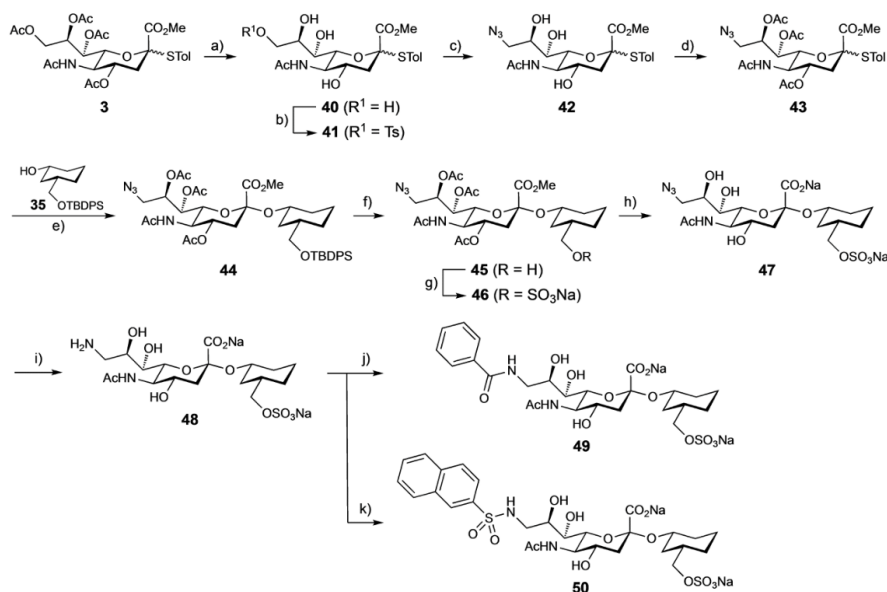
Modification of the 9-position of the Neu5Ac moiety. Amide formation in the 9-position of neuraminic acid is generally a successful approach to increase the affinity of siglec antagonists.^[8,27–33,51] Starting from the readily available Neu5Ac derivative **43** (Scheme 3) the cyclohexanol derivative **35** was sialidated to give intermediate **44**, but only in 25% yield. By desilylation (\rightarrow **45**), 6-O-sulfation (\rightarrow **46**) and hydrolysis of the ester function, azide **47** was obtained in an overall yield of 75%. After reduction of the 9'-azido group by catalytic hydrogenation (\rightarrow **48**), acylation yielded amide **49** and sulfonamide **50**. In accordance with a recent publication of Paulson *et al.*^[34] emphasizing that amide linked substituents at C-9 of the neuraminic acid moiety do not yield hits, benzamide **49** did not show any activity neither in the competitive binding assay nor in ITC experiments (Table 3, entry 8). When we, based on Paulson's findings, formed sulfonamide **50**, a Siglec-8 ligand with a K_D of 15 μM affinity was obtained (entry 9).

Thermodynamics of Siglec-8 antagonist/Siglec-8 interaction. Based on the thermodynamic fingerprints of the interaction of compounds **1b**, **2**, **29** and **50** with Siglec-8, a deeper insight into the binding process was intended. For this purpose, ITC data of the mimetics **2**, **29** and **50** were compared with the previous data for the parent tetrasaccharide 3-aminopropyl 6'-sulfo-sLe^x (**1b**).^[38] The K_D values determined by ITC (Table 4, Figure 2) correspond well with the data obtained from the competitive binding assay and by MST (Tables 1–3). Since the inventory of protonatable functional groups is constant throughout the compound series, we do not expect any superimposed effects from changes in protonation states upon binding.

The binding of 3-aminopropyl 6'-sulfo-sLe^x (**1b**) to Siglec-8 is driven by a strong binding enthalpy ($\Delta H^\circ = -32.6$ kJ mol⁻¹), which is partly offset by a large unfavorable entropic term ($-\Delta\Delta S^\circ = +12.4$ kJ mol⁻¹). Because the protein structure of apo-Siglec-8 and the complex of 6'-sulfo-sLe^x (**1b**) with Siglec-8 are identical to a large extent,^[38] a large entropy penalty resulting from induced fit can be excluded (Figure 3A & B). A potential reason for the entropy penalty could be related to a loss of conformational flexibility, especially of the Fuc and GlcNAc moiety as well as of the glycerol side chain. On the other hand, an extended network of perfect hydrogen bonds is the main reason for the large beneficial enthalpy term.^[52] For disaccharide **2** the enthalpic contribution is much less pronounced ($\Delta\Delta H^\circ_{2-1b} = 16.3$ kJ mol⁻¹), probably as a result of a slightly modified binding mode, aggravating a perfect alignment of the hydro-



Scheme 2. a) Chromatographic separation; b) vinyl butyrate, Novozyme 435, heptane, 23 °C, 2.5 h (35%); c) 2 M NaOH (aq), MeOH, 6 h (31%); d) DIBAL-*H*, THF, –15 °C, 1.5 h (94%); e) TBDPSCl, DMAP, imidazole, rt, 16 h (62%); f) (*R*)-(-)-MTPA-Cl, DMAP, DCM, 0 °C to rt; g) NIS, TfOH, MS 3 Å, DCM, MeCN, –40 °C, 6 h (81%); h) HF-pyr, pyridine, 0 °C, 5 h (88%); i) SO₃-pyr, DMF, 2 h (85%); j) NaOH (aq), overnight (83%).



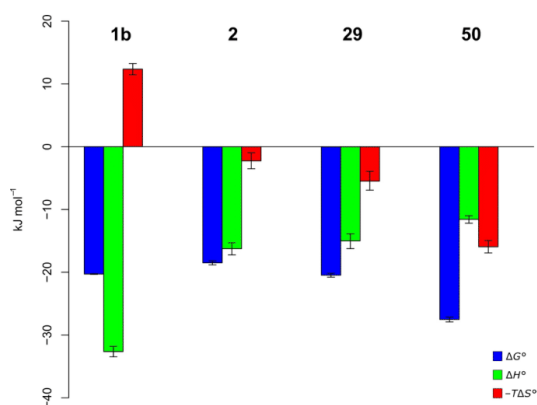
Scheme 3. a) NaOMe, MeOH, rt, 16 h (83%); b) TsCl, pyridine, 0 °C to rt, 16 h (35%); c) NaN₃, 15-crown-5, DMF, 60 °C, 16 h (96%); d) Ac₂O, pyridine, rt, 6 h (93%); e) NIS, TfOH, MS 3 Å, DCM, MeCN, –40 °C, 4 h (25%); f) HF-pyr, pyridine, 0 °C to rt, 5 h (91%); g) SO₃-pyr, DMF, 2 h (99%); h) NaOH (aq), rt, 6 h (82%); i) Pd(OH)₂/C, H₂ (1 atm), H₂O, rt, 16 h (85%); j) PhCO₂H, HATU, DIPEA, DMF, 6 h (72%); k) 2-naphthalenesulfonyl chloride, DMF/H₂O (2:1), rt, 5 h (42%).

phobic α -face of the Gal moiety and Tyr58. As a second consequence of the modified binding mode, the geometry of

the hydrogen bond interactions is slightly altered, further reducing the enthalpy term. Overall, the complex exhibits

Table 4. Thermodynamic parameters from ITC for selected Siglec-8 ligands. Error estimates for thermodynamic data correspond to the 68% confidence interval from global fitting of two independent experiments. Errors in binding kinetic data represent the standard error of a single measurement.

Compound	K_D [μM]	ΔG° [$\text{kJ}\cdot\text{mol}^{-1}$]	ΔH° [$\text{kJ}\cdot\text{mol}^{-1}$]	$-\text{T}\Delta S^\circ$ [$\text{kJ}\cdot\text{mol}^{-1}$]	k_{on} [$\text{M}^{-1}\cdot\text{s}^{-1}$]	k_{off} [s^{-1}]	Residence time τ [s]
1b ^[a]	279 (273–285)	–20.3 (–20.3––20.2)	–32.6 (–33.5––31.8)	12.4 (11.5–13.2)	N/A	N/A	N/A
2	574 (505–650)	–18.5 (–18.8––18.2)	–16.3 (–17.2––15.3)	–2.3 (–3.5––1.0)	$1.2\cdot 10^3$ ($\pm 5.1\cdot 10^2$)	$8.2\cdot 10^{-1}$ ($\pm 3.5\cdot 10^{-1}$)	1.2
29	259 (222–303)	–20.5 (–20.9––20.1)	–15.0 (–16.2––13.9)	–5.5 (–6.9––3.9)	$6.6\cdot 10^2$ ($\pm 7.5\cdot 10^1$)	$1.6\cdot 10^{-1}$ ($\pm 1.8\cdot 10^{-2}$)	6.2
50	15 (13–18)	–27.5 (–27.1––27.9)	–11.6 (–11.0––12.2)	–16.0 (–15.0––16.9)	$4.7\cdot 10^3$ ($\pm 7.1\cdot 10^2$)	$8.7\cdot 10^{-2}$ ($\pm 1.2\cdot 10^{-2}$)	11.5

[a] Data reproduced from Ref. [38] [b] N/A: Kinetic rate constants for **1b** have not been published in the cited reference.^[38]**Figure 2.** Thermodynamic signature (ΔG° , ΔH° and $-\text{T}\Delta S^\circ$) for 3-aminopropyl 6'-sulfo-sLe^x (**1b**) and the disaccharides **2**, **29** & **50**. Error estimates for thermodynamic data correspond to the 68% confidence interval from global fitting of two independent experiments.

higher flexibility, leading to a substantial improvement of the entropy term ($-\text{T}\Delta\Delta S^\circ_{2-1b} = -14.7 \text{ kJ mol}^{-1}$). Cyclohexane derivative **29** shows a slightly reduced binding enthalpy ($\Delta\Delta H^\circ_{29-2} = 1.3 \text{ kJ mol}^{-1}$) compared to disaccharide **2**, which is overcompensated by a beneficial entropy term ($-\text{T}\Delta\Delta S^\circ_{29-2} = -3.2 \text{ kJ mol}^{-1}$), resulting in a 2-fold higher binding affinity. Finally, the introduction of a benzamide in the 9-position of the Neu5Ac moiety ($\rightarrow 49$, Table 3) yielded an inactive compound in the competitive binding assay as well as in ITC experiments. This was initially surprising because in a number of other siglecs a substantial improvement of affinity could be realized by the introduction of aromatic amides.^[8,27–33,51] It is, however, in accordance with a recent publication of Paulson *et al.* emphasizing that amide linked substituents at C-9 of the Neu5Ac moiety did not yield Siglec-8 hits.^[34] Possible reasons could be the exit vector of the amide bond, causing the aromatic substituent to point into the water environment. In contrast, the exit vector of a sulfonamide substituent positions an aromatic group much closer to the protein surface. However, an inspection of the binding site in the apo-Siglec-8 structure obtained by NMR,^[38] (Figure 3A) revealed that Lys120 blocks the area for possible

aromatic contacts (Figure 3B). For docking purposes, we performed an *in silico* mutation of Lys120 to Ala and used this mutant for docking (for details see experimental part). After visual inspection of the generated docking poses, Ala120 was mutated back to Lys and minimized (Figure 3C). In the docking solution of **50**, the salt bridges of the Neu5Ac carboxylic acid to Arg105 and of the sulfate group to Arg56 and Glu59 are conserved, as are the hydrogen bonds to Tyr7 and the Lys115 backbone oxygen. The naphthyl substituent of sulfonamide **50** binds to a hydrophobic pocket generated by the displacement of Lys120. This additional hydrophobic interaction likely drives the high-affinity interaction to Siglec-8. Presumably, the angular geometry of the sulfonamide bond is required for access to this region. Whereas benzamide **49** was inactive, sulfonamide **50** proved to be the best Siglec-8 antagonist in the series with a K_D of 15 μM . Surprisingly, this became possible by a substantial improvement of the entropy term ($-\text{T}\Delta\Delta S^\circ_{50-29} = -10.5 \text{ kJ/mol}$) compared to benzamide **29**, which overcompensates a marked enthalpy penalty ($\Delta\Delta H^\circ_{50-29} = 3.4 \text{ kJ/mol}$).

The residence times $\tau = 1/k_{\text{off}}^{[53]}$ for carbohydrate/lectin interactions are regularly very short and represent one of the challenges to be addressed for therapeutic applications. We determined binding kinetic data for the interactions of the disaccharide mimetics **2**, **29**, and **50** with Siglec-8 from ITC data using the kinITC technology.^[54,55] This method analyses the equilibration time of each injection during a titration and fits this information to a kinetic model to derive rate constants. The binding kinetics of disaccharide **2** are characterized by a very short residence time of 1.2 s. For the mimetic **29**, the residence time is increased by a factor of 5, probably mainly based on the reduced polarity. The residence time of the complex with sulfonamide derivative **50** is even longer, *i.e.* 10-fold increased. Thus, structural modifications leading to improved affinities go in parallel with prolonged lifetimes of the protein–ligand complex, which is often correlated with beneficial pharmacological properties. In the association rate, the simplification of the carbohydrate core from disaccharide **2** to cyclohexane derivative **29** is associated with a reduction of the rate constant by a factor of 2. However, through the introduction of the sulfonamide substituent in mimetic **50**, an improvement of the association rate by a factor of 4 compared to disaccharide **2** was observed.

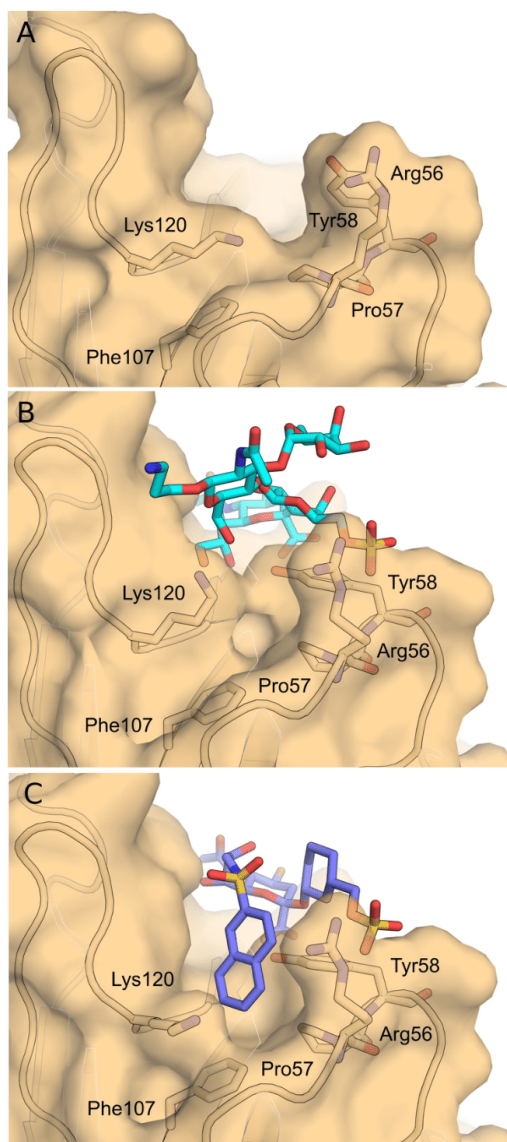


Figure 3. A) NMR structure of apo-Siglec-8 (PDB 2N7A) and B) the 3-aminopropyl 6'-sulfo-sLe^x (1b)/Siglec-8 complex (PDB 2N7B); C) Docking pose of antagonist 50/Siglec-8 (for details see experimental section).

Thus, the additional interactions of the hydrophobic naphthyl substituent influence both association and dissociation kinetics towards a higher binding affinity of sulfonamide 50. The discussion about the impact of receptor binding kinetics in early stage drug discovery is currently not fully settled. However, carbohydrates are often characterized by extremely short-lived interaction with their receptors. It, there-

fore, seems appropriate that dissociation kinetics represent an important optimization parameter when carbohydrate-based therapeutics are considered. The prolonged residence time of the high-affinity binder 50 is an indication that glycomimetic ligands have the potential to overcome one of the main drawbacks of carbohydrate ligands in the context of medicinal chemistry.

Conclusion

Siglec-8 is a CD33-related protein exclusively expressed on eosinophils, mast cells, and to some extent on basophils, cells playing a key role in the pathophysiology of asthma. However, the lack of a small molecule binding to Siglec-8 with high affinity and drug-like residence time τ limits therapeutic applications to monoclonal antibodies and polymeric displays of physiological ligands and derivatives thereof.^[15,20–24,34]

Here, in an extended study, we identified the pharmacophores of 6'-sulfo-Lewis^x (1a) and successfully developed the high-affinity mimetic 50. Its core is still neuraminic acid, however bearing a carbocyclic mimetic of the Gal moiety in the 2-position and a sulfonamide substituent in the 9-position. Compared to the lead structure 3-aminopropyl 6'-sulfo-Lewis^x (1b), the affinity could be improved 20-fold. We postulate a hypothetical binding mode that necessitates the formation of a hydrophobic pocket to accommodate the bulky aromatic substituent of sulfonamide 50. In addition, the residence time, which usually is the Achilles tendon of carbohydrate/lectin interactions could be substantially improved as well. Future activities will focus on further improvement of the pharmacokinetic profile, besides the exploration of the 4- and 5-position of the neuraminic acid core. Finally, a comparison of the best antagonists in their mono- and polyvalent presentation will give insight into possible therapeutic applications.

Experimental Section

General Methods. NMR spectra were recorded on a Bruker Avance DMX-500 (500 MHz) spectrometer. Assignment of ¹H and ¹³C NMR spectra was achieved using 2D methods (COSY, HSQC, HMBC). Chemical shifts are expressed in ppm using residual solvent signals (CHCl₃, CHD₂OD, HDO) as reference. Optical rotations were measured with a PerkinElmer polarimeter 341. Electrospray ionization mass spectrometry (ESI-MS) data were obtained on a Waters Micromass ZQ instrument. High resolution mass (HR-MS) analyses were carried out using an Agilent 1100 LC, equipped with a photodiode array detector and a Micromass QTOF I, equipped with a 4 GHz digital-time converter. Reactions were monitored by TLC using glass plates coated with silica gel 60 F254 (Merck) and visualized by using UV light and/or by charring with a molybdate solution (a 0.02 M solution of ammonium cerium sulfate dihydrate and ammonium molybdate tetrahydrate in 10% aq. H₂SO₄). Medium pressure chromatography (MPLC) separations were carried out on a CombiFlash Companion or R_f from Teledyne Isco equipped with RediSep normal phase or RP-18 reversed-phase flash columns. Size exclusion chromatography was performed on Biogel P-2 media (Bio-Rad Laboratories, Inc.). Reagents were purchased as reagent grade from Fluka, Aldrich, and Acros and used without further

purification. Solvents were purchased from Sigma-Aldrich (Buchs, Switzerland) or Acros Organics (Geel, Belgium) and were dried prior to use where indicated. MeOH was dried by reflux with sodium methoxide and distilled and stored under argon atmosphere. Dichloromethane (DCM), acetonitrile (MeCN) and toluene were dried by filtration over Al_2O_3 (Fluka, type 5016 A basic) and stored over activated molecular sieves (3 Å, 4 Å). Pyridine was distilled over KOH under argon atmosphere and stored over KOH pellets. Dry DMF was purchased from Acros Organics. Molecular sieves (3 Å, 4 Å) were activated under vacuum at 500 °C for 0.5 h immediately before use.

Methyl (methyl 5-acetamido-4,7,8,9-tetra-O-acetyl-3,5-dideoxy-D-glycero- α -D-galacto-2-nonulopyranosylonate)-(2 \rightarrow 3)-6-O-tert-butylidiphenylsilyl- β -D-galactopyranoside (5). To a suspension of **3**^[42] (3.65 g, 6.10 mmol), **4**^[41] (1.20 g, 2.77 mmol) and 3 Å molecular sieves in MeCN/DCM (5:3, 70 mL) at -40 °C, was added *N*-iodosuccinimide (2.74 g, 12.1 mmol), followed by dropwise addition of TfOH (98 μ L, 1.1 mmol). The reaction mixture was stirred at -40 °C for 16 h under argon and then was neutralized with NEt_3 . The suspension was warmed up to rt, filtered over celite and the solvents were evaporated. The residue was dissolved in DCM (60 mL), washed with 1 M $\text{Na}_2\text{S}_2\text{O}_3$ (30 mL) and H_2O (3 \times 30 mL), dried over Na_2SO_4 , filtered and evaporated. The crude product was purified by flash column chromatography (toluene/acetone, 1:0 to 1:1) to afford **5** (853 mg, 34%). $[\alpha]_{\text{D}}^{20} = -11.8$ ($c = 1.0$, CHCl_3); ^1H NMR (500 MHz, CDCl_3): $\delta = 7.79$ – 7.75 (m, 4H, Ar-H), 7.53–7.44 (m, 6H, Ar-H), 5.45 (ddd, $J = 2.7, 4.9, 9.3$ Hz, 1H, H-8'), 5.43 (dd, $J = 2.0, 9.2$ Hz, 1H, H-7'), 5.30 (d, $J = 9.8$ Hz, 1H, NH), 5.04 (ddd, $J = 4.6, 10.2, 12.2$ Hz, 1H, H-4'), 4.44 (d, $J = 7.7$ Hz, 1H, H-1), 4.36 (dd, $J = 2.8, 12.6$ Hz, 1H, H-9'a), 4.22–4.16 (m, 3H, H-3, H-6', H-9'b), 4.08 (q, $J = 10.2$ Hz, 1H, H-5'), 4.03 (dd, $J = 7.1, 10.1$ Hz, 1H, H-6a), 3.91 (dd, $J = 5.0, 10.2$ Hz, 1H, H-6b), 3.88 (d, $J = 3.6$ Hz, 1H, H-4), 3.85 (s, 3H, COOMe), 3.78 (ddd, $J = 1.1, 7.7, 9.2$ Hz, 1H, H-2), 3.68 (m, 1H, H-5), 3.63 (s, 3H, OMe), 2.89 (s, 1H, OH-4), 2.86 (dd, $J = 4.6, 12.9$ Hz, 1H, H-3'e), 2.59 (d, $J = 4.0$ Hz, 1H, OH-2), 2.24, 2.20, 2.13 (3 s, 9H, 3 OAc), 2.13 (m, 1H, H-3'a), 2.12 (s, 3H, OAc), 1.98 (s, 3H, NHAc), 1.13 ppm (s, 9H, $\text{C}(\text{CH}_3)_3$); ^{13}C NMR (126 MHz, CDCl_3): $\delta = 171.0, 170.7, 170.4, 170.2, 168.4$ (6 C, 6 C=O), 135.73, 135.67, 133.2, 133.1, 129.99, 129.95, 127.92, 127.88 (12 C, Ar-C), 104.0 (C-1), 97.4 (C-2'), 77.4 (C-3), 73.7 (C-5), 72.7 (C-6), 69.5 (C-2), 68.6 (C-4'), 68.0 (C-8'), 67.9 (C-4), 66.9 (C-7'), 62.6 (C-6), 62.4 (C-9'), 56.8 (OMe), 53.2 (COOMe), 49.8 (C-5'), 38.2 (C-3'), 26.9 (3 C, $\text{C}(\text{CH}_3)_3$), 23.3 (NHAc), 21.4, 21.0, 20.91, 20.90 (4 OAc), 19.4 ppm ($\text{C}(\text{CH}_3)_3$); MS (ESI): m/z calcd for $\text{C}_{43}\text{H}_{59}\text{NO}_{18}\text{Si}$: 928.4 $[\text{M} + \text{Na}]^+$; found: 928.4.

Methyl (methyl 5-acetamido-4,7,8,9-tetra-O-acetyl-3,5-dideoxy-D-glycero- α -D-galacto-2-nonulopyranosylonate)-(2 \rightarrow 3)-2,4-di-O-benzoyl-6-O-tert-butylidiphenylsilyl- β -D-galactopyranoside (6). To a solution of **5** (974 mg, 1.08 mmol) in pyridine (30 mL) was added DMAP (47 mg, 0.38 mmol) followed by portion-wise addition of Bz_2O (3.18 g, 14.0 mmol) at 0 °C. The mixture was warmed up to rt and stirred for 16 h. Then, the solvent was removed by co-evaporation with toluene. The residue was dissolved in EtOAc (30 mL), washed with H_2O (3 \times 10 mL), satd aq. CuSO_4 (3 \times 10 mL), H_2O (10 mL) and brine (10 mL), dried over Na_2SO_4 , filtered and evaporated. The crude product was purified by flash column chromatography (petroleum ether/acetone, 1:0 to 1:1) to afford **6** (1.10 g, 92%) as a brown vitreous solid. $[\alpha]_{\text{D}}^{20} = +61.7$ ($c = 1.00$, CHCl_3); ^1H NMR (500 MHz, CDCl_3): $\delta = 8.23$ – 8.14 (m, 2H, Ar-H), 8.13–8.02 (m, 2H, Ar-H), 7.70–7.62 (m, 6H, Ar-H), 7.62–7.52 (m, 2H, Ar-H), 7.52–7.34 (m, 4H, Ar-H), 7.29–7.24 (m, 3H, Ar-H), 7.12 (t, $J = 7.6$ Hz, 1H, Ar-H), 5.66 (ddd, $J = 2.4, 5.4, 9.5$ Hz, 1H, H-8'), 5.62 (d, $J = 3.2$ Hz, 1H, H-4), 5.36 (dd, $J = 7.9, 10.1$ Hz, 1H, H-2), 5.25 (dd, $J = 2.8, 9.7$ Hz, 1H, H-7), 5.00 (d, $J = 10.2$ Hz, 1H, NH), 4.96–4.86 (m, 2H, H-3, H-4'), 4.73 (d, $J = 7.9$ Hz, 1H, H-1), 4.36 (dd, $J = 2.3, 12.5$ Hz, 1H, H-9'a), 3.97 (s, 3H, COOMe), 4.02–3.93 (m, 2H, H-5, H-9'b), 3.81 (q, $J =$

10.4 Hz, 1H, H-5'), 3.74–3.64 (m, 2H, H-6), 3.58 (dd, $J = 2.8, 10.7$ Hz, 1H, H-6'), 3.47 (s, 3H, OMe), 2.51 (dd, $J = 4.7, 12.6$ Hz, 1H, H-3'e), 2.24, 2.10, 1.93, 1.79 (4 s, 12H, 4 OAc), 1.67 (t, $J = 12.4$ Hz, 1H, H-3'a), 1.46 (s, 3H, NHAc), 1.03 ppm (s, 9H, $\text{C}(\text{CH}_3)_3$); ^{13}C NMR (126 MHz, CDCl_3): $\delta = 170.8, 170.7, 170.6, 170.2, 170.1, 168.1, 165.5, 165.4$ (8 C=O), 135.6, 135.4, 132.91, 132.89, 130.4, 130.2, 130.0, 129.9, 129.7, 129.6, 128.3, 127.7, 127.5 (24 C, Ar-C), 102.4 (C-1), 96.9 (C-2'), 73.2 (C-5), 71.9 (C-3), 71.6 (C-6'), 71.4 (C-2), 69.6 (C-4'), 67.9 (C-4), 67.5 (C-8'), 66.4 (C-7'), 62.3 (C-9'), 60.9 (C-6), 57.1 (OMe), 53.2 (COOMe), 48.9 (C-5'), 37.3 (C-3'), 26.6 (3 C, $\text{C}(\text{CH}_3)_3$), 23.1 (NHAc), 21.5, 20.8, 20.7, 20.3 (4 OAc), 19.0 ppm ($\text{C}(\text{CH}_3)_3$); MS (ESI): m/z calcd for $\text{C}_{57}\text{H}_{67}\text{NO}_{26}\text{Si}$: 1136.4 $[\text{M} + \text{Na}]^+$; found: 1136.4.

Methyl (methyl 5-acetamido-4,7,8,9-tetra-O-acetyl-3,5-dideoxy-D-glycero- α -D-galacto-2-nonulopyranosylonate)-(2 \rightarrow 3)-2,4-di-O-benzoyl- β -D-galactopyranoside (7). To a solution of **6** (485 mg, 0.44 mmol) in pyridine (10 mL) in a Teflon container was added HF-pyr (3.0 mL) dropwise and the reaction mixture was stirred at rt for 2.5 h. The reaction was neutralized with satd aq. NaHCO_3 and the aqueous phase was extracted with DCM. The crude product was purified by flash chromatography (DCM/MeOH, 1:0 to 19:1) to afford **7** (360 mg, 93%) as a white solid. $[\alpha]_{\text{D}}^{20} = +58.2$ ($c = 0.8$, MeOH); ^1H NMR (500 MHz, CDCl_3): $\delta = 8.24$ – 8.15 (m, 2H, Ar-H), 8.14–8.04 (m, 2H, Ar-H), 7.63–7.56 (m, 2H, Ar-H), 7.50–7.47 (m, 4H, Ar-H), 5.65 (m, 1H, H-8'), 5.47 (dd, $J = 8.0, 10.1$ Hz, 1H, H-2), 5.21 (dd, $J = 2.6, 9.6$ Hz, 1H, H-7'), 5.13 (d, $J = 3.3$ Hz, 1H, H-4), 4.90 (d, $J = 10.1$ Hz, 1H, NH), 4.82–4.66 (m, 3H, H-1, H-3, H-4'), 4.33 (dd, $J = 2.4, 12.4$ Hz, 1H, H-9'a), 3.98 (dd, $J = 5.8, 12.4$ Hz, 1H, H-9'b), 3.88 (m, 1H, H-5), 3.84 (m, 1H, H-5'), 3.80 (s, 3H, COOMe), 3.76–3.70 (m, 2H, H-6a, H-6'), 3.53 (s, 3H, OMe), 3.52 (m, 1H, H-6b), 2.77 (dd, $J = 6.5, 8.4$ Hz, 1H, OH-6), 2.45 (dd, $J = 4.5, 12.7, 1H, H-3'e$), 2.24, 2.09, 1.91, 1.79 (4 s, 12H, 4 OAc), 1.72 (t, 1H, $J = 12.5$ Hz, H-3'a), 1.51 ppm (s, 3H, NHAc); ^{13}C NMR (126 MHz, CDCl_3): $\delta = 170.72, 170.70, 170.6, 170.2, 170.0, 168.3, 167.7, 165.4$ (8 C=O), 133.7, 133.0, 130.21, 130.18, 130.1, 128.8, 128.6, 128.4 (12 C, Ar-C), 102.4 (C-1), 96.8 (C-2'), 73.2 (C-5'), 72.0 (C-6'), 71.4 (C-3), 71.0 (C-2), 69.1 (2 C, C-4, C-4'), 69.1 (C-8'), 67.5 (C-7'), 62.4 (C-9'), 60.3 (C-6), 57.2 (OMe), 53.2 (COOMe), 48.8 (C-5'), 37.5 (C-3'), 23.1 (NHAc), 21.5, 20.8, 20.7, 20.3 ppm (4 OAc); MS (ESI): m/z calcd for $\text{C}_{41}\text{H}_{49}\text{NO}_{20}$: 898.3 $[\text{M} + \text{Na}]^+$; found: 898.5.

Methyl (methyl 5-acetamido-4,7,8,9-tetra-O-acetyl-3,5-dideoxy-D-glycero- α -D-galacto-2-nonulopyranosylonate)-(2 \rightarrow 3)-2,4-di-O-benzoyl-6-O-sulfonato- β -D-galactopyranoside (8). To a solution of **7** (280 mg, 0.32 mmol) in dry DMF (7 mL) was added SO_3pyr (508 mg, 3.20 mmol) at 0 °C under argon atmosphere. The reaction mixture was warmed up to rt and stirred for 2.5 h. Then, powdered NaHCO_3 was added and the suspension was stirred for 2 h. The suspension was filtered over celite, and the solvent removed by co-evaporation with xylenes. The crude product was purified by flash column chromatography (DCM/MeOH, 1:0 to 8:2) to afford **8** (290 mg, 93%) as a white solid. $[\alpha]_{\text{D}}^{20} = +48.2$ ($c = 1.1$, MeOH); ^1H NMR (500 MHz, CD_3OD): $\delta = 8.21$ – 8.15 (m, 2H, Ar-H), 8.14–8.05 (m, 2H, Ar-H), 7.65 (m, 2H, Ar-H), 7.57–7.51 (m, 4H, Ar-H), 5.66 (ddd, $J = 2.5, 5.9, 9.7$ Hz, 1H, H-8'), 5.40 (m, 1H, H-4), 5.32 (dd, $J = 7.9, 10.1$ Hz, 1H, H-2), 5.19 (dd, 1H, $J = 2.7, 9.7$ Hz, H-7'), 4.93 (dd, $J = 3.3, 10.1$ Hz, 1H, H-3), 4.85–4.79 (m, 2H, H-1, H-4'), 4.34 (dd, $J = 2.5, 12.4$ Hz, 1H, H-9'a), 4.21 (m, 1H, H-5), 4.06–4.05 (m, 2H, H-6), 3.95 (s, 3H, COOMe), 3.94 (m, 1H, H-9'b), 3.74 (dd, $J = 2.6, 10.7$ Hz, 1H, H-6'), 3.67 (m, 1H, H-5'), 3.55 (s, 3H, OMe), 2.42 (dd, $J = 4.7, 12.5$ Hz, 1H, H-3'e), 2.24, 2.05, 1.88, 1.73 (4 s, 12H, 4 OAc), 1.48 (m, 1H, H-3'a), 1.45 ppm (s, 3H, NHAc); ^{13}C NMR (126 MHz, CD_3OD): $\delta = 172.42, 172.38, 171.7, 171.4, 169.4, 167.2, 167.0$ (8 C, 8 C=O), 131.5, 131.2, 130.9, 129.8, 129.7, 124.6 (12 C, Ar-C), 103.4 (C-1), 98.3 (C-2'), 73.1 (C-5), 72.8 (2 C, C-6', C-3), 72.7 (C-2), 71.0 (C-4'), 70.5 (C-4), 68.8 (C-8'), 68.7 (C-7'), 67.3 (C-6), 63.6 (C-9'), 57.5 (OMe), 53.9 (COOMe), 49.3 (C-5'), 38.4 (C-3'), 22.7 (NHAc), 21.7, 20.6 ppm (4 C, 4 OAc); MS (ESI): m/z calcd for $\text{C}_{41}\text{H}_{48}\text{NNaO}_{23}\text{S}$: 1000.2 $[\text{M} + \text{Na}]^+$; found: 1000.3.

Methyl (sodium 5-acetamido-3,5-dideoxy-D-glycero- α -D-galacto-2-nonulopyranosylonate)-(2 \rightarrow 3)-6-O-sulfonato- β -D-galactopyranoside sodium salt (2). To a solution of **8** (70 mg, 0.07 mmol) in dry MeOH (2 mL) was added a freshly prepared solution of MeONa in MeOH (1.5 M, to pH 10). The reaction mixture was stirred for 5 h at 50 °C and then neutralized with Dowex 50X8 (H⁺ form) to pH 5. The suspension was filtered, concentrated and the crude product dissolved in 0.1 M NaOH. The reaction mixture was stirred for 1 h, then neutralized and concentrated. The crude product was purified by reversed-phase column chromatography (RP-18, H₂O) and size-exclusion column chromatography (P-2 gel, H₂O) to afford **2** (40 mg, 84%) as a white solid. $[\alpha]_D^{20} = +5.8$ ($c = 0.7$, H₂O); ¹H NMR (500 MHz, D₂O): $\delta = 4.44$ (d, $J = 8.0$ Hz, 1H, H-1), 4.22–4.20 (m, 2H, H-6), 4.13 (dd, $J = 3.2, 9.8$ Hz, 1H, H-3), 4.02 (m, 1H, H-4), 3.95 (m, 1H, H-5), 3.91–3.85 (m, 3H, H-5', H-8', H-9'a), 3.74–3.64 (m, 3H, H-4', H-6', H-9'b), 3.62 (dd, $J = 1.8, 8.9$ Hz, 1H, H-7'), 3.60 (s, 3H, OMe), 3.57 (dd, $J = 8.0, 9.8$ Hz, 1H, H-2), 2.78 (dd, $J = 4.6, 12.4$ Hz, 1H, H-3'e), 2.06 (s, 3H, NHAc), 1.83 ppm (m, 1H, H-3'a); ¹³C NMR (126 MHz, D₂O): $\delta = 175.7, 174.5$ (2 C=O), 104.1 (C-1), 100.6 (C-2'), 76.3 (C-3), 73.5 (C-6'), 73.2 (C-5), 72.4 (C-8'), 69.7 (C-2), 69.0 (C-4'), 68.8 (C-7'), 68.1 (C-4), 68.0 (C-6), 63.2 (C-9'), 57.8 (OMe), 52.3 (C-5'), 40.2 (C-3'), 22.7 ppm (NHAc); HRMS (ESI): m/z calcd for C₁₈H₂₉NNa₂O₁₇S: 632.0849 [M + Na]⁺; found: 632.0849.

Ethyl *cis*-3-hydroxycyclohexane-1-carboxylate (*rac-cis*-31). Racemic ethyl 3-hydroxycyclohexane-1-carboxylate (**31**, 4.00 g, 23.2 mmol) was separated by flash column chromatography on silica (petroleum ether/EtOAc, 7:3 to 6:4). The lower fraction was collected to yield the racemic *cis* isomers *rac-cis*-**31** (1.50 g, 38%) as a colorless oil. The diastereomeric purity was confirmed by conversion to the racemic analogue of Mosher ester **36** (for details see Supporting Information).

Ethyl (1*S*,3*R*)-3-(butyryloxy)cyclohexane-1-carboxylate (32). Racemic *rac-cis*-**31** (3.01 g, 17.5 mmol) was dissolved in heptane (18 mL). Vinyl butyrate (4.40 mL, 34.7 mmol) and lipase Novozyme 435 (61.5 mg) were added and the mixture was shaken in an incubator at 23 °C and 140 rpm for 3.5 h. The suspension was filtered over celite, washed with petroleum ether, and the solvent was removed under reduced pressure. The crude product was purified by flash column chromatography on silica (toluene/acetone, 1:0 to 6:4) to afford **32** (1.48 g, 35%) as a colorless oil. $[\alpha]_D^{20} = +44.0$ ($c = 1.00$, CHCl₃); ¹H NMR (500 MHz, CDCl₃): $\delta = 4.73$ (tt, $J = 4.3, 11.0$ Hz, 1H, H-3), 4.13 (q, $J = 7.1$ Hz, 2H, OCH₂CH₃), 2.40 (tt, $J = 3.5, 11.9$ Hz, 1H, H-1), 2.25 (t, $J = 7.3$ Hz, 2H, CH₂CH₂CH₃), 2.21 (m, 1H, H-2e), 1.99–1.85 (m, 3H, H-4e, H-5e, H-6e), 1.65 (sextet, $J = 7.4$ Hz, 2H, CH₂CH₂CH₃), 1.49 (q, $J = 12.2$ Hz, 1H, H-2a), 1.43–1.28 (m, 3H, H-4a, H-5a, H-6a), 1.25 (t, $J = 7.1$ Hz, 3H, OCH₂CH₃), 0.95 ppm (t, $J = 7.4$ Hz, 3H, CH₂CH₂CH₃); ¹³C NMR (126 MHz, CDCl₃): $\delta = 174.0, 172.5$ (2 C=O), 71.3 (C-3), 60.0 (OCH₂CH₃), 41.3 (C-1), 36.1 (CH₂CH₂CH₃), 33.7 (C-2), 30.9 (C-4), 27.7 (C-6), 22.9 (C-5), 18.2 (CH₂CH₂CH₃), 13.8 (OCH₂CH₃), 13.2 ppm (CH₂CH₂CH₃); MS (ESI): m/z calcd for C₁₃H₂₂O₄: 265.1 [M + Na]⁺; found: 265.0.

(1*S*,3*R*)-(+)-3-Hydroxycyclohexane-1-carboxylate (33). To a solution of **32** (31.1 mg, 0.128 mmol) in MeOH (0.5 mL) was added 2 M aq. NaOH (0.32 mL, 0.64 mmol) dropwise at 0 °C and the solution was stirred at 0 °C for 6 h. The reaction mixture was neutralized with HOAc and then concentrated at reduced pressure. The residue was purified by flash column chromatography on silica (DCM/MeOH, 9:1 to 4:1) to give **33** (5.7 mg, 31%) as white solid. $[\alpha]_D^{20} = +10.3$ ($c = 0.64$, MeOH), [Ref.:⁵⁰] $[\alpha]_D^{20} = +10.7$ ($c = 1.77$, MeOH); ¹H NMR (500 MHz, CD₃OD): $\delta = 3.54$ (tt, $J = 4.2, 11.0$ Hz, 1H), 2.33 (tt, $J = 3.5, 12.2$ Hz, 1H), 2.17 (dtt, $J = 2.0, 3.9, 12.1$ Hz, 1H), 1.98–1.76 (m, 3H), 1.47–1.03 ppm (m, 4H).

(1*R*,3*S*)-3-(Hydroxymethyl)cyclohexane-1-ol (34). Compound **32** (701 mg, 2.89 mmol) was dissolved in dry THF (28 mL) and cooled

to –15 °C. Then, DIBAL-*H* (1 M in toluene, 17.0 mL, 17.0 mmol) was added dropwise under argon and the mixture was stirred at –15 °C for 1.5 h. The reaction was quenched by the addition of satd aq. KNaC₄H₄O₆ (20 mL) and vigorously stirred for 30 min. The aqueous phase was extracted with Et₂O (4 × 20 mL) and the combined organic fractions were dried over Na₂SO₄, filtered and concentrated. The crude product was purified by flash column chromatography on silica (toluene/acetone, 1:0 to 1:1) to give **34** (352 mg, 94%). $[\alpha]_D^{20} = 0.0$ ($c = 0.4$, CHCl₃); ¹H NMR (500 MHz, CDCl₃): $\delta = 3.61$ (m, 1H, H-3), 3.48 (m, 2H, CH₂OH), 2.03 (m, 1H, H-2e), 1.98 (m, 1H, H-4e), 1.81 (dq, $J = 3.5, 13.5$ Hz, 1H, H-5e), 1.71 (m, 1H, H-6e), 1.62 (m, 1H, H-1), 1.30 (tq, $J = 3.5, 13.2$ Hz, 1H, H-5a), 1.18 (m, 1H, H-4a), 0.94 (q, $J = 11.5$ Hz, 1H, H-2a), 0.86 ppm (dq, $J = 3.8, 12.7$ Hz, 1H, H-6a); ¹³C NMR (126 MHz, CDCl₃): $\delta = 71.2$ (C-3), 68.3 (CH₂OH), 40.7 (C-1), 39.8 (C-2), 36.5 (C-4), 29.8 (C-6), 24.9 ppm (C-5).

(1*R*,3*S*)-3-(*tert*-Butyldiphenylsilyloxymethyl)cyclohexane-1-ol (35). To a solution of **34** (608 mg, 4.67 mmol) in dry DCM (14 mL) were consecutively added imidazole (471 mg, 6.92 mmol), DMAP (113 mg, 0.92 mmol) and TBDPSCI (1.32 mL, 5.08 mmol) and the mixture was stirred at rt under argon. After 16 h, additional TBDPSCI (0.24 mL, 0.92 mmol) was added, and after further 2 h another portion of TBDPSCI (0.24 mL, 0.92 mmol) was added. After additional 4 h, the mixture was diluted with DCM (40 mL) and washed with H₂O. The organic fraction was dried over Na₂SO₄, filtered and concentrated in vacuo. The crude product was purified by flash column chromatography on silica (DCM/MeOH, 1:0 to 95:5) to yield **35** (1.07 g, 62%). $[\alpha]_D^{20} = +1.3$ ($c = 1.0$, CHCl₃); ¹H NMR (500 MHz, CDCl₃): $\delta = 7.68$ –7.64 (m, 4H, Ar–H), 7.45–7.36 (m, 6H, Ar–H), 3.61 (m, 1H, H-3), 3.50 (dq, $J = 6.1, 9.8$ Hz, 2H, CH₂O), 2.08 (m, 1H, H-2e), 1.98 (m, 1H, H-4e), 1.80 (dq, $J = 3.4, 13.5$ Hz, 1H, H-5e), 1.70 (m, 1H, H-6e), 1.61 (m, 1H, H-1), 1.42 (d, $J = 4.4$ Hz, 1H, OH), 1.29 (tq, $J = 3.5, 13.2$ Hz, 1H, H-5a), 1.15 (m, 1H, H-4a), 1.05 (s, 9H, C(CH₃)₃), 0.98 (q, $J = 11.5$ Hz, 1H, H-2a), 0.88 ppm (dq, $J = 3.6, 12.1$ Hz, 1H, H-6a); ¹³C NMR (126 MHz, CDCl₃): $\delta = 135.6, 134.0, 129.6, 127.7, 12.7$ (12 C, Ar–C), 70.7 (C-3), 68.8 (CH₂O), 39.4 (C-1), 39.0 (C-2), 35.9 (C-4), 28.5 (C-6), 26.9 (3 C, C(CH₃)₃), 23.8 (C-5), 19.4 ppm (C(CH₃)₃); MS (ESI): m/z calcd for C₂₃H₃₂O₂Si: 391.2 [M + Na]⁺; found: 391.1.

(1*R*,3*S*)-3-(*tert*-Butyldiphenylsilyloxymethyl)cyclohexyl (*R*)-(-)- α -methoxy- α -(trifluoromethyl)phenylacetate (36). To a solution of **35** (9.5 mg, 0.026 mmol) in dry DCM (0.2 mL) were added DMAP (2.7 mg, 0.061 mmol) and (*R*)-(-)-MTPA-Cl (9.2 μ L, 0.038 mmol) at 0 °C. The reaction mixture was stirred at 0 °C for 15 min and then for 1 h at rt. The reaction mixture was diluted with Et₂O (5.0 mL), washed twice with 1 M aq. HCl, satd aq. NaHCO₃ and water, dried over Na₂SO₄, filtered, and concentrated under reduced pressure. The crude **36** was directly subjected to ¹⁹F NMR investigation without further purification. ¹⁹F NMR (470 MHz, CDCl₃): $\delta = -71.60$ ppm; Enantiomeric purity: 95% ee (for ¹⁹F NMR see Supporting Information).

(1*S*,3*R*)-3-(*tert*-Butyldiphenylsilyloxymethyl)cyclohexyl (methyl 5-acetamido-4,7,8,9-tetra-O-acetyl-3,5-dideoxy-D-glycero- α -D-galacto-2-nonulopyranosylonate) (37). A suspension of **35** (1.99 g, 5.40 mmol), **3**⁴² (6.49 g, 10.8 mmol) and MS 3 Å (11.4 g) in dry MeCN (39 mL) was cooled to –40 °C under argon. Then, *N*-iodosuccinimide (4.89 g, 21.7 mmol) was added, followed by dropwise addition of TfOH (195 μ L, 2.2 mmol). After stirring at –40 °C for 6 h, the mixture was neutralized with Et₃N, warmed to rt, filtered over celite and concentrated under reduced pressure. The residue was dissolved in DCM (40 mL) and washed with 1 M aq. Na₂S₂O₃ (2 × 30 mL) and H₂O (3 × 30 mL). The organic layer was dried over Na₂SO₄, filtered and concentrated in vacuo. The crude product was purified by flash column chromatography on silica (toluene/acetone, 3:1 to 1:3) to afford **37** (3.69 g, 81%) as a pale brown solid. $[\alpha]_D^{20} = -5.6$ ($c = 1.6$, CHCl₃); ¹H NMR (500 MHz, CDCl₃): $\delta = 7.66$ –7.62 (m, 4H, Ar–H), 7.44–7.35 (m, 6H, Ar–H), 5.38 (ddd, $J = 2.6,$

5.5, 8.2 Hz, 1H, H-8'), 5.32 (dd, $J=1.8, 8.4$ Hz, 1H, H-7'), 5.07 (d, $J=9.4$ Hz, 1H, NH), 4.82 (ddd, $J=4.6, 9.7, 12.4$ Hz, 1H, H-4'), 4.30 (dd, $J=2.6, 12.4$ Hz, 1H, H-9'a), 4.14–4.04 (m, 3H, H-5', H-6', H-9'b), 3.73 (s, 3H, OMe), 3.69 (m, 1H, H-3), 3.48 (dd, $J=5.5, 9.8$ Hz, 1H, CH₂O), 3.41 (dd, $J=6.4, 9.8$ Hz, 1H, CH₂O), 2.60 (dd, $J=4.6, 12.7$ Hz, 1H, H-3'e), 2.17, 2.14 (2 s, 6H, 2 OAc), 2.07–2.00 (m, 7H, H-4e, 2 OAc), 1.94 (t, $J=12.5$ Hz, 1H, H-3'a), 1.88 (s, 3H, NHAc), 1.82–1.73 (m, 2H, H-2e, H-5e), 1.61 (m, 2H, H-1, H-6e), 1.39 (tq, $J=2.6, 13.3$ Hz, 1H, H-5a), 1.23 (m, 1H, H-4a), 1.04 (s, 9H, C(CH₃)₃), 0.99 (m, 1H, H-2a), 0.82 ppm (dq, $J=3.2, 12.7$ Hz, 1H, H-6a); ¹³C NMR (126 MHz, CDCl₃): $\delta=171.2, 170.8, 170.4, 170.3, 170.1, 169.2$ (6 C=O), 135.7, 133.98, 133.95, 129.6, 127.7 (12 C, Ar-C), 98.8 (C-2'), 74.7 (C-3), 72.6 (C-6'), 69.4 (C-4'), 68.9 (C-8'), 68.8 (CH₂O), 67.6 (C-7'), 62.6 (C-9'), 52.6 (OMe), 49.5 (C-5'), 39.6 (C-1), 38.7 (C-3'), 36.6 (C-2), 35.2 (C-4), 28.4 (C-6), 27.0 (3 C, C(CH₃)₃), 23.7 (C-5), 23.3 (NHAc), 21.2, 20.97, 20.95, 20.88 (4 OAc), 19.4 ppm (C(CH₃)₃); MS (ESI): m/z calcd for C₄₃H₅₉NO₁₄S: 864.4 [M + Na]⁺; found: 864.2.

(15,3R)-3-(Hydroxymethyl)cyclohexyl (methyl 5-acetamido-4,7,8,9-tetra-O-acetyl-3,5-dideoxy-D-glycero- α -D-galacto-2-nonulopyranosylonate) (38). Compound **37** (201 mg, 0.239 mmol) was dissolved in pyridine (6.5 mL) in a Teflon container under argon at 0 °C. Then, HF-pyr (1.20 mL, 13.3 mmol) was added dropwise and the mixture was stirred at 0 °C for 5 h. The reaction mixture was neutralized with satd aq. NaHCO₃ and the aqueous phase was extracted with DCM (3 × 30 mL). The combined organic layers were dried over Na₂SO₄, filtered and concentrated in vacuo. The residue was purified by flash column chromatography on silica (toluene/acetone, 3:1 to 1:3) to give **38** (127 mg, 88%) as a pale brown solid. [α]_D²⁰ = -9.5 ($c=1.0$, CHCl₃); ¹H NMR (500 MHz, CDCl₃): $\delta=5.37$ (ddd, $J=2.6, 5.9, 8.4$ Hz, 1H, H-8'), 5.31 (m, 1H, H-7'), 5.12 (br d, $J=9.5$ Hz, 1H, NH), 4.83 (ddd, $J=4.6, 9.9, 12.3$ Hz, 1H, H-4'), 4.33 (dd, $J=2.5, 12.4$ Hz, 1H, H-9'a), 4.12–4.01 (m, 3H, H-5', H-6', H-9'b), 3.79 (s, 3H, OMe), 3.75 (m, 1H, H-3), 3.49 (m, 1H, CH₂O), 3.40 (m, 1H, CH₂O), 2.58 (dd, $J=4.6, 12.8$ Hz, 1H, H-3'e), 2.15, 2.14, 2.04, 2.02 (4 s, 12H, 4 OAc), 2.03 (m, 1H, H-4e), 1.95 (t, $J=12.5$ Hz, 1H, H-3'a), 1.88 (s, 3H, NHAc), 1.82–1.76 (m, 2H, H-2e, H-5e), 1.64 (br d, $J=12.4$ Hz, 1H, H-6e), 1.55 (t, $J=5.9$ Hz, 1H, H-1), 1.40 (tq, $J=3.6, 13.4$ Hz, 1H, H-5a), 1.25 (dq, $J=3.8, 12.7$ Hz, 1H, H-4a), 0.94 (q, $J=11.8$ Hz, 1H, H-2a), 0.82 ppm (dq, $J=3.8, 12.6$ Hz, 1H, H-6a); ¹³C NMR (126 MHz, CDCl₃): $\delta=171.0, 170.8, 170.3, 170.22, 170.17, 169.0$ (6 C=O), 98.5 (C-2'), 74.0 (C-3), 72.5 (C-6'), 69.2 (C-4'), 68.8 (C-8'), 68.0 (CH₂O), 67.4 (C-7'), 62.5 (C-9'), 52.7 (OMe), 49.5 (C-5'), 39.5 (C-1), 38.3 (C-3'), 36.2 (C-2), 34.8 (C-4), 28.3 (C-6), 23.5 (C-5), 23.2 (NHAc), 21.2, 20.88, 20.86, 20.8 ppm (4 OAc); MS (ESI): m/z calcd for C₂₇H₄₁NO₁₄: 626.2 [M + Na]⁺; found: 626.3.

(15,3R)-3-(Sulfonatooxymethyl)cyclohexyl (methyl 5-acetamido-4,7,8,9-tetra-O-acetyl-3,5-dideoxy-D-glycero- α -D-galacto-2-nonulopyranosylonate) sodium salt (39). To a solution of **38** (148 mg, 0.246 mmol) in dry DMF (12 mL) was added SO₃·pyr (391 mg, 2.46 mmol) under argon and the mixture was stirred at rt for 2 h. Solid NaHCO₃ was added to the solution, which was stirred vigorously for 10 min. Then, the suspension was filtered, and the solvents were removed via co-evaporation with toluene. The residue was purified by flash column chromatography on silica (DCM/MeOH, 1:0 to 7:3) to yield **39** (147 mg, 85%) as a pale white solid. [α]_D²⁰ = 0.0 ($c=1.0$, MeOH); ¹H NMR (500 MHz, CD₃OD): $\delta=5.39$ (ddd, $J=2.6, 5.4, 8.3$ Hz, 1H, H-8'), 5.32 (dd, $J=2.2, 9.1$ Hz, H-7'), 4.77 (ddd, $J=4.5, 10.5, 12.1$ Hz, 1H, H-4'), 4.30 (dd, $J=2.5, 12.4$ Hz, 1H, H-9'a), 4.12 (dd, $J=2.1, 10.8$ Hz, 1H, H-6'), 4.04 (dd, $J=5.5, 12.4$ Hz, 1H, H-9'b), 3.94 (t, $J=10.5$ Hz, 1H, H-5'), 3.86–3.71 (m, 3H, H-3, CH₂O), 3.82 (s, 3H, OMe), 2.62 (dd, $J=4.6, 12.6$ Hz, 1H, H-3'e), 2.15, 2.11 (2 s, 6H, 2 OAc), 2.03 (m, 1H, H-4e), 2.00, 1.97 (2 s, 6H, 2 OAc), 1.83 (s, 3H, NHAc), 1.75 (m, 3H, H-3'a, H-5e, H-2e), 1.67 (m, 2H, H-1, H-6e), 1.46 (qt, $J=3.0, 13.0$ Hz, 1H, H-5a), 1.20 (m, 1H, H-4a), 1.02–0.81 ppm (m, 2H, H-2a, H-6a); ¹³C NMR (126 MHz, CD₃OD): $\delta=173.5,$

172.4, 171.8, 171.64, 171.58, 170.1 (6 C=O), 99.9 (C-2'), 75.9 (C-3), 73.5 (CH₂O), 73.1 (C-6'), 70.8 (C-4'), 69.4 (C-8'), 68.7 (C-7'), 63.5 (C-9'), 53.2 (OMe), 50.1 (C-5'), 39.6 (C-3'), 38.0 (C-1), 37.4 (C-2), 36.1 (C-4), 29.4 (C-6), 24.5 (C-5), 22.7 (NHAc), 21.3, 20.8, 20.70, 20.65 ppm (4 OAc); MS (ESI): m/z calcd for C₂₇H₄₀NNaO₁₇S: 682.2 [M-Na]⁺; found: 682.3.

(15,3R)-3-(Sulfonatooxymethyl)cyclohexyl (sodium 5-acetamido-3,5-dideoxy-D-glycero- α -D-galacto-2-nonulopyranosylonate) sodium salt (29). Compound **39** (416 mg, 0.590 mmol) was dissolved in 0.1 M NaOH (19 mL) and the mixture was stirred at rt overnight. The solution was neutralized with 1 M HCl and concentrated in vacuo. The residue was purified by size-exclusion chromatography (P-2 gel, H₂O) to afford **29** (266 mg, 83%) as a white solid. [α]_D²⁰ = +18.3 ($c=0.2$, H₂O); ¹H NMR (500 MHz, D₂O): $\delta=3.96$ –3.78 (m, 6H, H-3, H-5', H-7', H-9'a, CH₂O), 3.71–3.59 (m, 4H, H-4', H-6', H-8', H-9'b), 2.77 (dd, $J=4.7, 12.4$ Hz, 1H, H-3'e), 2.07 (m, 1H, H-4e), 2.05 (s, 3H, NHAc), 1.92 (m, 1H, H-2e), 1.85–1.72 (m, 2H, H-1, H-5e), 1.70 (m, 1H, H-6e), 1.65 (t, $J=12.1$ Hz, 1H, H-3'a), 1.39–1.19 (m, 2H, H-4a, H-5a), 1.05 (q, $J=11.9$ Hz, 1H, H-2a), 0.92 ppm (dq, $J=3.7, 12.6$ Hz, 1H, H-6a); ¹³C NMR (126 MHz, D₂O): $\delta=176.0, 174.8$ (2 C=O), 102.0 (C-2'), 75.8 (C-3), 74.5 (CH₂O), 73.7, 73.0, 69.3 (C-4', C-6', C-7'), 69.0 (C-8'), 63.4 (C-9'), 52.8 (C-5'), 42.1 (C-3'), 37.1 (C-1), 36.6 (C-2), 35.2 (C-4), 28.5 (C-6), 24.2 (C-5), 23.0 ppm (NHAc); HRMS (ESI): m/z calcd for C₁₈H₂₉NNaO₁₃S: 568.1053 [M + Na]⁺; found: 568.1048.

p-Tolyl (methyl 5-acetamido-2,3,5-trideoxy-2-thio-D-glycero- β -D-galacto-2-nonulopyranosylonate) (40). To a solution of **3**^[42] (2.00 g, 3.35 mmol) in dry MeOH (60 mL) was added NaOMe (25% w/v, 70 μ L, 0.33 mmol) under argon and the solution was stirred at rt for 16 h. The mixture was neutralized with Amberlyst-15 and filtered over a pad of celite. The celite was washed with MeOH and the solvent was evaporated. The crude product was purified by flash column chromatography on silica (DCM/MeOH, 1:0 to 85:15) to give **40** (1.20 g, 83%) as an orange oil. [α]_D²⁰ = -27.7 ($c=0.13$, MeOH); ¹H NMR (500 MHz, CD₃OD): $\delta=7.46$ (d, $J=8.1$ Hz, 2H, Ar-H), 7.17 (d, $J=8.0$ Hz, 2H, Ar-H), 4.50 (dd, $J=0.8, 10.5$ Hz, 1H, H-6), 4.10 (m, 1H, H-4), 3.89 (t, $J=10.3$ Hz, 1H, H-5), 3.82 (m, 1H, H-9a), 3.78 (m, 1H, H-8), 3.66 (m, 1H, H-9b), 3.55 (m, 1H, H-7), 3.52 (s, 3H, OMe), 2.67 (dd, $J=4.7, 13.6$ Hz, 1H, H-3e), 2.33 (s, 3H, CH₃), 2.03 (s, 3H, NHAc), 1.94 ppm (dd, $J=11.7, 13.6$ Hz, 1H, H-3a); ¹³C NMR (126 MHz, CD₃OD): $\delta=173.5, 171.4$ (2 C=O), 141.1, 137.4, 130.7, 127.8 (6 C, Ar-C), 94.5 (C-2), 73.3 (C-6), 71.2 (C-8), 70.6 (C-7), 68.1 (C-4), 65.1 (C-9), 54.0 (C-5), 53.0 (OMe), 42.1 (C-3), 22.8 (NHAc), 21.4 ppm (CH₃); MS (ESI): m/z calcd for C₁₉H₂₇NO₈S: 452.2 [M + Na]⁺; found: 452.2.

p-Tolyl (methyl 5-acetamido-2,3,5-trideoxy-2-thio-9-O-tosyl-D-glycero- β -D-galacto-2-nonulopyranosylonate) (41). To a solution of **40** (1.90 g, 4.42 mmol) in dry pyridine was added tosyl chloride (1.01 g, 5.31 mmol) at 0 °C under argon. The reaction mixture was stirred at rt for 16 h. Then, MeOH was added and the mixture was stirred for 30 min. The solvents were evaporated under reduced pressure and the crude product was purified by flash column chromatography on silica (DCM/MeOH, 1:0 to 9:1) to give **41** (0.904 g, 35%). [α]_D²⁰ = -6.4 ($c=0.08$, CHCl₃); ¹H NMR (500 MHz, CDCl₃): $\delta=7.77$ (d, $J=8.3$ Hz, 2H, Ar-H), 7.34–7.31 (m, 4H, Ar-H), 7.11 (d, $J=8.0$ Hz, 2H, Ar-H), 4.62 (d, $J=7.1$ Hz, 1H, NH), 4.33–4.28 (m, 2H, H-6, H-9a), 4.14 (m, 1H, H-4), 4.09 (m, 1H, H-9b), 3.95 (m, 1H, H-8), 3.85 (m, 1H, H-5), 3.55 (m, 1H, H-7), 3.50 (s, 3H, OMe), 2.72 (dd, $J=4.6, 13.8$ Hz, 1H, H-3e), 2.34, 2.33 (2 s, 6H, 2 CH₃), 2.07 (s, 3H, NHAc), 1.98 ppm (m, 1H, H-3a); ¹³C NMR (126 MHz, CDCl₃): $\delta=173.6, 168.9$ (2 C=O), 145.2, 140.2, 135.7, 132.6, 130.1, 130.0, 128.2, 126.1 (12 C, Ar-C), 89.6 (C-2), 72.7 (C-9), 72.4 (C-6), 69.1 (C-7), 68.7 (C-8), 67.8 (C-4), 53.7 (C-5), 52.7 (OMe), 41.1 (C-3), 23.4 (NHAc), 21.8, 21.4 ppm (2 CH₃); MS (ESI): m/z calcd for C₂₆H₃₃NO₁₂S₂: 606.2 [M + Na]⁺; found: 606.0.

p-Tolyl (methyl 5-acetamido-9-azido-2,3,5,9-tetraoxy-2-thio-D-glycero-β-D-galacto-2-nonulopyranosylonate) (42). To a solution of 41 (570 mg, 0.98 mmol) in dry DMF (15 mL) were added Na₂S₂O₈ (313 mg, 4.82 mmol) and 15-crown-5 (0.1 mL, 0.49 mmol). The reaction mixture was stirred under argon at 60 °C for 16 h. The suspension was filtered through a pad of celite and the celite was washed with MeOH. The solvents were removed by co-evaporation with *n*-heptane and the crude product was purified by flash column chromatography on silica (DCM/MeOH, 1:0 to 9:1) to afford 42 (422 mg, 96%) as a white solid. [α]_D²⁰ = -141 (*c* = 0.33, MeOH); ¹H NMR (500 MHz, CD₃OD): δ = 7.42 (d, *J* = 8.1 Hz, 2H, Ar-H), 7.18 (d, *J* = 7.9 Hz, 2H, Ar-H), 4.44 (d, *J* = 10.5, 1H, H-6), 4.11 (m, 1H, H-4), 3.91–3.84 (m, 2H, H-5, H-8), 3.61–3.56 (m, 2H, H-7, H-9a), 3.54 (s, 3H, OMe), 3.41 (m, 1H, H-9b), 2.66 (dd, *J* = 4.7, 13.6 Hz, 1H, H-3e), 2.34 (s, 3H, CH₃), 2.04 (s, 3H, NHAc), 1.93 ppm (dd, *J* = 11.6, 13.7 Hz, 1H, H-3a); ¹³C NMR (126 MHz, CD₃OD): δ = 174.8, 170.8 (2 C=O), 141.2, 137.4, 130.8, 127.7 (6 C, Ar-C), 91.3 (C-2), 73.3 (C-6), 71.3 (C-7), 70.6 (C-8), 68.0 (C-4), 55.7 (C-9), 54.1 (C-5), 53.0 (OMe), 42.0 (C-3), 22.8 (NHAc), 21.3 ppm (CH₃); MS (ESI): *m/z* calcd for C₁₉H₂₆N₄O₅S: 477.2 [M + Na]⁺; found: 477.2.

p-Tolyl (methyl 5-acetamido-4,7,8-tri-O-acetyl-9-azido-2,3,5,9-tetraoxy-2-thio-D-glycero-β-D-galacto-2-nonulopyranosylonate) (43). A solution of 42 (330 mg, 0.73 mmol) in dry pyridine (3.2 mL) was cooled to 0 °C. Then, DMAP (15.4 mg, 0.13 mmol) and Ac₂O (1.6 mL, 16.7 mmol) were added. The reaction mixture was stirred at rt for 6 h under argon. The volatiles were co-evaporated with toluene and the crude product was purified by flash column chromatography on silica (DCM/MeOH, 1:0 to 96:4) to yield 43 (392 mg, 93%) as a white solid. [α]_D²⁰ = -89.4 (*c* = 0.23, CHCl₃); ¹H NMR (500 MHz, CDCl₃): δ = 7.30 (d, *J* = 8.1 Hz, 2H, Ar-H), 7.19 (d, *J* = 7.9 Hz, 2H, Ar-H), 5.49 (d, *J* = 10.2 Hz, 1H, NH), 5.43 (m, 1H, H-7), 5.37 (m, 1H, H-4), 4.76 (m, 1H, H-8), 4.58 (dd, *J* = 2.4, 10.5 Hz, 1H, H-6), 4.12 (m, 1H, H-5), 3.68 (s, 3H, OMe), 3.63 (dd, *J* = 2.4, 13.4 Hz, 1H, H-9a), 3.31 (dd, *J* = 9.4, 13.4 Hz, 1H, H-9b), 2.67 (dd, *J* = 4.8, 13.8 Hz, 1H, H-3e), 2.35 (s, 3H, CH₃), 2.15–2.10 (m, 4H, H-3a, OAc), 2.09, 2.04 (2 s, 6H, 2 OAc), 1.90 ppm (s, 3H, NHAc); ¹³C NMR (126 MHz, CDCl₃): δ = 171.5, 171.3, 170.7, 170.6, 168.6 (5 C=O), 141.2, 136.3, 130.5, 124.8 (6 C, Ar-C), 88.8 (C-2), 74.9 (C-8), 73.3 (C-6), 69.2 (C-4), 69.1 (C-7), 53.1 (OMe), 50.0 (C-9), 49.6 (C-5), 37.5 (H-3), 23.5 (NHAc), 21.6 (CH₃), 21.4, 21.2, 21.1 ppm (3 OAc); MS (ESI): *m/z* calcd for C₂₅H₃₂N₄O₁₀S: 603.2 [M + Na]⁺; found: 603.0.

(1S,3R)-3-(tert-Butyldiphenylsilyloxymethyl)cyclohexyl (methyl 5-acetamido-4,7,8-tri-O-acetyl-9-azido-3,5,9-trideoxy-D-glycero-α-D-galacto-2-nonulopyranosylonate) (44). A suspension of 43 (340 mg, 0.57 mmol), 35 (320 mg, 0.88 mmol) and MS 3 Å (620 mg) in dry MeCN (6 mL) was cooled to -40 °C under argon. Then, *N*-iodosuccinimide (1.53 g, 6.79 mmol) was added, followed by dropwise addition of TfOH (60 μL, 0.68 mmol). After stirring at -40 °C for 4 h, the mixture was neutralized with Et₃N, warmed to rt, filtered over celite and concentrated under reduced pressure. The residue was dissolved in DCM (20 mL) and washed with 1 M Na₂S₂O₃ (4 × 10 mL) and H₂O (2 × 10 mL). The organic layer was dried over Na₂SO₄, filtered and concentrated in vacuo. The crude product was purified by flash column chromatography on silica (toluene/acetone, 1:0 to 6:4) to afford 44 (110 mg, 25%). [α]_D²⁰ = -1.2 (*c* = 0.29, CHCl₃); ¹H NMR (500 MHz, CDCl₃): δ = 7.66–7.60 (m, 4H, Ar-H), 7.42–7.35 (m, 6H, Ar-H), 5.33–5.26 (m, 2H, H-6', H-8'), 5.21 (d, *J* = 10.1 Hz, 1H, NH), 4.81 (m, 1H, H-4'), 4.11 (m, 1H, H-5'), 4.01 (m, 1H, H-7'), 3.75 (s, 3H, OMe), 3.71 (m, 1H, H-3), 3.61 (dd, *J* = 2.9, 13.5 Hz, 1H, H-9'a), 3.45–3.39 (m, 2H, OCH₂), 3.28 (dd, *J* = 6.4, 13.5 Hz, 1H, H-9'b), 2.62 (dd, *J* = 4.6, 12.7 Hz, 1H, H-3'e), 2.18, 2.16, 2.02 (3 OAc), 2.00 (m, 1H, H-4e), 1.93 (t, *J* = 12.5 Hz, 1H, H-3'a), 1.87 (s, 3H, NHAc), 1.81–1.74 (m, 2H, H-2e, H-5e), 1.62–1.56 (m, 2H, H-1, H-6e), 1.40 (m, 1H, H-5a), 1.25 (m, 1H, H-4a), 1.04 (s, 9H, C(CH₃)₃), 0.99 (m, 1H, H-2a), 0.82 ppm (m, 1H, H-6a); ¹³C NMR (126 MHz, CDCl₃): δ = 171.5,

170.67, 170.66, 170.5 (5 C, 5 C=O), 135.8, 134.0, 129.8, 127.9 (12 C, Ar-C), 98.9 (C-2'), 74.7 (C-3'), 73.1 (C-7'), 70.5 (C-6'), 69.3 (C-4'), 68.8 (CH₂O), 68.3 (C-8'), 53.0 (OMe), 51.0 (C-9'), 49.5 (C-5'), 39.7 (C-1), 38.7 (C-3'), 36.7 (C-2), 35.4 (C-4), 28.5 (C-6), 27.1 (3 C, C(CH₃)₃), 23.5 (C-5), 23.5 (NHAc), 21.4, 21.24, 21.22 (3 OAc), 19.6 ppm (C(CH₃)₃); MS (ESI): *m/z* calcd for C₄₁H₅₆N₄O₁₂Si: 847.4 [M + Na]⁺; found: 847.2.

(1S,3R)-3-(Hydroxymethyl)cyclohexyl (methyl 5-acetamido-4,7,8-tri-O-acetyl-9-azido-3,5,9-trideoxy-D-glycero-α-D-galacto-2-nonulopyranosylonate) (45). To a solution of 44 (110 mg, 0.13 mmol) in dry pyridine (3.8 mL) was added HF-pyr (0.75 mL) dropwise at 0 °C under argon and the reaction mixture was stirred at rt for 5 h. The reaction mixture was neutralized with satd aq. NaHCO₃. The aqueous phase was extracted with DCM (3 × 20 mL), and the combined organic layers were dried over Na₂SO₄, filtered and evaporated. The crude product was purified by flash column chromatography on silica (toluene/acetone, 1:0 to 1:1) to afford 45 (71.4 mg, 91%). [α]_D²⁰ = -35.6 (*c* = 0.73, CHCl₃); ¹H NMR (500 MHz, CDCl₃): δ = 5.32–5.26 (m, 2H, H-6', H-8'), 5.12 (d, *J* = 10.0 Hz, 1H, NH), 4.82 (m, 1H, H-4'), 4.09 (m, 1H, H-5'), 4.02 (m, 1H, H-7'), 3.81 (s, 3H, OMe), 3.75 (m, 1H, H-3), 3.58 (dd, *J* = 2.9, 13.5 Hz, 1H, H-9'a), 3.51–3.38 (m, 2H, CH₂O), 3.28 (m, 1H, H-9'b), 2.60 (dd, *J* = 4.6, 12.7 Hz, 1H, H-3'b), 2.18, 2.17 (2 s, 6H, 2 OAc), 2.03–2.01 (m, 4H, H-4, OAc), 1.94 (t, *J* = 12.6 Hz, 1H, H-3'a), 1.88 (s, 3H, NHAc), 1.80 (m, 1H, H-5e), 1.75 (m, 1H, H-2e), 1.66 (m, 1H, H-6e), 1.42 (m, 1H, H-1), 1.37 (m, 1H, H-5a), 1.29 (m, 1H, H-4a), 0.95 (m, 1H, H-2a), 0.88 ppm (m, 1H, H-6a); ¹³C NMR (126 MHz, CDCl₃): δ = 170.8, 170.52, 170.51, 170.46, 170.3 (5 C=O), 98.5 (C-2'), 74.1 (C-3'), 72.9 (C-7'), 70.1 (C-6'), 69.1 (C-4'), 68.0 (CH₂O), 67.9 (C-8'), 52.9 (OMe), 50.9 (C-9'), 49.4 (C-5'), 39.5 (C-1), 38.5 (C-3'), 36.1 (C-2), 34.9 (C-4), 28.3 (C-6), 23.6 (C-5), 23.4 (NHAc), 21.3, 21.2, 21.1 ppm (3 OAc); MS (ESI): *m/z* calcd for C₂₅H₃₈N₄O₁₂: 609.3 [M + Na]⁺; found: 609.0.

(1S,3R)-3-(Sulfonatooxymethyl)cyclohexyl (methyl 5-acetamido-4,7,8-tri-O-acetyl-9-azido-3,5,9-trideoxy-D-glycero-α-D-galacto-2-nonulopyranosylonate) sodium salt (46). To a solution of 45 (65.0 mg, 0.11 mmol) in dry DMF (7 mL) was added SO₃pyr (176 mg, 1.11 mmol) and the reaction mixture was stirred under argon for 2 h at rt. Then, the reaction was quenched by the addition of solid NaHCO₃ and stirred vigorously for 10 min. The suspension was filtered, and the filtrate was co-evaporated with toluene. The crude product was purified by flash column chromatography on silica (DCM/MeOH, 1:0 to 4:1) to give 46 (75.6 mg, 99%). [α]_D²⁰ = +10.3 (*c* = 0.47, MeOH); ¹H NMR (500 MHz, CD₃OD): δ = 5.19 (s, 2H, H-7', H-8'), 4.64 (m, 1H, H-4'), 3.98 (d, *J* = 10.8 Hz, 1H, H-6'), 3.80 (t, *J* = 10.5 Hz, 1H, H-5'), 3.70 (s, 3H, OMe), 3.70–3.60 (m, 3H, H-3, CH₂O), 3.47 (d, *J* = 13.3 Hz, 1H, H-9'a), 3.14 (m, 1H, H-9'b), 2.50 (dd, *J* = 4.4, 12.6 Hz, 1H, H-3'e), 2.05, 1.99 (2 s, 6H, 2 OAc), 1.88 (m, 1H, H-4e), 1.85 (s, 3H, OAc), 1.70 (s, 3H, NHAc), 1.64–1.59 (m, 3H, H-2e, H-5e, H-3'a), 1.56–1.51 (m, 2H, H-1, H-6e), 1.37 (m, 1H, H-5a), 1.08 (m, 1H, H-4a), 0.83 (m, 1H, H-2a), 0.75 ppm (m, 1H, H-6a); ¹³C NMR (126 MHz, CD₃OD): δ = 173.6, 171.7, 171.5, 170.1 (5 C, 5 C=O), 99.9 (C-2'), 74.9 (C-3'), 73.5 (C-6'), 73.3 (CH₂O), 70.7 (C-4'), 70.5 (C-7'), 69.3 (C-8'), 53.3 (OMe), 52.0 (C-9'), 50.0 (C-5'), 39.5 (C-3'), 38.0 (C-1), 37.4 (C-2), 36.1 (C-4), 29.4 (C-6), 24.5 (C-5), 22.7 (NHAc), 21.3, 21.0, 20.8 ppm (3 OAc); MS (ESI): *m/z* calcd for C₂₅H₃₇N₄NaO₁₅S: 711.2 [M + Na]⁺; found: 711.1.

(1S,3R)-3-(Sulfonatooxymethyl)cyclohexyl (sodium 5-acetamido-9-azido-3,5,9-trideoxy-D-glycero-α-D-galacto-2-nonulopyranosylonate) sodium salt (47). Compound 46 (79.2 mg, 0.12 mmol) was treated with 0.1 M NaOH (11.5 mL, 1.15 mmol) at rt for 6 h. Then, the reaction mixture was neutralized with Amberlyst-15 (to pH 7), the suspension was filtered, and the solvent was evaporated. The crude product was purified by flash column chromatography on silica (DCM/MeOH, 1:0 to 1:1) and size-exclusion chromatography (P-2 gel, H₂O) to afford 47 (54.1 mg, 82%) as a white solid. [α]_D²⁰ = +25.4 (*c* = 1.00, H₂O); ¹H NMR (500 MHz, D₂O): δ = 3.97–3.79 (m, 4H,

H-3, CH₂O, H-8'), 3.75–3.58 (m, 4H, H-4', H-5', H-6', H-9'a), 3.54 (m, 1H, H-7'), 3.45 (m, 1H, H-9'b), 2.73 (m, 1H, H-3'e), 2.10–1.96 (m, 4H, H-4, NHAc), 1.89 (m, 1H, H-2e), 1.83–1.69 (m, 2H, H-1, H-5e), 1.69–1.54 (m, 2H, H-6, H-3'a), 1.36–1.14 (m, 2H, H-4a, H-5a), 1.02 (m, 1H, H-2a), 0.89 ppm (m, 1H, H-6a); ¹³C NMR (126 MHz, D₂O): δ = 176.1, 174.7 (2 C=O), 102.2 (C-2'), 75.9 (C-3), 74.5 (CH₂O), 73.7 (C-4'), 71.8 (C-8'), 70.0 (C-7'), 69.5 (C-6'), 54.1 (C-9'), 53.0 (C-5'), 42.4 (C-3'), 37.4 (C-1), 36.8 (C-2), 35.5 (C-4), 28.8 (C-6), 24.4 (C-5), 23.1 ppm (NHAc); MS (ESI): *m/z* calcd for C₁₈H₂₈N₄Na₂O₁₂S: 593.1 [M+Na]⁺; found: 593.2.

(15,3R)-3-(Sulfonatoxyethyl)cyclohexyl (sodium 5-acetamido-9-amino-3,5,9-trideoxy-D-glycero-α-D-galacto-2-nonulopyranosylonate) sodium salt (48). To a solution of **47** (38.3 mg, 0.07 mmol) in water (1.7 mL) was added Pd(OH)₂/C (10% Pd, 20.8 mg). The reaction mixture was hydrogenated at rt for 16 h (1 atm H₂). Then, the suspension was filtered over a pad of celite and the celite was washed with water. The solvent was evaporated, and the crude product was purified by size-exclusion chromatography (P-2 gel, H₂O) to afford **48** (31.1 mg, 85%) as a white solid. [α]_D²⁰ = +13.4 (c = 0.50, H₂O); ¹H NMR (500 MHz, D₂O): δ = 3.86 (m, 1H, H-8'), 3.76–3.66 (m, 3H, H-3, CH₂O), 3.61 (m, 1H, H-5'), 3.53–3.41 (m, 2H, H-4', H-6'), 3.36 (m, 1H, H-7'), 3.22 (m, 1H, H-9'a), 2.81 (m, 1H, H-9'b), 2.57 (dd, *J* = 4.5, 12.4 Hz, 1H, H-3'e), 1.89–1.82 (m, 4H, H-4e, NHAc), 1.75 (m, 1H, H-2e), 1.66–1.54 (m, 2H, H-1, H-5e), 1.53–1.44 (m, 2H, H-6e, H-3'a), 1.18–1.01 (m, 2H, H-4a, H-5a), 0.85 (m, 1H, H-2a), 0.73 ppm (m, 1H, H-6a); ¹³C NMR (126 MHz, D₂O): δ = 176.1, 174.9 (2 C=O), 102.0 (C-2'), 75.6 (C-3), 74.5 (CH₂O), 73.4 (C-4'), 71.1 (C-7'), 69.2 (2 C, C-6', C-8'), 52.7 (C-5'), 43.1 (C-9'), 41.8 (C-3'), 37.2 (C-1), 36.7 (C-2), 35.2 (C-4), 29.5 (C-6), 24.3 (C-5), 23.0 ppm (NHAc); MS (ESI): *m/z* calcd for C₁₈H₃₀N₄Na₂O₁₂S: 567.1 [M+Na]⁺; found: 567.3.

(15,3R)-3-(Sulfonatoxyethyl)cyclohexyl (sodium 5-acetamido-9-benzamido-3,5,9-trideoxy-D-glycero-α-D-galacto-2-nonulopyranosylonate) sodium salt (49). A solution of benzoic acid (10.3 mg, 0.084 mmol), HATU (23.3 mg, 0.061 mmol) and DIPEA (20 μL, 0.115 mmol) in dry DMF (0.5 mL) was stirred for 10 min and then added to a solution of **48** (21.0 mg, 0.039 mmol) in dry DMF (0.5 mL) under argon. The resulting mixture was stirred at rt for 6 h. The solvent was removed in vacuo and the residue was purified by flash chromatography on silica [DCM/(MeOH/H₂O, 10:1), 1:0 to 1:1] and size-exclusion chromatography (P-2 gel, H₂O) to give **49** (18.0 mg, 72%). [α]_D²⁰ = +39.6 (c = 1.00, H₂O); ¹H NMR (500 MHz, D₂O): δ = 7.80–7.76 (m, 2H, Ar-H), 7.63 (m, 1H, Ar-H), 7.57–7.52 (m, 2H, Ar-H), 4.03 (ddd, *J* = 3.0, 7.6, 8.9 Hz, 1H, H-8'), 3.93–3.85 (m, 3H, H-3, CH₂O), 3.85–3.77 (m, 2H, H-5', H-9'a), 3.73 (dd, *J* = 2.0, 10.4 Hz, 1H, H-6'), 3.66 (ddd, *J* = 4.6, 9.8, 11.9 Hz, 1H, H-4'), 3.57 (m, 2H, H-7', H-9'b), 2.75 (dd, *J* = 4.7, 12.4 Hz, 1H, H-3'e), 2.07 (m, 1H, H-4e), 2.01 (s, 3H, NHAc), 1.90 (m, 1H, H-2e), 1.79–1.68 (m, 2H, H-1, H-5e), 1.68–1.60 (m, 2H, H-6e, H-3'a), 1.29–1.17 (m, 2H, H-4a, H-5a), 1.03 (q, *J* = 12.1 Hz, 1H, H-2a), 0.88 ppm (qd, *J* = 3.8, 12.7 Hz, 1H, H-6a); ¹³C NMR (126 MHz, D₂O): δ = 176.0, 174.8, 172.2 (3 C=O), 134.7, 133.0, 129.7, 128.0 (6 C, Ar-C), 102.0 (C-2'), 75.8 (C-3), 74.4 (CH₂O), 73.6 (C-6'), 71.6 (C-8'), 70.8 (C-7'), 69.2 (C-4'), 52.8 (C-5'), 43.5 (C-9'), 42.0 (C-3'), 37.1 (C-1), 36.5 (C-2), 35.3 (C-4), 28.5 (C-6), 24.2 (C-5), 22.9 ppm (NHAc); HRMS (ESI): *m/z* calcd for C₂₅H₃₄N₄Na₂O₁₃S: 671.1469 [M+Na]⁺; found: 671.1468.

(15,3R)-3-(Sulfonatoxyethyl)cyclohexyl (sodium 5-acetamido-3,5,9-trideoxy-9-(naphthalene-2-sulfonamido)-D-glycero-α-D-galacto-2-nonulopyranosylonate) sodium salt (50). Compound **48** (20.6 mg, 0.038 mmol), NaHCO₃ (15.1 mg, 0.180 mmol) and 2-naphthalenesulfonyl chloride (10.1 mg, 0.045 mmol) were dissolved in DMF/H₂O (2:1, 1.8 mL) and the solution was stirred at rt for 5 h. The solution was neutralized with aq. HCl and evaporated to dryness. The residue was purified by flash chromatography on silica [DCM/(MeOH/H₂O, 10:1), 8:2 to 6:4] and size-exclusion chromatography (P-2 gel, H₂O) to afford **50** (11.7 mg, 42%). [α]_D²⁰ = +21.5 (c =

0.50, H₂O); ¹H NMR (600 MHz, D₂O): δ = 8.52 (d, *J* = 1.9 Hz, 1H, Ar-H), 8.12 (d, *J* = 8.8 Hz, 1H, Ar-H), 8.09 (d, *J* = 8.1 Hz, 1H, Ar-H), 8.03 (d, *J* = 8.1 Hz, 1H, Ar-H), 7.85 (dd, *J* = 2.0, 8.7 Hz, 1H, Ar-H), 7.73 (m, 1H, Ar-H), 7.69 (m, 1H, Ar-H), 3.77–3.72 (m, 2H, CH₂O), 3.72–3.66 (m, 2H, H-5', H-8'), 3.63–3.53 (m, 3H, H-3, H-4', H-6'), 3.47–3.42 (m, 2H, H-7', H-9'a), 3.09 (dd, *J* = 8.0, 14.2 Hz, 1H, H-9'b), 2.64 (dd, *J* = 4.6, 12.4 Hz, 1H, H-3'e), 1.97 (s, 3H, NHAc), 1.75–1.69 (m, 2H, H-2e, H-4e), 1.52 (t, *J* = 12.1 Hz, 1H, H-3'a), 1.41–1.35 (m, 2H, H-5e, H-6e), 1.32 (m, 1H, H-1), 0.90 (dq, *J* = 3.8, 12.4 Hz, 1H, H-4a), 0.83 (q, *J* = 11.9 Hz, 1H, H-5a), 0.74 (tq, *J* = 3.3, 13.2 Hz, 1H, H-2a), 0.65 ppm (dq, *J* = 3.6, 12.5 Hz, 1H, H-6a); ¹³C NMR (126 MHz, D₂O): δ = 176.0, 174.5 (2 C=O), 137.1, 135.7, 132.9, 130.9, 130.3, 130.2, 128.93, 128.91, 128.89, 122.5 (10 C, Ar-C), 101.9 (C-2'), 75.6 (C-3), 74.3 (CH₂O), 73.5 (C-6'), 71.9 (C-8'), 70.4 (C-7'), 69.2 (C-4'), 52.8 (C-5'), 46.3 (C-9'), 42.1 (C-3'), 36.8 (C-1), 36.4 (C-2), 35.0 (C-4), 28.3 (C-6), 23.9 (C-5), 22.9 ppm (NHAc); HRMS (ESI): *m/z* calcd for C₂₈H₃₆N₄Na₂O₁₄S₂: 757.1296 [M+Na]⁺; found: 757.1296.

Cloning of 6His-tagged Siglec-8-CRD. The Siglec-8 encoding sequence was amplified by PCR from cDNA clone MN_014442 (OriGene, Rockville, USA) and applied to site-directed mutagenesis to replace proline 173 and cysteine 23 by serines. The fragment was inserted into the NdeI and XhoI cloning site of the expression vector pET22b (Novagen). The resulting construct encoding a 6His tag at the C-terminus was amplified in chemo-competent *E. coli* DH5 and the correctness of the DNA sequence was confirmed by double-strand sequencing (Microsynth, Balgach, Switzerland).

Expression and purification of 6His-tagged Siglec-8-CRD. Protein expression was performed in *Escherichia coli* strain Rosetta-gami B (DE3). Bacterial culture was grown in LB medium (Luria-Bertani broth) containing 100 μg/mL of ampicillin at 30 °C and 300 rpm to reach an OD₆₀₀ of 0.7–1. The temperature was lowered gradually to reach 18 °C and isopropyl-β-D-1-thiogalactoside (IPTG) was added to a final concentration of 1 mM. The bacteria were further cultivated at 18 °C and 300 rpm for 36 h after induction and collected by centrifugation at 5000 rpm for 20 min at 4 °C. The bacterial lysis was performed in binding buffer (50 mM NaH₂PO₄, 300 mM NaCl, 10 mM imidazole, pH 8) containing 1 mg/mL lysozyme followed by sonication. After centrifugation at 11000 rpm for 20 min at 4 °C, the supernatant (cytoplasmic extract) was dialyzed overnight against binding buffer and applied to a Ni-NTA column (Sigma, Buchs, Switzerland) attached to a BioLogic fast protein liquid chromatography system (BioRad, Reinach BL, Switzerland). The column was washed with binding buffer and afterwards eluted with elution buffer (50 mM NaH₂PO₄, 300 mM NaCl and 250 mM imidazole, pH 8). The fractions containing 6His-Siglec-8-CRD were pooled and dialyzed against assay buffer (20 mM HEPES, 150 mM NaCl, 1 mM CaCl₂, pH 7.4). The purity of the protein was verified by non-reducing SDS-PAGE.

Competitive binding assay. The polyacrylamide-based competitive binding assay^[43] was used to evaluate the binding of Siglec-8 ligands. Microtiter plates (F96 MaxiSorp, Nunc) were coated with 100 μL/well of a 10 μg/mL solution of Siglec-8-CRD in 20 mM HEPES, 150 mM NaCl, and 1 mM CaCl₂, pH 7.4 (assay buffer), overnight at 4 °C. The coating solution was discarded, and the wells were blocked with 150 μL/well of 3% BSA in assay buffer for 2 h at 4 °C. After three washing steps with assay buffer (150 μL/well), a 3-fold serial dilution of the test compound (50 μL/well) in assay buffer and streptavidin-peroxidase coupled biotinylated polyacrylamide (PAA) glycopolymers (6'-sulfo-sLe^x-PAA, 50 μL/well of a 0.3 μg/mL solution) were added. The plate was incubated for 3 h at 25 °C and 350 rpm and then carefully washed four times with 150 μL/well assay buffer. After the addition of 100 μL/well of the horseradish peroxidase substrate (2,2'-azino-di(3-ethylbenzthiazoline-6-sulfonic acid), ABTS), the colorimetric reaction was allowed to develop for 3 min, then stopped by the addition of 2% aqueous oxalic acid

before the optical density (OD) was measured at 415 nm on a microplate-reader (Spectramax 190, Molecular Devices, CA). The IC_{50} values of the compounds were calculated with the prism software (GraphPad Software, Inc., La Jolla, CA). The IC_{50} defines the molar concentration of the test compound that reduces the maximal specific binding of 6'-sulfo-sLe^x-PAA polymer to Siglec-8-CRD by 50%.

Microscale thermophoresis. Microscale thermophoresis experiments were performed using a Monolith NT.115 (Nanotemper, Munich, Germany) instrument set to 25 °C, 50% LED power, and "medium" MST power. The Nanotemper MO.Affinity Analysis software suite was employed for analysis and nonlinear fitting of experimental data. In a typical experiment, a serial ligand dilution starting at 50 mM or 100 mM was incubated with an equal volume of 200 nM FITC labeled Siglec-8-CRD and measured directly using the green channel of the instrument.

Isothermal titration calorimetry. Isothermal titration calorimetric experiments were performed on an ITC200 instrument (MicroCal, Northampton, USA) at 25 °C using standard instrument settings (reference power 6 μ cal s^{-1} , stirring speed 750 rpm, feedback mode high, filter period 2 s). Protein solutions were dialyzed against ITC buffer (20 mM HEPES, 150 mM NaCl, pH 7.4) prior to the experiments and all samples were prepared using the dialysate buffer to minimize dilution effects. Protein concentrations were determined spectrophotometrically with the specific absorbance at 280 nm employing an extinction coefficient of 33240 $mol^{-1} cm^{-1}$. Binding affinities of Siglec-8 ligands in the μ M to mM range necessitated a low c titration setup. In a typical experiment, a 5–25 mM ligand solution was titrated to a solution containing 30–50 μ M Siglec-8-CRD to ensure > 70% saturation. Baseline correction, peak integration, and non-linear regression analysis of experimental data was performed using the NITPIC (version 1.2.2.)^[56] and SEDPHAT (version 12.1b)^[57] software packages. The stoichiometry parameter was manually constrained to a value of 1. Experiments were performed in duplicate and the 68% confidence intervals from global fitting of two experiments were calculated as an estimate of experimental error. For kinITC analysis, the AFFINImeter software suite (v2.1802.5, Software for Science Developments, Santiago de Compostela, Spain) was used. Raw ITC data was fit to a thermodynamic model assuming a stoichiometry of 1 to derive K_A . Dissociation rates were then determined from a fit of the equilibration time curve to a 1:1 interaction model. Association rate constants were calculated from K_A and k_{off} according to the equation:

$$k_{on} = K_A \times k_{off} = \frac{k_{off}}{K_D}$$

Errors in rate constants are given as the 68% standard error of the fit for a single experiment.

Generation of pseudo induced-fit docking pose for 50. Structure preparation and docking studies were carried out using programs from the Maestro suite version 2016-4.^[58] The ligand bound Siglec-8-CRD NMR solution structure 2N7B was retrieved from the PDB and frame 1 was chosen for the docking procedure. After *in silico* mutation of Lys120 to Ala, the protein was prepared for docking by protonation, bond order and hydrogen bond assignment, and subsequent restrained minimization using the OPLS3 force field.^[59,60] The LigPrep module employing the OPLS3 force field was used for the preparation of low energy conformations and charge assignment of 50. Receptor grid generation and ligand docking was carried out with Glide in standard precision mode using the ligand bound in 2N7B as the centroid of the bounding box.^[61] After visual inspection of the generated docking poses, Ala120 was mutated to Lys and minimized.

Acknowledgements

This project has received funding from the European Union's Horizon 2020 research and innovation programme under the Marie Skłodowska-Curie grant agreement No 765581.

Conflict of Interest

The authors declare no conflict of interest.

Keywords: Siglec-8 · asthma · 6'-sulfo-sialyl Lewis^x · glycosides · calorimetry

- [1] P. R. Crocker, J. C. Paulson, A. Varki, *Nat. Rev. Immunol.* **2007**, *7*, 255–266.
- [2] A. Varki, T. Angata, *Glycobiology* **2005**, *16*, 1R-27R.
- [3] M. S. Macauley, P. R. Crocker, J. C. Paulson, *Nat. Rev. Immunol.* **2014**, *14*, 653–666.
- [4] J. V. Ravetch, L. L. Lanier, *Science* **2000**, *290*, 84–89.
- [5] P. R. Crocker, P. Redelinghuys, *Biochem. Soc. Trans.* **2008**, *36*, 1467–1471.
- [6] J. C. Paulson, M. S. MacAuley, N. Kawasaki, *Ann. N. Y. Acad. Sci.* **2012**, *1253*, 37–48.
- [7] B. E. Collins, O. Blixt, A. R. DeSieno, N. Bovin, J. D. Marth, J. C. Paulson, *Proc. Natl. Acad. Sci. USA* **2004**, *101*, 6104–6109.
- [8] B. E. Collins, O. Blixt, S. Han, B. Duong, H. Li, J. K. Nathan, N. Bovin, J. C. Paulson, *J. Immunol.* **2006**, *177*, 2994–3003.
- [9] K. K. Kikly, B. S. Bochner, S. D. Freeman, K. B. Tan, K. T. Gallagher, K. J. D. Alessio, S. D. Holmes, J. A. Abrahamson, C. L. Erickson-Miller, P. R. Murdock, H. Tachimoto, P. Robert, J. R. White, *Clin. Exp. Allergy* **2009**, *39*, 1093–1100.
- [10] H. Floyd, J. Ni, A. L. Cornish, Z. Zeng, D. Liu, K. C. Carter, J. Steel, P. R. Crocker, *J. Biol. Chem.* **2000**, *275*, 861–866.
- [11] P. J. Barnes, *Nat. Rev. Immunol.* **2008**, *8*, 183–192.
- [12] J. V. Fahy, *Nat. Rev. Immunol.* **2015**, *15*, 57–65.
- [13] E. Nutku, H. Aizawa, S. A. Hudson, B. S. Bochner, *Blood* **2003**, *101*, 5014–5020.
- [14] H. Yokoi, O. H. Choi, W. Hubbard, H.-S. Lee, B. J. Canning, H. H. Lee, S.-D. Ryu, S. von Gunten, C. A. Bickel, S. A. Hudson, D. W. MacGlashan, B. S. Bochner, *J. Allergy Clin. Immunol.* **2008**, *121*, 499–505.
- [15] T. Angata, C. M. Nycholat, M. S. Macauley, *Trends Pharmacol. Sci.* **2015**, *36*, 645–660.
- [16] S. A. Hudson, N. V. Bovin, R. L. Schnaar, P. R. Crocker, B. S. Bochner, *J. Pharmacol. Exp. Ther.* **2009**, *330*, 608–612.
- [17] Y. Jia, H. Yu, S. M. Fernandes, Y. Wei, A. Gonzalez-Gil, B. S. Bochner, R. C. Kern, R. P. Schleimer, R. L. Schnaar, *J. Allergy Clin. Immunol.* **2015**, *135*, 799–810.
- [18] S. V. Gunten, M. Vogel, A. Schaub, B. M. Stadler, S. Miescher, P. R. Crocker, *J. Allergy Clin. Immunol.* **2007**, *119*, 1005–1011.
- [19] P.-S. Gao, K. Shimizu, A. V. Grant, N. Rafaels, L.-F. Zhou, S. A. Hudson, S. Konno, N. Zimmermann, M. I. Araujo, E. V. Ponte, A. A. Cruz, M. Nishimura, S.-N. Su, N. Hizawa, T. H. Beaty, R. A. Mathias, M. E. Rothenberg, K. C. Barnes, B. S. Bochner, *Eur. J. Hum. Genet.* **2010**, *18*, 713–719.
- [20] T. Kiwamoto, N. Kawasaki, J. C. Paulson, B. S. Bochner, *Pharmacol. Ther.* **2012**, *135*, 327–336.
- [21] S. Farid, A. Mirshafiey, A. Razavi, *Immunopharmacol. Immunotoxicol.* **2012**, *34*, 721–726.
- [22] F. Legrand, Y. Cao, J. B. Wechsler, X. Zhu, N. Zimmermann, S. Rampertaap, J. Monsale, K. Romito, B. A. Youngblood, E. C. Brock, M. A. Makiya, N. Tomasevic, C. Bebbington, I. Maric, D. D. Metcalfe, B. S. Bochner, A. D. Klion, *J. Allergy Clin. Immunol.* **2019**, *143*, 2227–2237.
- [23] D. Simon, H. U. Simon, *Curr. Opin. Pharmacol.* **2019**, *46*, 29–33.
- [24] J. A. O'Sullivan, D. J. Carroll, Y. Cao, A. N. Salicru, B. S. Bochner, *J. Allergy Clin. Immunol.* **2018**, *141*, 1774–1785.
- [25] R. T. Lee, Y. C. Lee, *Glycoconjugate J.* **2000**, *17*, 543–551.
- [26] T. K. Dam, T. A. Gerken, C. F. Brewer, *Biochemistry* **2009**, *48*, 3822–3827.
- [27] N. R. Zaccai, K. Maenaka, T. Maenaka, P. R. Crocker, R. Brossmer, S. Kelm, E. Y. Jones, *Structure* **2003**, *11*, 557–567.

- [28] S. Mesch, K. Lemme, M. Wittwer, H. Koliwer-Brandl, O. Schwardt, S. Kelm, B. Ernst, *ChemMedChem* **2012**, *7*, 134–143.
- [29] S. Kelm, J. Gerlach, R. Brossmer, C. P. Danzer, L. Nitschke, *J. Exp. Med.* **2002**, *195*, 1207–1213.
- [30] H. H. M. Abdu-Allah, K. Watanabe, G. C. Completo, M. Sadagopan, K. Hayashizaki, C. Takaku, T. Tamanaka, H. Takematsu, Y. Kozutsumi, J. C. Paulson, T. Tsubata, H. Ando, H. Ishida, M. Kiso, *Bioorg. Med. Chem.* **2011**, *19*, 1966–1971.
- [31] S. Mesch, D. Moser, D. S. Strasser, A. Kelm, B. Cutting, G. Rossato, A. Vedani, H. Koliwer-Brandl, M. Wittwer, S. Rabbani, O. Schwardt, S. Kelm, B. Ernst, *J. Med. Chem.* **2010**, *53*, 1597–1615.
- [32] S. V. Shelke, G.-P. Gao, S. Mesch, H. Gächje, S. Kelm, O. Schwardt, B. Ernst, *Bioorg. Med. Chem.* **2007**, *15*, 4951–4965.
- [33] H. Prescher, M. Frank, S. Gütgemann, E. Kuhfeldt, A. Schweizer, L. Nitschke, C. Watzl, R. Brossmer, *J. Med. Chem.* **2017**, *60*, 941–956.
- [34] C. M. Nycholat, S. Duan, E. Knuplez, C. Worth, M. Elich, A. Yao, J. O'Sullivan, R. McBride, Y. Wei, S. M. Fernandes, Z. Zhu, R. L. Schnaar, B. S. Bochner, J. C. Paulson, *J. Am. Chem. Soc.* **2019**, *141*, 14032–14037.
- [35] B. S. Bochner, R. A. Alvarez, P. Mehta, N. V. Bovin, O. Blixt, J. R. White, R. L. Schnaar, *J. Biol. Chem.* **2005**, *280*, 4307–4312.
- [36] H. F. Yu, A. Gonzalez-Gil, Y. D. Wei, S. M. Fernandes, R. N. Porell, K. Vajn, J. C. Paulson, C. M. Nycholat, R. L. Schnaar, *Glycobiology* **2017**, *27*, 657–668.
- [37] H. Tateno, P. R. Crocker, J. C. Paulson, *Glycobiology* **2005**, *15*, 1125–1135.
- [38] J. M. Pröpster, F. Yang, S. Rabbani, B. Ernst, F. H. T. Allain, M. Schubert, *Proceed. Natl. Acad. Sci. U. S. A.* **2016**, *113*, E4170–E4179.
- [39] The PyMOL Molecular Graphics System, Version 1.8 Schrödinger, LLC.
- [40] Functional Glycomics Gateway, **2010**. Available at: http://www.functionalglycomics.org/glycomics/H5Servlet?operation=view&sideMenu=no&psi d=primscreen_5605. Accessed: January 2017.
- [41] R. Dubey, D. Reynolds, S. A. Awas, K. L. Matta, *Carbohydr. Res.* **1988**, *183*, 155–162.
- [42] C.-S. Chao, M.-C. Chen, S.-C. Lin, K.-K. T. Mong, *Carbohydr. Res.* **2008**, *343*, 957–964.
- [43] S. Rabbani, X. Jiang, O. Schwardt, B. Ernst, *Anal. Biochem.* **2010**, *407*, 188–195.
- [44] T. S. Carter, T. J. Mooibroek, P. F. N. Stewart, M. P. Crump, M. C. Galan, A. P. Davis, *Angew. Chem. Int. Ed.* **2016**, *55*, 9311–9315; *Angew. Chem.* **2016**, *128*, 9457–9461.
- [45] M. Hendlich, A. Bergner, J. Gunther, G. Klebe, *J. Mol. Biol.* **2003**, *326*, 607–620.
- [46] G. A. Patani, E. J. LaVoie, *Chem. Rev.* **1996**, *96*, 3147–3176.
- [47] N. A. Meanwell, *J. Med. Chem.* **2011**, *54*, 2529–2591.
- [48] D. Rotticci, T. Norin, K. Hult, *Org. Lett.* **2000**, *2*, 1373–1376.
- [49] R. ter Halle, Y. Bernet, S. Billard, C. Bufferne, P. Carlier, C. Delaitre, C. Flouzat, G. Humblot, J. C. Laigle, F. Lombard, S. Wilmouth, *Org. Process Res. Dev.* **2004**, *8*, 283–286.
- [50] A. Numata, T. Suzuki, K. Ohno, S. Uyeo, *Yakugaku Zasshi* **1968**, *88*, 1298–1305.
- [51] S. Kelm, R. Brossmer, PCT patent WO 03/000709A2, **2003**.
- [52] J. Cramer, C. P. Sager, B. Ernst, *J. Med. Chem.* **2019**, *62*, 8915–8930.
- [53] R. A. Copeland, D. L. Pompliano, T. D. Meek, *Nat. Rev. Drug Discovery* **2006**, *5*, 730–739.
- [54] P. Dumas, E. Ennifar, C. Da Veiga, G. Bec, W. Palau, C. Di Primo, A. Piñeiro, J. Sabin, E. Muñoz, J. Rial, *Methods Enzymol.* **2016**, *567*, 157–180.
- [55] P. Zihlmann, M. Silbermann, T. Sharpe, X. Jiang, T. Mühlethaler, R. P. Jakob, S. Rabbani, C. P. Sager, P. Frei, L. Pang, T. Maier, B. Ernst, *Chem. Eur. J.* **2018**, *24*, 13049–13057.
- [56] T. H. Scheuermann, C. A. Brautigam, *Methods* **2015**, *76*, 87–98.
- [57] G. Piszczek, *Methods* **2015**, *76*, 137–148.
- [58] Schrödinger Release 2016–4: Maestro Schrödinger LLC. New York, NY (USA), **2016**.
- [59] G. Madhavi Sastry, M. Adzhigirey, T. Day, R. Annabhimoju, W. Sherman, *J. Comput.-Aided Mol. Des.* **2013**, *27*, 221–234.
- [60] E. Harder, W. Damm, J. Maple, C. Wu, M. Reboul, J. Y. Xiang, L. Wang, D. Lupyan, M. K. Dahlgren, J. L. Knight, J. W. Kaus, D. S. Cerutti, G. Krilov, W. L. Jorgensen, R. Abel, R. A. Friesner, *J. Chem. Theory Comput.* **2016**, *12*, 281–296.
- [61] R. A. Friesner, J. L. Banks, R. B. Murphy, T. A. Halgren, J. J. Klicic, D. T. Mainz, M. P. Repasky, E. H. Knoll, M. Shelley, J. K. Perry, D. E. Shaw, P. Francis, P. S. Shenkin, *J. Med. Chem.* **2004**, *47*, 1739–1749.

Manuscript received: June 10, 2020

Accepted manuscript online: August 3, 2020

Version of record online: August 31, 2020

Oligo- and Multivalent presentation of Siglec-8 ligand

Manuscript 1: Targeting Siglec-8 with Oligo- and Multivalent Ligands modulates immune cell activation

This manuscript describes the synthesis of oligomeric ligands displaying glycomimetics ligands targeting Siglec-8. In order to link the ligands with oligovalent scaffolds, a new glycosyl acceptor had to be developed. The attachment to the oligo- and multivalent scaffolds was performed by click chemistry. The multivalent Siglec-8 ligands were evaluated in terms of their binding affinities and respective thermodynamic fingerprints. Finally, the abilities of a multivalent polymer displaying Siglec-8 ligands and of small molecules were investigated in cell-based bioassays.

Contribution to the project:

Gabriele Conti designed and performed the synthesis of the compounds. He expressed and purified Siglec-8 CRD, which he used in nano differential scanning fluorimetry and isothermal titration calorimetry assays.

Targeting Siglec-8 with Oligo- and Multivalent Ligands modulates immune cell activation

Gabriele Conti,^{[a],[b]} Anne Bärenwaldt,^[c] Blijke S. Kroezen,^[a] Said Rabbani,^[a] Mirza Sarcevic,^[c] Oliver Schwardt,^[a] Daniel Ricklin,^[a] Roland J. Pieters,^{[b]*} Heinz Läubli,^{[c]*} and Beat Ernst^{[a]*}

^[a] Molecular Pharmacy Group, Department of Pharmaceutical Sciences, University of Basel, Klingelbergstrasse 50, 4056 Basel (Switzerland)

^[b] Chemical Biology and Drug Discovery Group, Department of Pharmaceutical Sciences, Utrecht University, Universiteitsweg 99, 3584 CG Utrecht (The Netherlands)

^[c] Laboratory for Cancer Immunotherapy, Department of Biomedicine, University of Basel, Hebelstrasse 20, 4051 Basel (Switzerland) and Division of Medical Oncology, University Hospital Basel Petersgraben 4, 4051 Basel (Switzerland)

Abstract

Carbohydrate-binding proteins are generally characterized by poor affinities for their natural glycan ligands, predominantly due to the shallow and solvent-exposed binding sites. To overcome this drawback, nature has exploited multivalency to strengthen the binding by establishing multiple interactions simultaneously. The development of oligovalent structures frequently proved to be successful, both for proteins with multiple binding sites, but also for proteins that possess a single recognition domain. Here we present the syntheses of a number of oligovalent ligands for Siglec-8, a monomeric I-type lectin found on eosinophils and mast cells, as well as the thermodynamic characterization of their binding. While the enthalpic contribution of each binding epitope was within a narrow range to the one of the monomeric ligand, larger differences in the solvation and conformation entropies were seen. Additionally, we observe a successful agonistic binding of the oligovalent ligands to Siglec-8 on immune cells and modulation of immune cell activation, whereas a monovalent ligand, despite binding with similar affinity, had only an antagonistic effect. Tetra- and hexavalency and to an even larger extent multivalency was a prerequisite to trigger a biological response.

Introduction

Siglecs are a family of sialic acid-binding immunoglobulin-like lectins that participate in the discrimination between ‘self’ and ‘non-self’ and regulate the function of cells in the innate and adaptive immune system by recognizing glycan ligands.^[1] They exhibit a sialic acid binding N-terminal domain, one or more C2-set immunoglobulin domains and a cytoplasmic tail.^[2] The cytoplasmic tail of most Siglecs contains an immunoreceptor tyrosine-based inhibitory motif (ITIM), which functions as inhibitory receptor and suppresses activation signals. Ligand-binding induces phosphorylation of the tyrosine motif by an Src family kinase, resulting in the recruitment of SH2 domain-containing phosphatases,^[3] which inhibit cellular processes through inactivation of essential kinases and therefore, can modulate crucial immune responses.^[4] In their resting state, most Siglecs are engaged in *cis*-interactions with sialylated glycans expressed on the surface of the same cell.^[5] As a result, Siglecs are essentially masked and can only interact with *trans*-ligands that display sufficient affinity or avidity to outcompete the *cis*- interactions.^[6]

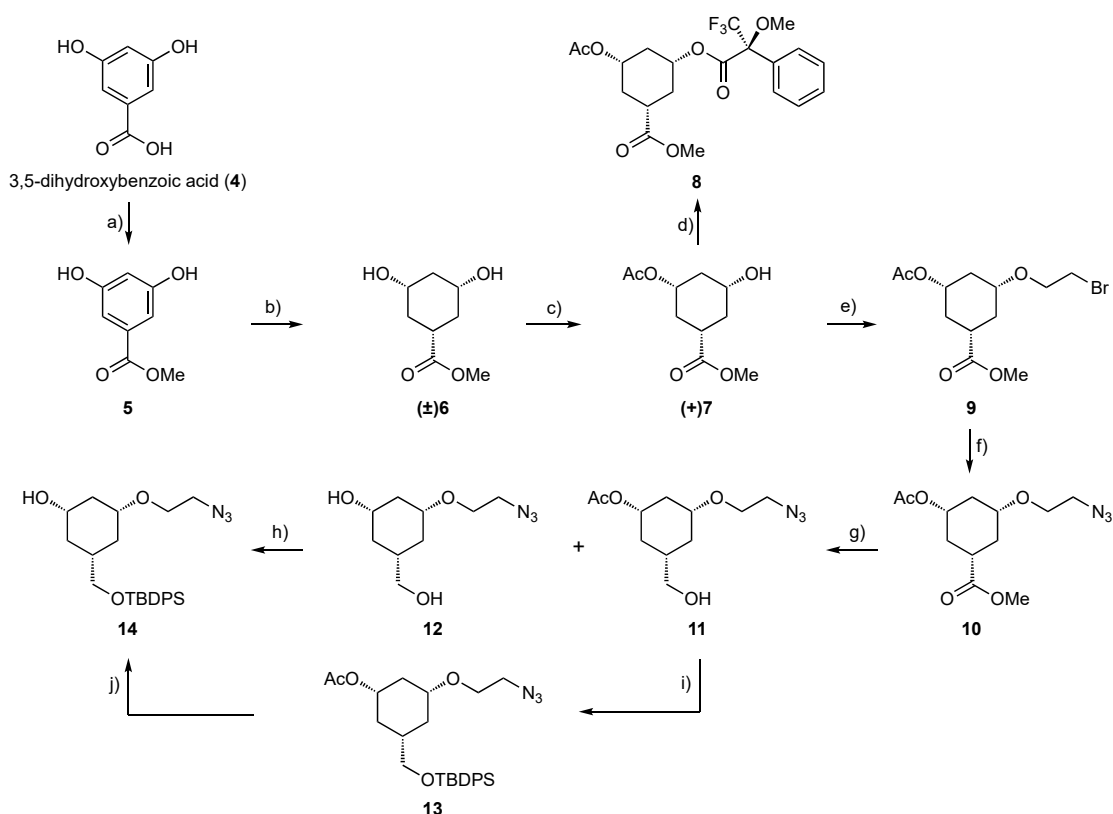
Due to the restricted expression of Siglecs on immune cells, their endocytic properties, and their ability to modulate receptor signalling, they evolved into attractive but challenging therapeutic targets for immune modulation. Among them, Siglec-8, expressed on eosinophils, mast cells and weakly on basophils, has proven to be a promising target for the treatment of a variety of eosinophil- and mast cell-associated disorders such as asthma, chronic rhinosinusitis, chronic urticaria, hypereosinophilic syndromes, mast cell and eosinophil malignancies and eosinophilic gastrointestinal disorders.^[7] The engagement of Siglec-8 with a monoclonal antibody^[8] or multivalent sialoglycan ligands^[9] induced apoptosis/cell death of eosinophils and inhibits mast cell degranulation. When anti-Siglec-8 antibody are administrated *in vivo* to humanized and transgenic mice selectively expressing Siglec-8 on eosinophils and mast cells, these findings could be confirmed. Currently, a Siglec-8 agonist, the humanized IgG1 antibody against Siglec-8 (AK002, lirentelimab), depleting eosinophils via antibody-dependent cellular cytotoxicity^[10] and inhibiting mast cell activation, is in clinical development for mast cell- and eosinophil-mediated diseases.^[11]

A promising alternative to target Siglec-8 with antibodies involves the multivalent display of Siglec ligands on liposomes,^[9a] polymers^[9b,c] and nanoparticles.^[9d] Thus, it was shown that apoptosis can be initiated by treating eosinophils with a synthetic polyvalent Siglec-8 ligand^[12] and immunohistochemical analyses exhibited an up-regulation of Siglec-8 ligands in inflamed compared to healthy tissue.^[13] Additionally, Siglec-8 ligands could be presented on liposomes. When encapsulating drugs, such liposomes could be exploited for the delivery of their payloads to eosinophil, thanks to their endocytic activity.^[14] Alternatively, liposomes simultaneously displaying

To further enhance binding, an oligo- and multivalent presentation of the carbohydrate ligand was explored. In this way, clustering of Siglec-8 in microdomains can be induced, which is a necessity for triggering the biological response.^[6] In addition, an oligo- and multivalent ligand with a proper spatial presentation of the individual epitopes increases its local concentration enabling fast rebinding upon dissociation.^[19]

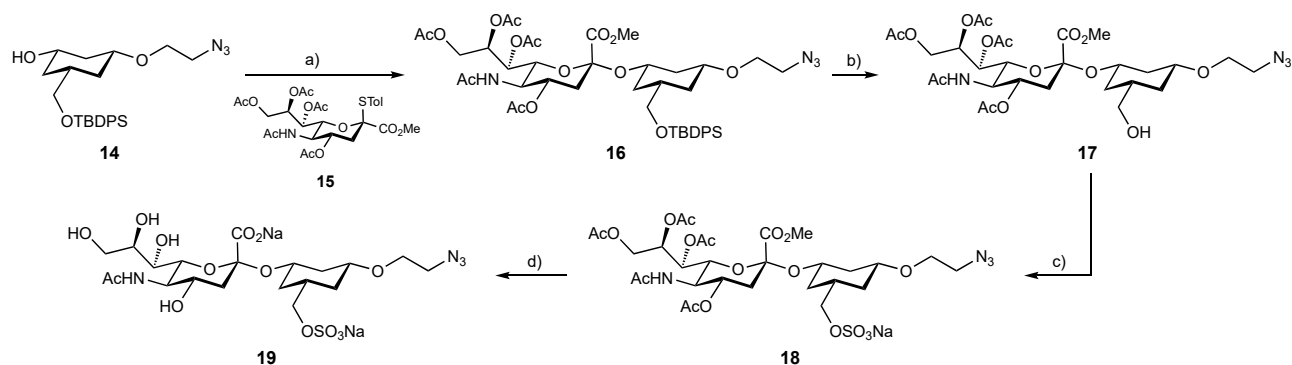
In order to achieve oligo- and multimeric presentations of epitope **3**, an additional exit vector is required. Importantly, it should not interfere with or preclude binding of the key functionality of the epitope. For this purpose, we extended the carbocycle with an additional hydroxy group that mimics the β 1-4 glycosidic linkage between the Gal and GlcNAc present in the parent tetrasaccharide **1**.

Synthesis of the Carbocyclic GlcNAc Mimetic. The synthesis of the glycosyl acceptor **14** equipped with side chain for oligomerization started from commercial 3,5-dihydroxybenzoic acid (Scheme 1). After esterification (\rightarrow **5**), rhodium-catalysed hydrogenation at 100 °C and 90 atm H₂ for 72 h yielded the all *cis*-derivative **6** quantitatively. Subsequent enzymatic asymmetrization^[20] with porcine pancreatic lipase, type II (PPL-II) and vinyl acetate led to the enantiomer **7** with an overall chemical yield of 95 % over three steps. Its optical rotation was in agreement with the reported value.^[21] In addition, to determine the enantiomeric purity, the corresponding Mosher ester **8** was formed, while the non-asymmetric monoacetylation of **6** subsequently esterified with Mosher chloride provided the diastereomeric mixture as reference. Surprisingly, ¹⁹F NMR analysis was inconclusive, as only a single peak could be detected for the Mosher derivative of racemic **6**, not allowing to distinguish the two diastereomers. However, in the ¹H NMR spectrum, the peaks of the signals for the methyl ester and acetate were split for the two diastereoisomers, indicating an enantiomeric excess > 99 % for **7** (for details see Supporting Information). Subsequent functionalization of the free hydroxyl group with freshly prepared 2-bromoethyltriflate^[22] afforded **9**, and by nucleophilic substitution with sodium azide compound **10**. Treatment of **10** with a stoichiometric amount of LiBH₄ resulted in a mixture of both alcohol **11** and diol **12** in 19 % and 45 % yield, respectively. To avoid double silylation, the TBDPS protection of the primary alcohol in diol **12** (\rightarrow **14**) had to be executed at 0° C and lasted 43 h. Because the acetate in **11** acted as protecting group, its silylation could be performed at rt, leading to **13** in only 19 h and the final deacetylation with aq. NaOH yielded **14**.



Scheme 1. Synthesis of the glycosyl acceptor 14. a) H₂SO₄, MeOH, reflux, 4 d (quant.); b) Rh/Al₂O₃, H₂ (90 bar), MeOH, 100 °C, 72 h (quant.); c) vinyl acetate, PPL (lipase from porcine pancreas, type II), rt, 20 h (95 %); d) (*R*)-(-)-MTPA-Cl, DCM, 0 °C to rt; e) 2-bromoethyltriflate, DIPEA, toluene, 25 to 100 °C, 48 h (quant.); f) NaN₃, DMF, rt, 24 h (quant.); g) LiBH₄, THF/MeOH, 0 °C to rt, 18 h (**11**, 19 % & **12**, 45 %) h) TBDPSCl, DMAP, imidazole, rt, 43 h (71 %); i) TBDPSCl, DMAP, imidazole, rt, 19 h; j) NaOH (aq), MeCN, rt, 19 h (71 % from **11**); for experimental details see Supporting Information.

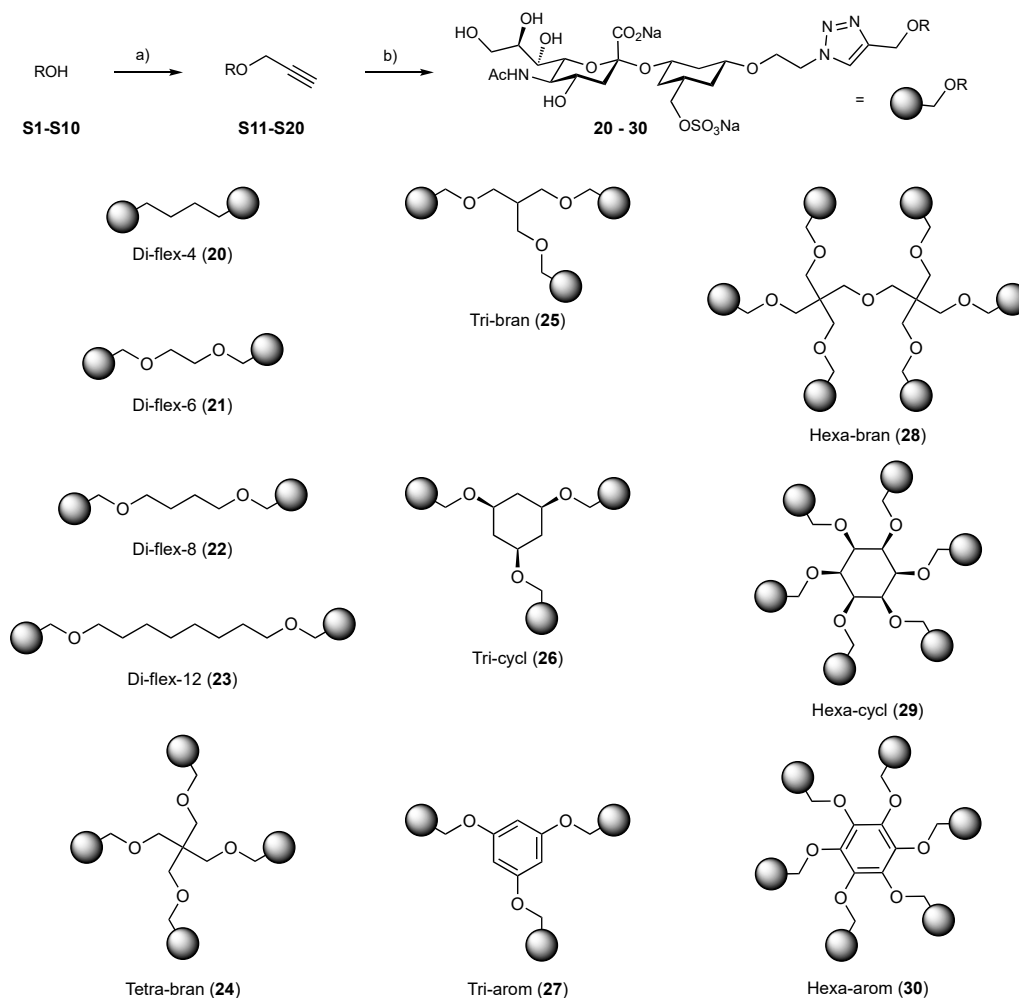
The aim of this work was to compare the monovalent ligand **3** with its oligo- and multivalent presentations and to study the impact of shape and flexibility of the scaffolds used. Therefore, the Gal mimetic **14** was sialidated using donor **15**^[23] (Scheme 2) to give pseudodisaccharide **16** in 50 % yield. Subsequent treatment with HF to remove the TBDPSCl protection (→ **17**) and sulfation of the primary hydroxyl group gave **18** in almost quantitative yield. Final deprotection with aqueous NaOH provided the monovalent ligand **19**.



Scheme 2. Synthesis of monovalent epitope. a) NIS, TfOH, MS 3 Å, MeCN, -40 °C, 14 h (50 %); b) HF·pyr, pyridine, 0 °C, 7 h (95 %); c) SO₃·pyr, DMF, rt, 5.5 h (99 %); d) NaOH (aq), rt, 48 h (84 %); for experimental details see Supporting Information.

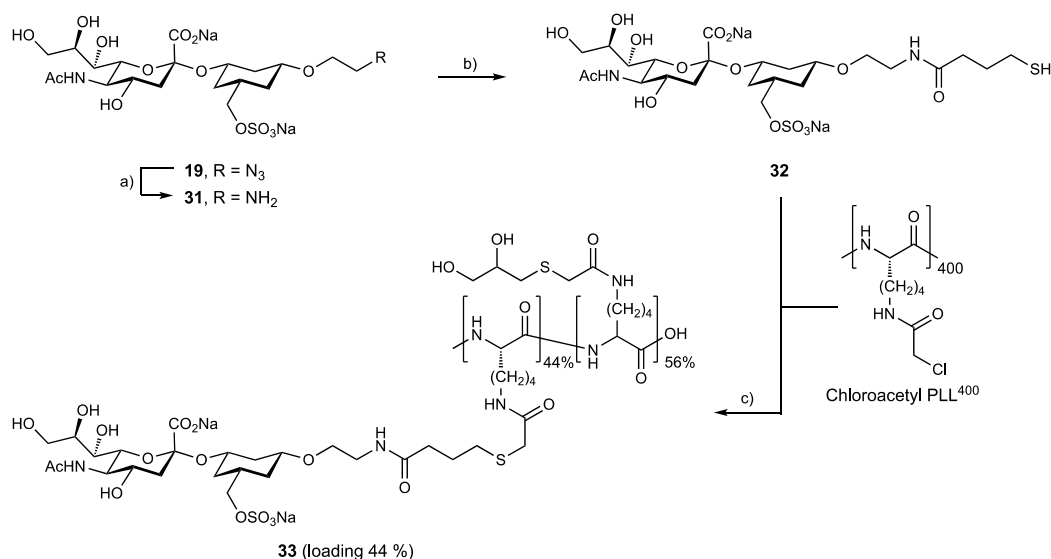
For optimizing simultaneous multiple interactions, the central scaffold used for the oligo- and multivalent presentation of the carbohydrate epitope has to meet specific requests regarding rigidity vs. flexibility to allow the proper spatial arrangement of the epitopes while keeping the entropic penalty as low as possible. Therefore, a number of flexible, branched, carbocyclic and aromatic scaffolds were decorated with the carbohydrate epitope **19** by click chemistry (Scheme 3).

The alkyne equipped scaffolds **S11-S20** to be used for CuAAC coupling^[24] with **19** were obtained by treatment of the corresponding alcohols **S1-S10** with propargyl bromide under basic conditions (Scheme 3). Various bases from mild K₂CO₃ for the phenolic hydroxyl groups to NaH or KOH for the primary alcohols were applied (for experimental details see Supporting Information). Click CuAAC reactions yielding the oligovalent compounds **20-30** were performed using CuBr as Cu(I) source, and tris((1-benzyl-4-triazolyl)methyl)amine (TBTA) as stabilizing agent to prevent copper oxidation and disproportionation.^[25]



Scheme 3. General synthesis of oligomeric ligands with various scaffolds. a) Propargyl bromide, base (for details see Supporting Information), DMF, 0 °C to rt (5 – 90 %); b) **19**, CuBr, TBTA, MeCN/H₂O, rt, overnight (19 – 63 %). The acronyms indicate the valency of the ligand, the type of scaffold [flexible with number of atoms (flex-No), branched (bran), cyclohexane-based (cycl), or benzene-based (arom)]. Compound Di-flex-4 (**20**) was synthesized from commercially available 1,7-octadiyne; for experimental details see Supporting Information.

For the synthesis of the multivalent representative **33**, compound **19** was further modified to enable the attachment to a L-lysine polymer, employing a previously published procedure that used γ -thiobutyrolactone as linker for attaching amines to chloroacetyl derivatives of PLL (Scheme 4).^[26] First, hydrogenation of **19** led to the primary amine **31**, which was then treated with γ -thiobutyrolactone yielding the functionalized ligand **32**. Finally, chlorine substitution on chloroacetyl PLL⁴⁰⁰ provided polymer **33**, whose loading was determined by ¹H NMR to be 44 % (for details see Supporting Information).



Scheme 4. Synthesis of glycopolymer 33. a) Pd(OH)₂/C, H₂ (1 atm), H₂O, rt, 24 h (96 %); b) γ -thiobutyrolactone, NaOH, MeOH/H₂O, rt, 24 h (45 %); c) DBU, DMF/H₂O, rt, 1 h; then thioglycerol, Et₃N, rt, overnight (91 %, loading 44 %); for experimental details see Supporting Information.

Qualitative binding assessment to Siglec-8 CRD with nanoDSF. For the qualitative assessment of the binding of the oligovalent ligands to the carbohydrate recognition domain of Siglec-8 (Siglec-8-CRD), differential scanning fluorimetry (nanoDSF) was employed. Thus, the protein was incubated with a constant concentration of ligand, and the thermal denaturation profile was measured by monitoring changes of the fluorescence signal of the aromatic residues of the protein as a function of temperature. Depending on the relative affinity, a ligand bound to the protein stabilizes its native state, causing a shift of the apparent melting temperature T_m to higher values.^[27]

DSF results for the various ligands are summarized in Table 1 (and Figure S3, Supporting Information). The Siglec-8-CRD alone showed a T_m of 45.5 °C. When incubated with the lead glycomimetic **3** or the monovalent ligand **19**, the ΔT_m s are +2.4 and +2.2 °C, respectively. The small difference of the ΔT_m s indicates that the additional azidoethyloxy substituent in **19** is not interfering with the protein and thus is optimally suited to link the carbohydrate epitope to the scaffolds. For the oligovalent compounds, positive temperature shifts with intensities increasing with rising valencies were obtained.

Table 1. T_m and ΔT_m (relative to reference compound **3**) values for various ligands. Siglec-8-CRD was used at a concentration of 20 μ M and incubated with 1 mM of each ligand except **33**. For polymer **33**, the assay concentration was 5 μ M and therefore 200-fold lower. Since polymer **33** displays 176 epitopes, the actual concentration of epitopes and therefore the T_m shifts is comparable to the monovalent ligands **3** and **19**.

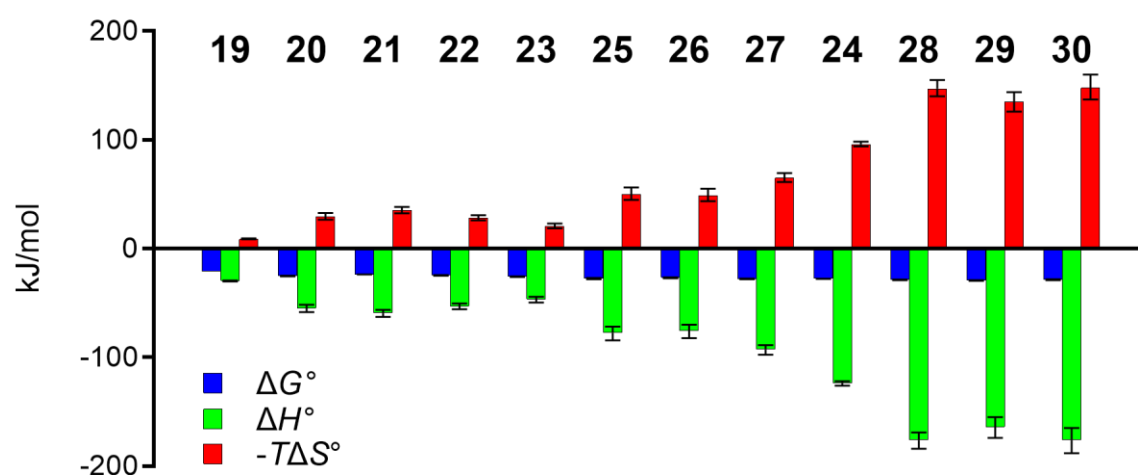
Compound	T_m (°C)	ΔT_m (°C)
Siglec-8-CRD	45.5	-
3 (reference compound)	47.9	+ 2.4
Monovalent 19	47.7	+ 2.2
Di-flex-4 (20)	50.8	+ 5.3
Di-flex-6 (21)	52.3	+ 6.8
Di-flex-8 (22)	49.2	+ 3.7
Di-flex-12 (23)	49.7	+ 4.2
Tri-bran (25)	50.5	+ 5.0
Tri-cycl (26)	50.0	+ 4.5
Tri-arom (27)	50.8	+ 5.3
Tetra-bran (24)	51.2	+ 5.7
Hexa-bran (28)	55.8	+ 10.3
Hexa-cycl (29)	55.2	+ 9.7
Hexa-arom (30)	55.1	+ 9.6
Glycopolymer 33	47.5	+2.2

Since both protein and ligand are present in solution and can freely move, multivalent ligands may bind, in addition to statistical rebinding, to more than one protein, leading to aggregation phenomena. This aggregation effect and its contribution to ΔT_m should be proportional to the contribution caused by the monovalent ligand **19**. Therefore, ΔT_m values may not only derive from statistical rebinding but also from an additional stabilization conferred by cross-linking of proteins.

Thermodynamic characterization of ligands. Besides the qualitative analysis of binding by DSF, a more detailed and quantitative analysis was obtained by isothermal titration calorimetry (ITC), providing information on affinity and thermodynamics of binding at the same time. According to Table 2, the affinity trend in ITC measurements roughly follows the increase of the functional valency N , which is defined as the inverse of the stoichiometry n ($N = 1/n$) and corresponds to the number of interacting epitopes of the oligomers. Indeed, divalent compounds gained on average a 5.1-fold increase in affinity compared to the monovalent ligand, while these benefits are 14.2-, 16.1- and 25.9-fold for trivalent, tetravalent and hexavalent ligands, respectively.

Furthermore, affinities also depend on nature and flexibility of the scaffold. As expected, entropy costs increase with valency but are cancelled out by a simultaneously improved enthalpy contribution. Surprisingly, the entropy costs related to branched, cyclic and aromatic scaffolds do not show any tendency, and, in addition, within a valency group, affinities vary only marginally, *i.e.* within a factor of 2.1 divalent to 1.3 for hexavalent ligands, probably as the result of entropy/enthalpy compensation.^[28]

Table 2. Thermodynamic fingerprints, binding affinities and stoichiometry of the interaction of oligovalent ligands with the Siglec-8-CRD. Error estimates resemble the 95 % confidence interval from global fitting of two or more independent experiments (for details see Supporting Information).



Compound	K_D [μM]	ΔG° [kJ·mol ⁻¹]	ΔH° [kJ·mol ⁻¹]	$\Delta H^\circ/\text{epitope}$ [kJ·mol ⁻¹]	$-T\Delta S^\circ$ [kJ·mol ⁻¹]	$T\Delta S^\circ/\text{epitope}$ [kJ·mol ⁻¹]	n-value (fixed)
19	230 (225 – 235)	-20.8 (-20.8 – -20.7)	-29.7 (-30.1 – -29.4)	-29.7 (-30.1 – -29.4)	8.9 (8.6 – 9.3)	8.9 (8.6 – 9.3)	1
Di-flex-4 (20)	37.7 (33.2 – 42.7)	-25.2 (-25.6 – -24.9)	-54.8 (-58.2 – -51.6)	-27.4 (-29.1 – -25.8)	29.5 (26.7 – 32.7)	3.9 (2.6 – 5.3)	0.5
Di-flex-6 (21)	64.6 (58.9 – 70.8)	-23.9 (-24.1 – -23.7)	-59.3 (-62.6 – -56.2)	-29.7 (-31.3 – -28.1)	35.4 (32.5 – 38.5)	7.5 (6.1 – 8.9)	0.5
Di-flex-8 (22)	47.7 (43.4 – 54.5)	-24.7 (-24.9 – -24.4)	-52.9 (-55.6 – -50.4)	-26.5 (-27.8 – -25.2)	28.3 (26.0 – 30.7)	3.5 (2.6 – 4.6)	0.5
Di-flex-12 (23)	29.8 (25.9 – 34.1)	-25.8 (-26.2 – -25.5)	-46.7 (-49.4 – -44.2)	-23.4 (-24.7 – -22.1)	20.8 (18.7 – 23.2)	-0.8 (-1.7 – 0.2)	0.5
Tri-bran (25)	15.1 (12.3 – 18.5)	-27.5 (-28.0 – -27.0)	-77.6 (-84.3 – -71.8)	-25.9 (-28.1 – -23.9)	50.1 (44.8 – 56.3)	1.1 (-0.4 – 2.8)	0.333
Tri-cycl (26)	20.2 (16.9 – 24.1)	-26.8 (-27.2 – -26.4)	-75.7 (-82.2 – -70.1)	-25.2 (-27.4 – -23.4)	48.9 (43.8 – 55.0)	1.2 (-0.3 – 2.9)	0.333
Tri-arom (27)	13.2 (11.6 – 14.9)	-27.9 (-28.2 – -27.6)	-93.0 (-97.6 – -88.8)	-31.0 (-32.5 – -29.6)	65.2 (61.3 – 69.4)	5.9 (4.8 – 7.1)	0.333
Tetra-bran (24)	14.3 (13.7 – 15.0)	-27.6 (-27.8 – -27.5)	-124 (-126 – -122)	-31.0 (-31.5 – -30.5)	96.2 (94.1 – 98.4)	6.8 (6.4 – 7.2)	0.25
Hexa-bran (28)	9.19 (8.30 – 10.2)	-28.7 (-29.0 – -28.5)	-176 (-184 – -169)	-29.3 (-30.7 – -28.2)	147 (140 – 155)	5.0 (4.1 – 6.1)	0.167
Hexa-cycl (29)	7.60 (6.60 – 8.75)	-29.2 (-29.6 – -28.9)	-164 (-174 – -155)	-27.3 (-29.0 – -25.8)	135 (126 – 144)	2.6 (1.4 – 3.9)	0.167
Hexa-arom (30)	9.90 (8.59 – 11.5)	-28.6 (-28.9 – -28.2)	-176 (-188 – -165)	-29.3 (-31.3 – -27.5)	148 (137 – 160)	5.2 (3.8 – 6.9)	0.167

The enthalpies $\Delta H^\circ/\text{epitope}$ of the oligovalent ligands are within a narrow range ($\Delta H^\circ/\text{epitope} - 27.8 \pm 2.5 \text{ kJ}\cdot\text{mol}^{-1}$), indicating comparable enthalpy contributions from each binding event including for the monovalent ligand **19**. The small deviations are probably related to desolvation enthalpies stemming from the various scaffolds. However, much larger deviations were registered for the entropy penalties ($-\Delta S/\text{epitope} 18.9 \pm 4.9$), when moving from monovalent **19** to oligovalent compounds. Whereas for the divalent ligands **20-23** the average entropy penalty/epitope is with $14.3 \pm 3.0 \text{ kJ}\cdot\text{mol}^{-1}$ rather small, it increases steadily with increasing valency to $24.5 \pm 1.2 \text{ kJ}\cdot\text{mol}^{-1}$ for the hexavalent ligand **28-30** and roughly follows the increase of the functional valency.

Immune cell-based assay

The ability of a synthetic polyacrylamide conjugate displaying Siglec-8 ligands to bind to its receptor on expressing cells was demonstrated by Bochner *et al.*^[29] To elucidate the effect of affinity and avidity of Siglec-8 ligands, we compared the branched oligovalent compounds **24** and **28** (syntheses see Scheme 3) and the poly-L-lysine glycopolymer **33** (PLL-33) (synthesis see Scheme 4). In addition, the sulfonamide derivative **34**^[18b], 15 times more active than the epitope used for **24**, **28** and **33**, was chosen as monovalent test compound (Table 6). These four compounds were evaluated for their ability to modulate the activation of Siglec-8 expressing immune cells.

Table 6. Compounds tested in the immune cell assay and their dissociation constants. Structures of the monomers **3** and **34**^[18b], tetravalent ligand **24**, hexavalent ligand **28** and glycopolymer **33**. Ligands **24** and **28** are oligovalent versions and **33** is a polymeric version of **3** (without linker) and **19** (with linker). Dissociation constant K_D were determined by ITC (for details see Supporting Information).

Comp.	Structure	K_D [μM]
3 ^[18b]		259
19		230
34 ^[18b]		15
24		14.3

Comp.	Structure	K_D [μ M]
28		9.2
33		0.042
35 (negative control)		no binding

For testing activity, we used Jurkat NFAT (Luc2) cells^[30] that were transduced with Siglec-8. This reporter cell line possesses a firefly luciferase gene regulated by the transcription factor NFAT (Nuclear Factor of Activated T cells) that is activated by T cell receptor-mediated cell stimulation. Previous results have shown that the presence of inhibitory Siglecs such as Siglec-7 and Siglec-9 on these cells negatively influences the signaling cascade leading to the detection of a lower luciferase signal after activation.^[30] In accordance with these finding, we also found that Siglec-8-expressing Jurkat NFAT (Luc2) cells showed a decreased luciferase signal compared to control transduced Jurkat cells (MOCK) after stimulation with an agonistic CD3 antibody (Figure 6A). Addition of the sulfonamide derivative **34** did not change the activation of MOCK or Siglec-8 Jurkat cells (Figure 6B). In contrast, the branched tetra- and hexavalent ligands **24** and **28** mediated an increased activation of Siglec-8 Jurkat cells, while there was no effect on MOCK control cells (Figure 6B). For the tetravalent ligand **24** this effect was dose dependent showing a higher activation with increasing concentrations. The hexavalent ligand **28** showed the main effect at lower concentrations (Figure 6B). The glycopolymer **33** increased the activity of Siglec-8-expressing Jurkat cells, while there was no effect on the MOCK control cells (Figure 6C). To exclude any interference caused by the structure of the polymer itself, a PLL⁴⁰⁰-based polymer displaying D-mannose (**35**, Man-PLL⁴⁰⁰) instead of the D-sialic acid derivative **19** as binding epitope, and so unable to ligate Siglec-8, was used as negative control. Indeed, treatment with this polymer did not result in a signal change, confirming that the result with glycopolymer **33** was dependent on Siglec-8 ligation (Figure 6C). Due to the increased

number of glycomimetic epitopes present in the glycopolymers **33** we used lower concentrations (pM range) compared to the μM concentrations of the branched oligovalent ligands **24** and **28**. When comparing the Siglec-8 glycomimetics at the same concentration of $1\mu\text{M}$ (Figure 6D), the degree of activation correlates with the number of glycomimetic-epitopes. Whereas glycopolymer **33** showed the strongest activation of Siglec-8-expressing Jurkats cells with a 3.3-fold increase in luminescence signal, the hexavalent compound **28** showed only a 2.6-fold and the tetravalent compound **24** a 2-fold increase. Finally, sulfonamide derivative **34** had no effect. Surprisingly, there was also some increase in the activity of MOCK control cells with the multivalent glycopolymer **33**. Thus, it is possible that with higher concentrations an off-target effect occurs (Figure 6D), which was not seen with lower concentrations (Figure 6C).

We further tested the role of *cis* ligands present on the Jurkat cells on the activation potential of the tested Siglec-8 ligands. Therefore, we pretreated the Jurkat cells with sialidase to remove naturally present ligands before stimulating the cells in presence of the glycopolymer **33**. In all cases, sialidase pre-treatment only led to a small increase in luciferase signal compared to the corresponding non-pre-treated situation (Figure 6E). Thus, sialidase pre-treatment influenced only minimally the inhibitory effect of glycopolymer **33** on Siglec-8-expressing Jurkats cells (Figure 6E).

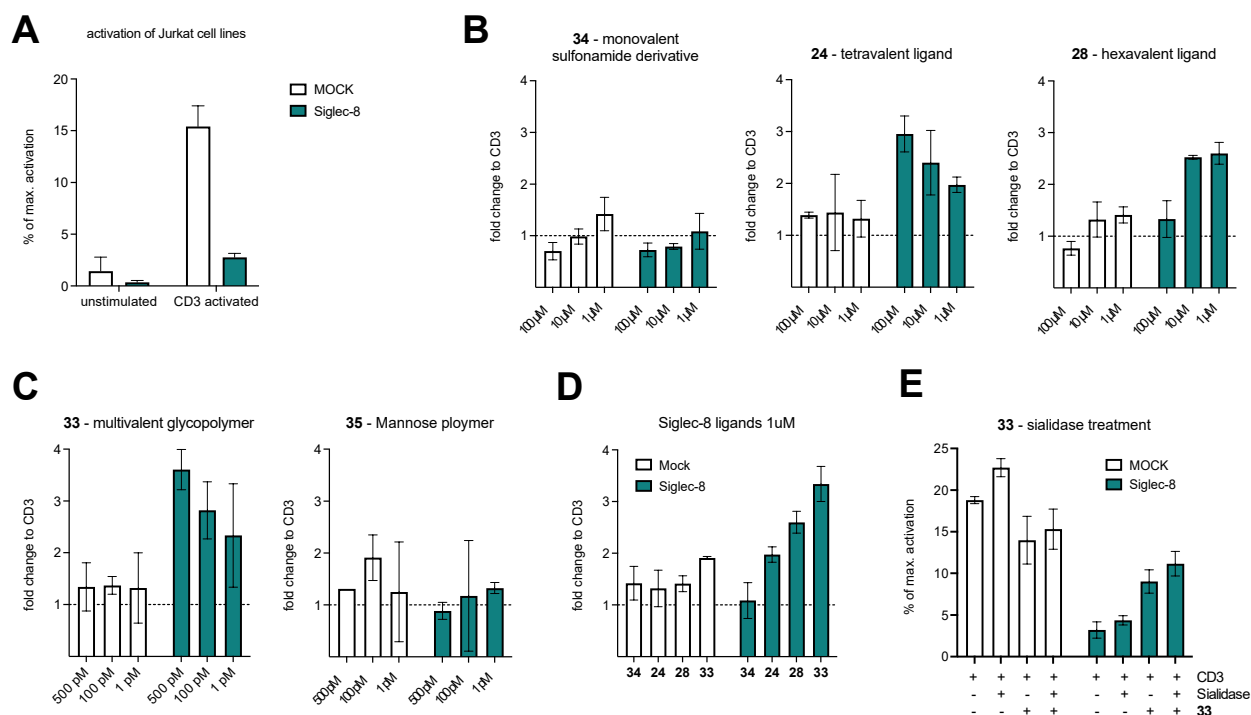


Figure 6. Multivalent Siglec-8 glycomimetics reduce inhibitory effect of Siglec-8 on immune cells. MOCK or Siglec-8 transduced Jurkat cells were left untreated (unstimulated) or activated with an activating CD3 antibody either in absence or presence of Siglec-8 ligands at various concentrations. Activation of cells was measured by luminescence signal that

is induced after CD3 stimulation. A) Comparison of activation of Siglec-8-expressing Jurkat cells and MOCK controls. Luminescence signal was normalized to the maximum luminescence signal achieved by PMA/Ionomycin stimulation. B-D) MOCK and Siglec-8 Jurkat cells were activated in presence of monovalent mimetic **34**, tetravalent mimetic **24** and the hexavalent mimetic **28** (B) or poly-L-lysine glycopolymer **33** in comparison to poly-L-lysine mannose polymer **35** as negative control (C). The activation with Siglec-8 ligands was normalized to the activation with CD3 alone (dashed line) for each cell line. D) Comparison of all Siglec-8 mimetics at a concentration of 1 μM . E) Siglec-8 and MOCK cells were treated with sialidase prior to activation with CD3 in presence or absence of glycomimetic **33** (500pM).

Overall, these results show that the oligovalent glycopolymers **24** and **28** and the multivalent glycomimetic **33** bind Siglec-8 on Siglec-8-expressing Jurkat NFAT (Luc2) cells causing an activation of Siglec-8 signaling. In contrast, the monovalent sulfonamide derivative **34** was not able to activate the immune cells, despite having a 17-fold higher affinity than the monovalent epitope **3** of the glycomimetics.

Conclusion

Siglecs are known to interact with glycans terminating in sialic acid on the same cell surface (in *cis*), blocking interactions with lower affinity ligands, thereby setting a threshold for productive Siglec signaling.^[31] To overcome the threshold set by *cis* ligands, we studied high-affinity oligo- and multivalent ligands competing with *cis* interactions.

The affinity of the preferred natural ligand 6'-sulfo-sLe^x for Siglec-8 is only 295 μM ^[16]. In a first step, we structurally simplified the natural epitope to yield Sia α (2-3)-6-sulfo-GlcOME (**2**) with a K_D of 733 μM . Replacement of the 6-sulfo-GlcOME moiety by (1*R*,3*S*)-(3-hydroxycyclohexyl)methyl-1-hydrogensulfate yielded the Siglec-8 ligand **3** with a K_D of 259 μM .^[18b]

In this communication, a further affinity improvement was realized by oligo- and multivalent presentations of Siglec-8 ligand **3**. To enable its oligo-/multivalent presentation, a linker was introduced (\rightarrow **19**, $K_D = 230 \mu\text{M}$). Further on, a special focus was laid on the type of scaffold employed (linear, cyclic, aromatic). When the oligovalent presentation of **19** (\rightarrow **20-30**) were thermodynamically characterized, we found enthalpy contributions for each epitope within a narrow range ($\Delta H^\circ/\text{epitope} = -27.8 \pm 2.4 \text{ kJ}\cdot\text{mol}^{-1}$). The normalized entropy penalties ($T\Delta S^\circ/\text{epitope} = 18.9 \pm 4.9 \text{ kJ}\cdot\text{mol}^{-1}$) for di- to hexavalent ligands differ roughly according valency, scaffold flexibility (from linear, branched, cyclic to aromatic) and numbers of rotational bonds per epitope (from 2 to 6). In summary, the scaffold has surprisingly not the dominant strong influence on activity, while the

valency of the ligands dominates. However, this opens the possibility to influence pharmacokinetic properties of the ligands such as solubility, polarity or metabolic stability via the scaffold structure.

Finally, a mono-, tetra-, hexa- and multivalent Siglec-8 ligand were tested in an immune cell bioassay to study their ability to bind to Siglec-8 and modulate immune activation. The monomeric glycomimetic **34** ($K_D = 15 \mu\text{M}$), was not able to activate Siglec-8 signaling, whereas the tetravalent ligand **24** exhibiting the same affinity showed a clear effect. Furthermore, the hexavalent ligand **28** induced receptor clustering to an even larger extent, reaching almost the capability of the multivalent ligand **33** (Figure 6D). In summary, not only synthetic polymers^[9] or antibodies^[10,11] but also tetravalent **24** and even more pronounced the hexavalent **28** were able to cluster Siglec-8 in microdomains necessary for producing the biological response. Small monovalent molecules, however, are not able to create these microdomains and only antagonistically bind the protein in the positions in which they are present on the cell surface.

Further studies with cells naturally expressing Siglec-8 will be conducted to test the effect on Siglec-8 induced apoptosis of eosinophils and mast cells by novel oligovalent Siglec-8 ligands. This would be an important step towards the application of such molecules for the treatment of eosinophil- or mast cell-associated disorders.

Experimental Part

Protein expression and purification. Protein expression was performed in *Escherichia coli* strain Rosetta-gami B (DE3), which were transfected as previously described.^[18b] Cells were initially cultivated overnight in 15 mL Terrific Broth medium substituted with 0.1 mg/mL ampicillin at 37 °C and then transferred into 1 L Terrific Broth medium substituted with 0.1 mg/mL ampicillin. Cells were incubated for 5 h at 37 °C and 160 rpm, then Siglec-8 expression was induced by addition of 1.0 mM IPTG. After 16 h, cells were harvested by centrifugation (5000 rpm, 30 min, 4 °C), resuspended in 20 mL lysis buffer (50 mM Tris·HCl, 10 mM MgCl₂, 0.1 % Triton X100, pH 7.5), and lysed by addition of 1.0 mg/mL lysozyme, incubating on ice for 4 h. The cell lysate was centrifuged (11000 rpm, 15 min, 4 °C), the supernatant discarded, and the precipitated material was washed three times with 25 mL washing buffer (50 mM Tris·HCl, 4 M urea, 500 mM NaCl, pH 8.0). The purified inclusion bodies were dissolved in 20 mL of denaturation buffer (6 M guanidine hydrochloride, 100 mM Tris·HCl, 1 mM DTT, pH 8.0) for 1 h at 37 °C. After ultracentrifugation (22000 rpm, 30 min, 4 °C), the denatured protein was refolded by slow dilution into 100 mL refolding

buffer (100 mM Tris·HCl, 1 M L-arginine, 150 mM NaCl, 120 mM sucrose, pH 8.0). The mixture was stirred for 2 d at 4 °C and dialyzed against binding buffer (50 mM NaH₂PO₄, 20 mM imidazole, 300 mM NaCl, pH 8.0). Precipitated protein was removed by ultracentrifugation (22000 rpm, 30 min, 4 °C) and the refolded soluble protein was purified by affinity chromatography on a Ni-NTA column (50 mM NaH₂PO₄, 250 mM imidazole, 300 mM NaCl, pH 8.0). The fractions containing 6His-Siglec-8-CRD were pooled and dialyzed against assay buffer (100 mM HEPES, 150 mM NaCl, pH 7.4). The purity of the protein was verified by non-reducing SDS-PAGE.

Differential scanning fluorimetry. Differential scanning fluorimetry assays were performed using a Prometheus NT.48 (Nanotemper, Munich, Germany) instrument set to 50 % excitation power and 1.0 °C/min temperature slope. The Nanotemper Pr.ThermControl software suite was employed for analysis of experimental data. In a typical experiment, a 20 µM solution of Siglec-8-CRD was incubated alone or with 1 mM solution of ligand and measured over a temperature range from 20 to 80 °C.

Isothermal Titration Calorimetry. Isothermal titration calorimetry experiments were performed at 25 °C (or a specified different temperature) on an ITC200 (MicroCal, Northampton, USA) instrument set to 6 µcal·s⁻¹ reference power, 750 rpm stirring speed, feedback mode high, 2 s filter period. Protein solutions were dialyzed against ITC buffer (100 mM HEPES, 150 mM NaCl, pH 7.4) prior to the experiments and all samples were prepared using the dialysate buffer to minimize dilution effects. Protein concentrations were determined spectrophotometrically with the specific absorbance at 280 nm employing an extinction coefficient of 33240 mol⁻¹·cm⁻¹. In a typical experiment, a 0.5 – 10 mM ligand solution was titrated to a solution containing 35 – 100 µM Siglec-8 to ensure more than 80 % saturation. For low c experiment, the stoichiometry parameter was constrained to 1, 0.5, 0.33, 0.25 and 0.167, according to valency. Baseline correction, peak integration, and non-linear regression analysis of experimental data were performed using the NITPIC (version 1.2.2.)^[32] and SEDPHAT (version 12.1b)^[33] software packages. Replicates were analyzed using global fitting, and the 95 % confidence intervals were calculated as an estimate of experimental error.

Cell-based Assay

Cell lines and culture conditions. Jurkat NFAT (Luc2) cells were cultured in RPMI1640 (Sigma) supplemented with 10 % heat-inactivated fetal bovine serum (PAN Biotech), 1 mM sodium pyruvate (Sigma), 1x non-essential amino acids (Sigma), 100 µg/mL streptomycin and penicillin (Sigma) and 50 nM β-mercaptoethanol (Gibco). Cells were routinely incubated at 37 °C and 5% CO₂.

Expression construct. The lentiviral plasmid (pLV-Sig8) containing the human Siglec-8 gene (NM_014442.3) followed by an eGFP reporter was purchased from VectorBuilder Inc. (ID: VB210104-1025kgy) as a bacterial stock (*E. coli*). Bacteria were plated on ampicillin plates and incubated at 37 °C overnight. A colony was picked, inoculated in 200 mL LB medium containing 100 µg/mL ampicillin and incubated overnight at 37 °C and 220 rpm. Plasmid DNA was purified using Nucleobond Xtra Midi plus kit (Macherey-Nagel) according to the manufacturer's protocol.

Production of lentivirus. Lentivirus was produced in HEK293T cells by transient cell transfection using the polyethylenimine (PEI) method. HEK293T cells were cultivated in 15 cm petri dishes to a confluency of 80 – 90% and were transfected with three plasmids: pCMV-dR8.9 (containing gag, pol and rev genes), pMD2G VSVg (containing envelope gene), and pLV-Sig8 or empty SFFV-eGFP plasmid in combination with PEI at a ratio of 1:3. Transfected HEK293T cells were incubated for 48 h at 37 °C and 5% CO₂. Supernatants containing the lentivirus were collected and replaced by fresh medium. Supernatants were centrifuged for 10 min at 2000 g and 4 °C, filtered through 0.45 µm filter and stored at 4 °C. After additional 24 h of incubation, supernatants were collected and centrifuged again. Lentiviruses were concentrated using 4x polyethylenglycol-8000 (PEG8000) buffer (40 % w/V PEG8000 (Sigma), 1.2 M NaCl (Sigma) in 1x PBS (Sigma) at pH 7.0). An appropriate volume of 4x PEG8000 buffer was added to supernatants to reach 1x buffer concentration and incubated for 24 h at 4 °C. The following day, supernatants were centrifuged for 45 min at 1500 g (4 °C) and discarded. Pellets containing the lentivirus were dissolved in 500 µL cold and sterile PBS. Lentiviruses were aliquoted and stored at -80 °C.

Transduction of Jurkat NFAT (Luc2) cells. 1 Mio. Jurkat NFAT (Luc2) cells per well were seeded in a 24-well plate. 100 µL of Siglec-8 or SFFV-eGFP containing lentivirus were added to corresponding wells and polybrene (Sigma) was added to a working concentration of 8 µg/mL. Subsequently, the plate was centrifuged at 1000 rpm for 10 min and incubated for 24 h at 37 °C and 5% CO₂. The medium was exchanged and cells were expanded in supplemented RPMI 1640 medium for one week. Ten days post transduction, GFP positive cells were sorted by flow cytometry. Cell lines were stored in DMSO/FBS (10:90) in liquid nitrogen until further usage.

Sialidase pre-treatment. An appropriate number of cells was resuspended to a concentration of 1 Mio. cells/mL in non-supplemented RPMI1640 medium containing 2% FBS. Vibrio Cholera sialidase (Roche) was added at a working concentration of 10 mU/mL and incubated for 30 min in an

end-over-end mixer at 37 °C and 5% CO₂. Afterwards, cells were washed once with and subsequently resuspended in full RPMI1640 medium before using them for the luciferase assay.

Luciferase assay. Anti-human CD3 (OKT3) antibodies (BioLegend) were diluted in 1x PBS (Sigma) to a concentration of 3 µg/mL. A 96 well flat bottom plate was coated with 50 µL anti-human CD3 antibodies overnight at 4 °C. Pre-coated wells were washed twice with 200 µL 1x PBS. 1·10⁵ Jurkat NFAT (Luc2) cells expressing either Siglec-8 or eGFP alone were added per well. Siglec-8 ligands were added to cells at varying concentrations. After incubation for 6 h at 37 °C and 5% CO₂, cells were transferred into a 96 well V-bottom plate, centrifuged for 3 min at 1500 rpm and 140 µL of supernatant were removed. 50 µL of ONE-Glo™ Luciferase buffer was added to each sample after preparing the reagent according to the protocol of ONE-Glo™ Luciferase Assay System (Promega). After an incubation time of 3-5 min, 80 µL of each sample were transferred into a white-bottom 96 well plate and, subsequently, luminescence was analyzed in a Synergy H1 microplate reader (BioTek).

Acknowledgement

This project has received funding from the European Union's Horizon 2020 research and innovation program under the Marie Skłodowska-Curie grant agreement No 765581. We also thank Dr. Pierre Thesmar (Organic Chemistry, Department of Chemistry, University of Basel, St. Johannis-Ring 19, 4056 Basel), and Ad van der Eerden and Thomas Dezaire (Inorganic Chemistry and Catalysis, Department of Chemistry, Utrecht University, Universiteitsweg 99, 3584 CG Utrecht) for their technical support in performing the hydrogenation at high pressure.

References

- 1 a) Varki, A.; Angata, T. Siglec - the major subfamily of I-type lectins, *Glycobiology* **2005**, *16*, 1R-27R; b) Macauley, M. S.; Crocker, P. R.; Paulson, J. C. Siglec-mediated regulation of immune cell function in disease. *Nat. Rev. Immunol.* **2014**, *14*, 653–666.
- 2 Crocker, P. R.; Paulson, J. C.; Varki, A. Siglecs and their roles in the immune system. *Nat. Rev. Immunol.* **2007**, *7*, 255–266.
- 3 Ravetch, J. V.; Lanier, L. L. Immune inhibitory receptors, *Science* **2000**, *290*, 84-89.
- 4 a) Crocker, P. R.; Redelinghuys, P. Siglecs as positive and negative regulators of the immune system, *Biochem. Soc. Trans.* **2008**, *36*, 1467-1471; b) Paulson, J. C.; MacAuley, M. S.; Kawasaki, N. Siglecs as sensors of self in innate and adaptive immune responses, *Ann. N. Y. Acad. Sci.* **2012**, *1253*, 37-48.

- 5 Collins, B. E.; Blixt, O.; DeSieno, A. R.; Bovin, N.; Marth, J. D.; Paulson, J. C. Masking of CD22 by cis ligands does not prevent redistribution of CD22 to sites of cell contact, *Proc. Natl. Acad. Sci. U. S. A.* **2004**, *101*, 6104-6109.
- 6 Collins, B. E.; Blixt, O.; Han, S.; Duong, B.; Li, H.; Nathan, J. K.; Bovin, N.; Paulson, J. C. High-Affinity Ligand Probes of CD22 Overcome the Threshold Set by *cis* Ligands to Allow for Binding, Endocytosis, and Killing of B Cells, *J. Immunol.* **2006**, *177*, 2994-3003.
- 7 a) Youngblood, B. A.; Leung, J.; Falahati, R.; Williams, J.; Schanin, J.; Brock, E. C.; Singh, B.; Chang, A. T.; O'Sullivan, J. A.; Schleimer, R. P.; Tomasevic, N.; Bebbington, C. R.; Bochner, B. S. Discovery, Function, and Therapeutic Targeting of Siglec-8, *Cells* **2021**, *10*, 19;
b) T. Kiwamoto, N. Kawasaki, J. C. Paulson, B. S. Bochner, Siglec-8 as a drugable target to treat eosinophil and mast cell-associated conditions, *Pharmacol. Ther.* **2012**, *135*, 327–336.
- 8 a) Youngblood, B. A.; Leung, J.; Falahati, R.; Williams, J.; Schanin, J.; Brock, E. C.; Singh, B.; Chang, A. T.; O'Sullivan, J. A.; Schleimer, R. P.; Tomasevic, N.; Bebbington, C. R.; Bochner, B. S. Discovery, function, and therapeutic targeting of Siglec-8. *Cell* **2021**, *10*, 19-32.
b) Kerr, S. C.; Gonzalez, J. R.; Schanin, J.; Peters, M. C.; Lambrecht, B. N.; Brock, E. C.; Charbit, A.; Ansel, K. M.; Youngblood, B. A.; Fahy, J. V. An anti-siglec-8 antibody depletes sputum eosinophils from asthmatic subjects and inhibits lung mast cells. *Clin. Exp. Allergy* **2020**, *50*; 904-914; c) Schanin, J.; Gebremeskel, S.; Korver, W.; Falahati, R.; Butuci, M.; Haw, T. J.; Nair, P. M.; Liu, G.; Handsbro, N. G.; Hansbro, P. M.; Eversen, E.; Brock, E. C.; Xu, A.; Wong, A.; Leung, J.; Bebbington, C.; Tomasevic, N.; Youngblood, B. A. A monoclonal antibody to Siglec-8 suppresses non-allergic airway inflammation and inhibits IgE-independent mast cell activation. *Mucosal Immun.* **2021**, *14*, 366-376.
- 9 a) Rillahan, C. D.; Schwartz, E.; Rademacher, C.; McBride, R.; Rangarajan, J.; Fokin, V. V.; Paulson, J. C.. On-Chip Synthesis and Screening of a Sialoside Library Yields a High Affinity Ligand for Siglec-7. *ACS Chem Biol.* **2013**, *8*, 1417–1422; b) Chibarev, A. A.; Galanina, O. E.; Bovin, N. V. Biotinylated multivalent glycoconjugates for surface coating. *Methods Mol. Biol.* **2010**, *600*, 67-78; c) Rapoport, E. M.; Pazynina, G. V.; Sablina, M. A.; Crocker, P. R.; Bovin, N. V. Probing sialic acid binding Ig-like lectins (siglecs) with sulfated oligosaccharides. *Biochem. (Moscow)*, **2006**, *71*, 496-504; d) S. Duan, B. M. Arlian, C. M. Nycholat, Y. Wei, H. Tateno, S. A. Smith, M. S. Macauley, Z. Zhu, B. S. Bochner, J. C. Paulson, Nanoparticles Displaying Allergen and Siglec-8 Ligands Suppress IgE-Fc ϵ RI-Mediated Anaphylaxis and Desensitize Mast Cells to Subsequent Antigen Challenge, *J. Immunol.* **2021**, *206*, 2290-2300.
- 10 a) Hudson, S. A.; Bovin, N. V.; Schnaar, R. L.; Crocker, P. R. Bochner, B. S. Eosinophil-selective binding and proapoptotic effect in vitro of a synthetic siglec-8 ligand, polymeric 6'-

- sulfated sialyl Lewis^x, *J. Pharmacol. Exp. Ther.* **2009**, *330*, 608-612; Nutku, E.; Alzawa, H.; Hudson, S. A.; Bochner, B. S. Ligation of Siglec-8: a selective mechanism for induction of human eosinophil apoptosis, *Blood* **2003**, *101*, 5014-5020.
- 11 a) Yokoi, H.; Choi, O. H.; Hubbard, W.; Lee, H.-S.; Canning, B. J.; Lee, H. H.; Ryu, S.-D.; von Gunten, S.; Bickel, C. A.; Hudson, S. A.; MacGlashan, D. W.; Bochner, B. S. Inhibition of FcεRI-dependent mediator release and calcium flux from human mast cells by sialic acid-binding immunoglobulin-like lectin 8 engagement, *J. Allergy Clin. Immunol.* **2008**, *121*, 499-505; b) Dellon, E. S.; Peterson, K. A.; Murray, J. A.; Falk, G. W.; Gonsalves, N.; Chehade, M.; R. Genta, R. M.; Leung, J.; Khoury, P.; Klion, A. D.; Hazan, S.; Vaezi, M.; Bledsoe, A. C.; Durrani, S. R.; Wang, C.; Shaw, C.; Chang, A. T.; Singh, B.; Kamboj, A. P.; Rasmussen, H. S.; Rothenberg, M. E.; Hirano, I. Anti-Siglec-8 Antibody for Eosinophilic Gastritis and Duodenitis, *N. Engl. J. Med.* **2020**, *383*, 1624-1634; c) Legrand, F.; Cao, Y.; Wechsler, J. B.; Zhu, X.; Zimmermann, N.; Rampertaap, S.; Monsale, J.; Romito, K.; Youngblood, B. A.; Brock, E. C.; Makiya, M. A.; Tomasevic, N.; Bebbington, C.; Maric, I.; Metcalfe, D. D.; Bochner, B. S.; Klion, A. D. Sialic acid-binding immunoglobulin-like lectin (Siglec) 8 in patients with eosinophilic disorders: Receptor expression and targeting using chimeric antibodies, *J. Allergy Clin. Immunol.* **2019**, *143*, 2227-2237; d) Youngblood, B. A.; Brock, E. C.; Leung, J.; Falahati, R.; Bryce, B. J.; Bright, J.; Williams, J.; Shultz, L. D.; Greiner, D. L.; Brehm, M. A.; Bebbington, C.; Tomasevic, N. AK002, a Humanized Sialic Acid-Binding Immunoglobulin-Like Lectin-8 Antibody that Induces Antibody-Dependent Cell-Mediated Cytotoxicity against Human Eosinophils and Inhibits Mast Cell-Mediated Anaphylaxis in Mice, *Int. Arch. Allergy Immunol.* **2019**, *180*, 91-102; e) Schanin, J.; Gebremeskel, S.; Korver, W.; Falahati, R.; Butuci, M.; Jhong Haw, T.; Nair, P. M.; Liu, G.; Hansbro, N. G.; Hansbro, P. M.; Evensen, E.; Brock, E. C.; Xu, A.; Wong, A.; Leung, J.; Bebbington, C.; Tomasevic, N.; Youngblood, B. A. A monoclonal antibody to Siglec-8 suppresses non-allergic airway inflammation and inhibits IgE-independent mast cell activation, *Mucosal Immunol.* **2021**, *14*, 366-276; f) Smith, B. A. H.; Bertozzi, C. R. The clinical impact of glycobiology: targeting selectins, siglecs and mammalian glycans. *Nat. Rev. Drug Discov.* **2021**, *20*, 217-243.
- 12 Hudson, S. A.; Bovin, N. V.; Schnaar, R. L. Crocker, P. R.; Bochner, B. S. Eosinophil-Selective Binding and Proapoptotic Effect in Vitro of a Synthetic Siglec-8 Ligand, Polymeric 6 -Sulfated Sialyl Lewis X, *J. Pharmacol. Exp. Ther.* **2009**, *330*, 608-612.
- 13 Jia, Y.; Yu, H.; Fernandes, S. M.; Wei, Y.; Gonzalez-Gil, A.; Bochner, B. S.; Kern, R. C.; Schleimer, R. P.; Schnaar, R. L. Expression of ligands for Siglec-8 and Siglec-9 in human airways and airway cells, *J. Allergy Clin. Immunol.* **2015**, *135*, 799-810.

- 14 Angata, T.; Nycholat, C. M.; Macauley, M. S. Therapeutic targeting of siglecs using antibody- and glycan-based approaches, *Trends Pharmacol. Sci.* **2015**, *36*, 645-660.
- 15 a) Tateno, H.; Crocker, P. R.; Paulson, J. C. Mouse Siglec-F and human Siglec-8 are functionally convergent paralogs that are selectively expressed on eosinophils and recognize 6'-sulfo-sialyl Lewis X as a preferred glycan ligand. *Glycobiology* **2005**, *15*, 1125–1135; b) Bochner, B. S.; Alvarez, R. A.; Mehta, P.; Bovin, N. V.; Blixt, O.; White J. R. , *et al.* Glycan array screening reveals a candidate ligand for Siglec-8. *J. Biol. Chem.* **2005**, *280*, 4307–4312.
- 16 Pröpster, J. M.; Yang, F.; Rabbani, S.; Ernst, B.; Allain, F. H.-T.; Schubert, M. Structural basis for sulfation-dependent self-glycan recognition by the human immune-inhibitory receptor Siglec-8, *PNAS* **2016**, *113*, E4170–E4179.
- 17 a) Abdu-Allah, H. H. M.; Watanabe, K.; Completo, G. C.; Sadagopan, M.; Hayashizaki, K.; Takaku, C.; Tamanaka, T.; Takematsu, H.; Kozutsumi, Y.; Paulson, J. C.; Tsubata, T.; Ando, H.; Ishida, H.; Kiso, M. CD22-Antagonists with Nanomolar Potency: The Synergistic Effect of Hydrophobic Groups at C-2 and C-9 of Sialic Acid Scaffold, *Bioorg. Med. Chem.* **2011**, *19*, 1966-1971; b) Mesch, S.; Lemme, K.; Wittwer, M.; Koliwer-Brandl, H.; Schwardt, O.; Kelm, S.; Ernst, B. From a library of MAG antagonists to nanomolar CD22 ligands, *ChemMedChem* **2012**, *7*, 134-143; c) Schwardt, O.; Kelm, S.; Ernst, B. Siglec-4 (MAG) antagonists: From the natural epitope to glycomimetics, *Top. Curr. Chem.* **2015**, *367*, 151-200; c) Prescher, H.; Frank, M.; Guütgemann, S.; Kuhfeldt, E.; Schweizer, A.; Nitschke, L.; Watzl, C.; Brossmer, R.; Design, Synthesis, and Biological Evaluation of Small, High-Affinity Siglec-7 Ligands: Toward Novel Inhibitors of Cancer Immune Evasion, *J. Med. Chem.* **2017**, *60*, 941-956.
- 18 a) Nycholat, C. M.; Duan, S.; Knuplez, E.; Worth, C.; Elich, M.; Yao, A.; O'Sullivan, J.; McBride, R.; Wei, Y.; Fernandes, S. M.; Zhu, Z.; Schnaar, R. L.; Bochner, B. S.; Paulson, J. C. A sulfonamide sialoside analogue for targeting Siglec-8 and-F on immune cells. *J. Am. Chem. Soc.* **2019**, *141*, 14032-14037; b) Kroezen, B. S.; Conti, G.; Girardi, B.; Cramer, J.; Jiang, X.; Rabbani, S.; Müller, J.; Kokot, M.; Luisoni, E.; Ricklin, D.; Schwardt, O.; Ernst, B. A Potent Mimetic of the Siglec-8 Ligand 6'-Sulfo-Sialyl Lewis^x, *ChemMedChem* **2020**, *15*, 1706-1719.
- 19 a) Pieters, R. J. Maximising multivalency effects in protein-carbohydrate interactions, *Org. Biomol. Chem.* **2009**, *7*, 2013–2025; b) Lundquist, J. J.; Toone, E. J. The cluster glycoside effect, *Chem. Rev.* **2002**, *102*, 555-578; c) Lu, W.; Pieters, R. J. Carbohydrate–protein interactions and multivalency: implications for the inhibition of influenza A virus infections, *Expert Opin. Drug Discov.* **2019**, *14*, 387–395.
- 20 a) Wagner, B.; Binder, F. P. C.; Jiang, X.; Mühlethaler, T.; Preston, R. C.; Rabbani, S.; Smieško, M.; Schwardt, O.; Ernst, B. A Structural-Reporter Group to Determine the Core Conformation

- of Sialyl Lewisx Mimetics. *Molecules* **2023**, *28*, 2595–2604; b) Rotticci, D.; Norin, T.; Hult, K. Mass transport limitation reduce the effective stereospecificity in enzyme-catalyzed kinetic resolution. *Org. Lett.* **2000**, *2*, 1373–1376; Ter Halle, R.; Bernet, Y.; Billard, S.; Bufferne, C.; Carlier, P.; Delaitre, C.; Flouzat, C.; Humbolt, G.; Laigle, J. C.; Lombard, F.; *et al.* Development of a practical multikilogram production of (*R*)-seudenol by enzymatic resolution. *Org. Process Res. Dev.* **2004**, *8*, 283–286.
- 21 Zhao, Y.; Wu, Y.; De Clercq, P.; Vandewalle, M.; Maillos, P.; Pascal, J. C. Asymmetrization of all-cis-3,5-dihydroxy-1-(methoxycarbonyl)cyclohexane and of the 4-methyl and 4-ethyl substituted homologues, *Tetrahedron Asymmetry* **2000**, *11*, 3887–3900.
- 22 Fritz, S. P. Diphenylvinylsulfonium triflate. *Synlett* **2012**, *23*, 480-481.
- 23 Chao, C. S.; Chen, M. C.; Lin, S. C.; Mong, K. K. T. Versatile acetylation of carbohydrate substrates with bench-top sulfonic acids and application to one-pot syntheses of peracetylated thioglycosides, *Carbohydr. Res.* **2008**, *343*, 957–964.
- 24 Kolb, H. C.; Finn, M. G.; Sharpless, K. B. Click chemistry: Diverse chemical function from a few good Reactions. *Angew. Chem., Int. Ed.* **2001**, *40*, 2004–2021.
- 25 Chan, T. R.; Hilgraf, R.; Sharpless, K. B.; Fokin, V. V. Polytriazoles as copper(I)-stabilizing ligands in catalysis, *Org. Lett.* **2004**, *6*, 2853–2855.
- 26 a) Cramer, J.; Aliu, B.; Jiang, X.; Sharpe, T.; Pang, L.; Hadorn, A.; Rabbani, S.; Ernst, B. Poly-L-lysine Glycoconjugates Inhibit DC-SIGN-mediated Attachment of Pandemic Viruses, *ChemMedChem* **2021**, *16*, 2345–2353; b) J. Cramer, J.; A. Lakkaichi, A.; B. Aliu, B.; R. P. Jakob, R. P.; S. Klein, S.; I. Cattaneo, J.; X. Jiang, X.; S. Rabbani, S.; O. Schwardt, O.; G. Zimmer, G.; M. Ciancaglini, M.; T. Abreu Mota, T.; T. Maier, T.; B. Ernst, B. Sweet Drugs for Bad Bugs: A Glycomimetic Strategy against the DCSIGN-Mediated Dissemination of SARS-CoV-2, *J. Amer. Chem. Soc.* **2021**, *143*, 17465-17478.
- 27 Niesen, F. H.; Berglund, H.; Vedadi, M. The use of differential scanning fluorimetry to detect ligand interactions that promote protein stability, *Nat. Protoc.* **2007**, *2*, 2212-2221.
- 28 Chodera, J. D.; Mobley, D. L. Entropy-enthalpy compensation: Role and ramifications in biomolecular ligand recognition and design, *Annu. Rev. Biophys.* **2013**, *42*, 121-141.
- 29 Hudson, S. A.; Bovin, N. V.; Schnaar, R. L.; Crocker, P. R.; Bochner, B. S. Eosinophil-selective binding and proapoptotic effect in vitro of a synthetic siglec-8 ligand, polymeric 6'-sulfated sialyl lewis X, *J. Pharmacol. Exp. Ther.* **2009**, *330*, 608–612.
- 30 Ikehara, Y.; Ikehara, S. K.; Paulson, J. C. Negative Regulation of T Cell Receptor Signaling by Siglec-7 (p70/AIRM) and Siglec-9, *J. Biol. Chem.* **2004**, *279*, 43117–43125.
- 31 Razi, N.; Varki, A. Masking and unmasking of the sialic acid-binding lectin activity of CD22

- (Siglec-2) on B lymphocytes. *Proc. Natl. Acad. Sci. U.S.A.* **1998**, *95*, 7469-7474.
- 32 Scheuermann, T. H.; Brautigam, C. A. High-precision, automated integration of multiple isothermal titration calorimetric thermograms: New features of NITPIC, *Methods* **2015**, *76*, 87–98.
- 33 Zhao, H.; Piszczek, G.; Schuck, P. SEDPHAT – A platform for global ITC analysis and global multi-method analysis of molecular interactions, *Methods* **2015**, *76*, 137–148.

Supporting Information

1. Synthesis

1.1. General methods. NMR spectra were recorded on Bruker Avance III 500 MHz, Bruker Ultrashield 600 MHz or Varian Mercury 400 MHz instruments. Assignment of ^1H and ^{13}C NMR spectra was achieved using 2D methods (COSY, HSQC, HMBC). Chemical shifts are expressed in ppm using residual solvent signals (CHCl_3 , CHD_2OD , HDO) as reference. Optical rotations were measured with a PerkinElmer polarimeter 341. Electrospray ionization mass spectrometry (ESI-MS) data were obtained on a Waters Micromass ZQ instrument. High resolution mass (HR-MS) analyses were done on an Agilent 1100 LC, equipped with a photodiode array detector and a Bruker QTOF I with a 4 GHz digital-time converter; or on a Thermo Fisher UPLC, equipped with a Bruker maxis 4G. Reactions were monitored by TLC using glass plates coated with silica gel 60 F254 (Merck) and visualized by using UV light and/or by charring with a molybdate solution (a 0.02 M solution of ammonium cerium sulfate dihydrate and ammonium molybdate tetrahydrate in 10 % aq. H_2SO_4). Flash chromatography was done on a CombiFlash Rf from Teledyne Isco (Lincoln, NE, USA) equipped with RediSep normal phase or RP-18 reversed-phase flash columns. Size exclusion chromatography was performed on Biogel P-2 (Bio-Rad Laboratories, Inc.) or Sephadex LH-20 (GE Healthcare) media. For purification of glycopolymers, Vivaspin ultrafiltration devices with a molecular weight cutoff of 6 kDa or 50 kDa (Sartorius, Göttingen, Germany) were used. Commercially available reagents and dry solvents were purchased as reagent grade from Sigma-Aldrich, Alfa Aesar and Acros and used without further purification. Molecular sieves (3Å, 4Å) were activated under vacuum at 500 °C for 0.5 h immediately before use. 2-Bromoethyltriflate was prepared according to [1], compound **13** was prepared according to [2], and chloroacetylated poly-L-lysine polymer was prepared according to [3].

1.2. Synthesis of oligo- and multivalent glycomimetic inhibitors

Methyl 3,5-dihydroxybenzoate (5). To a solution of 3,5-dihydroxybenzoic acid (50.0 g, 324 mmol) in MeOH (250 mL), H₂SO₄ (3.75 mL in 50 mL of MeOH) was added. The reaction mixture was refluxed for 4 d. Then, the solution was cooled to rt and concentrated *in vacuo*. The residue was dissolved in EtOAc, washed with satd. aq. NaHCO₃ and H₂O, dried over Na₂SO₄ and evaporated to afford **5** (56.00 g, quant.). ¹H NMR (500 MHz, DMSO-*d*₆): δ = 6.81 (d, *J* = 2.3 Hz, 2H, H-2, H-6), 6.44 (t, *J* = 2.3 Hz, 1H, H-4), 3.78 (s, 3H, OMe); ¹³C NMR (126 MHz, DMSO-*d*₆): δ = 166.4 (C=O), 158.8 (C-3, C-5), 131.3 (C-1), 107.3 (C-4), 107.1 (C-2, C-6), 52.0 (OMe); MS (ESI): *m/z* calcd for C₈H₈O₄: 191.0 [M+Na]⁺; found: 190.9.

Methyl (1*r*,3*R*,5*S*)-3,5-dihydroxycyclohexane-1-carboxylate (6). Compound **5** (6.02 g, 35.8 mmol) and Rh/Al₂O₃ (5 %, 936 mg) were dissolved in MeOH (50 mL) and AcOH (1.2 mL). The reactor was conditioned with H₂, then the mixture was stirred at 100 °C for 72 h (90 atm H₂). Then, the solution was cooled to rt and vented, filtered over celite and concentrated *in vacuo* to afford **6** (6.44 g, quant.) as a white solid. ¹H NMR (500 MHz, D₂O): δ = 3.78 – 3.70 (m, 2H, H-3, H-5), 3.73 (s, 3H, OMe), 2.53 (tt, *J* = 12.7, 3.5 Hz, 1H, H-1), 2.28 (d, *J* = 11.3 Hz, 1H, H-4e), 2.18 (d, *J* = 11.6 Hz, 2H, H-2e, H-6e), 1.31 (q, *J* = 12.0 Hz, 2H, H-2a, H-6a), 1.25 (q, *J* = 11.3 Hz, 1H, H-4a); ¹³C NMR (126 MHz, D₂O): δ = 178.2 (C=O), 68.0 (C-3, C-5), 53.3 (OMe), 43.4 (C-4), 39.1 (C-1), 36.8 (C-2, C-6); MS (ESI): *m/z* calcd for C₈H₁₄O₄: 197.1 [M+Na]⁺, found: 196.9.

Methyl (1*S*,3*S*,5*R*)-3-acetoxy-5-hydroxycyclohexane-1-carboxylate (7). Compound **6** (3.16 g, 18.2 mmol) and PPL (lipase from porcine pancreas, type II; 10.01 g) were suspended in vinyl acetate (100 mL). The mixture was stirred at rt under argon in the dark. After 20 h, the solution was filtered over celite and concentrated *in vacuo*. The crude product was purified by flash column chromatography (DCM/MeOH, 1:0 to 9:1) to give **7** (3.72 g, 95 %). $[\alpha]_D^{20} = +23.3$ (*c* = 1.0, DCM); ¹H NMR (600 MHz, CDCl₃): δ = 4.73 (tt, *J* = 11.4, 4.3 Hz, 1H, H-5), 3.72 (tt, *J* = 11.2, 4.2 Hz, 1H, H-3), 3.68 (s, 3H, OMe), 2.41 (tt, *J* = 12.6, 3.6 Hz, 1H, H-1), 2.29 (ddq, *J* = 11.6, 4.1, 2.0 Hz, 1H, H-4e), 2.25 – 2.19 (m, 2H, H-2e, H-6e), 2.04 (s, 3H, OAc), 1.47 – 1.32 (m, 3H, H-2a, H-4a, H-6a); ¹³C NMR (126 MHz, CDCl₃): δ = 174.4, 170.7 (2 C=O), 69.7 (C-3), 67.3 (C-5), 52.2 (OMe), 40.2 (C-4), 38.1 (C-1), 36.8 (C-6), 33.0 (C-2), 21.3 (OAc); MS (ESI): *m/z* calcd for C₁₀H₁₆O₅: 239.1 [M+Na]⁺, found: 238.8.

Methyl (1*R*,3*R*,5*S*)-5-acetoxy-3-((*R*)-(-)- α -methoxy- α -(trifluoromethyl)phenylacetoxy)cyclohexane-1-carboxylate (8). To a solution of compound **7** (7.3 mg, 0.048 mmol) in dry DCM (0.4 mL), DMAP (9.8 mg, 0.080 mmol) and (*R*)-(-)-MTPA-Cl (9 μ L, 0.048 mmol) were added at 0

°C. The reaction mixture was stirred at 0 °C for 15 min and then for 1 h at rt. The reaction mixture was diluted with Et₂O (5.0 mL), washed twice with 1 M aq. HCl (5.0 mL), satd. aq. NaHCO₃ (5.0 mL) and water (5.0 mL), dried over Na₂SO₄, filtered, and concentrated *in vacuo*. Crude **8** was directly subjected to ¹H NMR investigation without further purification. ¹H NMR (500 MHz, CDCl₃): δ = 7.51 – 7.46 (m, 2H, Ar-H), 7.43 – 7.38 (m, 3H, Ar-H), 5.04 (tt, *J* = 11.6, 4.4 Hz, 1H, H-3), 4.79 (tt, *J* = 11.6, 4.3 Hz, 1H, H-5), 3.69 (s, 3H, CO₂Me), 3.54 (s, 3H, OMe), 2.51 (tt, *J* = 12.8, 3.5 Hz, 1H, H-1), 2.38 (dtd, *J* = 14.0, 3.8, 1.8 Hz, 1H, H-4e), 2.35 – 2.27 (m, 2H, H-2e, H-6e), 2.03 (s, 3H, OAc), 1.58 (q, *J* = 12.4 Hz, 1H, H-4a), 1.52 – 1.39 (m, 2H, H-2a, H-6a); ¹³C NMR (126 MHz, CDCl₃): δ = 173.6, 170.3, 165.7 (3 C=O), 132.1, 129.8, 128.6, 127.2 (6C, Ar-C), 123.3 (q, *J* = 288.7 Hz, CF₃), 71.5 (C-5), 68.8 (C-3), 55.6 (OMe), 52.4 (CO₂Me), 37.8 (C-1), 36.2 (C-2), 33.1, 32.9 (C-4, C-6), 21.3 (OAc).

Methyl (1S,3S,5R)-3-acetoxy-5-(2-bromoethoxy)cyclohexane-1-carboxylate (9). To a solution of **7** (2.31 g, 10.7 mmol) in toluene (150 mL), DIPEA (9.3 mL, 53.4 mmol) was added, followed by 2-bromoethyltriflate (8.6 mL, 63.7 mmol) under nitrogen. The solution was stirred at rt for 24 h, then additional 2-bromoethyltriflate (1 mL, 7.41 mmol) was added and the mixture heated to 80 °C. After another 24 h, additional 2-bromoethyltriflate (1 mL, 7.41 mmol) was added and the temperature raised to 100 °C. Following complete conversion of the starting material, the solution was cooled to rt, washed with satd. aq. NaHCO₃ and H₂O, dried over Na₂SO₄, filtered and concentrated *in vacuo*. The crude product was purified by flash column chromatography (petroleum ether/EtOAc, 8:2 to 7:3) to give **9** (3.63 g, quant.). $[\alpha]_D^{20} = -1.2$ (*c* = 1.0, DCM); ¹H NMR (600 MHz, CDCl₃): δ = 4.70 (tt, *J* = 11.5, 4.8 Hz, 1H, H-3), 3.78 (q, *J* = 6.5 Hz, 2H, OCH₂), 3.68 (s, 3H, OMe), 3.48 – 3.36 (m, 3H, H-5, CH₂Br), 2.40 – 2.28 (m, 3H, H-1, H-4e, H-6e), 2.22 (d, *J* = 12.7 Hz, 1H, H-2e), 2.03 (s, 3H, OAc), 1.44 (q, *J* = 12.2 Hz, 1H, H-2a), 1.38 – 1.29 (m, 2H, H-4a, H-6a); ¹³C NMR (151 MHz, CDCl₃): δ = 174.0, 170.4 (2 C=O), 75.4 (C-5), 69.6 (C-3), 68.7 (OCH₂), 52.1 (OMe), 38.1 (C-1), 37.6 (C-6), 34.0 (C-4), 33.4 (C-2), 30.7 (CH₂Br), 21.3 (OAc); MS (ESI): *m/z* calcd for C₁₂H₁₉BrO₅: 345.0 [M+Na]⁺, found: 344.9.

Methyl (1S,3S,5R)-3-acetoxy-5-(2-azidoethoxy)cyclohexane-1-carboxylate (10). To a solution of **9** (4.85 g, 15.0 mmol) in DMF (60 mL), NaN₃ (2.48 mL, 38.1 mmol) was added under nitrogen and the mixture was stirred at rt. After 24 h, the solvent was removed under *vacuo* and the crude product was purified by flash column chromatography (petroleum ether/EtOAc, 8:2 to 7:3) to afford **10** (4.11 g, 96 %). $[\alpha]_D^{20} = -1.4$ (*c* = 1.0, DCM); ¹H NMR (600 MHz, CDCl₃): δ = 4.71 (tt, *J* = 11.7, 4.3 Hz, 1H, H-3), 3.70 – 3.63 (m, 5H, OCH₂, OMe), 3.39 (tt, *J* = 11.0, 4.0 Hz, 1H, H-5), 3.34 (td, *J* = 4.7,

4.3, 2.5 Hz, 2H, CH₂N₃), 2.41 – 2.31 (m, 3H, H-1, H-4e, H-6e), 2.26 – 2.20 (m, 1H, H-2e), 2.04 (s, 3H, OAc), 1.45 (q, $J = 12.2$ Hz, 1H, H-2a), 1.39 – 1.30 (m, 2H, H-4a, H-6a); ¹³C NMR (151 MHz, CDCl₃): $\delta = 174.1, 170.5$ (2 C=O), 75.5 (C-5), 69.6 (C-3), 67.6 (OCH₂), 52.2 (OMe), 51.0 (CH₂N₃), 38.2 (C-1), 37.5 (C-6), 34.0 (C-4), 33.4 (C-2), 21.3 (OAc); MS (ESI): m/z calcd for C₁₂H₁₉N₃O₅: 308.1 [M+Na]⁺, found: 308.1.

(1S,3R,5S)-3-(2-Azidoethoxy)-5-(hydroxymethyl)cyclohexyl acetate (11) and (1S,3R,5R)-3-(2-Azidoethoxy)-5-(hydroxymethyl)cyclohexan-1-ol (12). Compound **10** (5.28 g, 18.5 mmol) was dissolved in THF/MeOH (5:1, 300 mL) and cooled to 0 °C under argon. Then, LiBH₄ (2 M in THF, 9.5 mL, 19.0 mmol) was added dropwise. The mixture was allowed to reach rt. After 18 h, the solution was cooled to 0 °C, quenched by the addition of H₂O, filtered and concentrated *in vacuo*. The crude product was purified by flash column chromatography (DCM/MeOH, 1:0 to 9:1) to give **11** (0.916 g, 19 %) and **12** (1.79 g, 45 %).

11: ¹H NMR (500 MHz, CD₃OD): $\delta = 4.67$ (tt, $J = 11.6, 4.4$ Hz, 1H, H-1), 3.68 – 3.60 (m, 2H, OCH₂), 3.44 – 3.36 (m, 3H, H-3, CH₂O), 3.29 – 3.26 (m, 2H, CH₂N₃), 2.32 (dtd, $J = 12.4, 4.1, 2.1$ Hz, 1H, H-2e), 2.07 (dddd, $J = 12.2, 5.5, 3.5, 2.0$ Hz, 1H, H-4e), 1.97 (m, 4H, H-6e, OAc), 1.53 (dddp, $J = 12.7, 9.5, 6.1, 3.1$ Hz, 1H, H-5), 1.20 (q, $J = 11.4$ Hz, 1H, H-2a), 0.98 (q, $J = 12.1$ Hz, 1H, H-6a), 0.86 (td, $J = 12.4, 11.0$ Hz, 1H, H-4a); ¹³C NMR (101 MHz, CD₃OD): $\delta = 77.1$ (C-3), 72.1 (C-1), 68.5 (OCH₂), 67.5 (CH₂O), 52.0 (CH₂N₃), 39.1 (C-2), 36.6 (C-5), 35.7 (C-4), 35.4 (C-6), 21.1 (OAc); MS (ESI): m/z calcd for C₁₁H₁₉N₃O₄: 280.1 [M+Na]⁺, found: 280.2.

12: $[\alpha]_D^{20} = -0.9$ ($c = 1.0$, DCM); ¹H NMR (500 MHz, CD₃OD): $\delta = 3.63 - 3.55$ (m, 2H, OCH₂), 3.49 (tt, $J = 11.2, 4.2$ Hz, 1H, H-1), 3.35 (d, $J = 6.2$ Hz, 2H, CH₂O), 3.30 (ddd, $J = 11.2, 7.0, 4.1$ Hz, 1H, H-3), 3.23 (t, $J = 4.9$ Hz, 2H, CH₂N₃), 2.25 (dtd, $J = 11.8, 4.0, 1.9$ Hz, 1H, H-2e), 2.01 (dtd, $J = 11.8, 3.6, 1.7$ Hz, 1H, H-4e), 1.87 (dtd, $J = 11.9, 3.7, 1.8$ Hz, 1H, H-6e), 1.42 (ttt, $J = 12.7, 6.4, 3.4$ Hz, 1H, H-5), 1.05 (q, $J = 11.4$ Hz, 1H, H-2a), 0.85 – 0.70 (m, 2H, H-4a, H-6a); ¹³C NMR (151 MHz, CD₃OD): $\delta = 76.2$ (C-3), 67.6 (C-1), 67.0 (OCH₂), 66.4 (CH₂O), 50.6 (CH₂N₃), 41.3 (C-2), 37.6 (C-6), 35.5 (C-5), 34.4 (C-4); MS (ESI): m/z calcd for C₉H₁₇N₃O₃: 238.1 [M+Na]⁺, found: 237.9.

(1S,3R,5S)-3-(2-Azidoethoxy)-5-(tert-butyldiphenylsilyloxymethyl)cyclohexyl acetate (13). To a solution of **11** (841 mg, 3.27 mmol) in DCM (33 mL) were added imidazole (339 mg, 4.97 mmol) and DMAP (80.9 mg, 0.66 mmol) at 0 °C under argon, followed by dropwise addition of TBDPSCl (0.950 mL, 3.65 mmol). The mixture was stirred and allowed to reach rt. After 19 h, the reaction mixture was diluted with DCM (50 mL) and washed with H₂O (2 x 50 mL). The combined organic layers were dried over Na₂SO₄, filtered and concentrated *in vacuo*. The crude product **13** was directly

used in the next step without further purification. ^1H NMR (500 MHz, CDCl_3): δ = 7.68 – 7.61 (m, 4H, Ar-H), 7.47 – 7.35 (m, 6H, Ar-H), 4.74 (m, 1H, H-1), 3.70 – 3.63 (m, 2H, OCH_2), 3.55 (d, J = 5.8 Hz, 2H, CH_2O), 3.44 – 3.32 (m, 3H, H-3, CH_2N_3), 2.40 (dt, J = 10.4, 4.1, 2.0 Hz, 1H, H-2e), 2.11 (ddt, J = 14.0, 4.0, 1.8 Hz, 1H, H-4e), 2.05 (s, 3H, OAc), 2.00 (ddt, J = 13.9, 3.4, 1.8 Hz, 1H, H-6e), 1.63 (m, 1H, H-5), 1.29 (m, 1H, H-2a), 1.06 (s, 11H, H-4a, H-6a, *t*Bu); ^{13}C NMR (151 MHz, CDCl_3): δ = 135.9, 130.1, 127.8 (12C, Ar-C), 76.2 (C-3), 70.7 (C-1), 68.1 (CH_2O), 67.5 (OCH_2), 51.0 (CH_2N_3), 37.8 (C-2), 35.5 (C-5), 34.9 (C-6), 34.2 (C-4), 27.1 (*t*Bu), 21.3 (OAc); MS (ESI): m/z calcd for $\text{C}_{27}\text{H}_{37}\text{N}_3\text{O}_4\text{Si}$: 518.3 $[\text{M}+\text{Na}]^+$, found: 518.1.

(1S,3R,5R)-3-(2-Azidoethoxy)-5-(tert-butyldiphenylsilyloxymethyl)cyclohexan-1-ol (14). Crude compound **13** was dissolved in MeCN (50 mL) and NaOH (0.1 M, 50 mL) and the mixture was stirred at rt. After 19 h, the solution was neutralized with HCl (1 M) and concentrated *in vacuo*. The residue was purified by flash column chromatography (DCM/MeOH, 1:0 to 9:1) to give **14** (1.06 g, 71 % over two steps from **11**). $[\alpha]_D^{20}$ = -2.4 (c = 1.0, DCM); ^1H NMR (400 MHz, CDCl_3): δ = 7.68 – 7.63 (m, 4H, Ar-H), 7.46 – 7.35 (m, 6H, Ar-H), 3.72 – 3.61 (m, 3H, H-1, OCH_2), 3.55 (d, J = 5.9 Hz, 1H, CH_2O), 3.41 – 3.30 (m, 3H, H-3, CH_2N_3), 2.39 (m, 1H, H-2e), 2.12 – 2.00 (m, 2H, H-4e, H-6e), 1.60 (m, 1H, H-5), 1.23 (q, J = 11.1 Hz, 1H, H-2a), 1.09 – 0.92 (m, 11H, H-4a, H-6a, *t*Bu); ^{13}C NMR (101 MHz, CDCl_3): δ = 135.7, 133.8, 129.8, 127.8 (12C, Ar-C), 76.6 (C-3), 68.7 (C-1), 68.2 (CH_2O), 67.3 (OCH_2), 51.1 (CH_2N_3), 41.9 (C-2), 38.4 (C-6), 35.8 (C-5), 34.6 (C-4), 27.0 (*t*Bu), 19.4 (*q-t*Bu); MS (ESI): m/z calcd for $\text{C}_{25}\text{H}_{35}\text{N}_3\text{O}_3\text{Si}$: 476.2 $[\text{M}+\text{Na}]^+$, found: 476.3.

(1S,3R,5R)-3-(2-Azidoethoxy)-5-(tert-butyldiphenylsilyloxymethyl)cyclohexan-1-ol (14). To a solution of **12** (502 mg, 2.33 mmol) in DCM (23 mL) were added imidazole (242 mg, 3.56 mmol) and DMAP (59.2 mg, 0.48 mmol) at 0 °C under argon, followed by dropwise addition of TBDPSCl (0.675 mL, 2.60 mmol). The reaction was continued for 38 h, with subsequent additions of TBDPSCl (0.250 mL, 0.961 mmol), imidazole (86.5 mg, 1.27 mmol), and DMAP (22.6 mg, 0.185 mmol) until the reaction was complete (checking by TLC). The solution was then diluted with H_2O (60 mL) and extracted with DCM (4 x 40 mL). The combined organic layers were dried over Na_2SO_4 , filtered and concentrated *in vacuo*. The crude product was purified by flash column chromatography (DCM/MeOH, 1:0 to 9:1) to give **12** (749 mg, 71 %).

(1S,3R,5S)-3-(2-Azidoethoxy)-5-(tert-butyldiphenylsilyloxymethyl)cyclohexyl (methyl 5-acetamido-4,7,8,9-tetra-O-acetyl-3,5-dideoxy-D-glycero- α -D-galacto-2-nonulopyranosylonate) (16). To a suspension of **14** (284mg, 0.621 mmol), **15** (1.12 g, 1.88 mmol) and MS 3Å (1.13 g) in dry

MeCN (3.4 mL), *N*-iodosuccinimide (581 mg, 2.58 mmol) was added, followed by dropwise addition of TfOH (22 μ L, 0.249 mmol) at -40 °C under argon. The reaction mixture was stirred for 8 h at -40 °C, and then allowed to reach rt over 14 h. The suspension was neutralized with Et₃N, then filtered over a pad of celite. The solvent was evaporated, and the residue was dissolved in DCM (40 mL), washed with satd. aq. Na₂S₂O₃ (30 mL) and H₂O (30 mL), dried over Na₂SO₄, filtered and concentrated *in vacuo*. The crude product was purified by flash column chromatography (toluene/acetone, 9:1 to 1:1) to give **16** (290 mg, 50 %). $[\alpha]_D^{20} = -3.9$ ($c = 0.2$, DCM); ¹H NMR (500 MHz, CDCl₃): $\delta = 7.66 - 7.61$ (m, 4H, Ar-H), 7.45 - 7.35 (m, 6H, Ar-H), 5.41 (ddd, $J = 8.9, 5.9, 2.7$ Hz, 1H, H-8'), 5.31 (dd, $J = 9.2, 1.9$ Hz, 1H, H-7'), 5.11 (m, 1H, NH), 4.82 (ddd, $J = 12.5, 10.1, 4.6$ Hz, 1H, H-4'), 4.28 (dd, $J = 12.4, 2.7$ Hz, 1H, H-9'a), 4.09 - 4.03 (m, 3H, H-5', H-6', H-9'b), 3.73 (s, 3H, OMe), 3.72 - 3.65 (m, 3H, H-1, OCH₂), 3.55 - 3.44 (m, 3H, H-3, CH₂O), 3.35 (dt, $J = 6.1, 4.3$ Hz, 2H, CH₂N₃), 2.59 (dd, $J = 12.7, 4.5$ Hz, 1H, H-3'e), 2.48 (m, 1H, H-2e), 2.17, 2.15, 2.03, 2.02 (4 s, 12H, 4 OAc), 1.97 (m, 1H, H-4e), 1.93 (t, $J = 12.6$ Hz, 1H, H-3'a), 1.88 (s, 3H, NHAc), 1.73 (m, 1H, H-6e), 1.56 (ddq, $J = 9.9, 6.7, 3.5, 2.9$ Hz, 1H, H-5), 1.27 (m, 1H, H-2a), 1.08 - 0.97 (m, 10H, H-6a, *t*Bu), 0.91 (q, $J = 12.4$ Hz, 1H, H-4a); ¹³C NMR (126 MHz, CDCl₃): $\delta = 171.2, 170.7, 170.5, 170.4, 170.1$ (5 C=O), 169.0 (C-1'), 135.7, 133.8, 129.7, 127.8 (12C, Ar-C), 98.9 (C-2'), 75.9 (C-3), 72.4 (C-6'), 72.3 (C-1), 69.2 (C-4'), 68.3 (CH₂O), 68.1 (C-8'), 67.30 (C-7'), 67.27 (OCH₂), 62.7 (C-9'), 52.7 (OMe), 50.9 (CH₂N₃), 49.5 (C-5'), 41.2 (C-2), 38.6 (C-3'), 35.8 (C-6), 35.7 (C-5), 34.6 (C-4), 27.0 (*t*Bu), 23.3 (NHAc), 21.3, 21.0, 20.8 (4C, 4 OAc), 19.4 (*t*Bu); MS (ESI): m/z calcd for C₄₅H₆₂N₄O₁₅Si: 949.4 [M+Na]⁺, found: 949.2.

(1S,3R,5S)-3-(2-Azidoethoxy)-5-(hydroxymethyl)cyclohexyl (methyl 5-acetamido-4,7,8,9-tetra-O-acetyl-3,5-dideoxy-D-glycero- α -D-galacto-2-nonulopyranosylonate) (17). To a solution of **16** (245 mg, 0.264 mmol) in dry pyridine (7.4 mL) in a Teflon container, HF \cdot py (1.43 mL) was added dropwise at 0 °C under argon. The reaction mixture was stirred for 7 h, then satd. aq. NaHCO₃ was added to neutralize the reaction. The aqueous phase was extracted with DCM (6 x 30 mL), and the combined organic layers were dried over Na₂SO₄, filtered and concentrated *in vacuo*. The crude product was purified by flash column chromatography (toluene/acetone, 3:1 to 1:1) to afford **17** (173 g, 95 %). $[\alpha]_D^{20} = -14.5$ ($c = 0.06$, DCM); ¹H NMR (500 MHz, CDCl₃): $\delta = 5.39$ (ddd, $J = 8.9, 6.1, 2.7$ Hz, 1H, H-8'), 5.30 (dd, $J = 9.0, 2.0$ Hz, 1H, H-7'), 5.11 (dd, $J = 7.2, 3.1$ Hz, 1H, NH), 4.83 (dddd, $J = 12.4, 7.3, 4.6, 2.7$ Hz, 1H, H-4'), 4.30 (dd, $J = 12.4, 2.7$ Hz, 1H, H-9'a), 4.09 - 4.00 (m, 3H, H-5', H-6', H-9'b), 3.79 (s, 3H, OMe), 3.78 - 3.66 (m, 3H, H-1, OCH₂), 3.57 - 3.42 (m, 3H, H-3, CH₂O), 3.35 (td, $J = 4.7, 2.9$ Hz, 2H, CH₂N₃), 2.57 (dd, $J = 12.8, 4.6$ Hz, 1H, H-3'e), 2.47 (m, 1H, H-2e), 2.15 (s, 3H, OAc), 2.15 (s, 3H, OAc), 2.05 - 2.00 (m, 7H, H-4e, 2 OAc), 1.93 (t, $J = 12.6$ Hz, 1H, H-3'a),

1.88 (s, 3H, NHAc), 1.73 (m, 1H, H-6e), 1.53 (m, 1H, H-5), 1.28 (q, $J = 11.4$ Hz, 1H, H-2a), 0.94 (q, $J = 12.2$ Hz, 1H, H-6a), 0.87 (m, 1H, H-4a); ^{13}C NMR (126 MHz, CDCl_3): $\delta = 171.2, 170.8, 170.5, 170.4, 170.3$ (5 C=O), 169.1 (C-1'), 98.7 (C-2'), 75.8 (C-3), 72.5 (C-6'), 71.8 (C-1), 69.2 (C-4'), 68.3 (C-8'), 67.7 (CH₂O), 67.37 (C-7'), 67.36 (OCH₂), 62.8 (C-9'), 52.8 (OMe), 51.0 (CH₂N₃), 49.6 (C-5'), 41.0 (C-2), 38.4 (C-3'), 35.7 (C-5), 35.6 (C-6), 34.6 (C-4), 23.4 (NHAc), 21.3, 21.0, 20.9 (4C, 4 OAc); MS (ESI): m/z calcd for C₂₉H₄₄N₄O₁₅Si: 711.3 [M+Na]⁺; found: 711.2.

(1S,3R,5S)-3-(2-Azidoethoxy)-5-(sulfonatooxymethyl)cyclohexyl (methyl 5-acetamido-4,7,8,9-tetra-O-acetyl-3,5-dideoxy-D-glycero- α -D-galacto-2-nonulopyranosylonate) sodium salt (18).

To a solution of **17** (168 mg, 0.244 mmol) in dry DMF (12 mL), SO₃·py (389 mg, 2.44 mmol) was added at 0 °C under argon. The reaction mixture was stirred for 5.5 h at rt and was then quenched with powdered NaHCO₃. The suspension was stirred vigorously for 15 min, then filtered and concentrated *in vacuo* to give **18** (191 mg, 99 %). $[\alpha]_D^{20} = -14.5$ ($c = 0.06$, DCM); ^1H NMR (500 MHz, CD₃OD): $\delta = 5.45$ (ddd, $J = 9.6, 6.0, 2.7$ Hz, 1H, H-8'), 5.31 (dd, $J = 9.5, 2.4$ Hz, 1H, H-7'), 4.77 (ddd, $J = 12.2, 10.2, 4.4$ Hz, 1H, H-4'), 4.28 (dd, $J = 12.4, 2.7$ Hz, 1H, H-9'a), 4.17 (dd, $J = 10.8, 2.4$ Hz, 1H, H-6'), 4.02 (dd, $J = 12.4, 6.0$ Hz, 1H, H-9'b), 3.96 (t, $J = 10.5$ Hz, 1H, H-5'), 3.87 (dd, $J = 9.6, 6.0$ Hz, 1H, CH₂O), 3.84 – 3.79 (m, 4H, OMe, CH₂O), 3.76 – 3.71 (m, 3H, H-1, OCH₂), 3.56 (tt, $J = 11.3, 4.2$ Hz, 1H, H-3), 3.37 – 3.32 (m, 2H, CH₂N₃), 2.62 (dd, $J = 12.7, 4.6$ Hz, 1H, H-3'e), 2.48 (m, 1H, H-2e), 2.16, 2.11 (2 s, 6H, OAc), 2.08 (m, 1H, H-4e), 2.00, 1.98 (2 s, 6H, OAc), 1.83 (s, 3H, NHAc), 1.78 (t, $J = 12.4$ Hz, 1H, H-3'a), 1.74 (m, 1H, H-6e), 1.68 (m, 1H, H-5), 1.20 (q, $J = 11.4$ Hz, 1H, H-2a), 0.97 (q, $J = 12.3$ Hz, 1H, H-6a), 0.88 (q, $J = 12.2$ Hz, 1H, H-4a); ^{13}C NMR (126 MHz, CD₃OD): $\delta = 173.5, 171.8, 171.72, 171.67$ (4 C=O), 170.1 (C-1'), 100.2 (C-2'), 76.8 (C-3), 73.1 (C-6'), 72.98 (CH₂O), 72.97 (C-1), 70.7 (C-4'), 69.1 (C-8'), 68.7 (C-7'), 68.6 (OCH₂), 63.8 (C-9'), 53.3 (OMe), 51.8 (CH₂N₃), 50.1 (C-5'), 42.4 (C-2), 39.5 (C-3'), 36.6 (C-6), 35.5 (C-4), 34.2 (C-5), 22.7 (NHAc), 21.3, 20.9, 20.69, 20.67 (4 OAc); MS (ESI): m/z calcd for C₂₉H₄₃N₄NaO₁₈S: 813.2 [M+Na]⁺; found: 813.1.

(1S,3R,5S)-3-(2-Azidoethoxy)-5-(sulfonatooxymethyl)cyclohexyl (sodium 5-acetamido-3,5-dideoxy-D-glycero- α -D-galacto-2-nonulopyranosylonate) sodium salt (19).

Compound **18** (185 mg, 0.234 mmol) was dissolved in 0.1 M NaOH (13 mL) and stirred for 48 h. The solution was neutralized by addition of Amberlite IR 120, filtered and concentrated *in vacuo*. The crude product was purified by size-exclusion chromatography (P-2 gel, H₂O) to yield **19** (124 mg, 84 %). $[\alpha]_D^{20} = -2.1$ ($c = 0.8$, H₂O); ^1H NMR (500 MHz, D₂O): $\delta = 4.01 - 3.91$ (m, 3H, H-1, CH₂O), 3.92 – 3.83 (m, 2H, H-7', H-9'a), 3.83 – 3.74 (m, 3H, H-5', OCH₂), 3.71 – 3.65 (m, 3H, H-4', H-6', H-9'b), 3.62 (dd,

$J = 9.0, 2.0$ Hz, 1H, H-8'), 3.57 (tt, $J = 11.4, 4.1$ Hz, 1H, H-3), 3.50 – 3.45 (m, 2H, CH₂N₃), 2.77 (dd, $J = 12.3, 4.7$ Hz, 1H, H-3'e), 2.57 (m, 1H, H-2e), 2.13 (d, $J = 9.8$ Hz, 1H, H-4e), 2.05 (s, 3H, NHAc), 1.91 (d, $J = 10.5$ Hz, 1H, H-6e), 1.82 (m, 1H, H-5), 1.66 (t, $J = 12.1$ Hz, 1H, H-3'a), 1.27 (q, $J = 11.4$ Hz, 1H, H-2a), 1.09 (q, $J = 12.2$ Hz, 1H, H-6a), 1.00 (q, $J = 12.2$ Hz, 1H, H-4a); ¹³C NMR (126 MHz, D₂O): $\delta = 176.0$ (NHC=O), 174.5 (C-1'), 102.2 (C-2'), 76.8 (C-3), 73.8 (C-6'), 73.6 (CH₂O), 73.2 (C-7'), 73.0 (C-1), 69.2 (C-4'), 69.0 (C-8'), 67.7 (OCH₂), 63.4 (C-9'), 52.7 (C-5'), 51.3 (CH₂N₃), 42.0 (C-3'), 40.9 (C-2), 35.6 (C-6), 34.4 (C-4), 33.1 (C-5), 23.0 (NHAc); HR-MS (ESI): m/z calcd for C₂₀H₃₂N₄Na₂O₁₄S: 653.1323 [M+Na]⁺; found: 653.1324.

Di-flex-4 (20). A solution of **19** (15.2 mg, 24.0 μ mol), 1,7-octadiyne (1.2 mg, 10.8 μ mol), CuBr (0.7 mg, 4.9 μ mol) and TBTA (1.1 mg, 2.1 μ mol) in MeCN/H₂O (1:1, 1 mL) was stirred overnight at rt. QuadraSil MP resin was added and the mixture was stirred for 15 min, then the solution was filtered and directly applied to size exclusion chromatography (Sephadex LH-20, MeOH) to give **20** (2.8 mg, 19 %). ¹H NMR (500 MHz, D₂O): $\delta = 7.80$ (s, 2H, H-triazole), 4.55 (dd, $J = 6.3, 4.5$ Hz, 4H, CH₂N), 4.01 (m, 2H, OCH₂), 3.95 (m, 2H, OCH₂), 3.92 – 3.77 (m, 12H, H-1, CH₂O, H-5', H-7', H-9'a), 3.68 – 3.58 (m, 8H, H-4', H-6', H-8', H-9'b), 3.38 (m, 2H, H-3), 2.78 – 2.70 (m, 6H, H-3'e, L-1), 2.39 (d, $J = 11.4$ Hz, 2H, H-2e), 2.04 (s, 6H, NHAc), 1.90 (m, 2H, H-4e), 1.85 (d, $J = 12.5$ Hz, 2H, H-6e), 1.72 – 1.66 (m, 6H, H-5, L-2), 1.63 (t, $J = 12.1$ Hz, 2H, H-3'a), 1.13 (q, $J = 11.4$ Hz, 2H, H-2a), 0.99 (q, $J = 12.1$ Hz, 2H, H-6a), 0.83 (q, $J = 12.1$ Hz, 2H, H-4a); ¹³C NMR (126 MHz, D₂O): $\delta = 124.6$ (CH-triazole), 102.1 (C-2'), 77.0 (C-3), 73.8 (C-6'), 73.4 (CH₂O), 73.3 (C-7'), 72.8 (C-1), 69.3 (C-4'), 69.0 (C-8'), 67.4 (OCH₂), 63.5 (C-9'), 52.8 (C-5'), 51.2 (CH₂N), 42.0 (C-3'), 40.9 (C-2), 35.6 (C-6), 34.4 (C-4), 33.1 (C-5), 28.8 (L-2), 25.0 (L-1), 23.0 (NHAc); HR-MS (ESI): m/z calcd for C₄₈H₇₄N₈Na₄O₂₈S₂: 1343.3753 [M-Na]⁻; found: 1343.3762.

Di-flex-6 (21). A solution of **19** (14.9 mg, 24.0 μ mol), alkyne **S11** (1.5 mg, 10.9 μ mol), CuBr (0.7 mg, 4.9 μ mol) and TBTA (1.2 mg, 2.3 μ mol) in MeCN/H₂O (1:1, 1 mL) was stirred overnight at rt. QuadraSil MP resin was added and the mixture was stirred for 15 min, then the solution was filtered and directly applied to size exclusion chromatography (Sephadex LH-20, MeOH) to give **19** (9.6 mg, 63 %). ¹H NMR (500 MHz, D₂O): $\delta = 4.70$ (s, 4H, L-1), 4.61 (t, $J = 5.2$ Hz, 4H, CH₂N), 4.06 – 3.94 (m, 4H, OCH₂), 3.93 – 3.78 (m, 12H, H-1, CH₂O, H-5', H-7', H-9'a), 3.74 – 3.62 (m, 10H, H-4', H-6', H-9'b, L-2), 3.59 (dd, $J = 8.9, 1.9$ Hz, 2H, H-8'), 3.41 (td, $J = 11.5, 5.7$ Hz, 2H, H-3), 2.73 (dd, $J = 12.3, 4.7$ Hz, 2H, H-3'e), 2.40 (d, $J = 11.7$ Hz, 2H, H-2e), 2.04 (s, 6H, NHAc), 1.93 (d, $J = 11.6$ Hz, 2H, H-4e), 1.87 (d, $J = 11.1$ Hz, 2H, H-6e), 1.73 (br s, 2H, H-5), 1.66 (t, $J = 12.1$ Hz, 2H, H-3'a), 1.15 (q, $J = 11.4$ Hz, 2H, H-2a), 1.01 (q, $J = 12.1$ Hz, 2H, H-6a), 0.85 (q, $J = 12.1$ Hz, 2H, H-4a); ¹³C

NMR (126 MHz, D₂O): δ = 176.0 (C=O), 174.1 (C-1'), 144.6 (q-C-triazole), 126.3 (CH-triazole), 101.7 (C-2'), 76.9 (C-3), 73.8 (C-6'), 73.4 (CH₂O), 73.1 (C-7'), 72.8 (C-1), 69.7 (L-2), 69.1 (C-4', C-8'), 67.3 (OCH₂), 63.9 (L-1), 63.6 (C-9'), 52.7 (C-5'), 51.4 (CH₂N), 41.8 (C-3'), 40.8 (C-2), 35.6 (C-6), 34.3 (C-4), 33.1 (C-5), 23.0 (NHAc); HR-MS (ESI): m/z calcd for C₄₈H₇₄N₈Na₄O₃₀S₂: 1377.3807 [M+2H-Na]⁻; found: 1377.3774.

Di-flex-8 (22). A solution of **19** (14.5 mg, 23.0 μ mol), alkyne **S12** (1.8 mg, 10.9 μ mol), CuBr (0.2 mg, 1.4 μ mol) and TBTA (1.0 mg, 1.9 μ mol) in MeCN/H₂O (1:1, 1 mL) was stirred overnight at rt. QuadraSil MP resin was added and the mixture was stirred for 15 min, then the solution was filtered and directly applied to size exclusion chromatography (Sephadex LH-20, MeOH) to give **22** (8.8 mg, 57 %). ¹H NMR (500 MHz, D₂O): δ = 8.05 (s, 2H, H-triazole), 4.66 (s, 4H, L-1), 4.63 – 4.58 (m, 4H, CH₂N), 4.06 – 3.94 (m, 4H, OCH₂), 3.93 – 3.77 (m, 12H, H-1, CH₂O, H-5', H-7', H-9'a), 3.69 – 3.62 (m, 6H, H-4', H-6', H-9'b), 3.62 – 3.55 (m, 6H, H-8', L-2), 3.42 (tt, J = 11.1, 4.2 Hz, 2H, H-3), 2.74 (dd, J = 12.3, 4.7 Hz, 2H, H-3'e), 2.41 (m, 2H, H-2e), 2.04 (s, 6H, NHAc), 1.94 (d, J = 11.7 Hz, 2H, H-4e), 1.86 (d, J = 13.0 Hz, 2H, H-6e), 1.74 (m, 2H, H-5), 1.68 – 1.58 (m, 6H, H-3'a, L-3), 1.15 (q, J = 11.4 Hz, 2H, H-2a), 1.01 (q, J = 12.1 Hz, 2H, H-6a), 0.86 (q, J = 12.1 Hz, 2H, H-4a); ¹³C NMR (126 MHz, D₂O): δ = 176.0 (C=O), 174.5 (C-1'), 145.0 (q-C-triazole), 126.4 (CH-triazole), 102.1 (C-2'), 76.9 (C-3), 73.8 (C-6'), 73.4 (CH₂O), 73.3 (C-7'), 72.8 (C-1), 70.8 (L-2), 69.2 (C-4'), 69.0 (C-8'), 67.3 (OCH₂), 63.6 (2C, C-9', L-1), 52.8 (C-5'), 51.3 (CH₂N), 42.0 (C-3'), 40.9 (C-2), 35.6 (C-6), 34.4 (C-4), 33.1 (C-5), 26.2 (L-3), 23.0 (NHAc); HR-MS (ESI): m/z calcd for C₅₀H₇₈N₈Na₄O₃₀S₂: 1403.3964 [M-Na]⁻; found: 1403.3963.

Di-flex-12 (23). A solution of **19** (14.9 mg, 23.6 μ mol), alkyne **S13** (2.5 mg, 11.2 μ mol), CuBr (1.5 mg, 10.1 μ mol) and TBTA (1.1 mg, 2.1 μ mol) in MeCN/H₂O (1:1, 1 mL) was stirred overnight at rt. QuadraSil MP resin was added and the mixture was stirred for 15 min, then the solution was filtered and directly applied to size exclusion chromatography (Sephadex LH-20, MeOH) to give **23** (9.5 mg, 57 %). ¹H NMR (500 MHz, D₂O): δ = 7.97 (s, 2H, H-triazole), 4.58 (s, 4H, L-1), 4.52 (t, J = 5.4 Hz, 4H, CH₂N), 3.98 – 3.86 (m, 4H, OCH₂), 3.86 – 3.68 (m, 12H, H-1, CH₂O, H-5', H-7', H-9'a), 3.62 – 3.45 (m, 12H, H-4', H-6', H-8', H-9'b, L-2), 3.33 (tt, J = 11.4, 4.0 Hz, 2H, H-3), 2.65 (dd, J = 12.4, 4.7 Hz, 2H, H-3'e), 2.34 (d, J = 11.3 Hz, 2H, H-2e), 1.95 (s, 6H, NHAc), 1.85 (d, J = 11.6 Hz, 2H, H-4e), 1.78 (d, J = 12.2 Hz, 2H, H-6e), 1.65 (br s, 2H, H-5), 1.59 – 1.50 (m, 6H, H-3'a, L-3), 1.25 – 1.16 (m, 8H, L-4, L-5), 1.06 (q, J = 11.4 Hz, 2H, H-2a), 0.93 (q, J = 12.1 Hz, 2H, H-6a), 0.77 (q, J = 12.1 Hz, 2H, H-4a); ¹³C NMR (126 MHz, D₂O): δ = 176.0 (C=O), 174.5 (C-1'), 145.1 (q-C-triazole), 126.4 (CH-triazole), 102.1 (C-2'), 76.9 (C-3), 73.7 (C-6'), 73.4 (CH₂O), 73.3 (C-7'), 72.8 (C-1), 71.2

(L-2), 69.2 (C-4'), 69.0 (C-8'), 67.3 (OCH₂), 63.53 (C-9'), 63.47 (L-1), 52.8 (C-5'), 51.3 (CH₂N), 42.0 (C-3'), 40.9 (C-2), 35.6 (C-6), 34.4 (C-4), 33.1 (C-5), 29.4 (L-3), 29.2 (L-4), 26.0 (L-5), 23.0 (NHAc); HR-MS (ESI): *m/z* calcd for C₅₄H₈₆N₈Na₄O₃₀S₂: 1459.4590 [M-Na]⁻; found: 1459.4586.

Tri-bran (25). A solution of **19** (15.5 mg, 24.5 μmol), alkyne **S14** (1.6 mg, 7.3 μmol), CuBr (0.3 mg, 2.1 μmol) and TBTA (0.9 mg, 1.7 μmol) in MeCN/H₂O (1:1, 1 mL) was stirred overnight at rt. QuadraSil MP resin was added and the mixture was stirred for 15 min, then the solution was filtered and directly applied to size exclusion chromatography (Sephadex LH-20, MeOH) to give **25** (6.8 mg, 44 %). ¹H NMR (500 MHz, D₂O): δ = 8.03 (s, 3H, H-triazole), 4.66 – 4.57 (m, 12H, CH₂N, L-1), 4.05 – 3.94 (m, 6H, OCH₂), 3.94 – 3.77 (m, 18H, H-1, CH₂O, H-5', H-7', H-9'a), 3.70 – 3.54 (m, 18H, H-4', H-6', H-8', H-9'b, L-2), 3.44 (tt, *J* = 11.3, 4.1 Hz, 3H, H-3), 2.74 (dd, *J* = 12.4, 4.7 Hz, 3H, H-3'e), 2.42 (dd, *J* = 9.8, 5.5 Hz, 3H, H-2e), 2.19 (td, *J* = 11.4, 10.8, 5.4 Hz, 3H, L-3), 2.04 (s, 9H, NHAc), 1.97 – 1.90 (m, 3H, H-4e), 1.87 (d, *J* = 12.5 Hz, 3H, H-6e), 1.74 (br s, 3H, H-5), 1.63 (t, *J* = 12.1 Hz, 3H, H-3'a), 1.16 (q, *J* = 11.4 Hz, 3H, H-2a), 1.02 (q, *J* = 12.2 Hz, 3H, H-6a), 0.86 (q, *J* = 12.1 Hz, 3H, H-4a); ¹³C NMR (126 MHz, D₂O): δ = 176.0 (C=O), 174.5 (C-1'), 144.9 (q-C-triazole), 126.4 (CH-triazole), 102.1 (C-2'), 76.9 (C-3), 73.7 (C-6'), 73.4 (CH₂O), 73.3 (C-7'), 72.8 (C-1), 69.3 (C-4'), 69.0 (C-8'), 68.9 (L-2), 67.3 (OCH₂), 64.1 (L-1), 63.5 (C-9'), 52.8 (C-5'), 51.3 (CH₂N), 43.0 (C-3'), 40.9 (C-2), 40.0 (L-3), 35.7 (C-6), 34.4 (C-4), 33.1 (C-5), 23.0 (NHAc); HR-MS (ESI): *m/z* calcd for C₇₃H₁₁₂N₁₂Na₆O₄₅S₃: 2087.5501 [M-Na]⁻; found: 2087.5550.

Tri-cycl (26). A solution of **19** (15.4 mg, 24.4 μmol), alkyne **S15** (1.8 mg, 7.3 μmol), CuBr (0.6 mg, 4.2 μmol) and TBTA (0.6 mg, 1.1 μmol) in MeCN/H₂O (1:1, 1 mL) was stirred overnight at rt. QuadraSil MP resin was added and the mixture was stirred for 15 min, then the solution was filtered and directly applied to size exclusion chromatography (Sephadex LH-20, MeOH) to give **26** (9.5 mg, 61 %). ¹H NMR (500 MHz, D₂O): δ = 8.06 (s, 3H, H-triazole), 4.75 (s, 6H, L-1), 4.62 (t, *J* = 5.3 Hz, 6H, CH₂N), 4.07 – 3.96 (m, 6H, OCH₂), 3.96 – 3.75 (m, 18H, H-1, CH₂O, H-5', H-7', H-9'a), 3.70 – 3.57 (m, 15H, H-4', H-6', H-8', H-9'b, L-2), 3.44 (td, *J* = 11.7, 6.0 Hz, 3H, H-3), 2.74 (dd, *J* = 12.4, 4.7 Hz, 3H, H-3'e), 2.54 (d, *J* = 11.0 Hz, 3H, H-2e), 2.43 (d, *J* = 11.0 Hz, 3H, L-3e), 2.03 (s, 9H, NHAc), 1.96 (d, *J* = 11.6 Hz, 3H, H-4e), 1.87 (d, *J* = 11.9 Hz, 3H, H-6e), 1.75 (m, 3H, H-5), 1.63 (t, *J* = 12.2 Hz, 3H, H-3'a), 1.30 – 1.11 (m, 6H, H-2a, L-3a), 1.02 (q, *J* = 12.0 Hz, 3H, H-6a), 0.87 (q, *J* = 11.8 Hz, 3H, H-4a); ¹³C NMR (126 MHz, D₂O): δ = 176.0 (C=O), 174.5 (C-1'), 145.1 (q-C-triazole), 126.4 (CH-triazole), 102.1 (C-2'), 76.9 (C-3), 73.9 (L-2), 73.8 (C-6'), 73.5 (CH₂O), 73.3 (C-7'), 72.8 (C-1), 69.3 (C-4'), 69.0 (C-8'), 67.3 (OCH₂), 63.5 (C-9'), 61.7 (L-1), 52.8 (C-5'), 51.3 (CH₂N), 42.0

(C-3'), 40.9 (C-2), 38.1 (L-3), 35.6 (C-6), 34.4 (C-4), 33.1 (C-5), 23.0 (NHAc); HR-MS (ESI): m/z calcd for $C_{75}H_{114}N_{12}Na_6O_{45}S_3$: 1045.2882 $[M-2Na]^2^-$; found: 1045.2897.

Tri-arom (27). A solution of **19** (14.9 mg, 23.7 μ mol), alkyne **S16** (1.7 mg, 7.1 μ mol), CuBr (2.3 mg, 16.0 μ mol) and TBTA (1.2 mg, 2.3 μ mol) in MeCN/H₂O (1:1, 1 mL) was stirred overnight at rt. QuadraSil MP resin was added and the mixture was stirred for 15 min, then the solution was filtered and directly applied to size exclusion chromatography (Sephadex LH-20, MeOH) to give **27** (9.0 mg, 60 %). ¹H NMR (500 MHz, D₂O): δ = 8.12 (s, 3H, H-triazole), 6.44 (s, 3H, L-3), 5.27 (s, 6H, L-1), 4.61 (t, J = 5.3 Hz, 6H, CH₂N), 4.07 – 3.91 (m, 6H, OCH₂), 3.92 – 3.76 (m, 18H, H-1, CH₂O, H-5', H-7', H-9'a), 3.70 – 3.57 (m, 12H, H-4', H-6', H-8', H-9'b), 3.40 (ddt, J = 11.4, 8.4, 3.9 Hz, 3H, H-3), 2.73 (dd, J = 12.4, 4.7 Hz, 3H, H-3'e), 2.41 (d, J = 11.3 Hz, 3H, H-2e), 2.03 (s, 9H, NHAc), 1.90 – 1.83 (m, 6H, H-4e, H-6e), 1.71 (m, 3H, H-5), 1.63 (t, J = 12.1 Hz, 3H, H-3'a), 1.11 (q, J = 11.4 Hz, 3H, H-2a), 0.99 (q, J = 12.1 Hz, 3H, H-6a), 0.76 (q, J = 12.0 Hz, 3H, H-4a); ¹³C NMR (126 MHz, D₂O): δ = 176.0 (C=O), 174.5 (C-1'), 160.3 (L-2), 144.0 (q-C-triazole), 126.7 (CH-triazole), 102.1 (C-2'), 97.4 (L-3), 76.9 (C-3), 73.7 (C-6'), 73.4 (CH₂O), 73.3 (C-7'), 72.8 (C-1), 69.3 (C-4'), 69.0 (C-8'), 67.2 (OCH₂), 63.5 (C-9'), 62.2 (L-1), 52.8 (C-5'), 51.4 (CH₂N), 42.0 (C-3'), 40.9 (C-2), 35.7 (C-6), 34.2 (C-4), 33.1 (C-5), 23.0 (NHAc); HR-MS (ESI): m/z calcd for $C_{75}H_{108}N_{12}Na_6O_{45}S_3$: 1042.2648 $[M-2Na]^2^-$; found: 1042.2666.

Tetra-bran (24). A solution of **19** (15.7 mg, 24.9 μ mol), alkyne **S17** (1.6 mg, 5.5 μ mol), CuBr (0.3 mg, 2.1 μ mol) and TBTA (0.6 mg, 1.1 μ mol) in MeCN/H₂O (1:1, 1 mL) was stirred overnight at rt. QuadraSil MP resin was added and the mixture was stirred for 15 min, then the solution was filtered and directly applied to size exclusion chromatography (Sephadex LH-20, MeOH) to give **24** (7.6 mg, 49 %). ¹H NMR (500 MHz, D₂O): δ = 7.98 (s, 4H, H-triazole), 4.62 – 4.49 (m, 16H, CH₂N, L-1), 4.05 – 3.93 (m, 8H, OCH₂), 3.92 – 3.77 (m, 24H, H-1, CH₂O, H-5', H-7', H-9'a), 3.69 – 3.58 (m, 16H, H-4', H-6', H-8', H-9'b), 3.48 – 3.37 (m, 12H, H-3, L-2), 2.74 (dd, J = 12.3, 4.7 Hz, 4H, H-3'e), 2.42 (d, J = 10.2 Hz, 4H, H-2e), 2.04 (s, 12H, NHAc), 1.93 (d, J = 10.2 Hz, 4H, H-4e), 1.88 (d, J = 11.7 Hz, 4H, H-6e), 1.73 (m, 4H, H-5), 1.63 (t, J = 12.1 Hz, 4H, H-3'a), 1.15 (q, J = 11.4 Hz, 4H, H-2a), 1.01 (q, J = 12.5 Hz, 4H, H-6a), 0.85 (q, J = 12.5 Hz, 4H, H-4a); ¹³C NMR (126 MHz, D₂O): δ = 176.0 (C=O), 174.6 (C-1'), 145.5 (q-C-triazole), 126.5 (CH-triazole), 102.1 (C-2'), 76.9 (C-3), 73.7 (C-6'), 73.4 (CH₂O), 73.3 (C-7'), 72.8 (C-1), 69.3 (C-4'), 69.1 (L-2), 69.0 (C-8'), 67.2 (OCH₂), 64.5 (L-1), 63.5 (C-9'), 52.8 (C-5'), 51.3 (CH₂N), 42.0 (C-3'), 40.9 (C-2), 35.7 (C-6), 34.3 (C-4), 33.1 (C-5), 23.0 (NHAc); HR-MS (ESI): m/z calcd for $C_{98}H_{149}N_{15}Na_8O_{60}S_4$: 913.2512 $[M+H-3Na]^3^-$; found: 913.2506.

Hexa-bran (28). A solution of **19** (15.0 mg, 23.8 μmol), alkyne **S18** (1.8 mg, 3.7 μmol), CuBr (1.1 mg, 7.7 μmol) and TBTA (0.3 mg, 0.6 μmol) in MeCN/H₂O (1:1, 1 mL) was stirred overnight at rt. QuadraSil MP resin was added and the mixture was stirred for 15 min, then the solution was filtered and directly applied to size exclusion chromatography (Sephadex LH-20, MeOH) to give **28** (7.9 mg, 50 %). ¹H NMR (500 MHz, D₂O): δ = 7.97 (s, 6H, H-triazole), 4.64 – 4.48 (m, 24H, CH₂N, L-1), 4.03 – 3.92 (m, 12H, OCH₂), 3.92 – 3.75 (m, 36H, H-1, CH₂O, H-5', H-7', H-9'a), 3.73 – 3.57 (m, 24H, H-4', H-6', H-8', H-9'b), 3.42 (m, 18H, H-3, L-2), 3.26 (d, J = 9.2 Hz, 6H, L-4), 2.74 (dd, J = 12.4, 4.6 Hz, 6H, H-3'e), 2.42 (d, J = 10.4 Hz, 6H, H-2e), 2.04 (d, J = 2.0 Hz, 18H, NHAc), 1.96 – 1.86 (m, 12H, H-4e, H-6e), 1.74 (br s, 6H, H-5), 1.65 (t, J = 12.1 Hz, 6H, H-3'a), 1.16 (q, J = 11.2 Hz, 6H, H-2a), 1.01 (q, J = 12.1 Hz, 6H, H-6a), 0.85 (q, J = 11.5 Hz, 6H, H-4a); ¹³C NMR (126 MHz, D₂O): δ = 175.9 (C=O), 174.5 (C-1'), 145.2 (q-C-triazole), 126.2 (CH-triazole), 102.0 (C-2'), 76.9 (C-3), 73.7 (C-6'), 73.5 (CH₂O), 73.2 (C-6'), 72.7 (C-7'), 69.4 (L-2), 69.3 (C-4'), 69.1 (C-8'), 67.2 (OCH₂), 64.6 (L-1), 63.5 (C-9'), 52.8 (C-5'), 51.3 (CH₂N), 46.0 (L-3), 41.9 (C-3'), 40.9 (C-2), 35.8 (C-6), 34.4 (C-4), 33.1 (C-5), 23.0 (NHAc); HR-MS (ESI): m/z calcd for C₁₄₈H₂₂₆N₂₄Na₁₂O₉₁S₆: 829.6286 [M-5Na]⁵⁻; found: 829.6281.

Hexa-cycl (29). A solution of **19** (20.0 mg, 31.6 μmol), alkyne **S19** (1.9 mg, 4.7 μmol), CuBr (0.1 mg, 0.7 μmol) and TBTA (0.6 mg, 1.1 μmol) in MeCN/H₂O (1:1, 1 mL) was stirred overnight at rt. QuadraSil MP resin was added and the mixture was stirred for 15 min, then the solution was filtered and directly applied to size exclusion chromatography (Sephadex LH-20, MeOH) to give **29** (6.1 mg, 31 %). ¹H NMR (500 MHz, D₂O): δ = 8.04, 7.96 (2 s, 2H, H-triazole), 5.09 (br s, 2H, L-1), 4.62 – 4.40 (m, 4H, CH₂N, L-1), 4.60 (br s, 2H, CH₂N), 4.06 – 3.85 (m, 4H, OCH₂), 3.94 – 3.66 (m, 12H, H-1, CH₂O, H-5', H-7', H-9'a), 3.73 – 3.45 (m, 8H, H-4', H-6', H-8', H-9'b), 3.48 (br s, 1H, H-3), 3.43 – 3.25 (m, 1H, H-3), 2.76 – 2.69 (m, 1H, H-3'e), 2.65 (dd, J = 12.4, 4.8 Hz, 1H, H-3'e), 2.44 – 2.36 (m, 1H, H-2e), 2.34 (br s, 1H, H-2e), 2.03, 1.95 (2 s, 6H, NHAc), 1.94 – 1.71 (m, 4H, H-4e, H-6e), 1.73, 1.65 (2 br s, 2H, H-5), 1.65 (t, J = 12.1 Hz, 1H, H-3'a), 1.56 (t, J = 12.0 Hz, 1H, H-3'a), 1.15 (q, J = 11.3 Hz, 1H, H-2a), 1.14 – 0.98 (m, 1H, H-2a), 1.00 (q, J = 12.2 Hz, 1H, H-6a), 0.98 – 0.83 (m, 1H, H-6a), 0.85 (q, J = 11.6 Hz, 1H, H-4a), 0.83 – 0.63 (m, 1H, H-4a); ¹³C NMR (126 MHz, D₂O): δ = 176.0 (C=O), 174.4 (C-1'), 146.1 (q-C-triazole), 120.5 (CH-triazole), 101.9 (C-2'), 76.8 (L-2a), 76.9 (C-3), 73.8 (C-6'), 73.4 (CH₂O), 73.2 (C-6'), 72.7 (C-7'), 71.5 (L-2e), 69.2 (C-4'), 69.1 (C-8'), 67.3 (OCH₂), 63.6 (C-9'), 52.8 (C-5'), 51.4 (CH₂N), 41.9 (C-3'), 40.9 (C-2), 35.7 (C-6), 33.1 (C-4), 31.2 (C-5), 23.0 (NHAc).

Hexa-arom (30). A solution of **19** (18.5 mg, 29.4 μmol), alkyne **S20** (1.7 mg, 4.2 μmol), CuBr (0.4 mg, 2.8 μmol) and TBTA (0.5 mg, 0.9 μmol) in MeCN/H₂O (1:1, 1 mL) was stirred overnight at rt. QuadraSil MP resin was added and the mixture was stirred for 15 min, then the solution was filtered and directly applied to size exclusion chromatography (Sephadex LH-20, MeOH) to give **30** (3.7 mg, 21 %). ¹H NMR (500 MHz, D₂O): δ = 8.04 (s, 6H, H-triazole), 5.09 (br s, 12H, L-1), 4.60 (br s, 12H, CH₂N), 4.06 – 3.94 (m, 12H, OCH₂), 3.94 – 3.75 (m, 12H, H-1, CH₂O, H-5', H-7', H-9'a), 3.73 – 3.56 (m, 24H, H-4', H-6', H-8', H-9'b), 3.48 (br s, 6H, H-3), 2.73 (m, 6H, H-3'e), 2.40 (m, 6H, H-2e), 2.03 (s, 18H, NHAc), 1.94 – 1.82 (m, 12H, H-4e, H-6e), 1.73 (br s, 6H, H-5), 1.65 (t, J = 12.1 Hz, 6H, H-3'a), 1.15 (q, J = 11.3 Hz, 6H, H-2a), 1.00 (q, J = 12.2 Hz, 6H, H-6a), 0.85 (q, J = 11.6 Hz, 6H, H-4a); ¹³C NMR (126 MHz, D₂O): δ = 175.9 (C=O), 175.1 (C-1'), 154.1 (L-2), 129.9 (CH-triazole), 101.8 (C-2'), 76.9 (C-3), 73.8 (C-6'), 73.5 (CH₂O), 73.1 (C-6'), 72.7 (C-7'), 69.2 (C-4'), 69.1 (C-8'), 67.2 (OCH₂), 65.3 (L-1), 63.5 (C-9'), 52.8 (C-5'), 51.3 (CH₂N), 41.8 (C-3'), 40.9 (C-2), 35.8 (C-6), 34.3 (C-4), 33.1 (C-5), 23.0 (NHAc); HR-MS (ESI): m/z calcd for C₁₄₄H₂₁₀N₂₄Na₁₂O₉₀S₆: 1022.7530 [M-4Na]⁴⁺; found: 1022.7472.

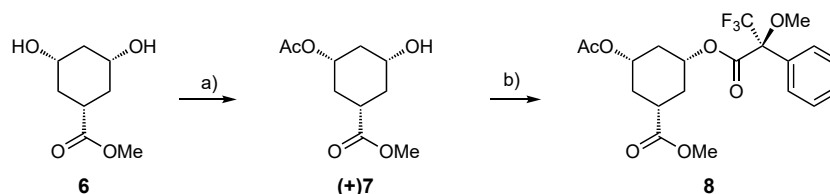
(1S,3R,5S)-3-(2-Aminoethoxy)-5-(sulfonatooxymethyl)cyclohexyl (sodium 5-acetamido-3,5-dideoxy-D-glycero- α -D-galacto-2-nonulopyranosylonate) sodium salt (31). Compound **19** (30.5 mg, 0.048 mmol) and Pd(OH)₂/C (20 %, 16.9 mg) were suspended in H₂O (5 mL). The mixture was hydrogenated (1 atm H₂) and stirred at rt for 24 h. Then, the suspension was filtered over a pad of celite, and the celite was washed with water. The solvent was removed under *vacuo*, affording compound **31** (28.1 mg, 96 %). ¹H NMR (500 MHz, D₂O): δ = 4.00 – 3.88 (m, 4H, H-1, CH₂O, H-7'), 3.87 – 3.75 (m, 4H, H-5', H-9'a, OCH₂), 3.69 – 3.61 (m, 3H, H-4', H-6', H-9'b), 3.58 (dd, J = 9.0, 2.0 Hz, 1H, H-8'), 3.53 (tt, J = 11.3, 4.0 Hz, 1H, H-3), 3.19 (t, J = 5.2 Hz, 2H, CH₂NH₂), 2.76 (dd, J = 12.4, 4.7 Hz, 1H, H-3'e), 2.54 (br d, J = 8.7 Hz, 1H, H-2e), 2.12 (br d, J = 13.9 Hz, 1H, H-4e), 2.04 (s, 3H, NHAc), 1.89 (m, 1H, H-6e), 1.80 (m, 1H, H-5), 1.64 (t, J = 12.1 Hz, 1H, H-3'a), 1.26 (q, J = 11.4 Hz, 1H, H-2a), 1.08 (q, J = 12.0 Hz, 1H, H-6a), 1.00 (q, J = 12.0 Hz, 1H, H-4a); ¹³C NMR (126 MHz, D₂O): δ = 176.0 (C=O), 174.4 (C-1'), 102.2 (C-2'), 76.9 (C-3), 73.8 (C-6'), 73.5 (CH₂O), 73.4 (C-7'), 73.0 (C-1), 69.2 (C-8'), 69.1 (C-4'), 64.7 (OCH₂), 63.7 (C-9'), 52.8 (C-5'), 42.0 (C-3'), 40.8 (C-2), 40.3 (CH₂NH₂), 35.6 (C-6), 34.4 (C-4), 33.1 (C-5), 23.0 (NHAc); MS (ESI): m/z calcd for C₂₀H₃₄N₂Na₂O₁₄S: 627.1 [M+Na]⁺; found: 627.0.

(1S,3R,5S)-3-(2-(4-Mercaptobutanamido)ethoxy)-5-(sulfonatooxymethyl)cyclohexyl (sodium 5-acetamido-3,5-dideoxy-D-glycero- α -D-galacto-2-nonulopyranosylonate) sodium salt (32). To a solution of **31** (24.2 mg, 0.040 mmol) in H₂O (150 μL) were added 1 M NaOH (4 μL), γ -

thiobutyrolactone (35 μ L, 0.404 mmol) and MeOH (200 μ L). The reaction mixture was checked by TLC every 2 h, and additional 1 M NaOH (4 μ L) was added until pH > 7.0. After 24 h, MeOH was removed under reduced pressure and the aqueous phase was washed with EtOAc (3 x 3 mL). After removal of insoluble material by centrifugation, lyophilization afforded the crude compound, which was purified by flash column chromatography (DCM/(MeOH/H₂O, 10:1), 8:2 to 1:1) and size-exclusion chromatography (P-2 gel, H₂O) to afford **32** (12.8 mg, 45 %). ¹H NMR (500 MHz, D₂O): δ = 4.00 – 3.83 (m, 5H, H-1, CH₂O, H-7', H-9'a), 3.81 (d, J = 10.2 Hz, 1H, H-5'), 3.74 – 3.58 (m, 6H, H-4', H-6', H-8', H-9'b, OCH₂), 3.50 (tt, J = 11.3, 4.0 Hz, 1H, H-3), 3.42 – 3.32 (m, 2H, CH₂N), 2.76 (dd, J = 12.4, 4.7 Hz, 1H, H-3'e), 2.57 (t, J = 7.1 Hz, 2H, CH₂S), 2.53 (m, 1H, H-2e), 2.40 (t, J = 7.4 Hz, 2H, COCH₂), 2.10 – 2.04 (m, 4H, H-4e, NHAc), 1.95 – 1.86 (m, 3H, H-6e, CH₂CH₂S), 1.81 (m, 1H, H-5), 1.66 (t, J = 12.1 Hz, 1H, H-3'a), 1.24 (q, J = 11.4 Hz, 1H, H-2a), 1.08 (q, J = 12.2 Hz, 1H, H-6a), 0.98 (q, J = 12.2 Hz, 1H, H-4a); ¹³C NMR (126 MHz, D₂O): δ = 177.2, 176.0 (2 C=O), 174.5 (C-1'), 102.1 (C-2'), 76.6 (C-3), 73.7 (C-6'), 73.5 (CH₂O), 73.3 (C-7'), 72.9 (C-1), 69.2 (C-4'), 69.0 (C-8'), 67.2 (OCH₂), 63.5 (C-9'), 52.8 (C-5'), 42.0 (C-3'), 41.0 (C-2), 40.3 (CH₂N), 35.6 (C-6), 35.3 (NCOCH₂), 34.6 (C-4), 33.2 (C-5), 30.4 (CH₂CH₂S), 24.0 (CH₂S), 23.0 (NHAc); MS (ESI): m/z calcd for C₂₄H₄₀N₂Na₂O₁₄S₂: 683.2 [M-Na]⁻; found: 683.1.

Glycopolymer 33. To a solution of chloroacetylated L-polylysine⁴⁰⁰ (3.005 mg, 36.6 μ mol) in DMF (145 μ L) a solution of **32** [(5.266 mg, 7.452 μ mol) in 24 μ L of water], was added under argon. Then, 1,8-diazabicyclo(5.4.0)undec-7-ene (2.19 μ L, 14.6 μ mol) was added. The reaction mixture was shaken in an Eppendorf tube at 25 °C for 1 h on an Eppendorf thermomixer at 300 rpm. Then, thioglycerol (3.8 μ L, 43.9 μ mol) and Et₃N (6.12 μ L, 43.9 μ mol) were added and the mixture was shaken overnight. Next, the reaction mixture was dropped into a stirred solution of ethyl acetate/ethanol (1:1; 3.0 mL), leading to precipitation of the product. The precipitate was collected by centrifugation, washed with ethanol (3 x 3.0 mL), and then dissolved in water (3.0 mL). The aqueous solution was purified by ultracentrifugation using a Vivaspin centrifugal concentrator (Sartorius, Germany; 6 mL, MWCO 50 kDa, three times from 6.0 mL to 0.5 mL). The product was lyophilized from 1 mL aqueous solution within 6 h yielding product **33** as a white solid (7.15 mg, 91 %, loading percentage based on ¹H NMR: 44 %, for details see Supporting Information).

1.3 Determination of stereochemical purity of compound 7



Scheme S1. a) Ac₂O, DMAP, pyridine, rt, overnight (16 %); b) d) (R)-(-)-MTPA-Cl, DCM, 0 °C to rt.

Methyl *rac-cis*-3-acetoxy-5-hydroxycyclohexane-1-carboxylate (*rac-cis*-7). Compound 6 (24.0 mg, 0.14 mmol) and DMAP (16.2 mg, 0.16 mmol) were dissolved in pyridine (0.5 mL) under argon, and Ac₂O (1.5 μ L, 0.16 mmol) was added. The solution was stirred overnight at rt, then concentrated *in vacuo*. The crude product was purified by flash column chromatography (DCM/MeOH, 1:0 to 9:1) to give *rac-cis*-7 (4.2 mg, 16 %) which was directly used in the next step.

Methyl *rac-cis* 5-acetoxy-3-((R)-(-)- α -methoxy- α -(trifluoromethyl)phenylacetoxy) cyclohexane-1-carboxylate (*rac-cis*-8). To a solution of compound *rac-cis*-7 (4.2 mg, 0.019 mmol) in dry DCM (0.4 mL), DMAP (6.8 mg, 0.027 mmol) and (R)-(-)-MTPA-Cl (5 μ L, 0.027 mmol) were added at 0 °C. The reaction mixture was stirred at 0 °C for 15 min and then for 1 h at rt. The reaction mixture was diluted with Et₂O (5.0 mL), washed twice with 1 M aq. HCl (5.0 mL), satd. aq. NaHCO₃ (5.0 mL) and water (5.0 mL), dried over Na₂SO₄, filtered, and concentrated *in vacuo*. The crude *rac-cis*-8 was directly subjected to ¹H NMR investigation without further purification.

The ¹H NMR spectra of crude compounds 8 and *rac-cis*-8 showed the presence of two distinct signals corresponding to the carboxylic esters CO₂Me and OAc for the two diastereoisomers in *rac-cis*-8, while a single peak each was detected for pure 8, confirming the presence of a single enantiomer (ee > 99 %, Figure S1).

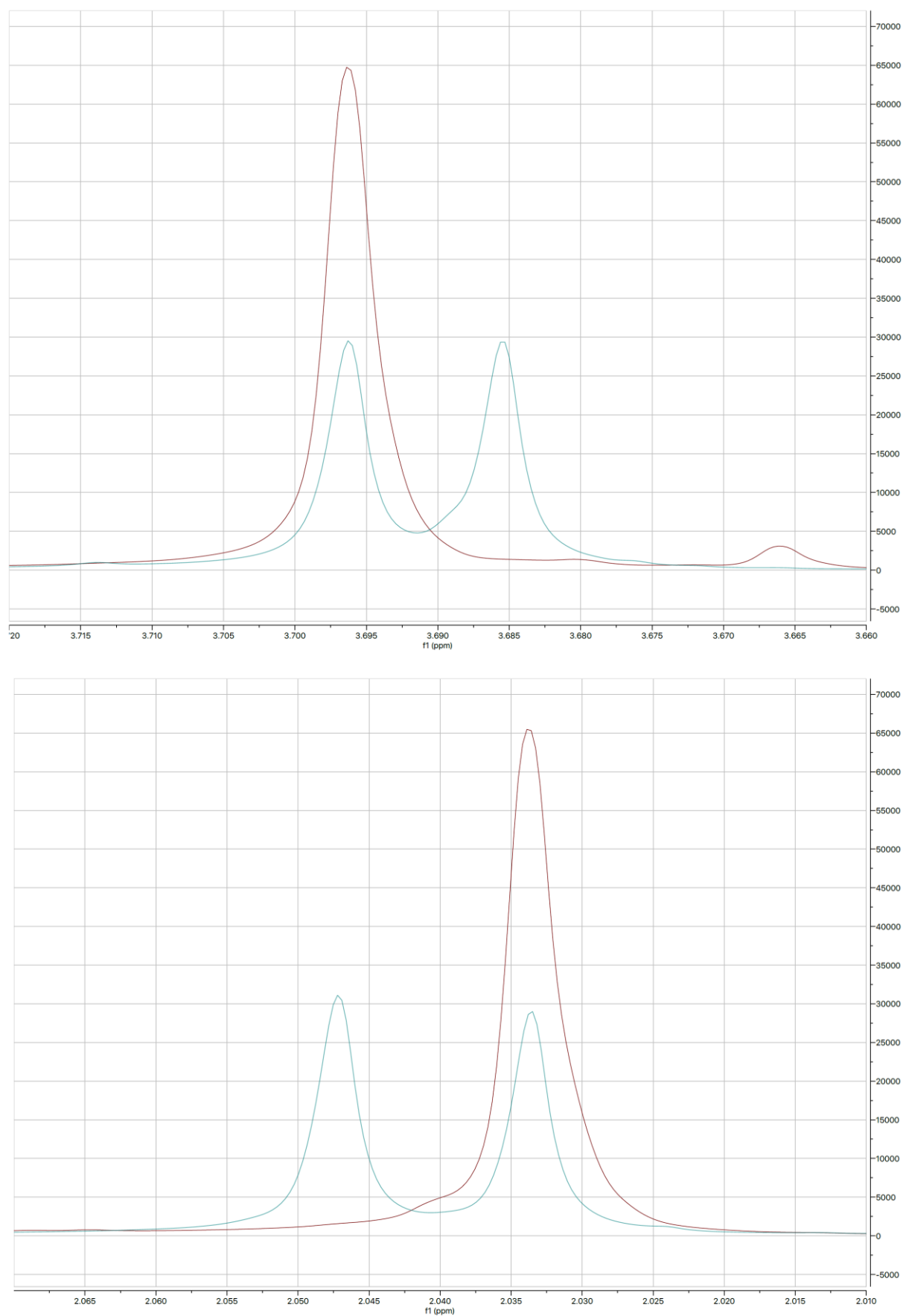
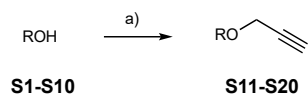


Figure S1. Enlargement overlays of ¹H NMR spectra of Mosher ester **8** (maroon) and *rac-cis-8* (teal) in regions 3.720 – 3.660 (CO₂Me signal) and 2.070 – 2.010 (OAc signal).

1.4. Synthesis of alkyne building blocks



Scheme S2. a) Propargyl bromide, base, DMF, 0 °C to rt (5-90%).

1,2-Ethanediol bis(2-propynyl) ether (S11). To a solution of 1,2-ethanediol (**S1**, 0.5 mL, 8.97 mmol) in DMF (10 mL), NaH (60% in mineral oil, 1.48 g, 37.0 mmol) was added, and the mixture was stirred at 0 °C for 15 min under argon. Then propargyl bromide (80 % in toluene, 2.7 mL, 25.1 mmol) was added, and the solution was stirred overnight allowing to reach rt. The solvent was evaporated, and the residue was diluted with H₂O (20 mL), extracted with DCM (3 x 20 mL), dried over Na₂SO₄, filtered and concentrated *in vacuo*. The crude product was purified by flash column chromatography (petroleum ether/EtOAc, 8:2 to 7:3) to give **S11** (620 mg, 50 %). ¹H NMR (600 MHz, CDCl₃): δ = 4.21 (d, *J* = 2.4 Hz, 4H, CH₂CCH), 3.72 (s, 4H, H-1), 2.43 (t, *J* = 2.4 Hz, 2H, CCH); ¹³C NMR (151 MHz, CDCl₃): δ = 79.5 (CCH), 74.8 (CCH), 68.9 (C-1), 58.5 (CH₂CCH); MS (ESI): *m/z* calcd for C₈H₁₀O₂: 161.1 [M+Na]⁺, found: 161.0.

1,4-Butanediol bis(2-propynyl) ether (S12). 1,4-Butanediol (**S2**, 502 mg, 5.57 mmol) and KOH (3.12 g, 55.6 mmol) were dissolved in DMF (10 mL) and stirred at 0 °C for 5 min under argon, then propargyl bromide (80 % in toluene, 3.0 mL, 27.8 mmol) was added dropwise, and the solution was stirred overnight allowing to reach rt. The solution was diluted with H₂O (70 mL), extracted with EtOAc (4 x 50 mL), dried over Na₂SO₄, filtered and concentrated *in vacuo*. The crude product was purified by flash column chromatography (petroleum ether/EtOAc, 10:1 to 8:2) to give **S12** (636 mg, 69 %). ¹H NMR (600 MHz, CDCl₃): δ = 4.11 (d, *J* = 2.5 Hz, 4H, CH₂CCH), 3.54 – 3.50 (m, 4H, H-1), 2.40 (t, *J* = 2.4 Hz, 2H, CCH), 1.68 – 1.64 (m, 4H, H-2); ¹³C NMR (151 MHz, CDCl₃): δ = 80.1 (CCH), 74.2 (CCH), 69.8 (C-1), 58.1 (CH₂CCH), 26.2 (C-2); MS (ESI): *m/z* calcd for C₁₀H₁₄O₂: 167.1 [M+H]⁺, found: 167.0.

1,8-Octanediol bis(2-propynyl) ether (S13). 1,8-Octanediol (**S3**, 501 mg, 3.43 mmol) and KOH (2.01 g, 35.8 mmol) were dissolved in DMF (10 mL) and stirred at 0 °C for 5 min under argon, then propargyl bromide (80 % in toluene, 1.5 mL, 13.9 mmol) was added dropwise, and the solution was stirred overnight allowing to reach rt. The solution was diluted with H₂O (70 mL), extracted with EtOAc (4 x 50 mL), dried over Na₂SO₄, filtered and concentrated *in vacuo*. The crude product was

purified by flash column chromatography (petroleum ether/EtOAc, 10:1 to 8:2) to give **S13** (646 mg, 85 %). ¹H NMR (600 MHz, CDCl₃): δ = 4.10 (d, *J* = 2.5 Hz, 4H, CH₂CCH), 3.47 (t, *J* = 6.6 Hz, 4H, H-1), 2.39 (t, *J* = 2.4 Hz, 2H, CCH), 1.56 (dq, *J* = 8.0, 6.6 Hz, 4H, H-2), 1.36 – 1.27 (m, 8H, H-3, H-4); ¹³C NMR (151 MHz, CDCl₃): δ = 80.1 (CCH), 74.1 (CCH), 70.3 (C-1), 58.1 (CH₂CCH), 30.0 (C-2), 29.4 (C-3), 26.1 (C-4); MS (ESI): *m/z* calcd for C₁₄H₂₂O₂: 245.1 [M+H]⁺, found: 245.0.

2-(Hydroxymethyl)-1,3-propanediol tris(2-propynyl) ether (S14). 2-Hydroxymethyl-1,3-propanediol (**S4**, 250 mg, 2.35 mmol) and KOH (1.35 mg, 24.1 mmol) were dissolved in DMF (5 mL) and stirred at 0 °C for 5 min under argon, then propargyl bromide (80 % in toluene, 1.5 mL, 13.9 mmol) was added dropwise, and the solution was stirred overnight allowing to reach rt. The solution was diluted with H₂O (40 mL), extracted with EtOAc (4 x 50 mL), dried over Na₂SO₄, filtered and concentrated *in vacuo*. The crude product was purified by flash column chromatography (petroleum ether/EtOAc, 10:1 to 9:1) to give **S14** (258 mg, 50 %). ¹H NMR (500 MHz, CDCl₃): δ = 4.11 (d, *J* = 2.4 Hz, 6H, CH₂CCH), 3.56 (d, *J* = 6.0 Hz, 6H, H-1), 2.41 (t, *J* = 2.4 Hz, 3H, CCH), 2.19 (hept, *J* = 5.8 Hz, 1H, H-2); ¹³C NMR (126 MHz, CDCl₃): δ = 80.0 (CCH), 74.4 (CCH), 68.4 (CH₂CCH), 58.5 (C-1), 40.1 (C-2); MS (ESI): *m/z* calcd for C₁₃H₁₆O₃: 243.1 [M+H]⁺, found: 242.9.

cis,cis-1,3,5-Cyclohexanetriol tris(2-propynyl) ether (S15). To a solution of *cis,cis*-1,3,5-cyclohexanetriol (**S5**, 496 mg, 3.75 mmol) in THF (14 mL), NaH (60 % in mineral oil, 921 mg, 23.0 mmol) was added, and the mixture was stirred at 0 °C for 15 min under argon. Then propargyl bromide (80 % in toluene, 1.35 mL, 12.5 mmol) was added, and the solution was stirred overnight allowing to reach rt. The solution was diluted with H₂O (20 mL), extracted with EtOAc (4 x 30 mL), dried over Na₂SO₄, filtered and concentrated *in vacuo*. The crude product was purified by flash column chromatography (petroleum ether/EtOAc, 10:1 to 8:2) to give **S15** (47.7 mg, 5 %). ¹H NMR (600 MHz, CDCl₃): δ = 4.19 (d, *J* = 2.5 Hz, 6H, CH₂CCH), 3.50 (tt, *J* = 11.5, 4.1 Hz, 3H, H-1), 2.44 – 2.39 (m, 6H, H-2e, CCH), 1.21 (q, *J* = 11.6 Hz, 1H, H-2a); ¹³C NMR (151 MHz, CDCl₃): δ = 79.9 (CCH), 74.5 (CCH), 72.0 (C-1), 55.6 (CH₂CCH), 37.5 (C-2); MS (ESI): *m/z* calcd for C₁₅H₁₈O₃: 269.1 [M+Na]⁺, found: 269.1.

Benzene-1,3,5-triol tris(2-propynyl) ether (S16). Benzene-1,3,5-triol (**S6**, 500 mg, 3.97 mmol) and K₂CO₃ (1.67 g, 12.1 mmol) were dissolved in DMF (15 mL) and stirred at rt for 10 min under argon, then propargyl bromide (80 % in toluene, 1.5 mL, 13.9 mmol) was added dropwise, and the solution was stirred overnight allowing to reach rt. The solution was poured into ice-cold H₂O (100 mL) and stirred to precipitate the product, which was purified by flash column chromatography (petroleum

ether/EtOAc, 10:1 to 8:2) to give **S16** (860 mg, 90 %). ^1H NMR (500 MHz, CDCl_3): δ = 6.27 (s, 3H, H-2), 4.65 (d, J = 2.4 Hz, 6H, CH_2CCH), 2.53 (t, J = 2.4 Hz, 3H, CCH); ^{13}C NMR (126 MHz, CDCl_3): δ = 159.5 (C-1), 95.6 (C-2), 78.4 (CCH), 75.9 (CCH), 56.1 (CH_2CCH); MS (ESI): m/z calcd for $\text{C}_{15}\text{H}_{12}\text{O}_3$: 263.1 $[\text{M}+\text{Na}]^+$, found: 262.9.

2,2-Bis(hydroxymethyl)propane-1,3-diol tetrakis(2-propynyl) ether (S17). Pentaerythritol (**S7**, 508 mg, 3.73 mmol) and KOH (3.10 g, 55.3 mmol) were dissolved in DMF (10 mL) and stirred at 0 °C for 5 min under argon, then propargyl bromide (80 % in toluene, 4.3 mL, 39.9 mmol) was added dropwise, and the solution was stirred overnight allowing to reach rt. The solution was diluted with H_2O (70 mL), extracted with EtOAc (4 x 50 mL), dried over Na_2SO_4 , filtered and concentrated *in vacuo*. The crude product was purified by flash column chromatography (petroleum ether/EtOAc, 10:1 to 8:2) to give **S17** (910 mg, 85 %). ^1H NMR (600 MHz, CDCl_3): δ = 4.11 (d, J = 2.5 Hz, 8H, CH_2CCH), 3.52 (s, 8H, H-1), 2.40 (t, J = 2.4 Hz, 4H, CCH); ^{13}C NMR (151 MHz, CDCl_3): δ = 80.3 (CCH), 74.2 (CCH), 69.1 (CH_2CCH), 58.8 (C-1), 44.8 (C-2); MS (ESI): m/z calcd for $\text{C}_{17}\text{H}_{20}\text{O}_4$: 311.1 $[\text{M}+\text{Na}]^+$, found: 311.1.

2-[[3-Hydroxy-2,2-bis(hydroxymethyl)propoxy]methyl]-2-(hydroxymethyl)propane-1,3-diol hexakis(2-propynyl) ether (S18). Dipentaerythritol (**S8**, 503 mg, 1.98 mmol) and KOH (5.45 g, 97.1 mmol) were dissolved in DMF (20 mL) and stirred at 0 °C for 5 min under argon, then propargyl bromide (80 % in toluene, 6.0 mL, 55.7 mmol) was added dropwise, and the solution was stirred overnight allowing to reach rt. The solution was diluted with H_2O (50 mL), extracted with EtOAc (4 x 50 mL), dried over Na_2SO_4 , filtered and concentrated *in vacuo*. The crude product was purified by flash column chromatography (petroleum ether/EtOAc, 10:1 to 9:1) to give **S18** (589 mg, 62 %). ^1H NMR (500 MHz, CDCl_3): δ = 4.11 (d, J = 2.4 Hz, 12H, CH_2CCH), 3.51 (s, 12H, H-1), 3.38 (s, 4H, H-3), 2.41 (t, J = 2.4 Hz, 6H, CCH); ^{13}C NMR (126 MHz, CDCl_3): δ = 80.3 (CCH), 74.2 (CCH), 69.9 (C-3), 69.3 (C-1), 58.8 (CH_2CCH), 45.2 (C-2); MS (ESI): m/z calcd for $\text{C}_{28}\text{H}_{34}\text{O}_7$: 485.2 $[\text{M}+\text{Na}]^+$, found: 485.0.

cis-Inositol hexakis(2-propynyl) ether (S19). *cis*-Inositol (**S9**, 25.0 mg, 0.14 mmol) and KOH (161 mg, 2.87 mmol) were dissolved in DMF (0.5 mL) and stirred at 0 °C for 5 min under argon, then propargyl bromide (80 % in toluene, 0.19 mL, 1.76 mmol) was added dropwise, and the solution was stirred overnight allowing to reach rt. The solution was diluted with H_2O (10 mL), extracted with EtOAc (4 x 10 mL), dried over Na_2SO_4 , filtered and concentrated *in vacuo*. The crude product was purified by flash column chromatography (petroleum ether/EtOAc, 8:2 to 1:1) to give **S19** (12.5 mg,

22 %). ^1H NMR (500 MHz, CDCl_3): δ = 4.54 (s, 6H, CH_2CCHa), 4.42 (d, J = 11.9 Hz, 9H, H-e, CH_2CCHb), 3.58 (s, 3H, H-a), 2.50 – 2.37 (m, 6H, CCH); ^{13}C NMR (126 MHz, CDCl_3): δ = 81.1 (CCHa), 79.5 (CCHb), 76.2 (C-Ha), 75.3 (CCHa), 74.8 (CCHb), 72.1 (C-He), 59.1 (CH_2CCHa), 56.0 (CH_2CCHb); MS (ESI): m/z calcd for $\text{C}_{24}\text{H}_{24}\text{O}_6$: 431.1 $[\text{M}+\text{Na}]^+$, found: 431.1.

Benzenehexol hexakis(2-propynyl) ether (S20). Benzenehexol (**S10**, 444 mg, 2.55 mmol) and K_2CO_3 (2.75 g, 19.9 mmol) were dissolved in DMF (11 mL) and stirred at rt for 10 min under argon, then propargyl bromide (80 % in toluene, 2.5 mL, 23.2 mmol) was added dropwise, and the solution was stirred overnight allowing to reach rt. The solution was poured into ice-cold H_2O (100 mL) and stirred to precipitate the product, which was purified by flash column chromatography (petroleum ether/EtOAc, 10:1 to 8:2) to give **S20** (51.6 mg, 5 %). ^1H NMR (500 MHz, CDCl_3): δ = 4.80 (d, J = 2.6 Hz, 12H, CH_2CCH), 2.51 (t, J = 2.5 Hz, 6H, CCH); ^{13}C NMR (126 MHz, CDCl_3): δ = 141.6 (C-1), 79.0 (CCH), 75.9 (CCH), 61.3 (CH_2CCH); MS (ESI): m/z calcd for $\text{C}_{24}\text{H}_{18}\text{O}_6$: 425.1 $[\text{M}+\text{Na}]^+$, found: 425.0.

2. Determination of polymer 33 loading

Loading of polymer **33** was calculated with the formula:

$$\% \text{ loading} = \frac{I_e}{I_e + I_t} \cdot 100 \% \quad (\text{S1})$$

Where I_e and I_t are the integrals corresponding to ^1H signals for epitope and thioglycerol moieties, respectively. I_e was calculated as the average of the integrals related to protons H-2e, L2, H-6a and H-4a, while for $I_e + I_t$ the signal at $\delta = 2.79$, corresponding to the protons H-3'e and A', was selected.

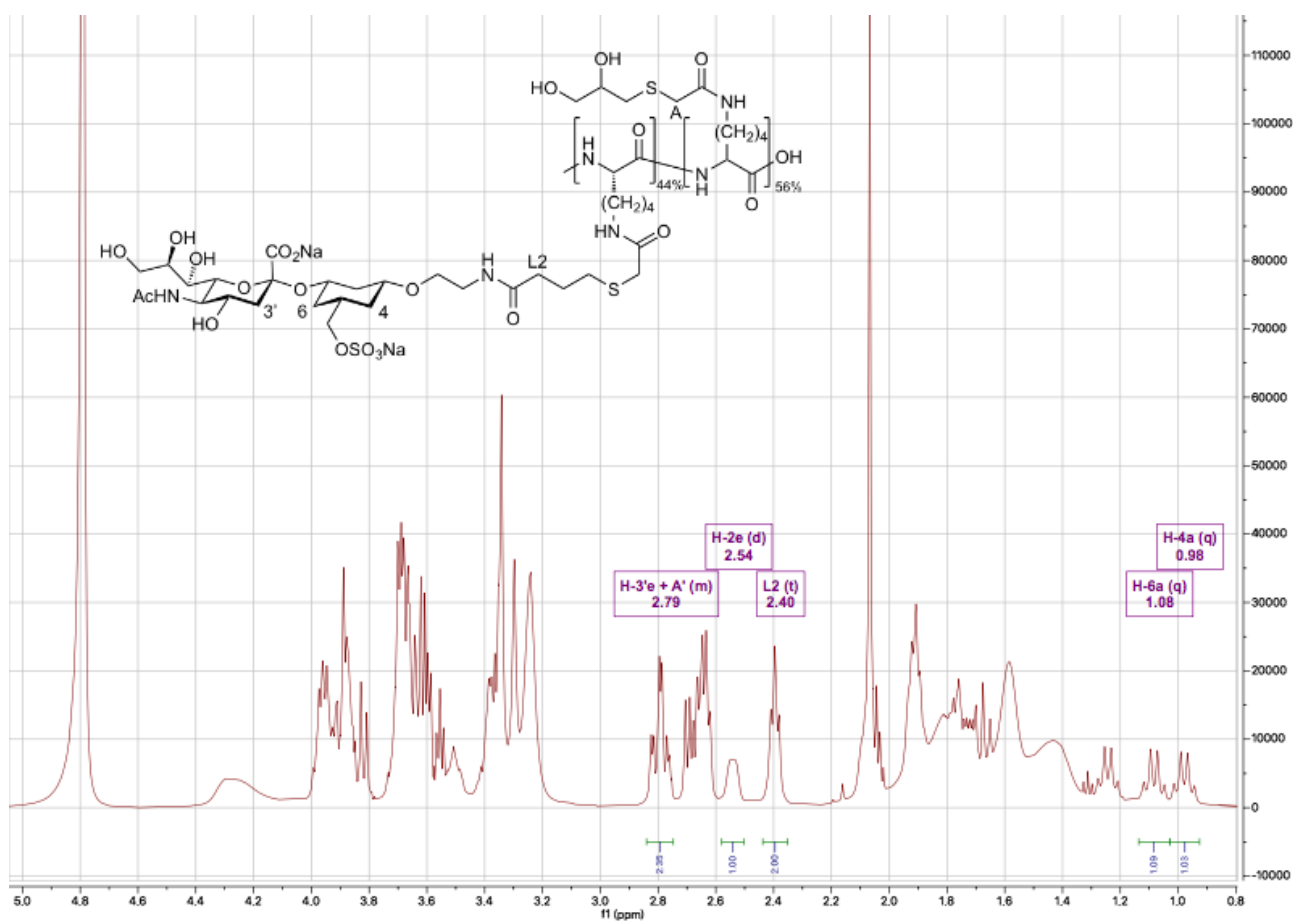


Figure S2. ^1H NMR spectrum of **33**.

3. Differential Scanning Fluorimetry

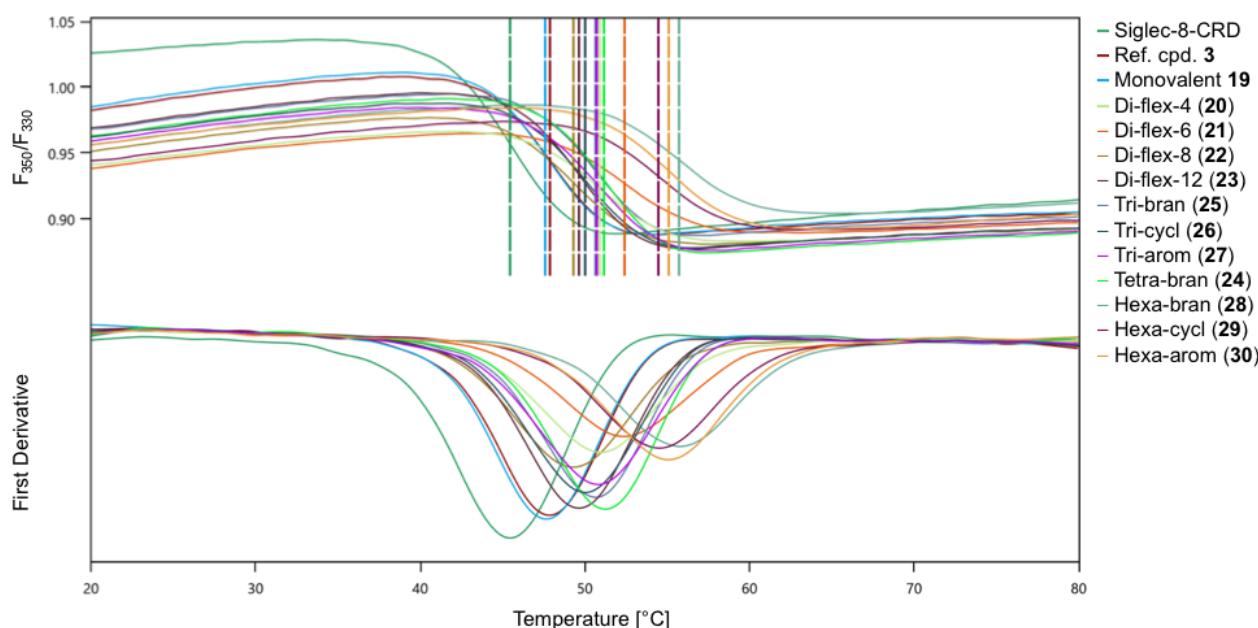


Figure S3. NanoDSF analysis of multivalent ligands. The upper graph represents the ratio between the fluorescence measured at 350 and 330 nm, while the lower one depicts the related first derivatives are depicted.

4. Isothermal Titration Calorimetry

4.1. General methods. Isothermal titration calorimetry experiments were performed at 25 °C (or a specified different temperature) on an ITC200 (MicroCal, Northampton, USA) instrument set to 6 $\mu\text{cal}\cdot\text{s}^{-1}$ reference power, 750 rpm stirring speed, feedback mode high, 2 s filter period). Protein solutions were dialyzed against ITC buffer (100 mM HEPES, 150 mM NaCl, pH 7.4) prior to the experiments and all samples were prepared using the dialysate buffer to minimize dilution effects. Protein concentrations were determined spectrophotometrically with the specific absorbance at 280 nm employing an extinction coefficient of $33240\text{ mol}^{-1}\cdot\text{cm}^{-1}$. In a typical experiment, a 0.5-10 mM ligand solution was titrated to a solution containing 35-100 μM Siglec-8 to ensure more than 80 % saturation. For low c experiments, the stoichiometry parameter was constrained to 1. Baseline correction, peak integration, and non-linear regression analysis of experimental data were performed using the NITPIC (version 1.2.2.) [4] and SEDPHAT (version 12.1b) [5] software packages. Replicates were analyzed using global fitting, and the 68 % confidence intervals were calculated as an estimate of experimental error.

4.2. Thermodynamic data and errors

Table S1. ITC results for oligovalent compounds. Error estimates resemble the 68 % confidence interval from global fitting of two or more independent experiments. n.d.: not determined.

Compound	K_D [μM]	ΔG° [$\text{kJ}\cdot\text{mol}^{-1}$]	ΔH° [$\text{kJ}\cdot\text{mol}^{-1}$]	$-\text{T}\Delta S^\circ$ [$\text{kJ}\cdot\text{mol}^{-1}$]	N
Monovalent 19	229.9 (226.4 – 233.4)	-20.8 (-20.8 – -20.7)	-29.7 (-30.0 – -29.5)	8.9 (8.7 – 9.2)	1 (fixed)
Di-flex-4 (20)	52.9 (45.2 – 62.7)	-24.4 (-24.8 – -24.0)	-79.5 (-101 – -66.6)	55.1 (41.8 – 77.4)	2.6 (2.3 – 3.2)
Di-flex-6 (21)	82.5 (72.4 – 95.0)	-23.3 (-23.6 – -23.0)	-88.5 (-119 – -72.0)	65.2 (48.4 – 95.6)	2.8 (2.4 – 3.5)
Di-flex-6 (22)	75.2 (70.2 – 80.9)	-23.5 (-23.7 – -23.4)	-100.9 (-117.9 – -88.9)	77.4 (65.2 – 94.5)	3.2 (2.9 – 3.7)
Di-flex-12 (23)	48.3 (43.2 – 54.3)	-24.6 (-24.9 – -24.3)	-80.4 (-95.7 – -69.9)	55.7 (44.9 – 71.4)	2.9 (2.6 – 3.4)
Tri-bran (25)	25.4 (23.1 – 28.0)	-26.2 (-26.5 – -26.0)	-122.8 (-136.4 – -112.3)	96.6 (85.8 – 110)	4.2 (3.9 – 4.5)
Tri-cycl (26)	30.0 (24.5 – 37.6)	-25.8 (-26.3 – -25.3)	-116.3 (-161.0 – -93.6)	90.5 (67.3 – 136)	4.1 (3.5 – 5.2)
Tri-arom (27)	16.9 (15.0 – 19.0)	-27.2 (-27.5 – -26.9)	-111.1 (-120.7 – -103.2)	83.8 (75.6 – 93.7)	3.4 (3.2 – 3.6)
Tetra-bran (24)	15.7 (13.5 – 18.5)	-27.4 (-27.8 – -27.0)	-132.3 (-152.0 – -117.9)	104.8 (90.1 – 125.0)	4.1 (3.8 – 4.5)
Hexa-bran (28)	7.9 (6.9 – 9.2)	-29.1 (-29.5 – -28.7)	-154.0 (-166.7 – -143.7)	124.9 (114.2 – 138.0)	5.2 (5.0 – 5.4)
Hexa-cycl (29)	8.1 (7.4 – 9.0)	-29.0 (-29.3 – -28.8)	-173.6 (-185.4 – -163.7)	144.6 (134.4 – 156.6)	6.3 (6.1 – 6.6)
Hexa-arom (30)	7.7 (6.8 – 8.8)	-29.2 (-29.5 – -28.9)	-150.4 (-160.8 – -141.8)	121.3 (112.3 – 131.9)	5.4 (5.3 – 5.6)
PLL-glycopolymer 33	0.042 (0.023 – 0.079)	-42.1 (-43.6 – -40.5)	n.d.	n.d.	n.d.

Table S2. Normalized ITC results for oligovalent compounds. Parameters were calculated from the experimental ITC results with the formula $\Delta X^\circ_{\text{norm}} = \Delta X^\circ / N$. Error estimates resemble the 68 % confidence interval from global fitting of two or more independent experiments. ^[a] Dissociation constants are calculated according to Kitov-Bundle model:

$$K_{D \text{ norm}} = K_D \cdot N.$$

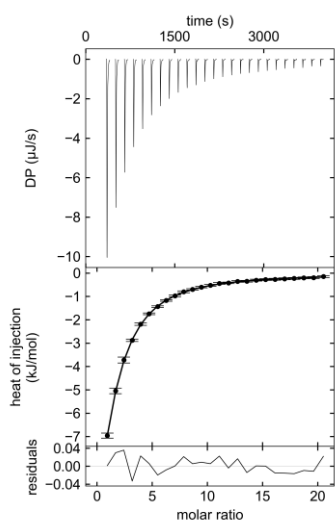
Compound	$K_{D \text{ norm}}^{\text{[a]}}$ [μM]	$\Delta G^\circ_{\text{norm}}$ [$\text{kJ}\cdot\text{mol}^{-1}$]	$\Delta H^\circ_{\text{norm}}$ [$\text{kJ}\cdot\text{mol}^{-1}$]	$-\text{T}\Delta S^\circ_{\text{norm}}$ [$\text{kJ}\cdot\text{mol}^{-1}$]
Monovalent 17	229.9 (226.4 – 233.4)	-20.8 (-20.8 – -20.7)	-29.7 (-30.0 – -29.5)	8.9 (8.7 – 9.2)
Di-flex-4 (20)	139.3 (119.0 – 165.1)	-9.3 (-9.4 – -9.1)	-30.2 (-38.5 – -25.3)	20.9 (15.9 – 29.4)
Di-flex-6 (21)	229.0	-8.4	-31.9	23.5

Compound	K_D norm ^[a] [μ M]	ΔG° norm [kJ·mol ⁻¹]	ΔH° norm [kJ·mol ⁻¹]	$-T\Delta S^\circ$ norm [kJ·mol ⁻¹]
Di-flex-6 (22)	(201.0 – 263.8)	(-8.5 – -8.3)	(-42.7 – -25.9)	(17.4 – 34.4)
	244.1	-7.3	-31.1	23.8
Di-flex-12 (23)	(227.7 – 262.6)	(-7.3 – -7.2)	(-36.3 – -27.4)	(20.1 – 29.1)
	142.2	-8.4	-27.3	19.0
Tri-bran (25)	(127.2 – 159.6)	(-8.5 – -8.3)	(-32.6 – -23.8)	(15.3 – 24.3)
	106.3	-6.3	-29.4	23.1
Tri-cycl (26)	(96.6 – 117.2)	(-6.3 – -6.2)	(-32.6 – -26.9)	(20.5 – 26.4)
	121.9	-6.3	-28.6	22.2
Tri-arom (27)	(99.6 – 117.2)	(-6.5 – -6.2)	(-39.6 – -23.0)	(16.5 – 33.4)
	57.2	-8.0	-32.8	24.7
Tetra-bran (24)	(50.9 – 64.4)	(-8.1 – -7.9)	(-35.6 – -30.4)	(22.3 – 27.6)
	64.5	-6.7	-32.2	25.6
Hexa-bran (28)	(55.2 – 75.7)	(-6.8 – -6.6)	(-37.1 – -28.7)	(22.0 – 30.5)
	40.8	-5.7	-29.9	24.2
Hexa-cycl (29)	(35.4 – 47.4)	(-5.7 – -5.6)	(-32.4 – -27.9)	(22.2 – 26.8)
	51.5	-4.6	-27.4	22.8
Hexa-arom (30)	(46.7 – 57.0)	(-4.6 – -4.6)	(-29.3 – -25.9)	(21.2 – 24.7)
	42.1	-5.4	-27.6	22.3
	(37.2 – 47.8)	(-5.4 – -5.3)	(-29.5 – -26.0)	(20.6 – 24.2)

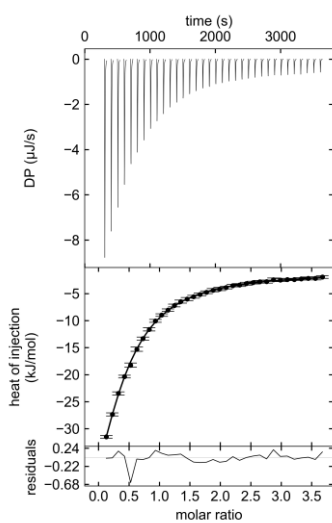
Table S3. ITC experiments for the determination of ΔC_p . Error estimates resemble the 68 % confidence interval from global fitting of two or more independent experiments. n.d.: not defined.

Compound	T [°C]	K_D [μ M]	ΔG° [kJ·mol ⁻¹]	ΔH° [kJ·mol ⁻¹]	$-T\Delta S^\circ$ [kJ·mol ⁻¹]	N
Monovalent 19	15	150.9	-21.8	-22.2	0.4	1 (fixed)
		(145.3 – 156.8)	(-21.9 – -21.7)	(-22.7 – -21.8)	(-0.1 – 1.0)	
Monovalent 19	35	345.3	-19.8	-24.7	4.9	1 (fixed)
		(337.0 – 354.6)	(-19.8 – -19.7)	(-25.1 – -24.3)	(4.5 – 5.4)	
Tetra-bran (24)	15	7.8	-29.2	-109.5	80.4	4.1
		(6.4 – 9.5)	(-29.6 – -28.7)	(-121.7 – -100.0)	(70.4 – 93.0)	(3.9 – 4.3)
Tetra-bran (24)	35	17.1	-27.2	-121.0	93.8	4.5
		(15.4 – 19.1)	(-27.5 – -26.9)	(-134.7 – -110.4)	(82.9 – 107.8)	(4.3 – 4.9)
Hexa-bran (28)	21.2	6.8	-29.5	-145.3	115.9	5.7
		(6.1 – 7.7)	(-29.8 – -29.2)	(-154.6 – -137.5)	(107.7 – 125.4)	(5.5 – 5.9)
Hexa-bran (28)	32	10.3	-28.5	-162.0	133.5	6.1
		(7.8 – 14.0)	(-29.1 – -27.7)	(-202.2 – -138.3)	(109.2 – 174.5)	(5.6 – 6.9)

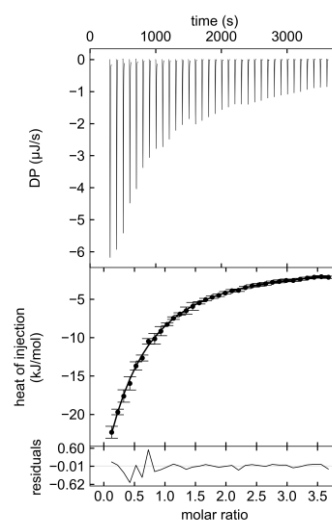
4.3. Representative thermograms of ITC experiments



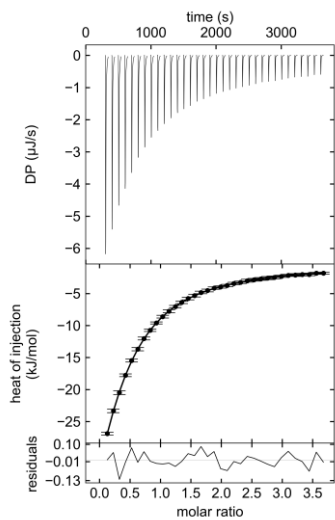
Compound 19



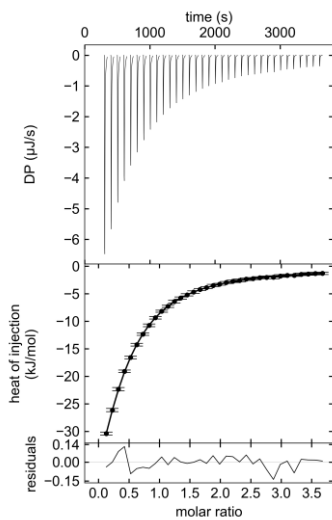
Compound 20



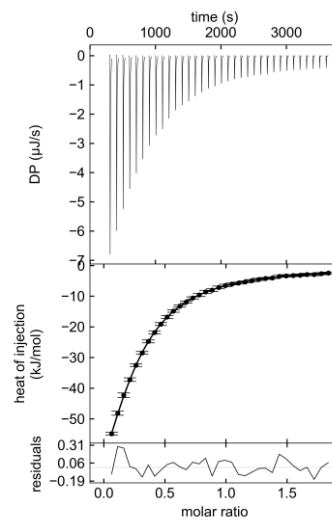
Compound 21



Compound 22

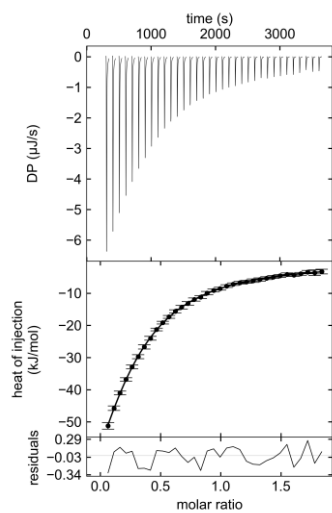


Compound 23

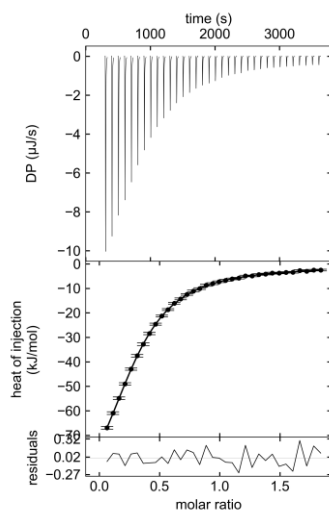


Compound 25

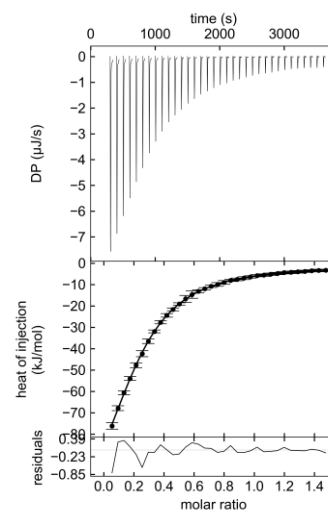
Oligo- and Multivalent presentation of Siglec-8 ligand



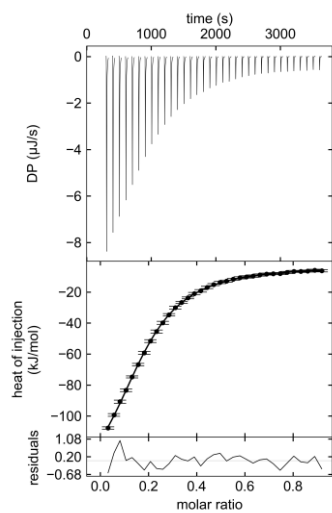
Compound 26



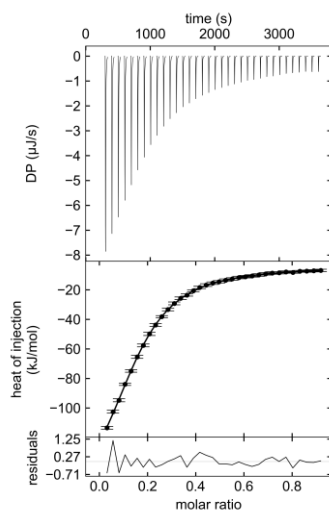
Compound 27



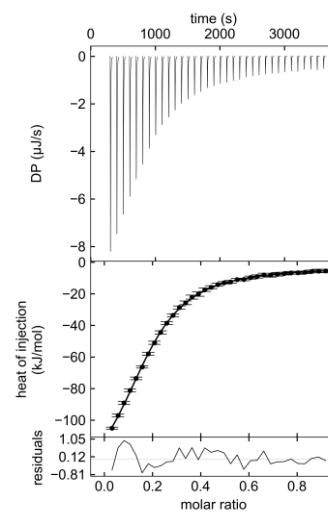
Compound 24



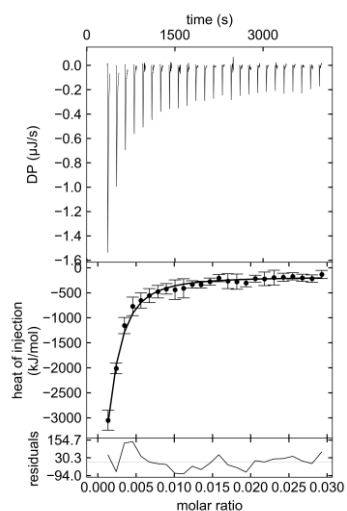
Compound 28



Compound 29



Compound 30



Compound 31

Figure S3. Exemplifying ITC analysis. Thermograms and binding isotherms for analyzed oligovalent compounds.

The ITC thermograms show no inflection points, reflecting the low c experiment shape (Figure S3). In such a case, the fitting parameters n and ΔH° are strictly correlated to each other and usually cannot be determined. The correlation between the two parameters was checked for each experiment using two-dimensional error surface projection (2D ESP) of the X^2 function (Figure S4).

The 2D ESP for compound **19** showed no minimum, as the two parameters are strictly dependent on each other. For this compound, therefore, the N parameter was fixed to 1, indicating the formation of the 1:1 complex with the protein. For the oligovalent compounds, such as **28**, a minimum region was found, together with the 68 % and 95 % confidence intervals, and so both n and ΔH° can be determined with the respective errors. Only for the polymer **31**, this correlation could not be obtained with the used experimental conditions, and additional experiments with increased amount of protein would be necessary.

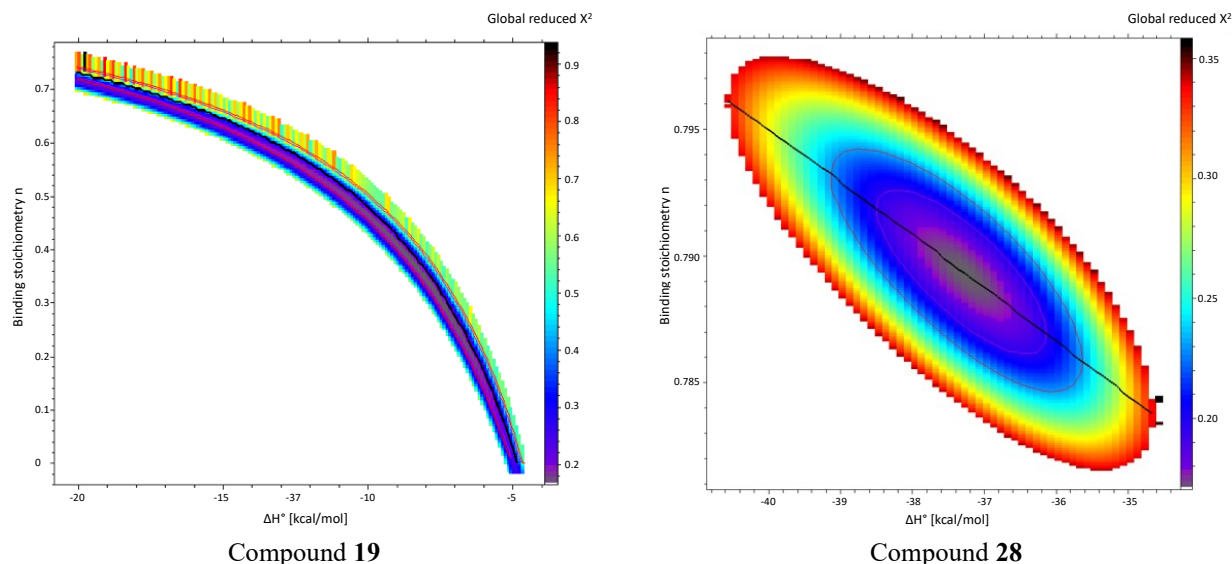
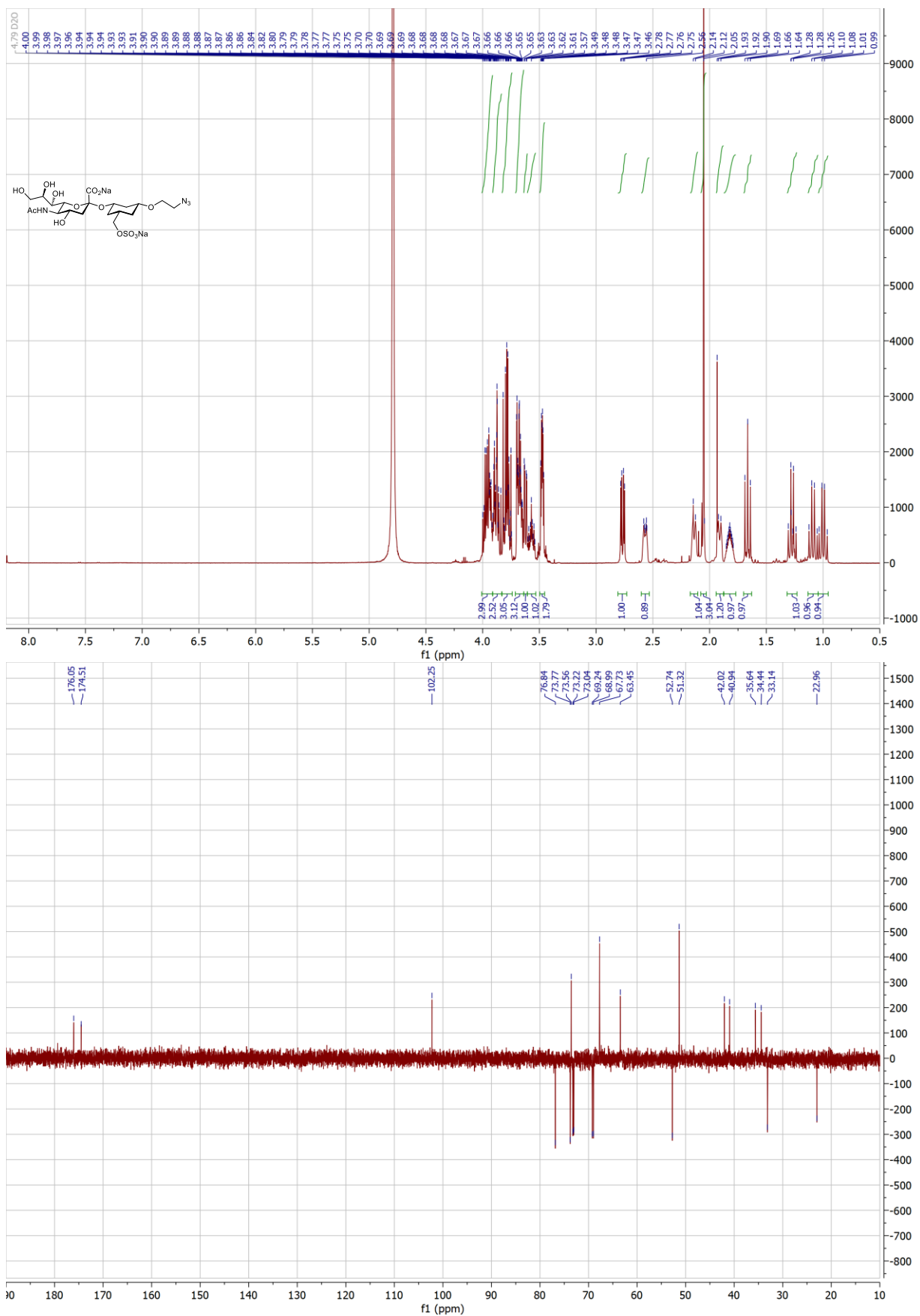


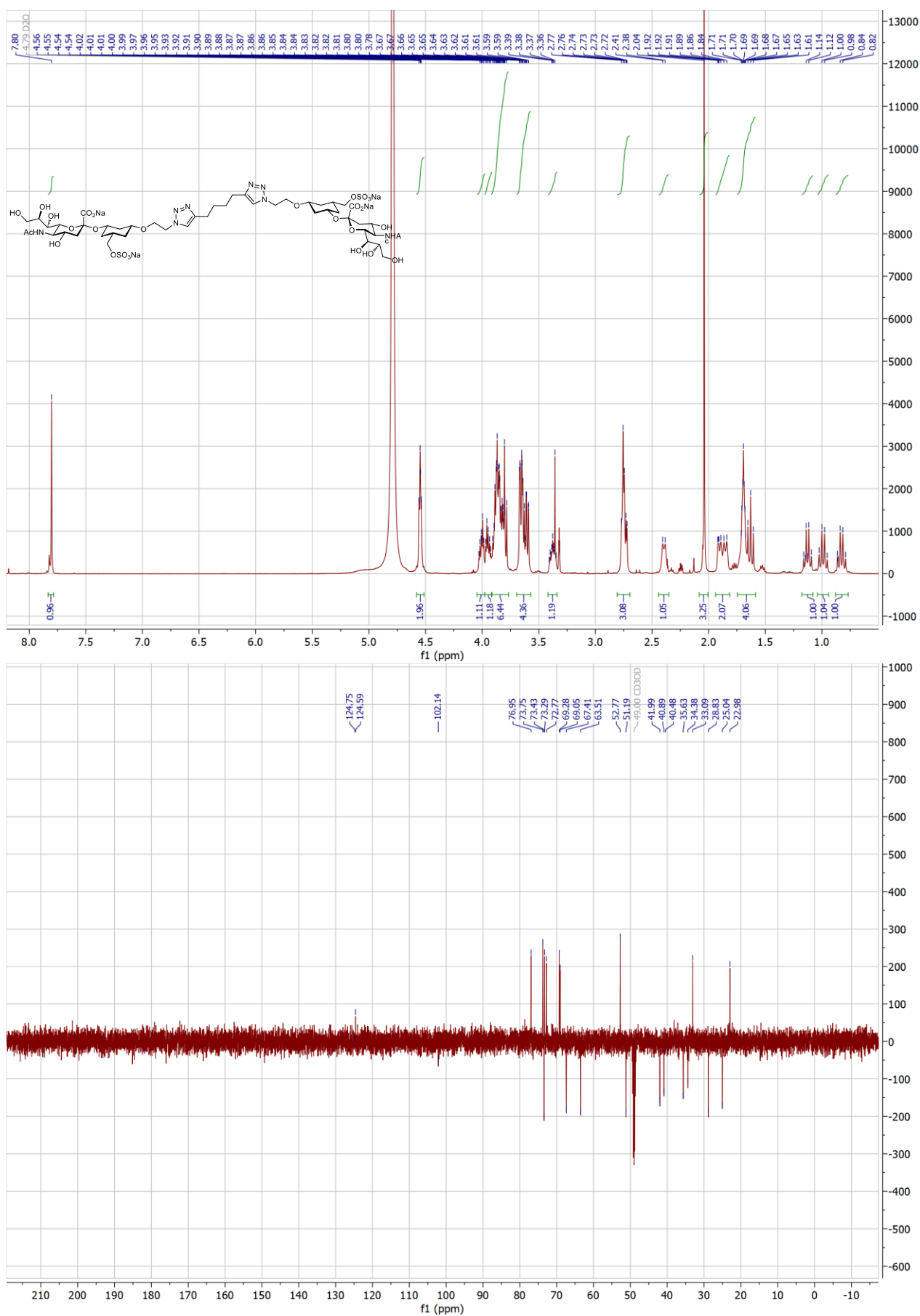
Figure S4. Examples of 2D ESP for compounds 19 and 28. Correlation between the fitting parameter n and the ΔH° . For compound **19**, the two values are strictly dependent on each other, and no minimum for both can be determined. For compound **28**, inner and outer confidence regions, corresponding to 68 and 95 % confidence thresholds, can be identified.

5. NMR and MS identification of target compounds

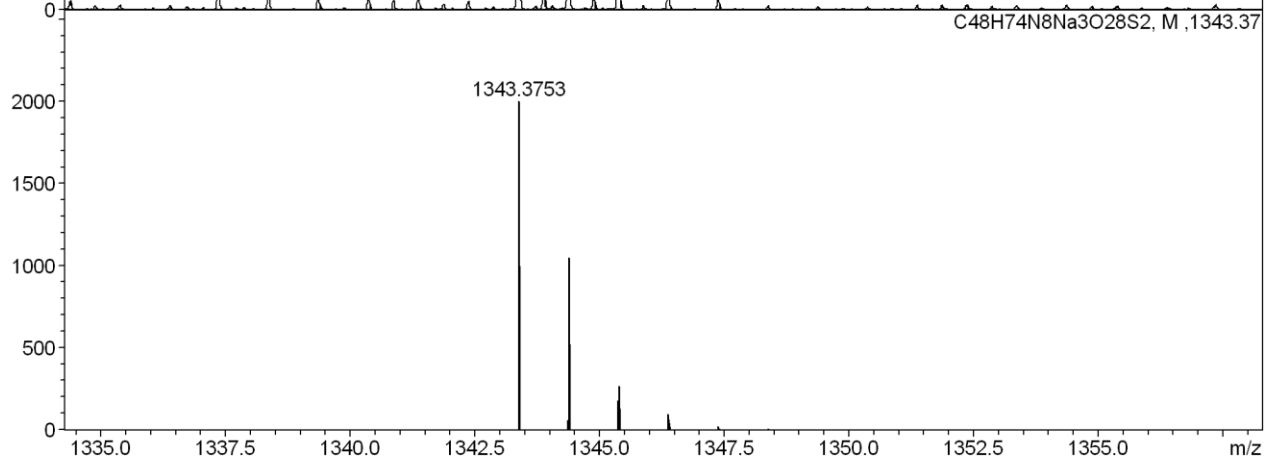
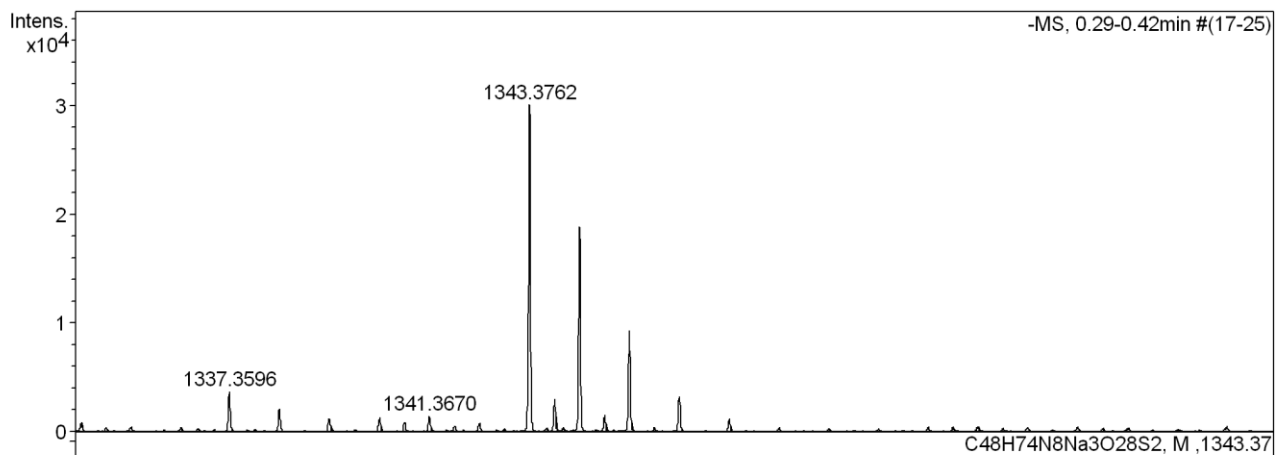
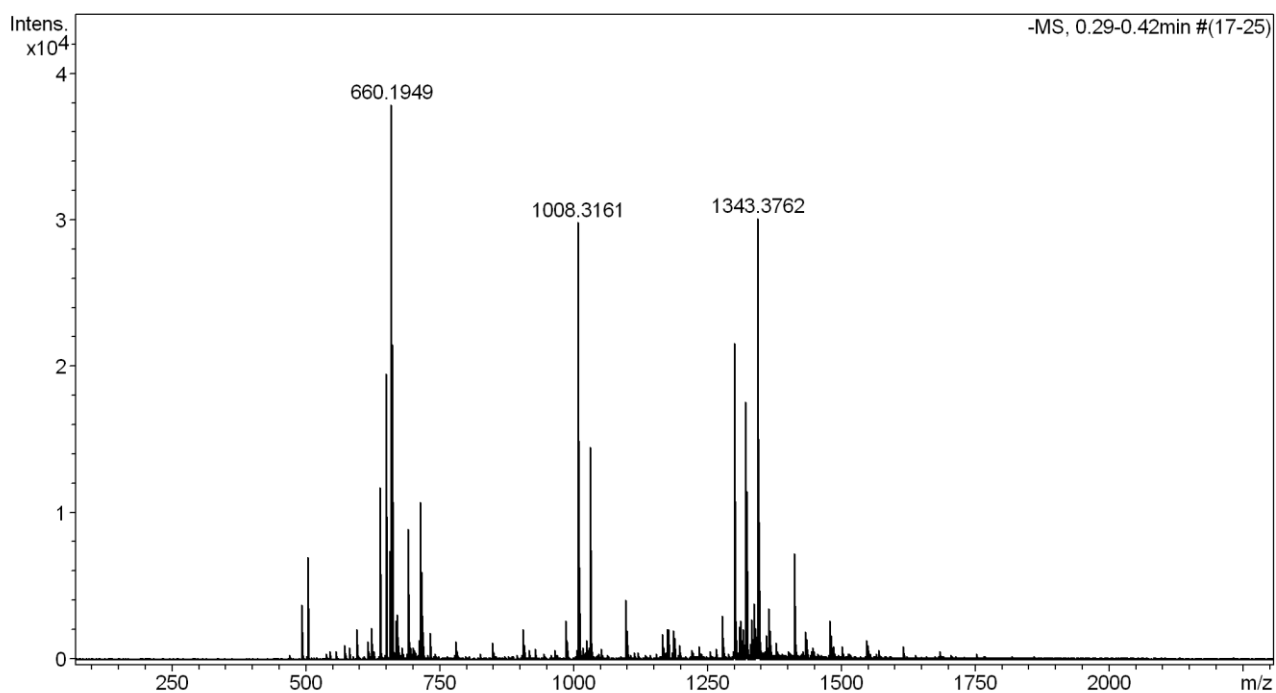
Compound **19**: ^1H NMR (500 MHz, D_2O) and ^{13}C APT-NMR (126 MHz, D_2O)



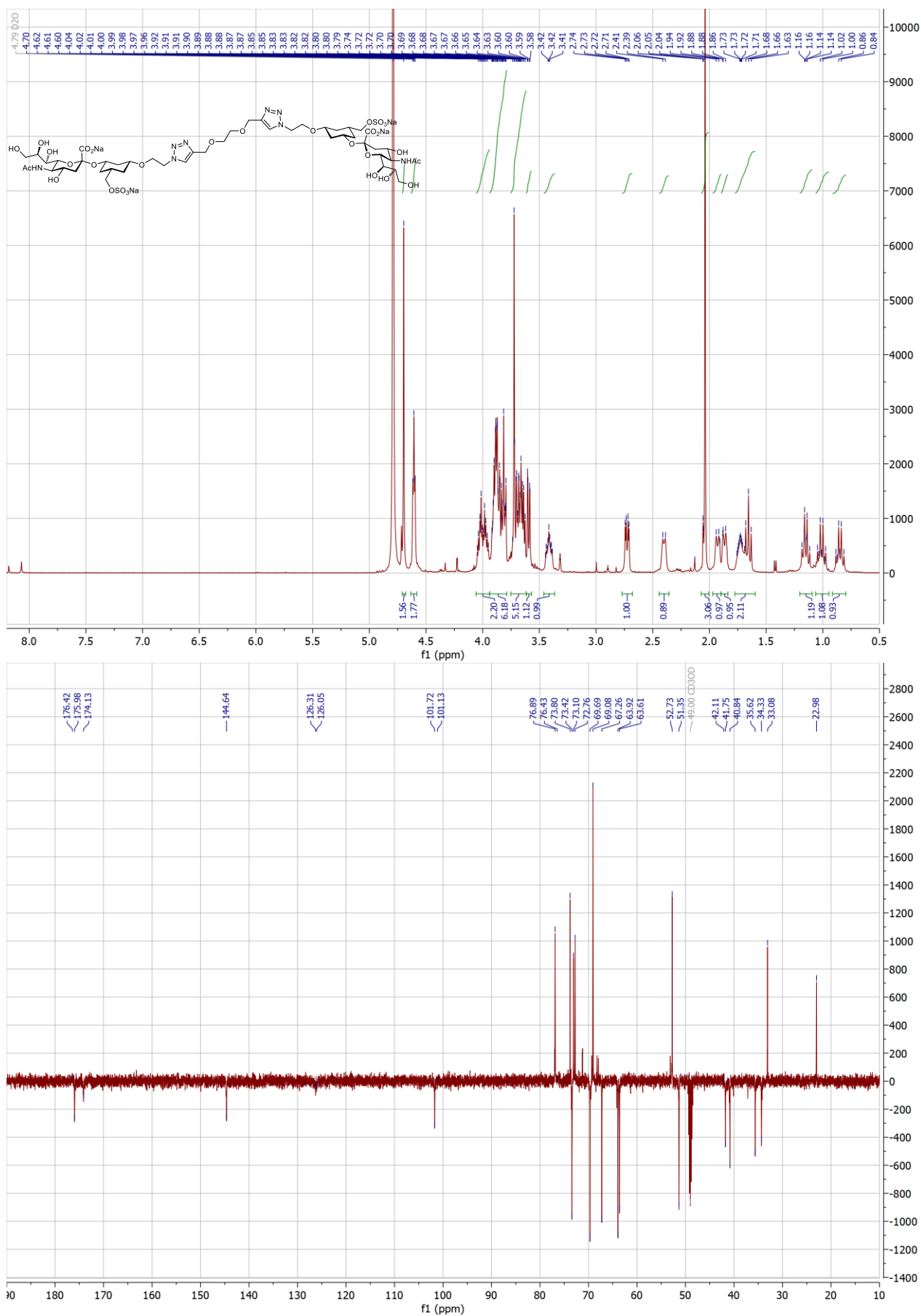
Compound **20**: ^1H NMR (500 MHz, D_2O), ^{13}C APT-NMR (126 MHz, D_2O) and HR-MS (ESI).



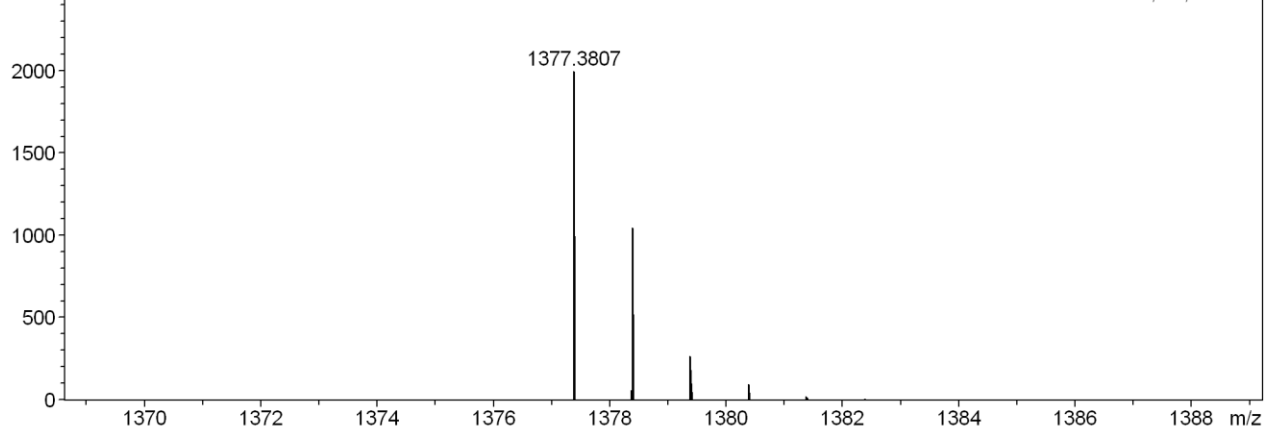
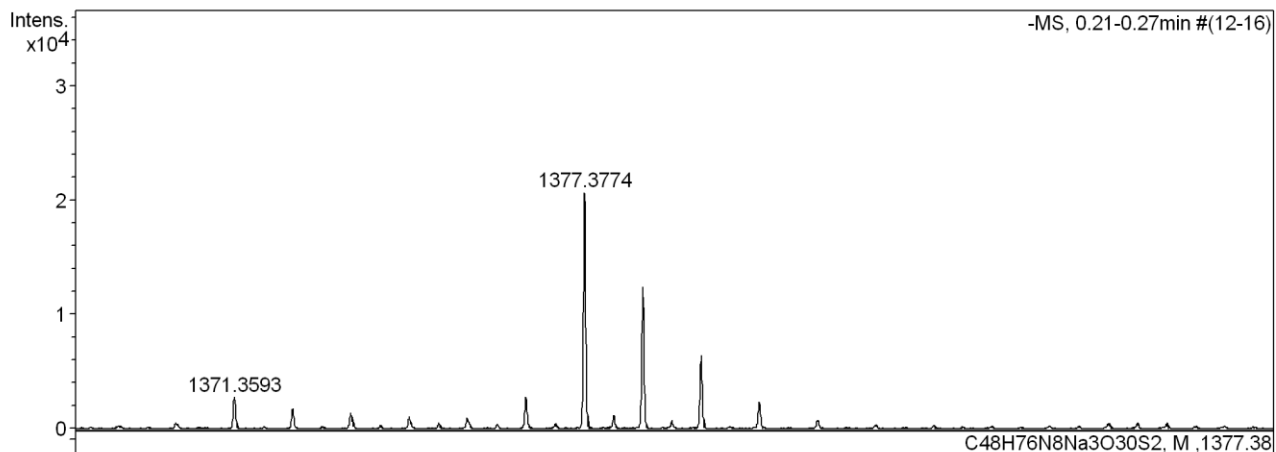
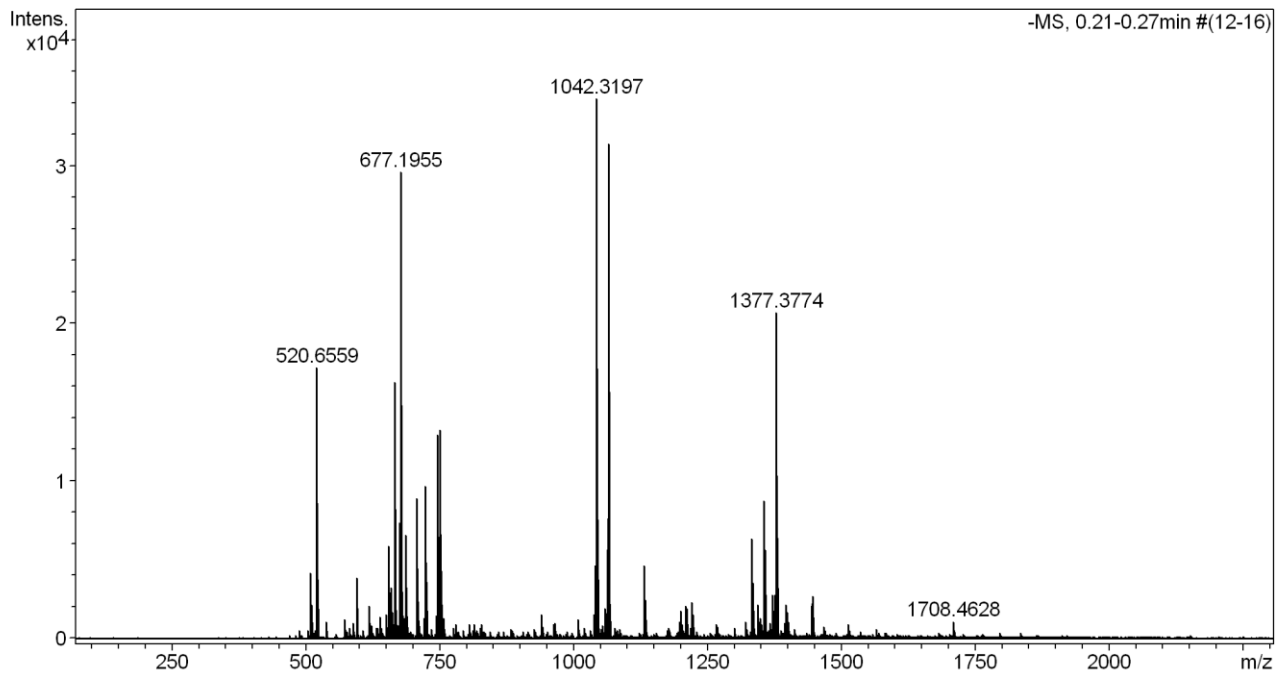
Oligo- and Multivalent presentation of Siglec-8 ligand



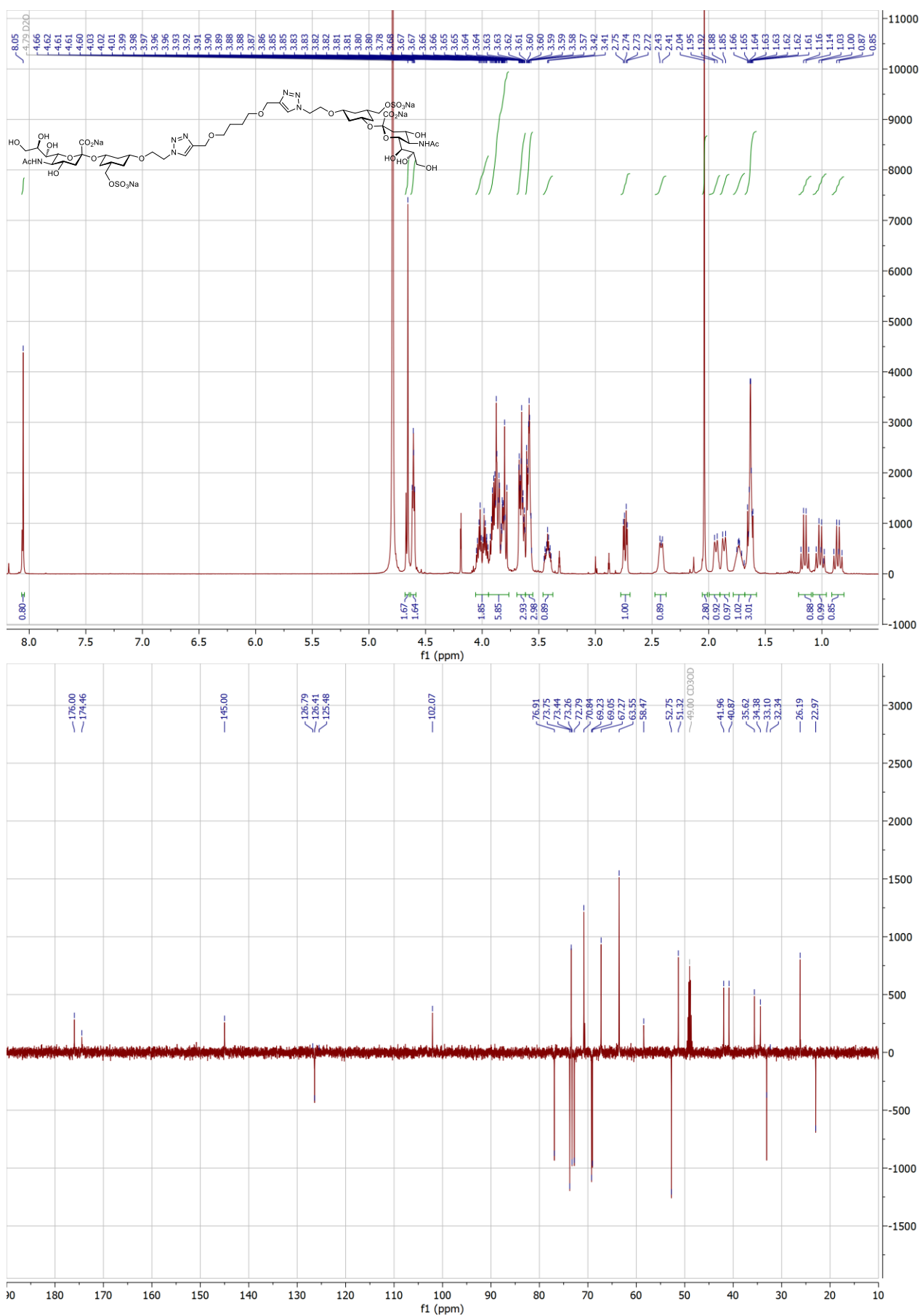
Compound **21**: ^1H NMR (500 MHz, D_2O), ^{13}C APT-NMR (126 MHz, D_2O) and HR-MS (ESI).



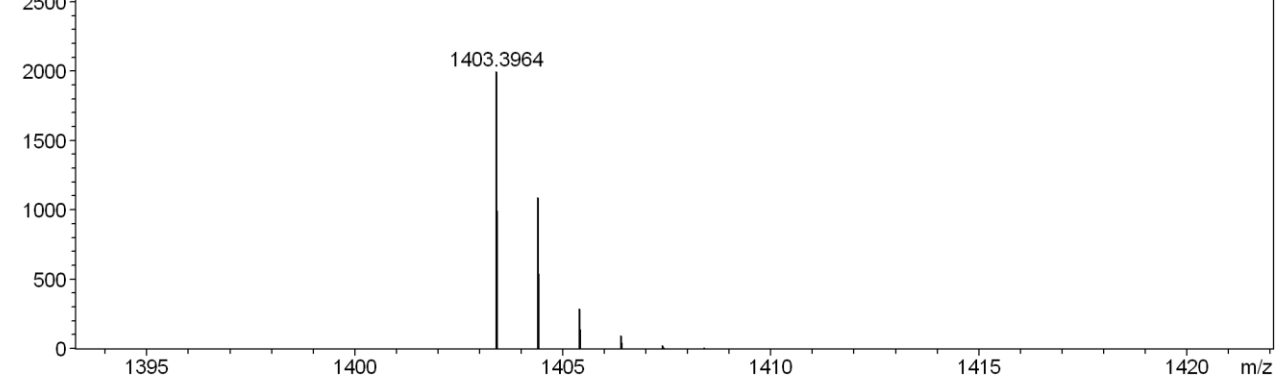
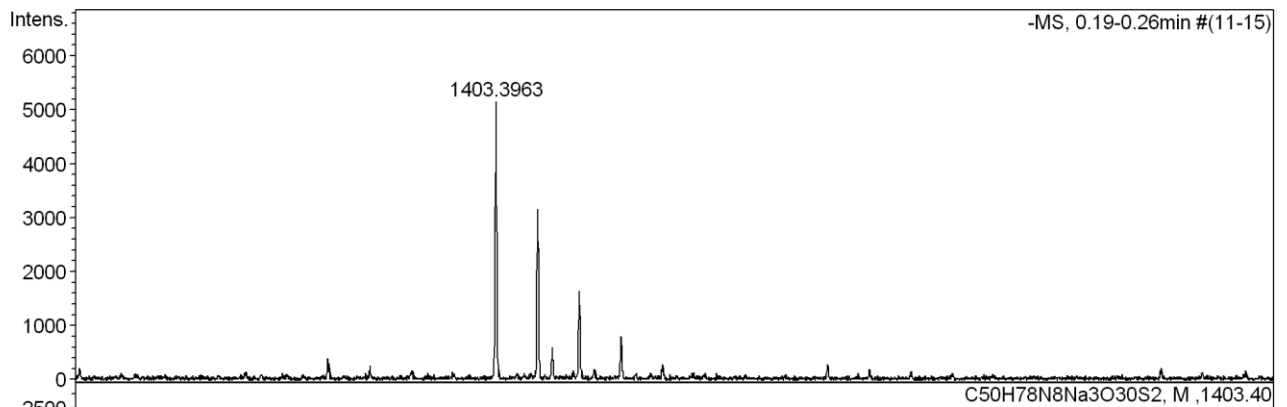
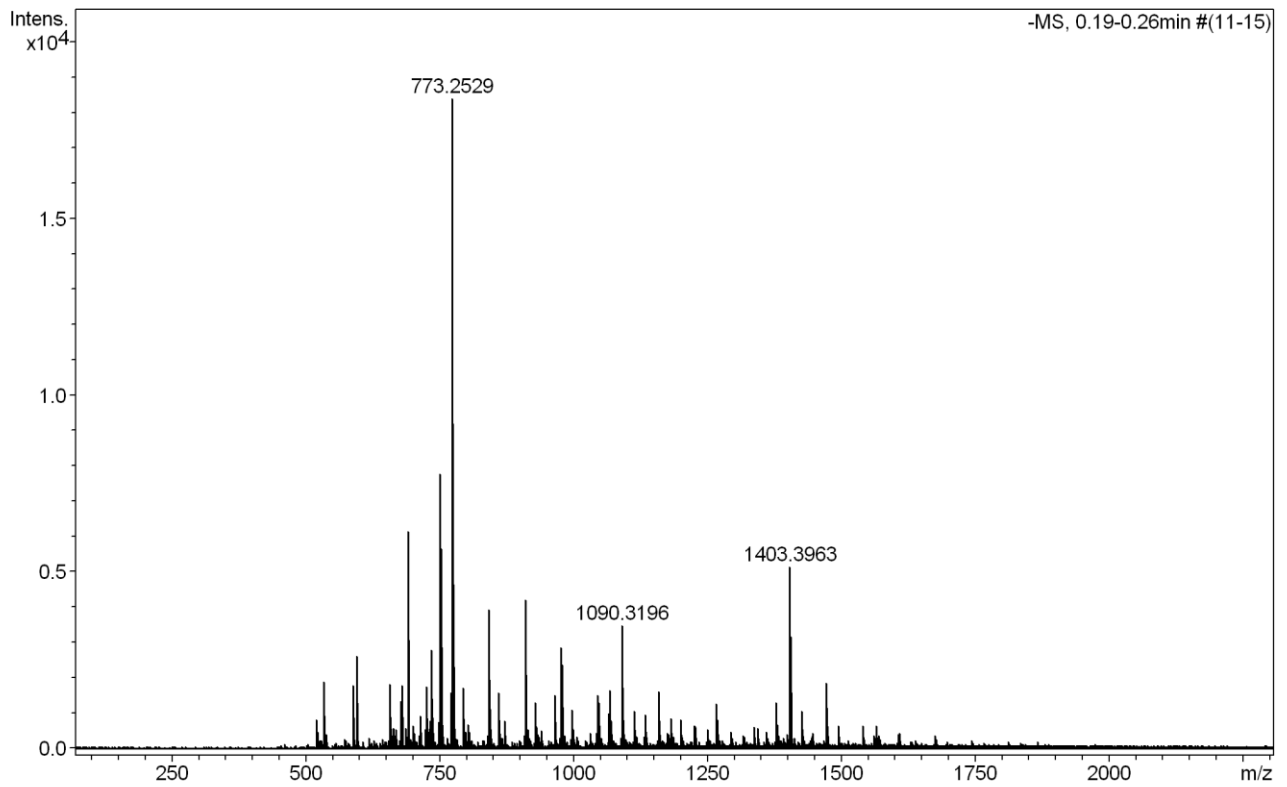
Oligo- and Multivalent presentation of Siglec-8 ligand



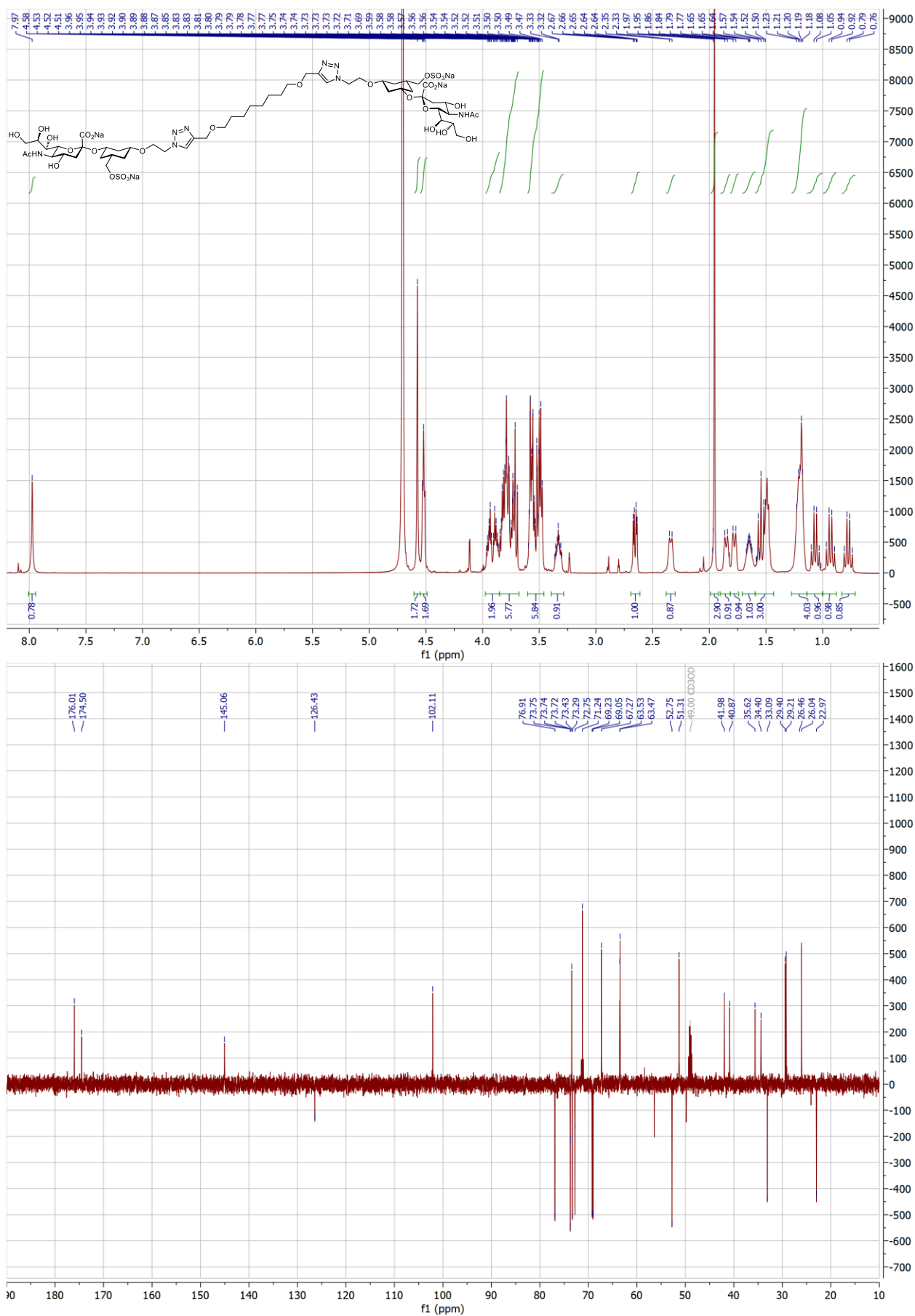
Compound 22: ^1H NMR (500 MHz, D_2O), ^{13}C APT-NMR (126 MHz, D_2O) and HR-MS (ESI).



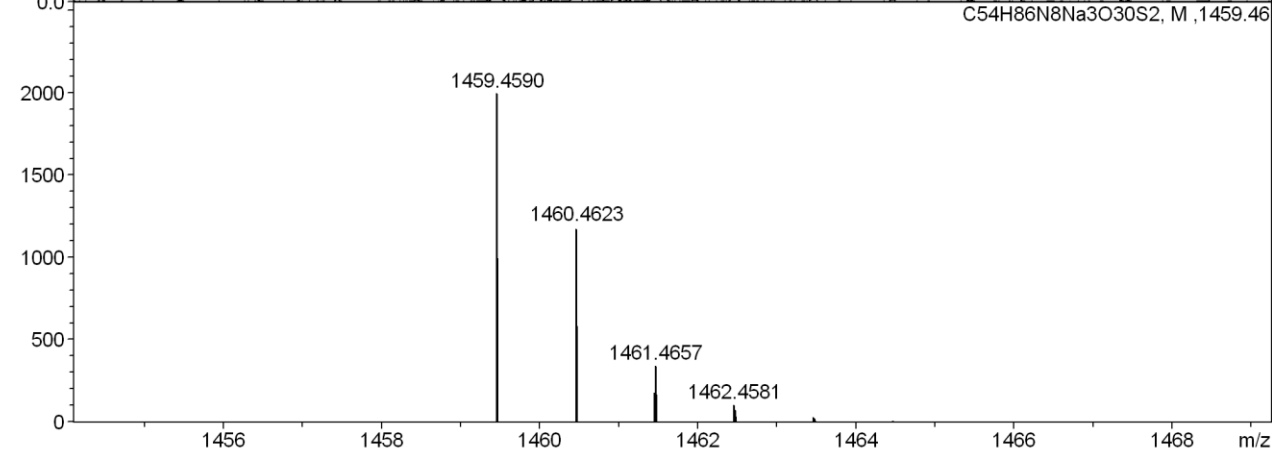
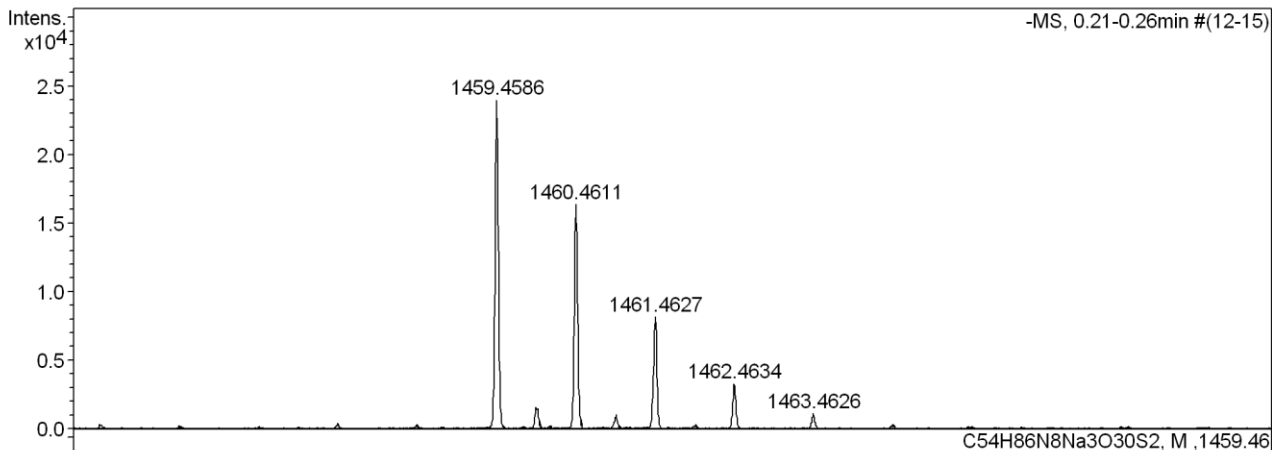
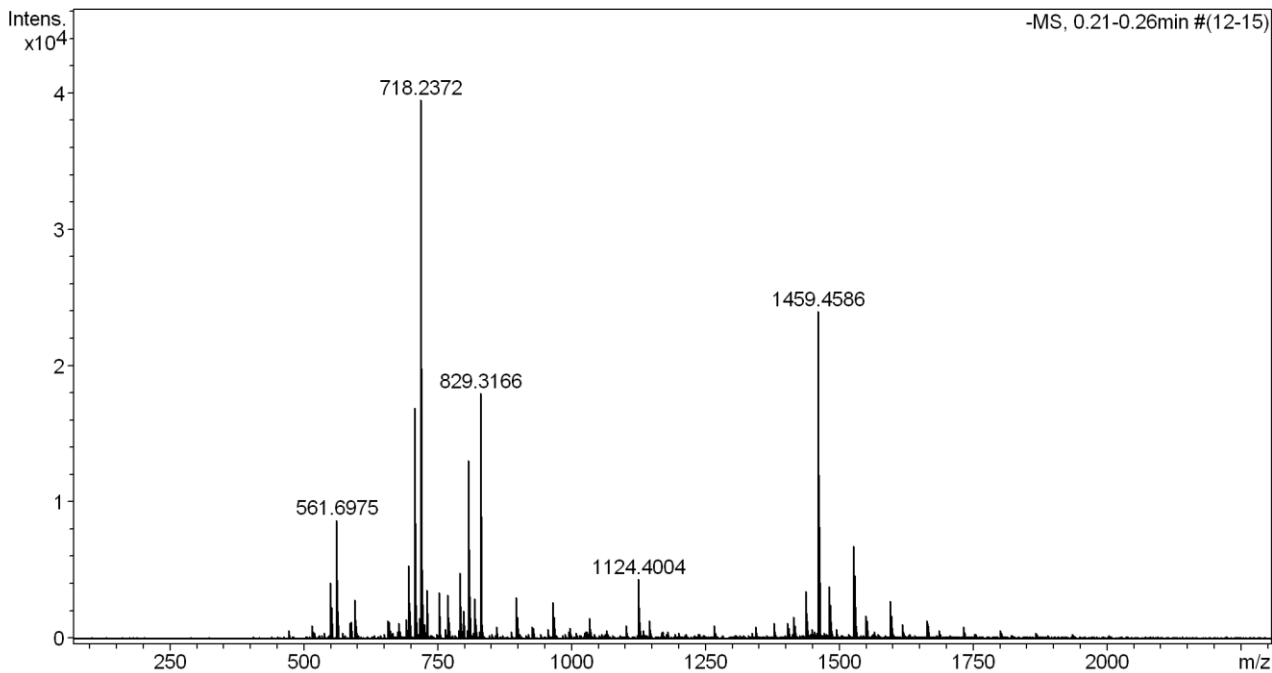
Oligo- and Multivalent presentation of Siglec-8 ligand



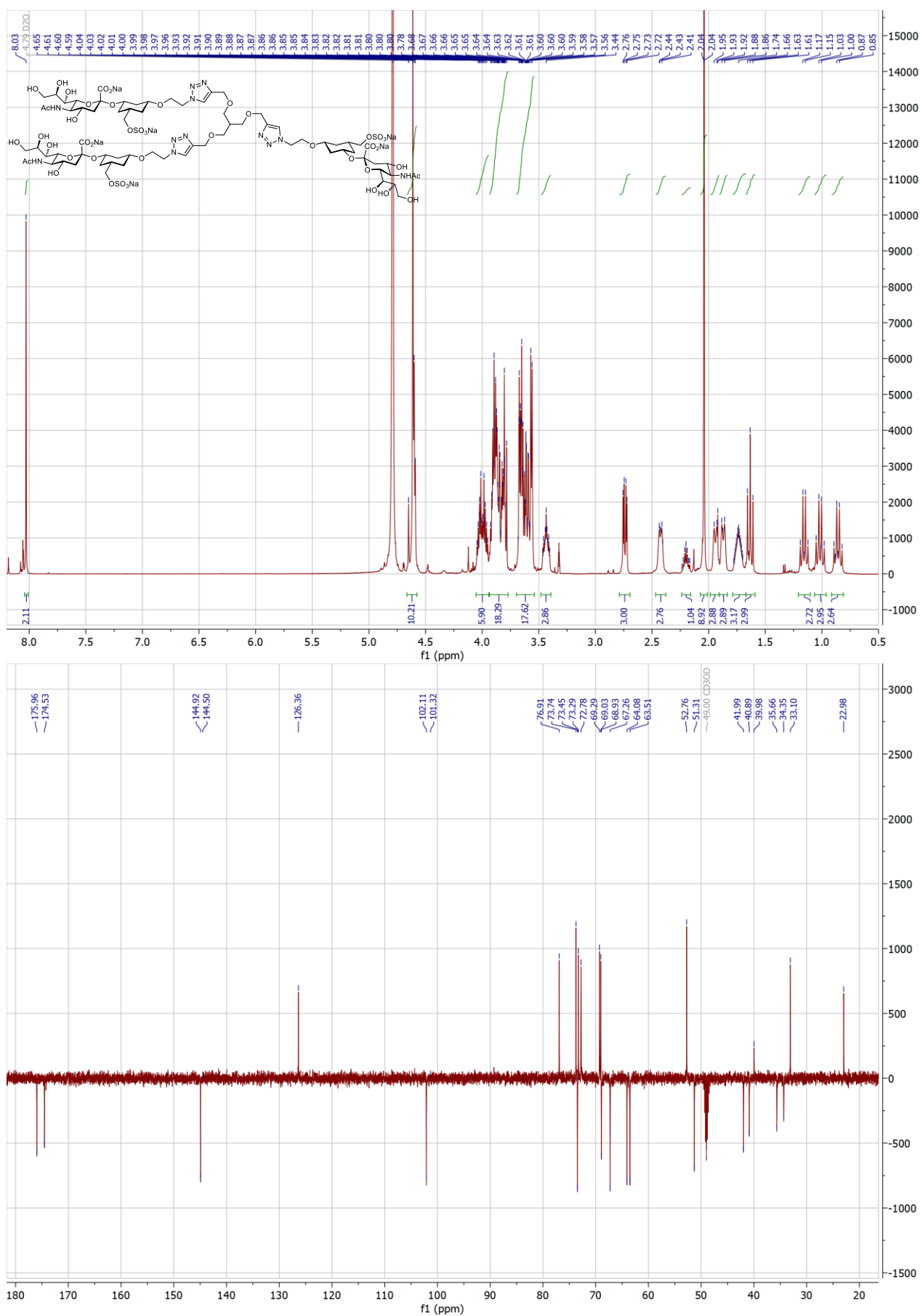
Compound **23**: ^1H NMR (500 MHz, D_2O), ^{13}C APT-NMR (126 MHz, D_2O) and HR-MS (ESI).



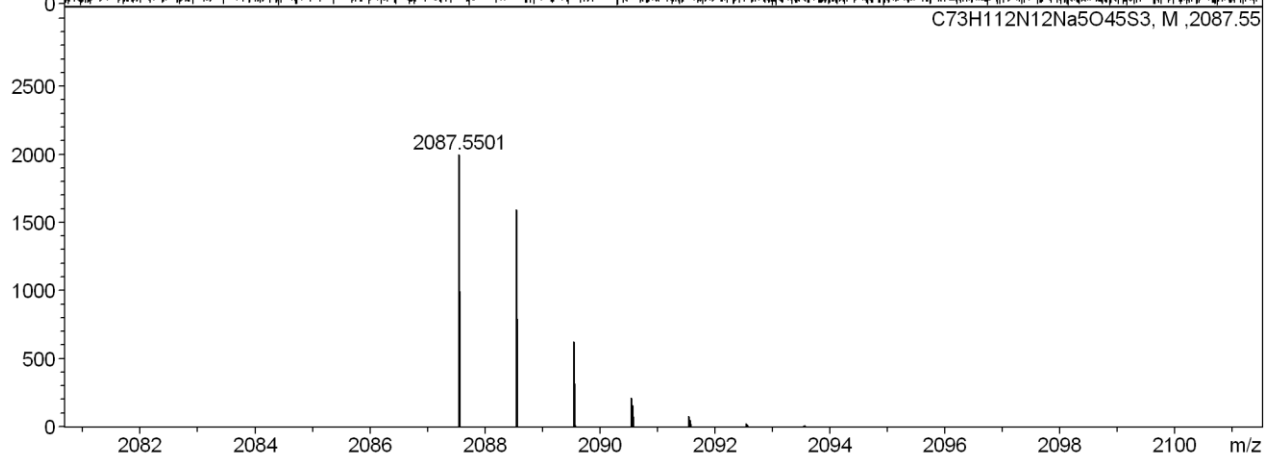
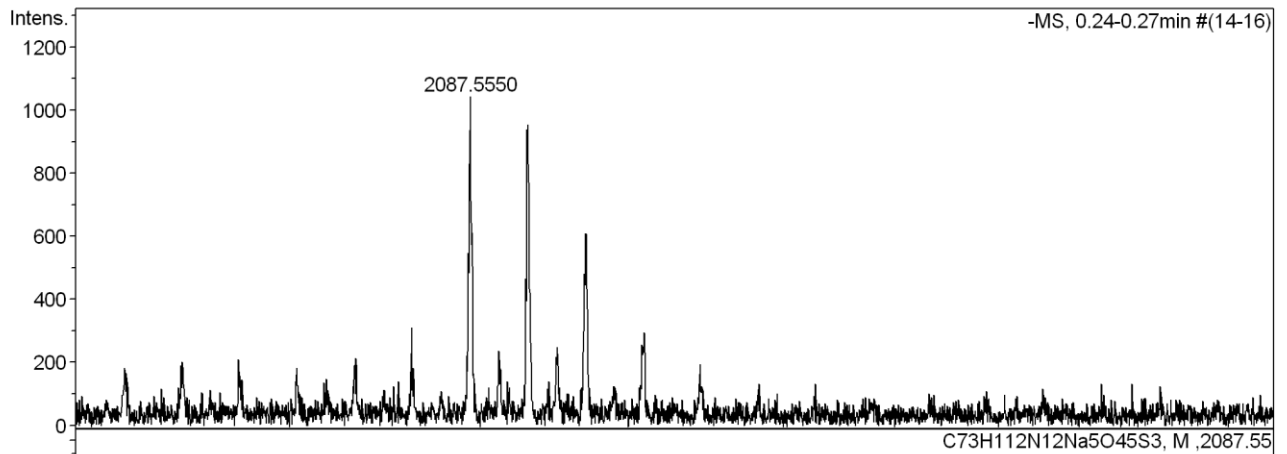
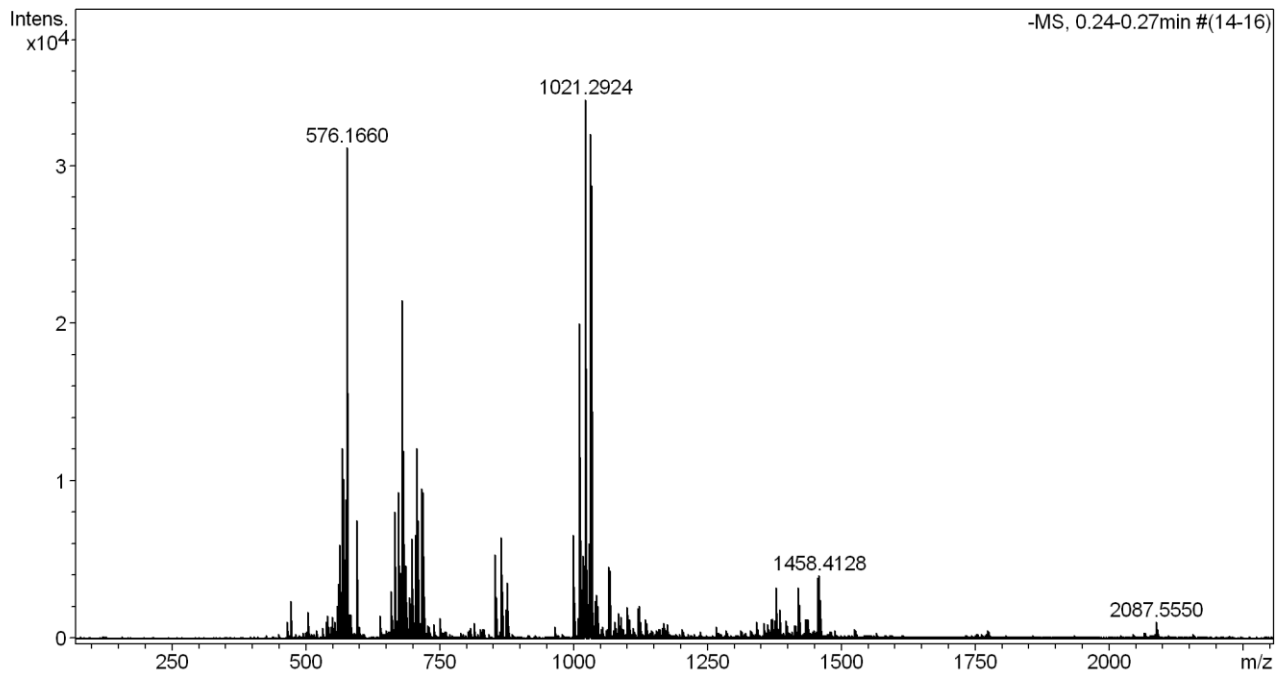
Oligo- and Multivalent presentation of Siglec-8 ligand



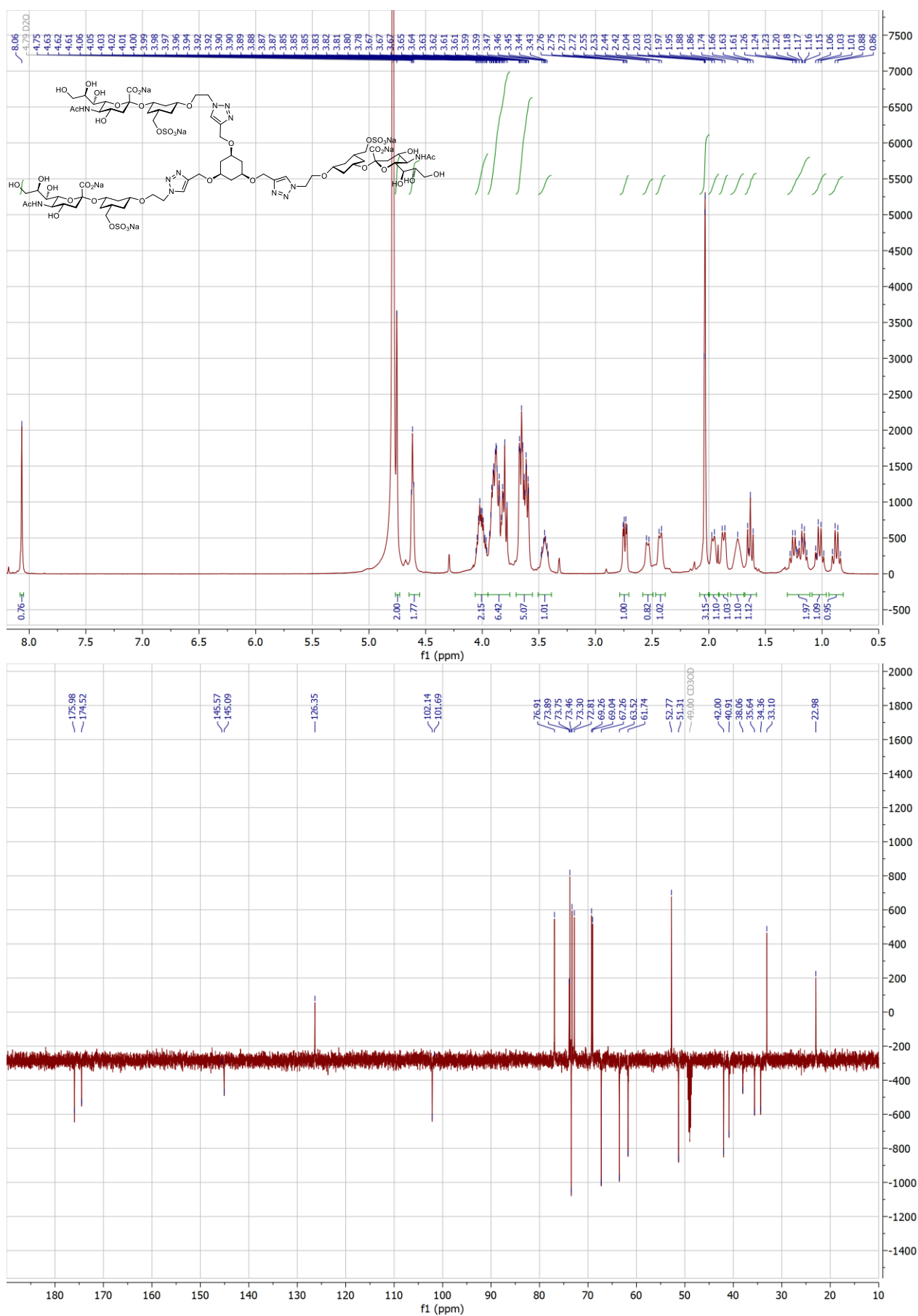
Compound 25: ^1H NMR (500 MHz, D_2O), ^{13}C APT-NMR (126 MHz, D_2O) and HR-MS (ESI).



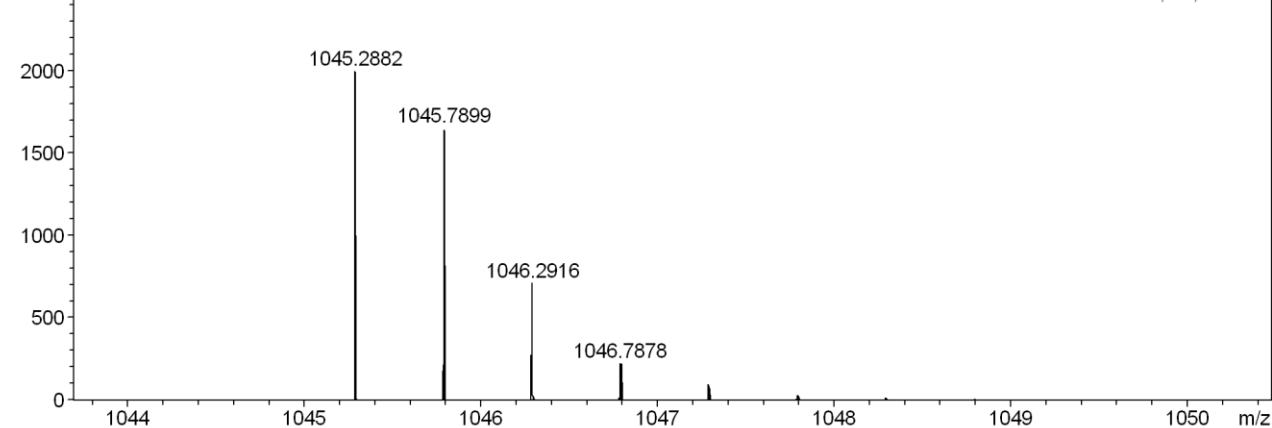
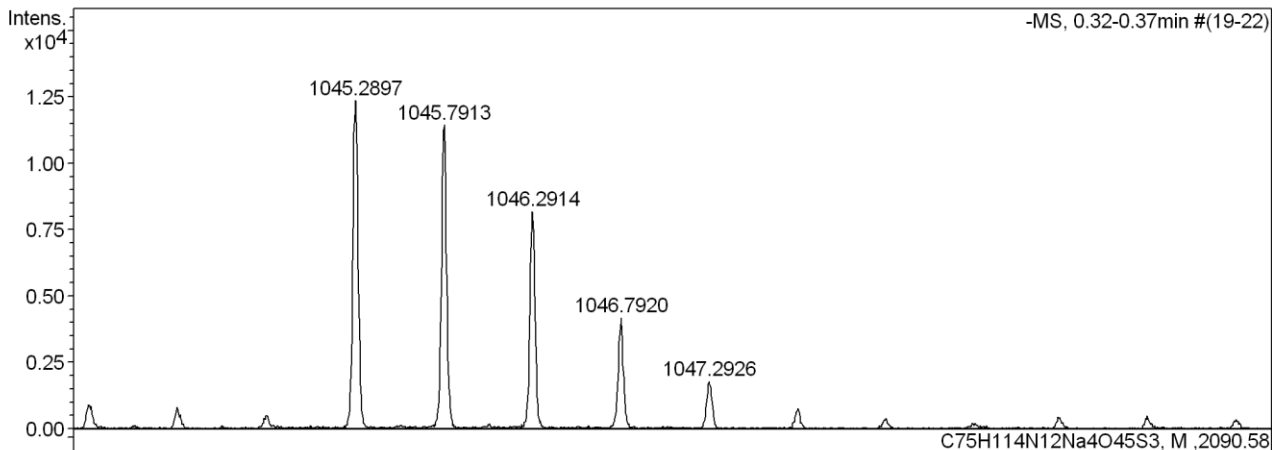
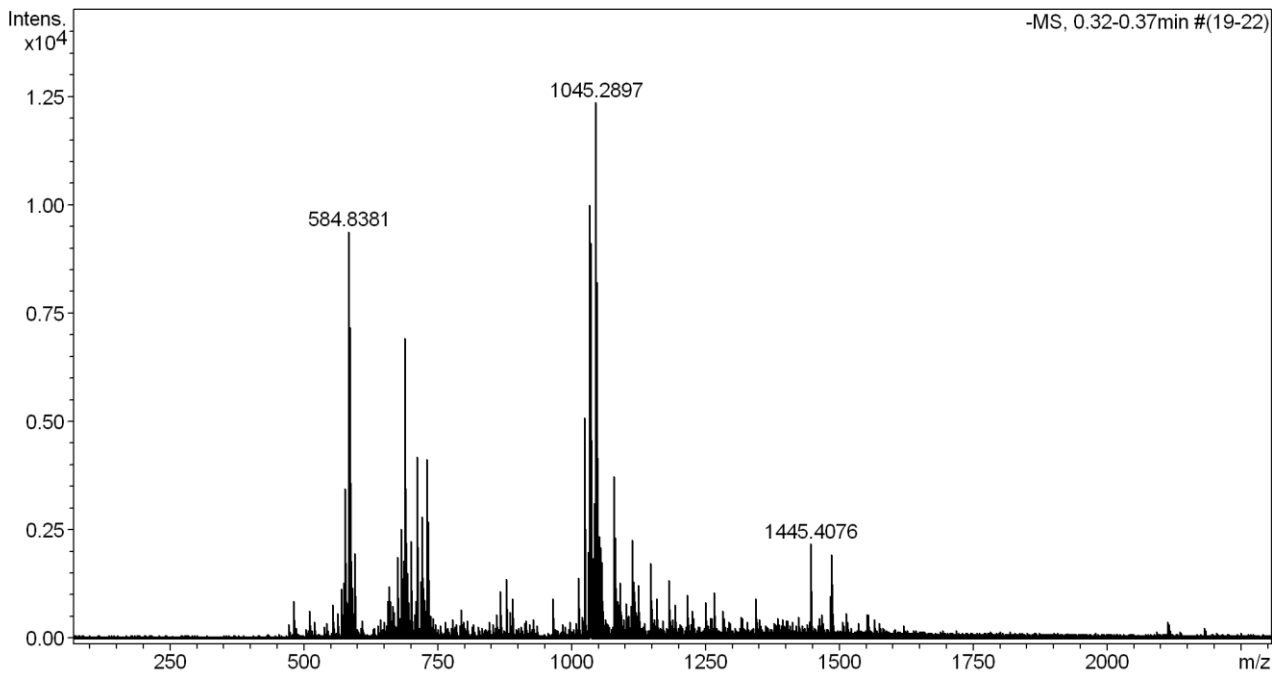
Oligo- and Multivalent presentation of Siglec-8 ligand



Compound 26: ^1H NMR (500 MHz, D_2O), ^{13}C APT-NMR (126 MHz, D_2O) and HR-MS (ESI).

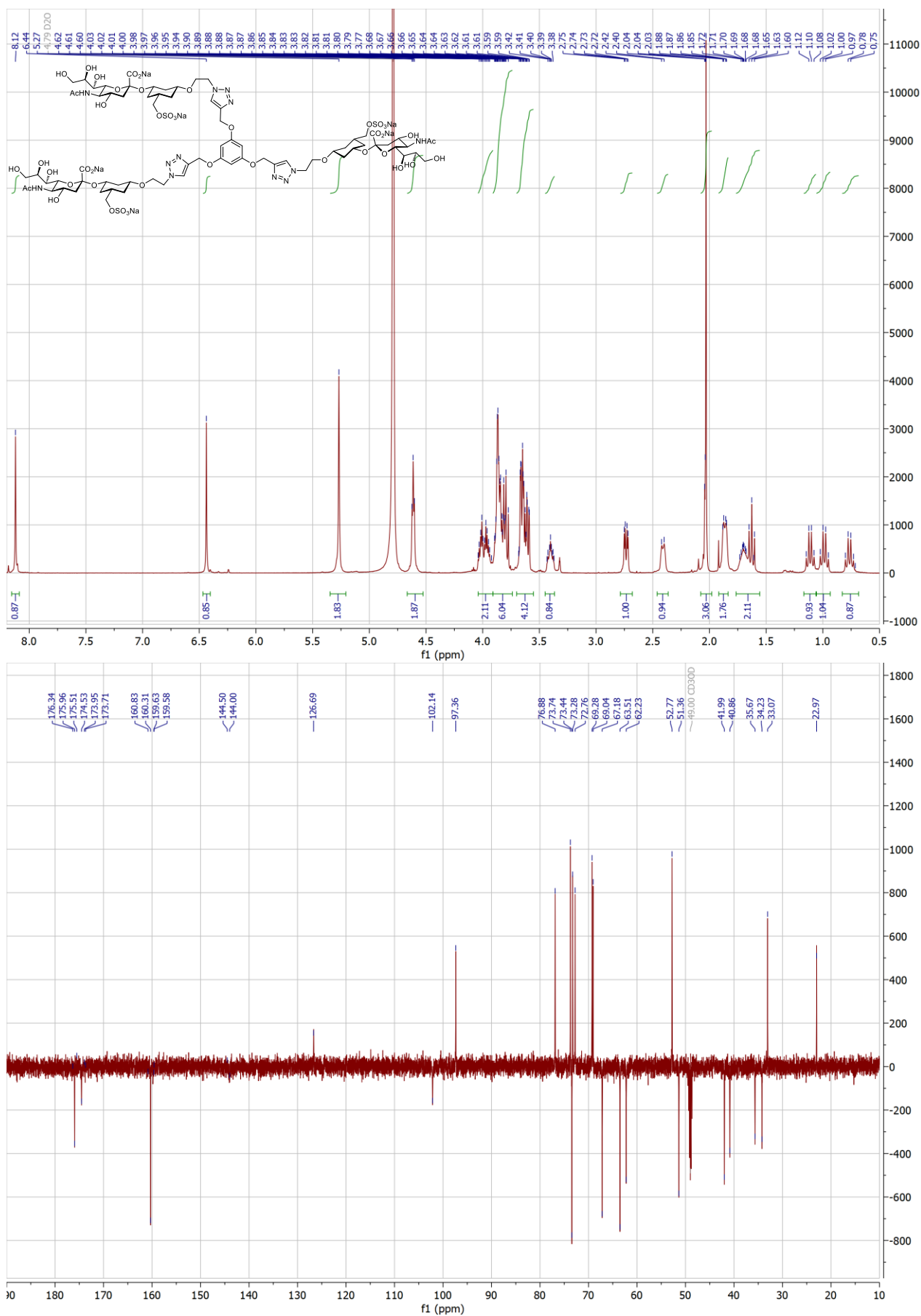


Oligo- and Multivalent presentation of Siglec-8 ligand

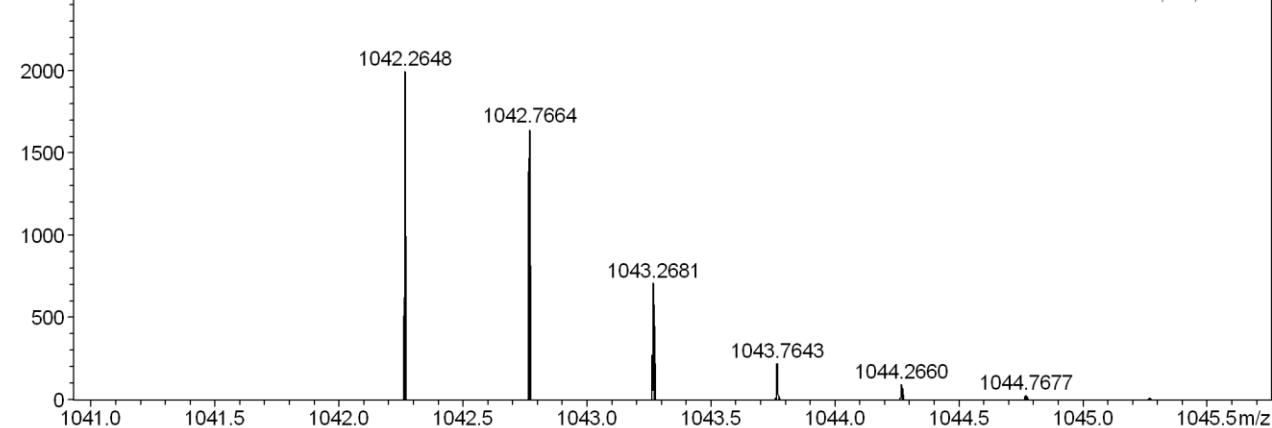
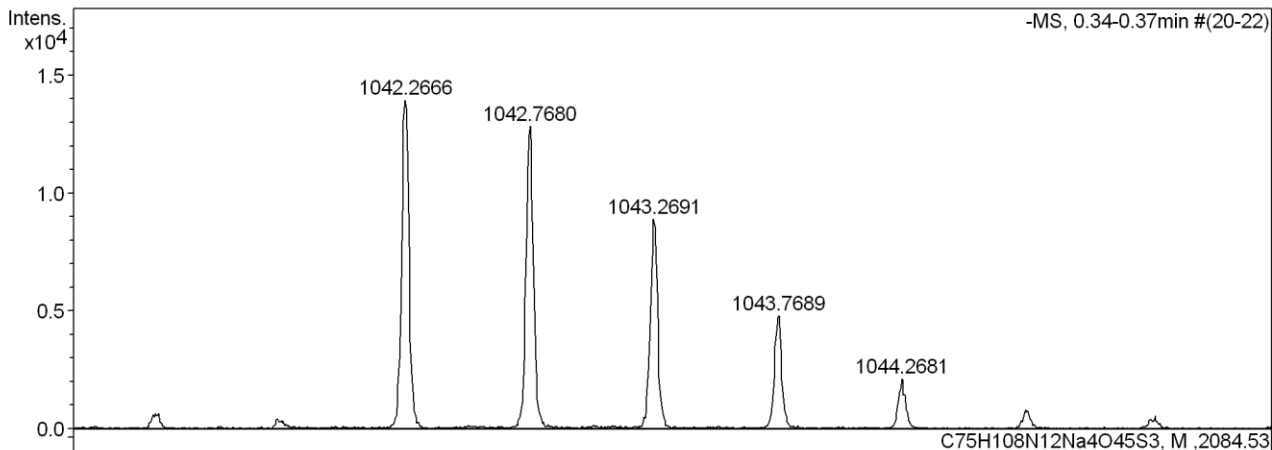
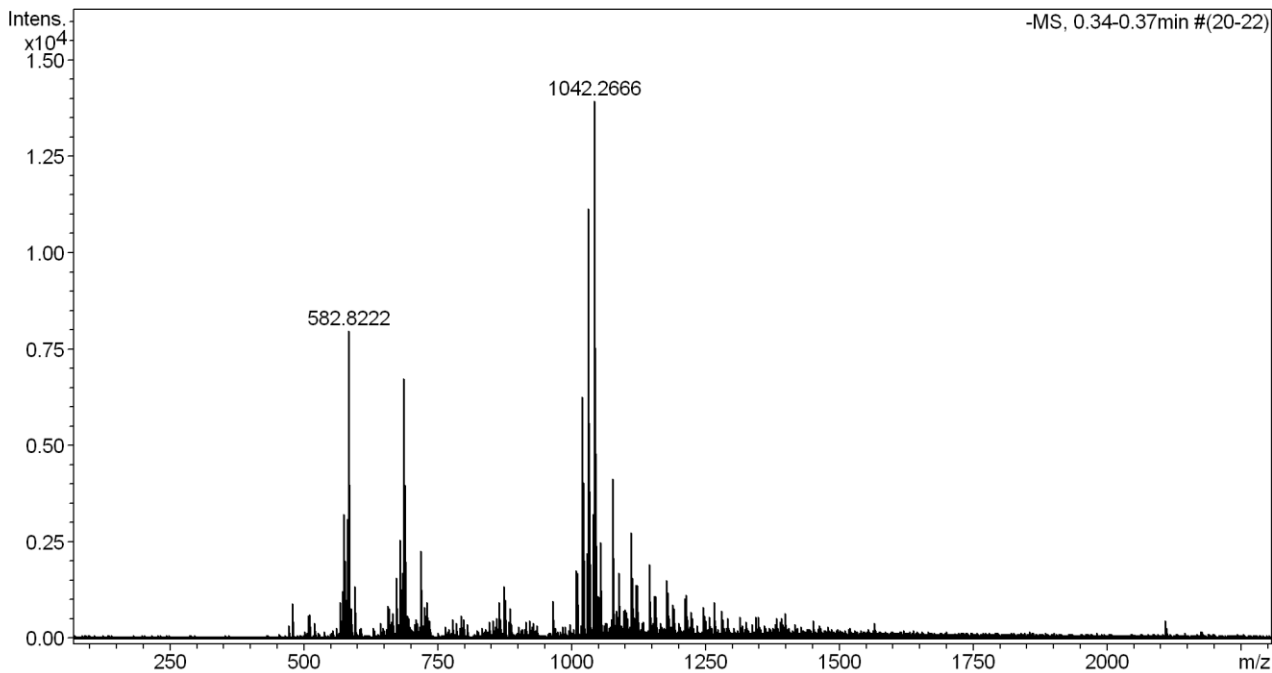


Oligo- and Multivalent presentation of Siglec-8 ligand

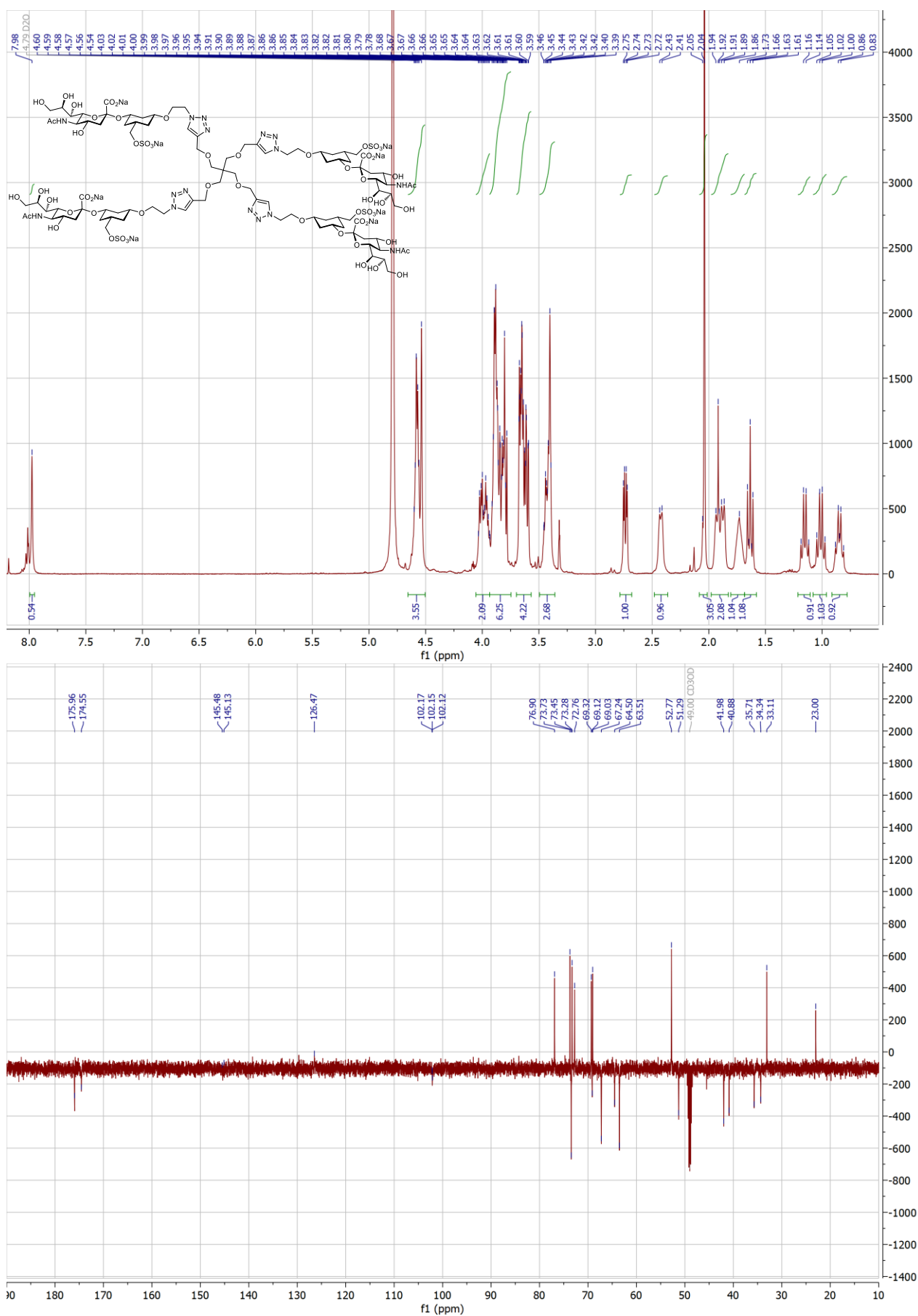
Compound 27: ^1H NMR (500 MHz, D_2O), ^{13}C APT-NMR (126 MHz, D_2O) and HR-MS (ESI).



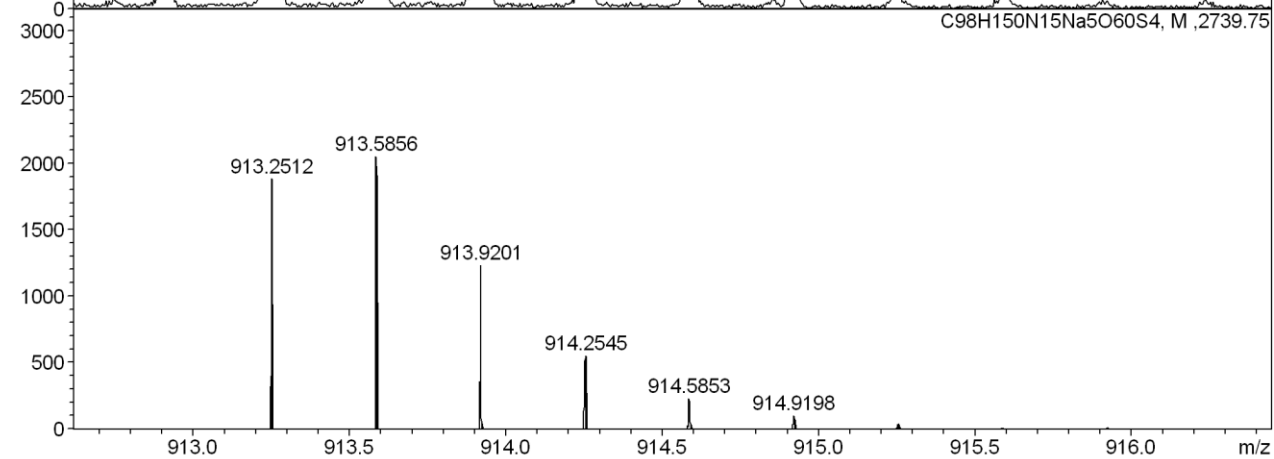
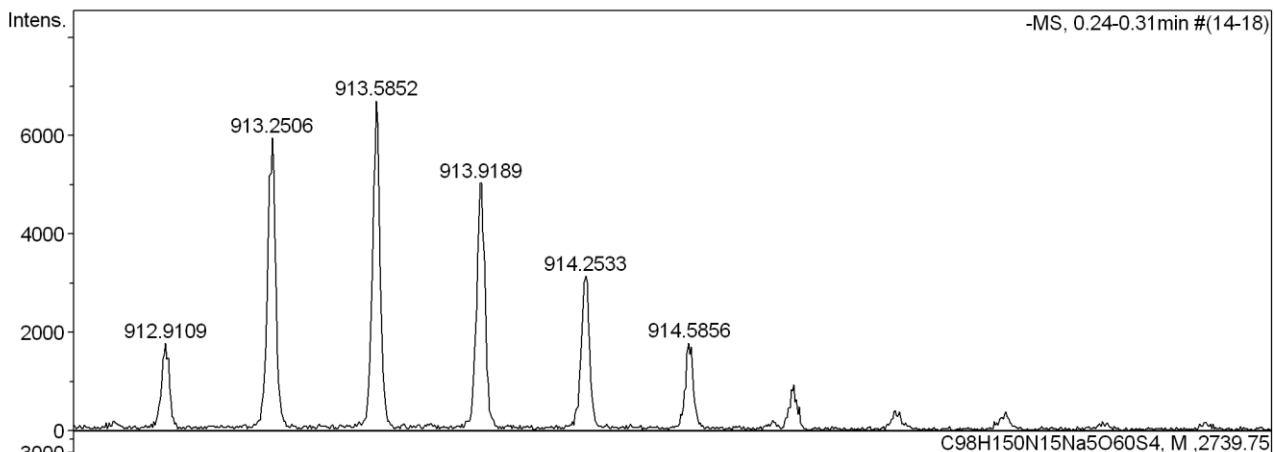
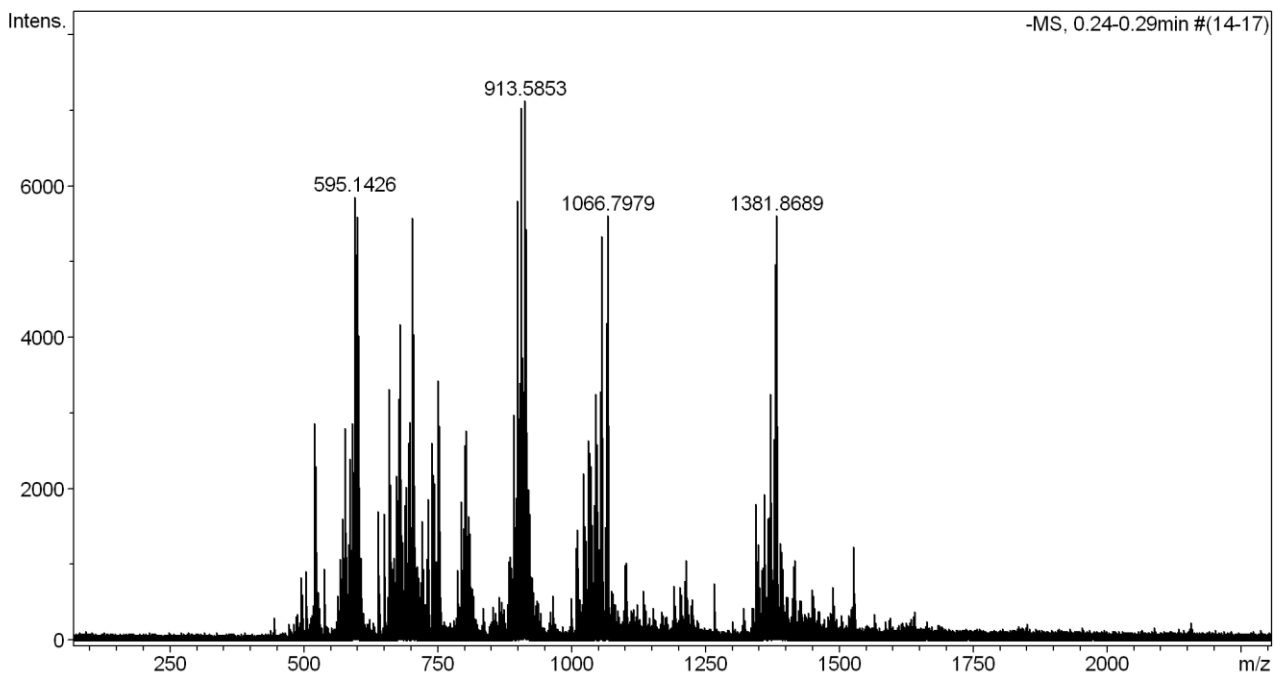
Oligo- and Multivalent presentation of Siglec-8 ligand



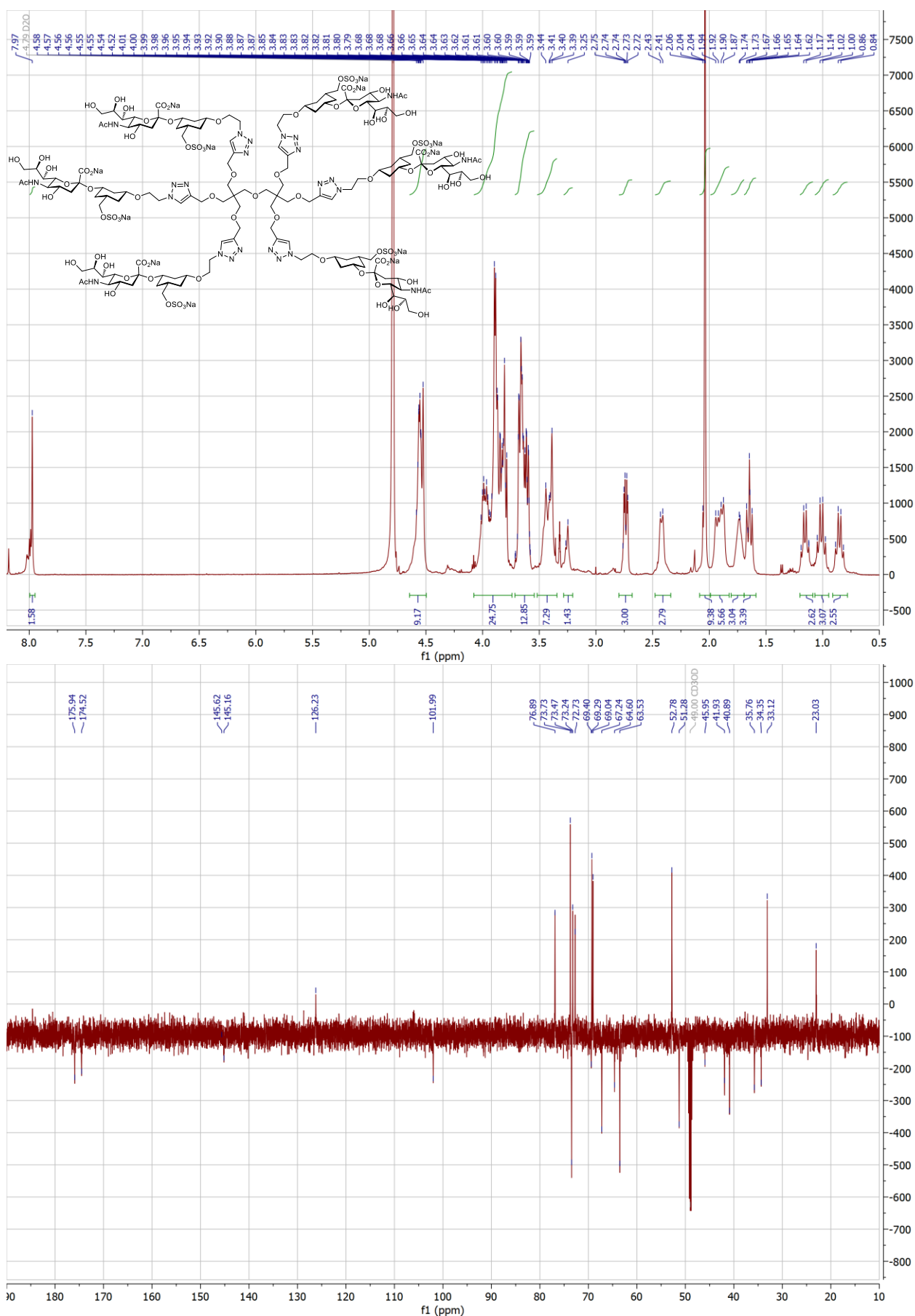
Compound 24: ^1H NMR (500 MHz, D_2O), ^{13}C APT-NMR (126 MHz, D_2O) and HR-MS (ESI).



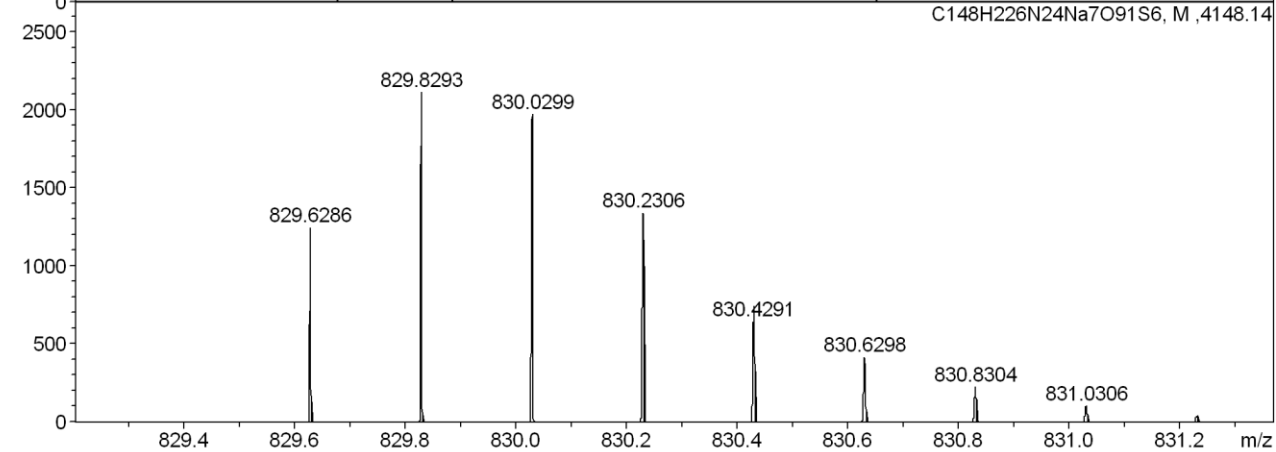
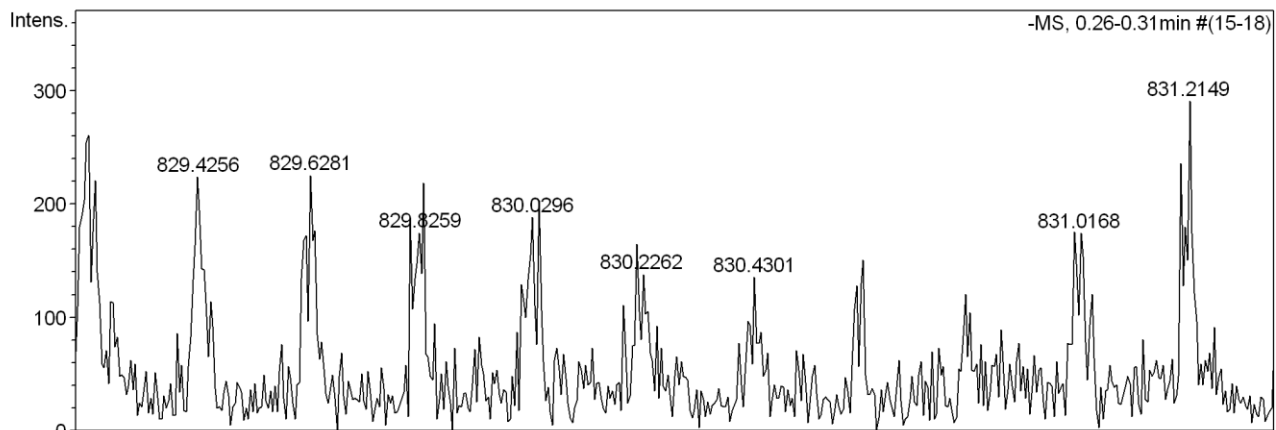
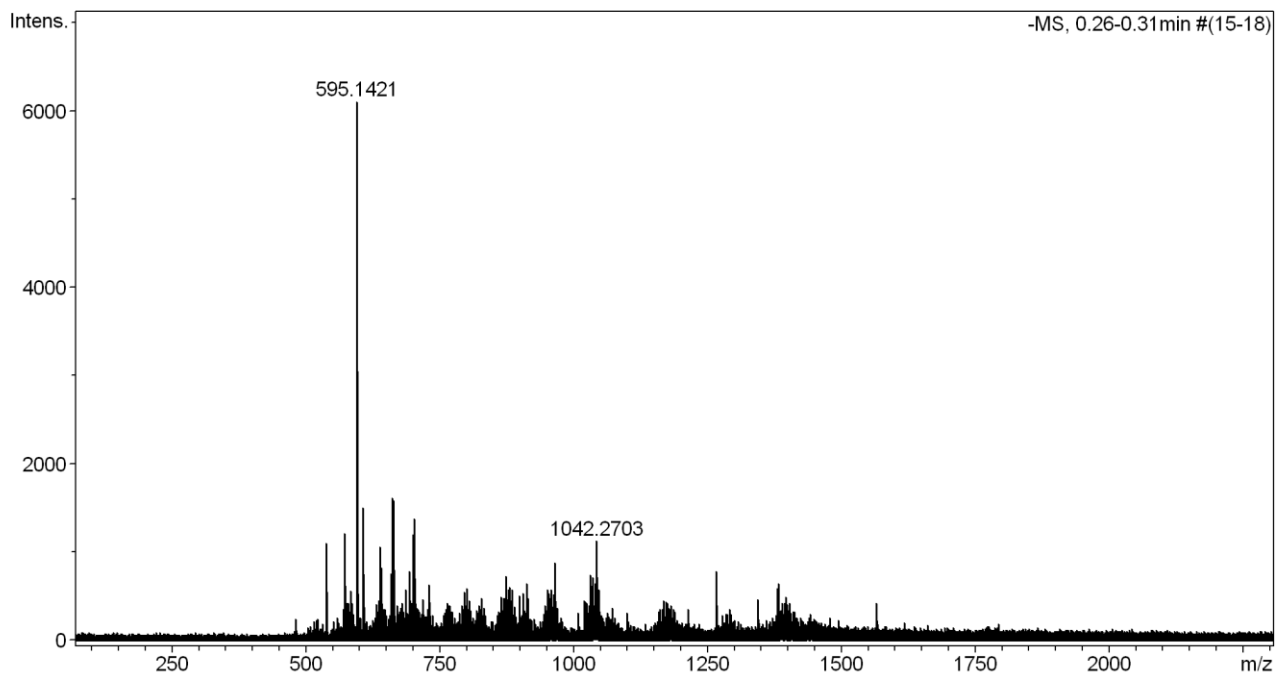
Oligo- and Multivalent presentation of Siglec-8 ligand



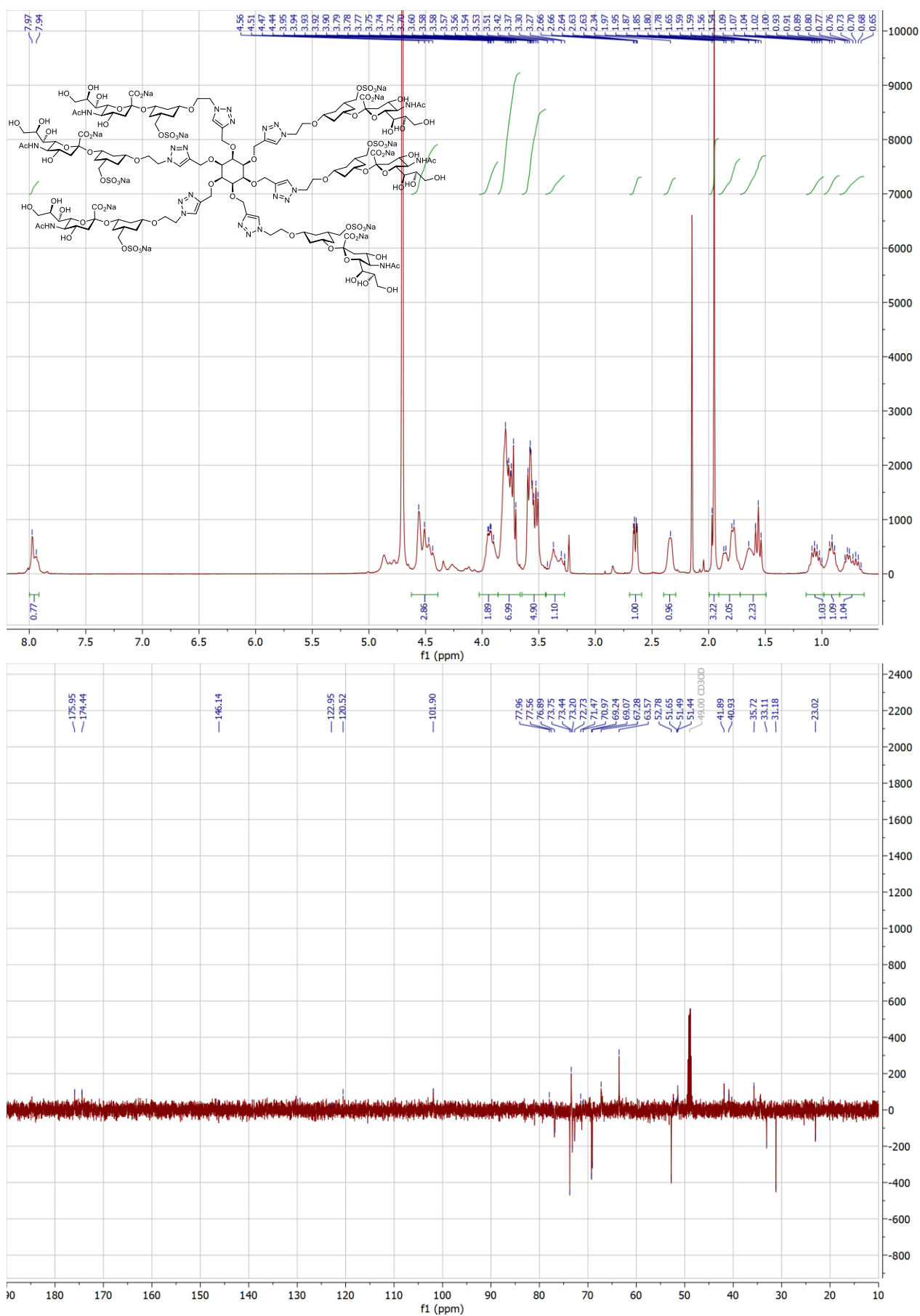
Compound **28**: ^1H NMR (500 MHz, D_2O), ^{13}C APT-NMR (126 MHz, D_2O) and HR-MS (ESI).



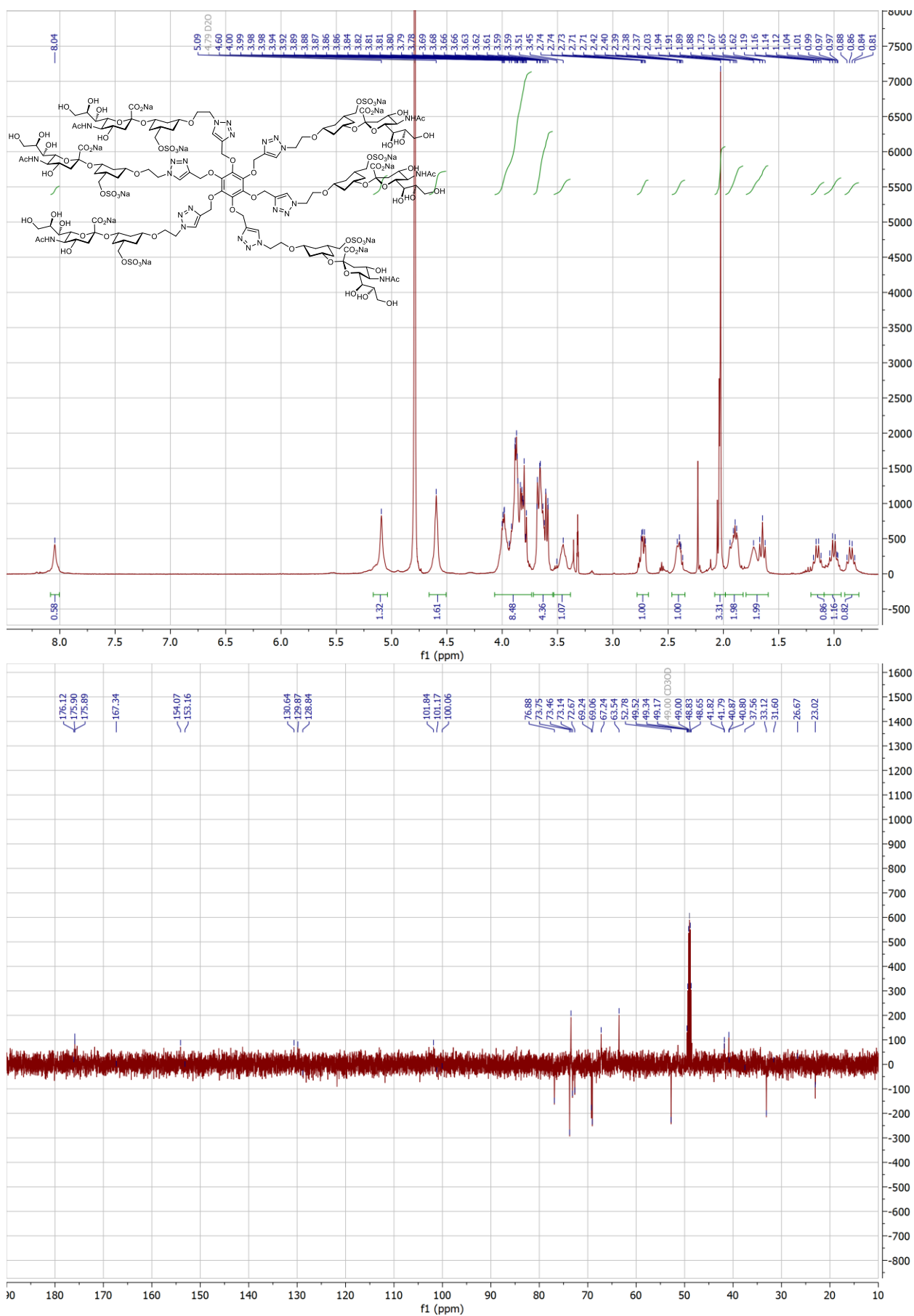
Oligo- and Multivalent presentation of Siglec-8 ligand



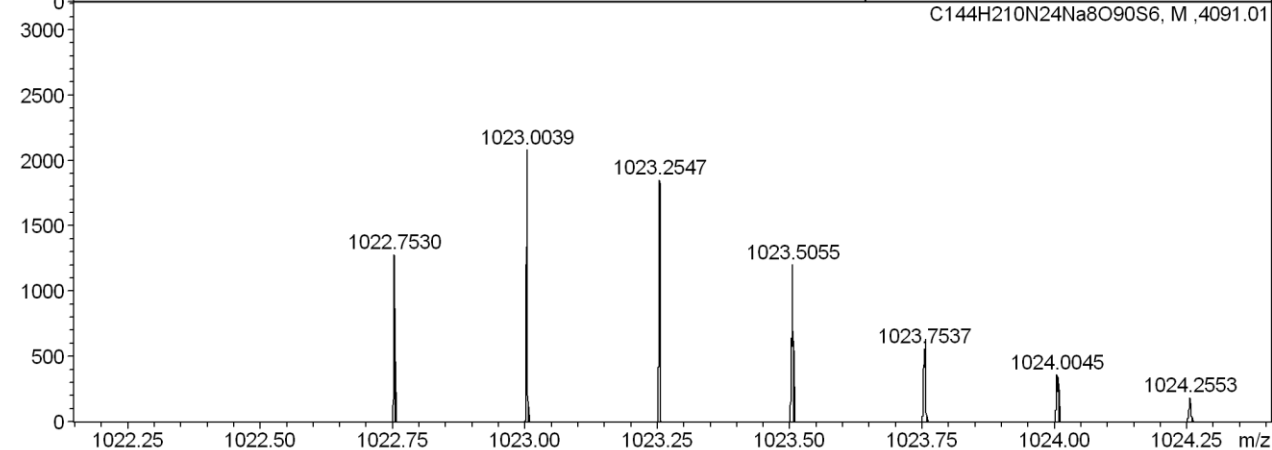
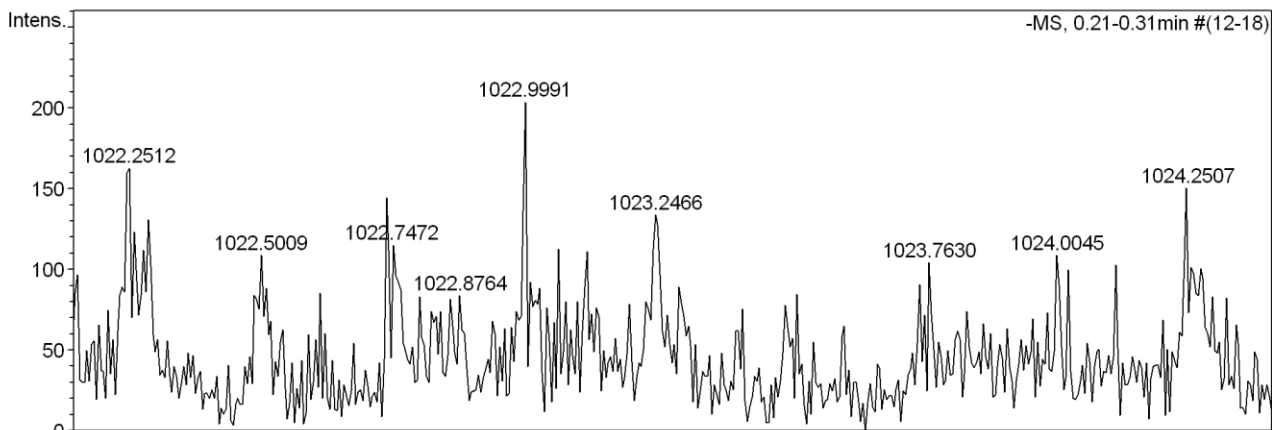
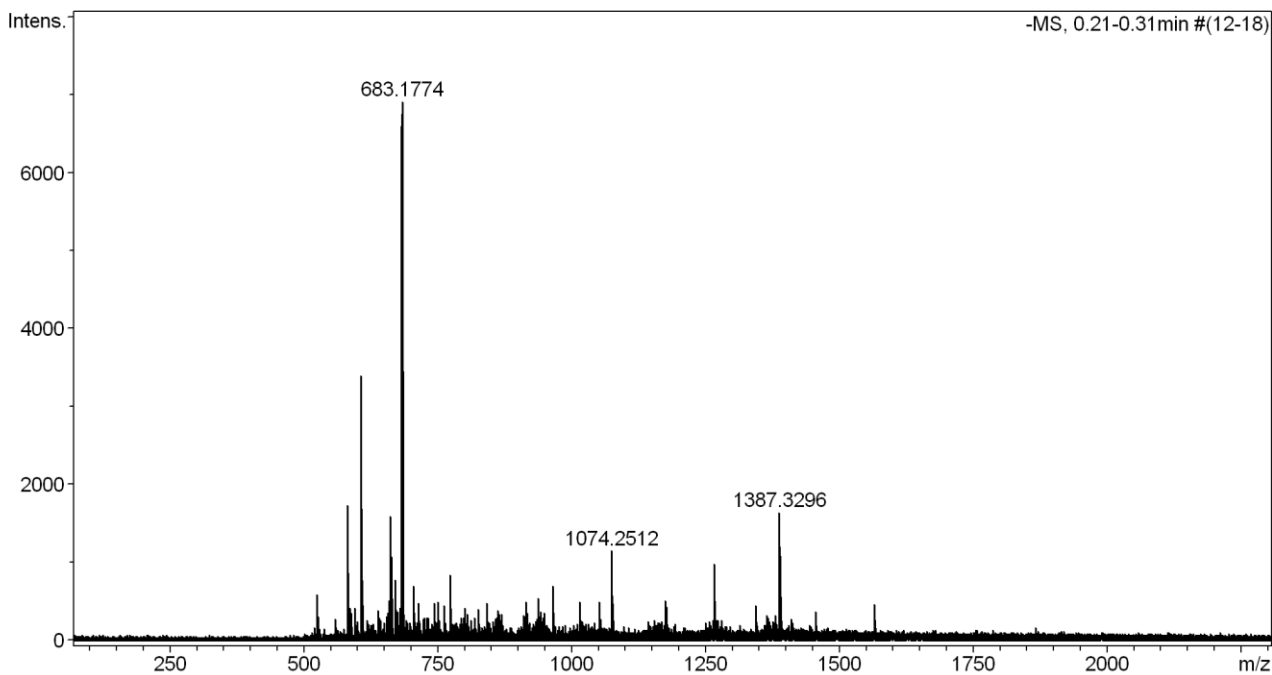
Compound 29: ^1H NMR (500 MHz, D_2O) and ^{13}C APT-NMR (126 MHz, D_2O).



Compound **30**: ^1H NMR (500 MHz, D_2O), ^{13}C APT-NMR (126 MHz, D_2O) and HR-MS (ESI).



Oligo- and Multivalent presentation of Siglec-8 ligand



6. References

1. M. Sajadi, F. Berndt, C. Richter, M. Gerecke, R. Mahrwald, N. P. Ernsting, Observing the hydration layer of trehalose with a linked molecular terahertz probe, *J. Phys. Chem. Lett.* **2014**, *5*, 1845–1849.
2. C. S. Chao, M. C. Chen, S. C. Lin, K. K. T. Mong, Versatile acetylation of carbohydrate substrates with bench-top sulfonic acids and application to one-pot syntheses of peracetylated thioglycosides, *Carbohydr. Res.* **2008**, *343*, 957–964.
3. J. Cramer, B. Aliu, X. Jiang, T. Sharpe, L. Pang, A. Hadorn, S. Rabbani, B. Ernst, Poly-L-lysine Glycoconjugates Inhibit DC-SIGN-mediated Attachment of Pandemic Viruses, *ChemMedChem* **2021**, DOI 10.1002/cmdc.202100348.
4. T. H. Scheuermann, C. A. Brautigam, High-precision, automated integration of multiple isothermal titration calorimetric thermograms: New features of NITPIC, *Methods* **2015**, *76*, 87–98.
5. H. Zhao, G. Piszczek, P. Schuck, SEDPHAT – A platform for global ITC analysis and global multi-method analysis of molecular interactions, *Methods* **2015**, *76*, 137–148.

2nd Generation of Siglec-8 ligands

Manuscript 2: 2nd Generation Siglec-8 Ligands: Effects of Bioisosteric Modification at C-4 and C-9

This manuscript describes the applied strategies for the synthesis of a second generation of ligands targeting Siglec-8. The lead molecule was previously identified (Paper 1) and served as starting point for ligands modified at different sites. This includes the introduction of bioisosteres for the carboxylate and the sulfate group, the synthesis of a small library of amides and sulfonamides at the C-9, as well as the modification of the C-4 of sialic acid.

Contribution to the project:

Gabriele Conti designed and performed the synthesis of the compounds. He expressed and purified Siglec-8 CRD, which he used in differential scanning fluorimetry, microscale thermophoresis and isothermal titration calorimetry assays.

2nd Generation Siglec-8 Ligands: Effects of Bioisosteric Modification at C-4 and C-9

Gabriele Conti,^{[a],[b]} Oliver Schwardt,^[a] Roland J. Pieters,^[b] and Beat Ernst^[a]

^[a] Molecular Pharmacy Group, Department of Pharmaceutical Sciences, University of Basel, Klingelbergstrasse 50, 4056 Basel (Switzerland)

^[b] Chemical Biology and Drug Discovery Group, Department of Pharmaceutical Sciences, Utrecht University, Universiteitsweg 99, 3584 CG Utrecht (The Netherlands)

Abstract

Siglec-8 is an immunoreceptor with inhibitory functions expressed on eosinophils and mast cells. When Siglec-8 is activated via binding to antibodies or synthetic polymers, eosinophils apoptosis and inhibition of mast cell degranulation are triggered. Therefore, targeting Siglec-8 for treating eosinophil- and mast cell-associated diseases caused by overexpression of these cell types appears to be a promising strategy. An extensive study on the pharmacophores of the tetrasaccharide 6'-sulfo-sialyl Lewis^x (6'-S-sLe^x), the preferred Siglec-8 ligand identified via a glycan array approach, led to the identification of a glycomimetic sulfonamide with improved activity. Here, we present a study on modifications of different positions of a glycomimetic lead molecule, as well as the analysis of a second generation of sulfonamides. While the carboxylic acid and the sulfate group proved to be essential for binding, the C-4 proved to be a suitable site for modifications increasing the binding affinity.

Introduction

Siglecs are a family of I-type transmembrane lectins primarily expressed on immune cells, which are involved in numerous physiological and pathological conditions, with functions depending on their structure and cell type expressing them.¹⁻⁶ Human siglecs are distinguished into conserved siglecs found in different species, and CD33-related siglecs, which are rapidly evolving proteins that share high sequence similarity. Among them, Siglec-8 is an inhibitory receptor present on eosinophils and mast cells, and to some extent on basophils.⁷⁻¹⁰ Its extracellular domain consists of an *N*-terminal V-set domain, called the carbohydrate recognition domain (CRD), and two C2-set domains, which intracellularly present the inhibitory motifs ITIM and ITIM-like. When Siglec-8 binds to antibodies or

synthetic polymers displaying Siglec-8 ligands, it triggers eosinophil cell death and inhibits mast cell degranulation.¹¹⁻¹⁴ Thus, targeting Siglec-8 represents a promising strategy for the treatment of conditions resulting from huge overexpression of these cell types, like asthma and allergic inflammation.^{15,16}

Although the pharmacological relevance of Siglec-8 has already been proven, the development of small molecules targeting Siglec-8 is still at a very early phase.¹⁷ Indeed, the flattened and solvent-exposed binding sites of lectins usually account for low affinities in the micromolar range. Additionally, carbohydrates are associated with poor drug-like properties, and tedious and long synthetic procedures with regio- and stereoselectivity issues that hamper the overall yield of the process. However, the development of glycomimetic structures proved to be a successful solution for a number of siglecs.¹⁸ Common ways to derive glycomimetics from their respective saccharides mostly rely on the replacement of carbohydrate moieties with non-carbohydrate ones, the use of bioisosteres and the introduction of new functionalities to target different protein residues. In this work, we describe the results of various modifications of the lead glycomimetic ligand for Siglec-8 that was previously identified in our laboratory.¹⁷

Results and discussion

Our approach to identify a potent Siglec-8 ligand was recently published.¹⁷ Pharmacophore analysis of the tetrasaccharide 6'-sulfo-sialyl Lewis^x (6'-sulfo-sLe^x), the preferred Siglec-8 ligand identified by a glycan array approach, allowed the development of glycomimetic structures with improved affinity. To achieve this, the tetrasaccharide structure was first shortened to the corresponding disaccharide Neu5Ac-Gal6S (**GB30**), which represents the minimal binding moiety. The replacement of the galactose ring with cyclohexane (\rightarrow **GC10**), together with the introduction of sulfonamide modification at C-9 of sialic acid provided **GC35**, a compound with improved affinity and drug-like properties (Figure 1).

In this perspective, glycomimetic **GC10** can be considered as the lead compound in the development of new high-affinity ligands for Siglec-8. Here we present further modifications including bioisosteres for the carboxylic acid and the sulfate, the modification of the C-4 position of sialic acid, as well as the introduction of different aromatic sulfonamides at C-9.

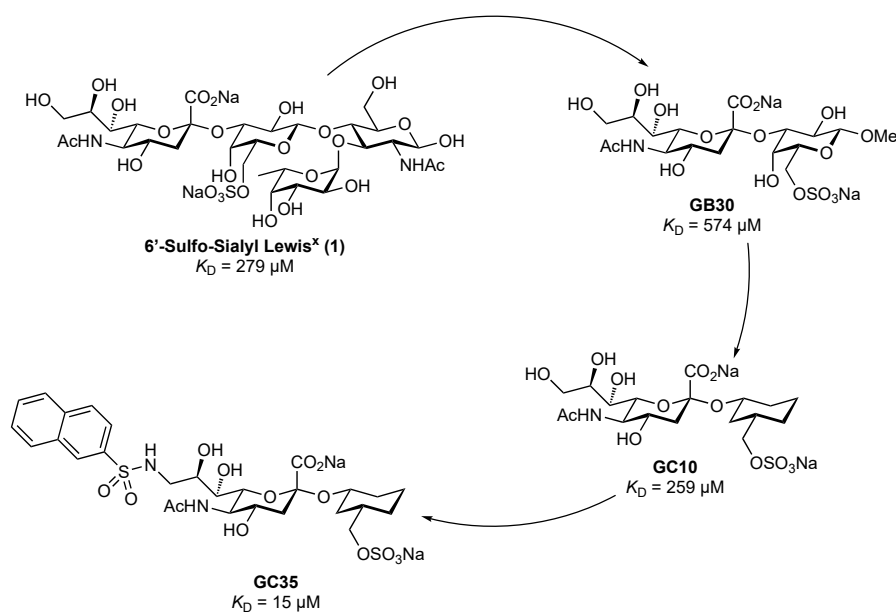
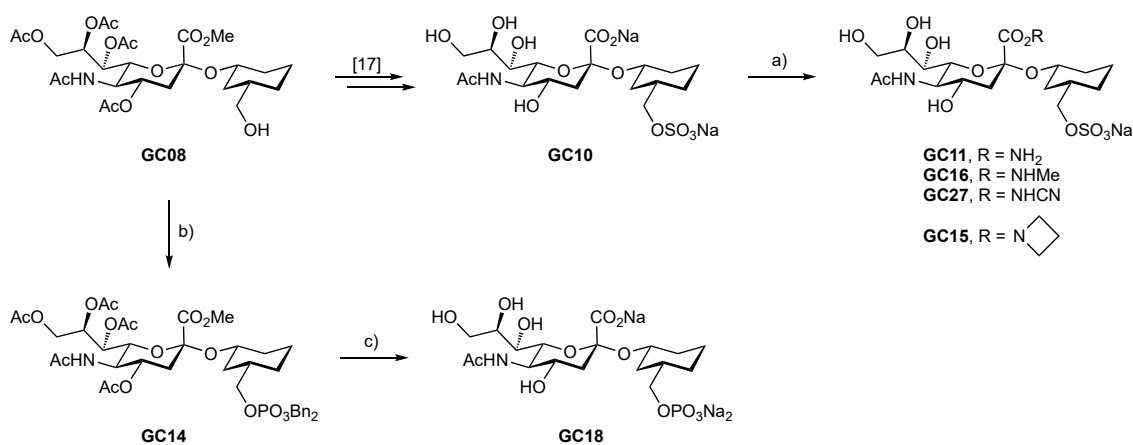


Figure 1. Development of a high-affinity sulfonamide ligand for Siglec-8. Pharmacophore analysis of the preferred tetrasaccharide 6'-sulfo-sLe^x led to the identification of disaccharide **GB30** as minimal binding epitope, with a 2-fold loss affinity. Replacement of the galactose ring with cyclohexane allowed the glycomimetic **GC10** with affinity similar to the tetrasaccharide. Additional modification by the introduction of a naphthalenesulfonamide moiety led to a further improvement of improved affinity.¹⁷

Bioisosteres of the carboxylic acid and the sulfate group

With bioisosteres of the carboxylate and the sulfate group of **GB30**, no affinity improvement was observed.¹⁷ In order to confirm this trend, a small series of amide bioisosteres, as well as a phosphate analogue of **GC10** were synthesised and tested. The synthesis of amides was achieved via classic peptide synthesis from glycomimetic **GC10**, using HATU as activating agent, while the phosphate



Scheme 1. Synthesis of amide and phosphate bioisosteres. a) RH, HATU, DIPEA, DMF, rt, (33 – 63 %); b) dibenzyl *N,N*-diisopropylphosphoramidite, 1,2,4-triazole, MeCN, 0 °C to rt, overnight; then *t*BuOOH, rt, 1 h (29 %); c) Pd/C, H₂ (1 atm), MeOH, rt, overnight; then NaOH (aq.), rt, 5 h (92 %).

derivative **GC18** was obtained in two steps from compound **GC08**¹⁷ (Scheme 1). These compounds were then tested with differential scanning fluorimetry (Figure 2 and Table 1).

When a ligand binds to Siglec-8, the stabilized complex exhibits a higher apparent melting temperature T_m . This was indeed the case of **GC10**, whose binding to Siglec-8 caused a ΔT_m of + 2.9 °C. The amide and phosphate modifications of glycomimetic lead molecules elicited no significant difference in T_m , clearly indicating that no binding to Siglec-8 was taking place. These results were further confirmed by microscale thermophoresis (MST) and isothermal titration calorimetry (ITC) assays, as in both cases no binding for these compounds was detected. These results are in agreement with the previous findings that altering these functionalities in the disaccharide **GB30** led to inactive compounds,¹⁷ confirming their key role in substrate recognition and supporting the idea of an identical binding mode between the glycomimetic **GC10** and **GB30**.

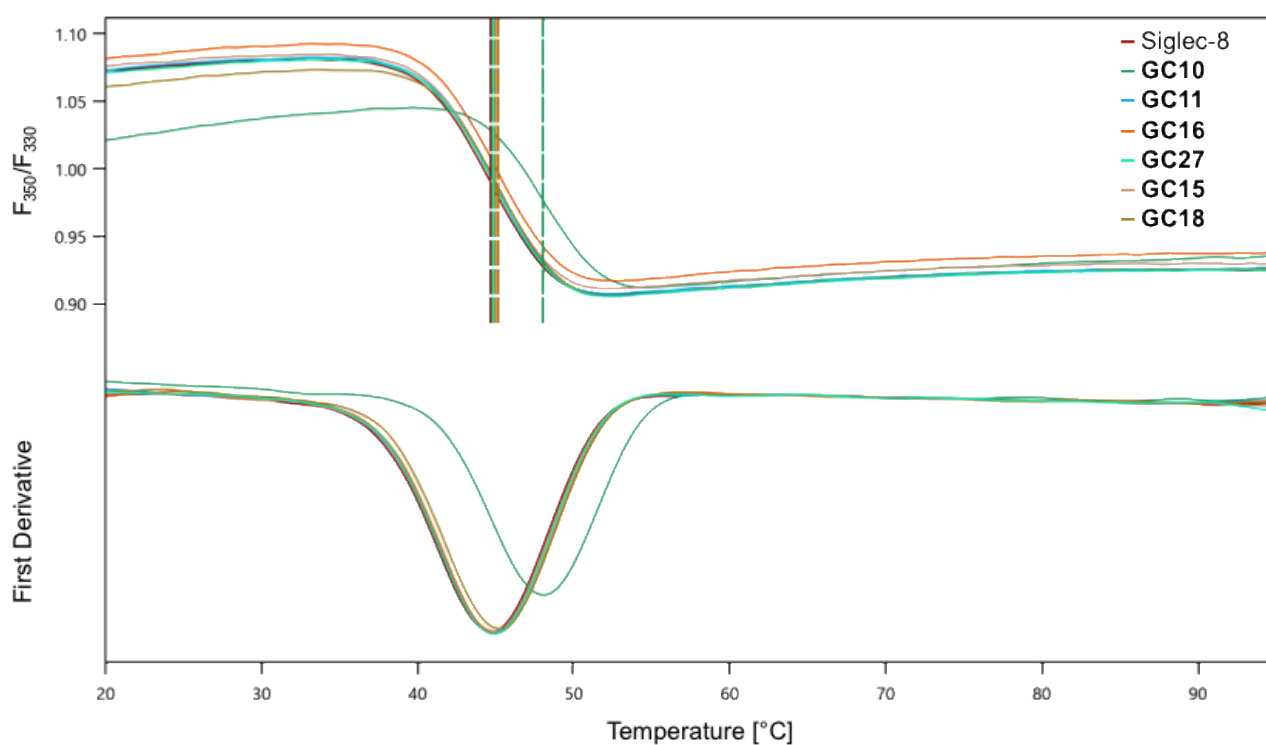
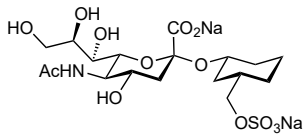
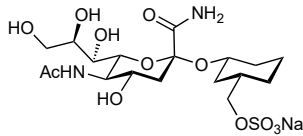
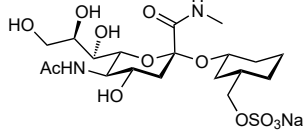
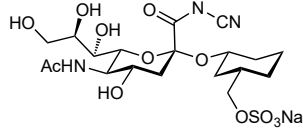
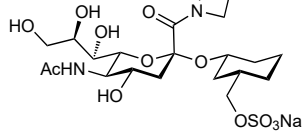
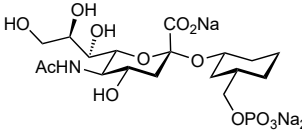


Figure 2. NanoDSF analysis of bioisosteres of GC10. The upper graph represents the ratio between the fluorescence measured at 350 and 330 nm, while the lower one depicts the related first derivatives are depicted.

Table 1. T_m and ΔT_m values for various ligands. Siglec-8-CRD was used with a concentration of 20 μ M and incubated with 1 mM of each ligand.

Compound	Structure	T_m ($^{\circ}$ C)	ΔT_m ($^{\circ}$ C)
Siglec-8		44.7	-
Reference compound			
GC10		47.6	+ 2.9
Carboxylic acid bioisosteres			
GC11		44.7	+ 0.0
GC16		44.8	+ 0.1
GC27		44.9	+ 0.2
GC15		44.8	+ 0.1
Sulfate bioisostere			
GC18		45.1	+ 0.4

Modification of the 4-position of the Neu5Ac moiety.

The development of compound **GC10** starting from the natural ligand, tetrasaccharide 6'-sulfo-sLe^x, was guided by rational design based on the available NMR solution structure.¹⁹ By keeping the important functionalities, and removing the moieties not essential for binding based on the NMR structure, first disaccharide **GB30** and then its glycomimetic **GC10** were obtained. In such an approach, where the binding epitope is not altered, no major changes in the binding pose between the compounds are expected. This is also supported by equal loss of affinity for the **GC10**- and the **GB30**-series of bioisosteres. Finally, the docking pose of compound **GC10** also provided additional proof that this compound binds similarly to 6'-sulfo-sLe^x (Figure 3).

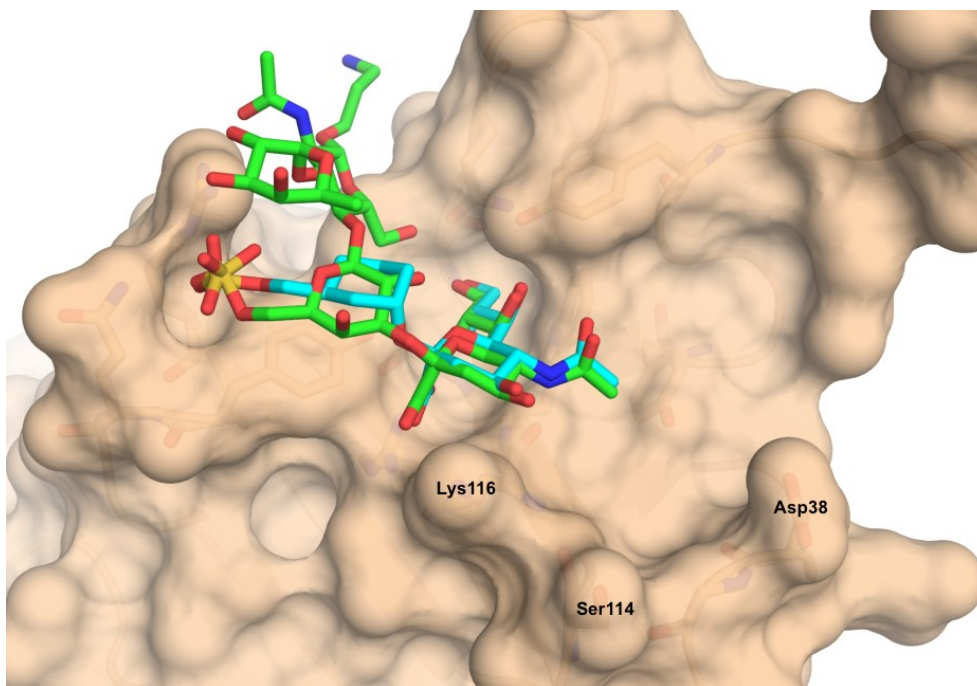
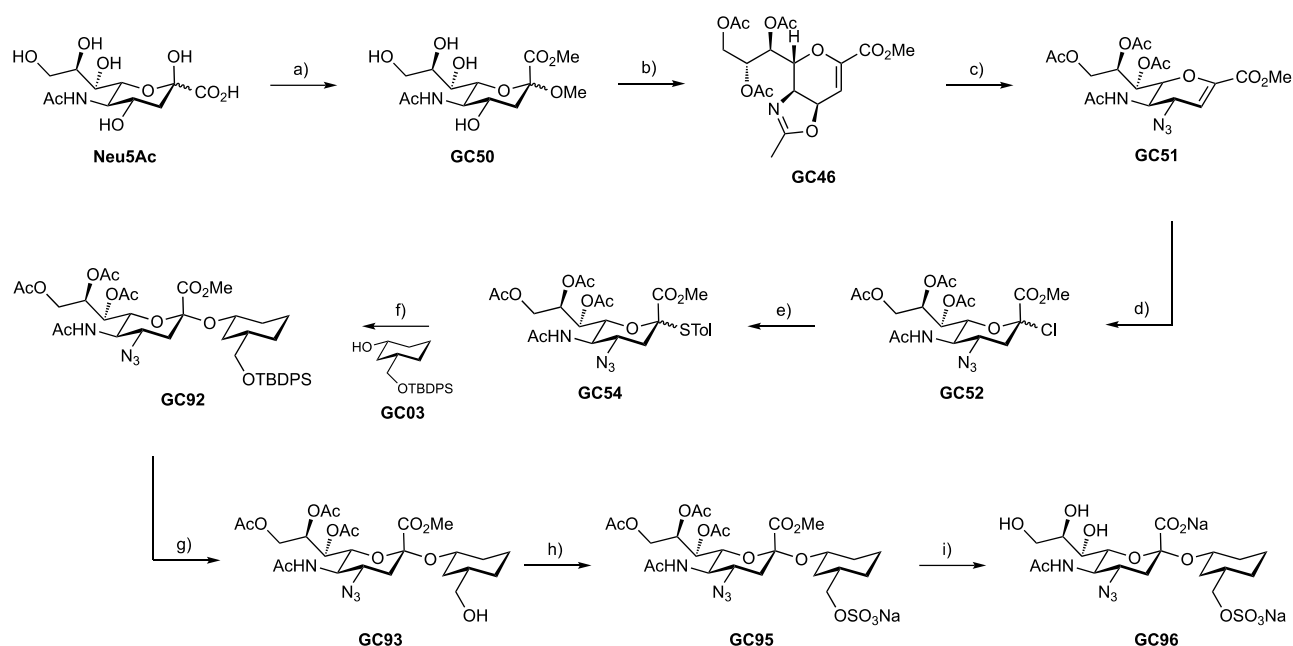


Figure 3. Docking poses of 3-aminopropyl 6'-sulfo-sLe^x and GC10. 3-Aminopropyl 6'-sulfo-sLe^x (green), GC10 (cyan). Structure preparation and docking studies were performed with Maestro suite,²⁰ using the NMR solution structure 2N7B as input. The figure was generated using Pymol.²¹ Colour code: N: blue, O: red, S: yellow.

In this binding pose, the hydroxyl group at C-4 of Neu5Ac lays next to the amino group of Lys116, pointing towards a pocket limited by Asp38, Ser114, and Lys116. The introduction of a proper substituent at this position, which could establish new interactions with these residues, could possibly lead to an increase in binding enthalpy and thus improve affinity. In order to achieve this, the hydroxyl group was replaced by an azide, a useful strategy to open the route to different classes of compounds, such as amides, amines or triazole derivatives.

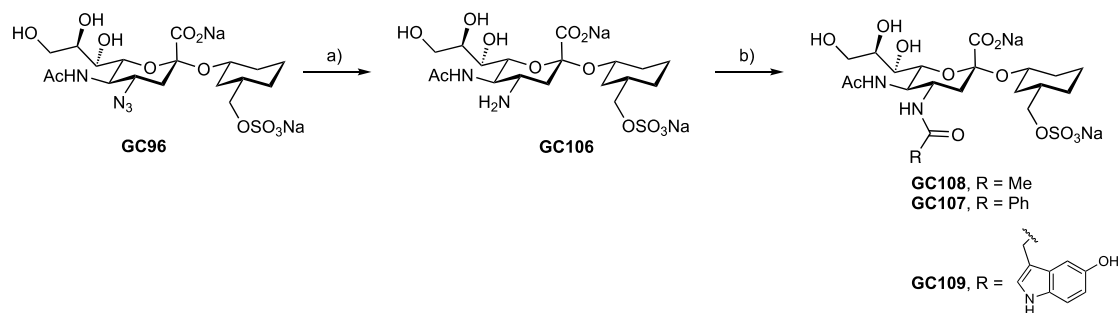
Starting from the commercially available Neu5Ac, the synthesis of the 4-azido analogue of glycomimetic GC10 is achieved in 9 steps (Scheme 2). First, the sialic acid was subjected to methylation of the carboxylic acid and anomeric hydroxyl by treatment with methanol and Dowex 50W X8 at 60 °C (→ GC50).²² Next, peracetylation with acetic anhydride in the presence of sulfuric acid yielded oxazoline GC46. The azido group was then inserted via S_N2 opening of the oxazoline ring at C-4 with TMSN₃ (→ GC51). Markovnikov addition of hydrogen chloride to the glycal GC51 allowed the restoration of the original oxidation states of C-2 and C-3. The introduction of a chlorine leaving group (→ GC52), and conversion into the thio derivative GC54 by treatment with *p*-thiocresol was possible. Glycosylation of acceptor GC03 using NIS and TfOH as activators and MeCN and DCM as solvent, yielded compound GC92, however, only in a moderate yield of 16%. Finally, desilylation with HF (→ GC93) and sulfation of the deprotected hydroxyl (→ GC95), followed by ester hydrolysis with aqueous NaOH yielded the 4-azido analogue GC96.

2nd Generation of Siglec-8 ligands



Scheme 2. Synthesis of 4-azido analogue of glycomimetic lead. a) Dowex 50W X8, MeOH, 60 °C, 90 h (74 %); b) Ac₂O, H₂SO₄, rt, 70 h (70 %); c) TMSN₃, *t*BuOH, 80 °C, 16 h (95 %); d) HCl (g), LiCl, MS 3 Å, -30 °C to rt, 120 h (54 %); e) *p*-thiocresol, DIPEA, DCM, 0 °C to rt, 24 h (66 %); f) NIS, TfOH, MeCN, DCM, MS 3 Å, -40 °C, 24 h (16 %); g) HF·py, pyridine, 0 °C, 24 h (81 %); h) SO₃·py, DMF, rt, 24 h (85 %); i) NaOH (aq.), rt, 120 h (80 %).

Next, a small library of amides was synthesised (Scheme 3). First, the azido group was reduced to the primary amine via Pd-catalysed hydrogenation (→ **GC106**). Subsequent acylation with the corresponding carboxylic acids in the presence of HATU as activating agent afforded amides **GC108**, **GC107** and **GC109**.



Scheme 3. Synthesis of amide derivatives at C-4. a) Pd(OH)₂/C, H₂ (1 atm), H₂O, rt, 24 h (97 %); b) RCO₂H, HATU, DIPEA, DMF, rt, (37 – 63 %).

These three amides, as well as the 4-amino and 4-azido compounds, were then tested with MST (Table 2).

Lead glycomimetic **GC10** showed a *K_D* of 256 μM, which is in agreement with the reported result from ITC (259 μM).¹⁷ The replacement of the hydroxyl group by azide (→ **GC96**) improved the

Table 2. MST analysis of C-4 modified derivatives of GC10.

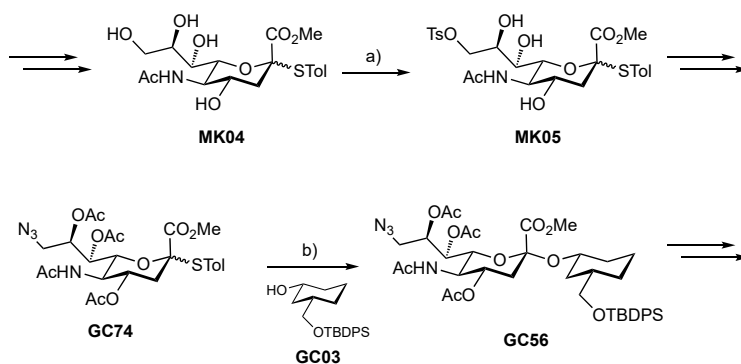
Compound	Structure	K_D [μ M]
GC10		256
GC96		162
GC106		421
GC108		193
GC107		161
GC109		262

affinity to 162 μ M, *i.e.* 1.6-fold improvement. This result is an indication that the 4-OH of the sialic acid is not involved in key interactions with the protein, therefore its modification can indeed represent a valuable strategy to improve the affinity of Siglec-8 ligands. However, when the azide is converted into the primary amine (\rightarrow **GC106**) the K_D dropped to 421 μ M. This may be due to the energetic costs associated with the additional positive charge of the protonated amine at physiological pH. When the amine was converted to amides, small improvements were observed. The acetamide derivatives **GC108** and **GC107** showed affinities of 161 and 193 μ M, respectively. The docking pose of these two compounds indicates the possible formation of an additional hydrogen bond between the oxygen of the new carbonyl group and Lys116. Interestingly, the amide made from the 5-hydroxyindole-3-acetic acid (**GC109**) exhibited a K_D of 262 μ M, which is worse than the other two amides despite showing a better docking score.

Even if this small library of compounds was not based on proper computational studies, affinity enhancements of 1.6-fold compared to the lead glycomimetic **GC10** were observed for both the azide and the benzylamide analogues. More in-depth computer-aided studies hopefully could provide valuable information regarding the amides to be tested. In addition, it would be interesting also to see whether other substitution patterns, such as triazole derivatives which are readily available through copper-catalysed azide-alkyne cycloaddition, could lead to ligands with improved affinity.

Modification of the 9-position of the Neu5Ac moiety.

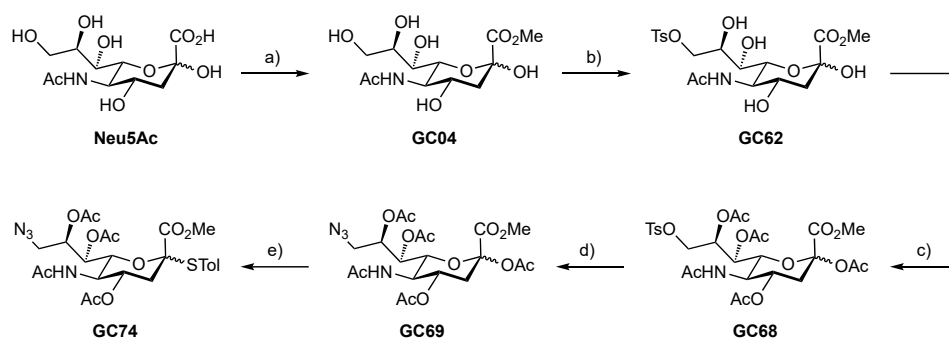
The introduction of sulfonamide functionalities at the 9-position of sialic acid proved to be a valuable strategy to enhance the affinity of Siglec-8 ligands.^{17,23} The reported synthesis of the 9-amino analogue of glycomimetic **GC10**, however, suffers from two low-yielding steps: the selective activation of the 9-hydroxyl group of the glycosyl donor, and the glycosylation reaction (Scheme 4). These two steps were described with 35 and 25 % yield, respectively, drastically diminished the overall yield.



Scheme 4. Critical steps in the reported synthesis of 9-azido derivatives. a) TsCl, pyridine, 0 °C to rt, 16 h (35 %); b) NIS, TfOH, MeCN, DCM, MS 3 Å, -40 °C, 4 h (25 %).

In attempts to improve the synthesis compound **GC56**, two different alternatives were explored. First, since **GC74** was synthesised from the glycosyl donor **GC06**, also used for the synthesis of glycomimetic **GC10**, a 7-steps procedure was necessary. We envisaged that the same compound could be obtained in a shorter route from the same starting point, the commercially available Neu5Ac (Scheme 5).

In this procedure, similar to the reported one, the sialic acid was first esterified to the methylester in presence of the acidic resin Amberlyst-15 (\rightarrow **GC04**). At this stage, however, the compound was treated with tosyl chloride for the selective activation of the primary alcohol, affording **GC62**, which was then immediately subjected to the next peracetylation without any workup procedure (\rightarrow **GC68**).

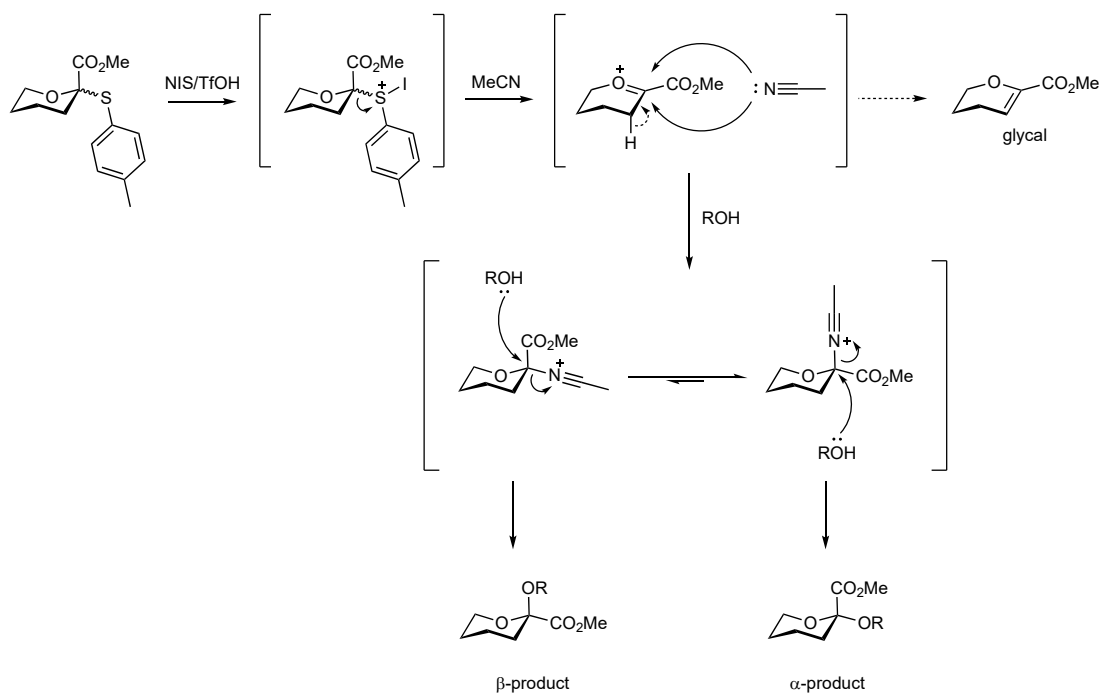


Scheme 5. Alternative synthesis of glycosyl donor **GC74.** a) Amberlyst-15, MeOH, rt, 120 h (98 %); b) **TsCl**, pyridine, 0 °C to rt, on; c) **Ac₂O**, pyridine, 0 °C to rt, 96 h (\approx 73 % from **GC04**); d) **NaN₃**, **DMF**, 60 °C, on; e) *p*-thiocresol, **BF₃·Et₂O**, **DCM**, 0 °C to rt, 24 h (18 % from **GC68**).

After introducing the azido group via reaction with **NaN₃** (\rightarrow **GC69**), the substitution of the anomeric acetate with *p*-thiocresol yielded the thioly glycosyl donor **GC74**, but only in 24 % yield. It needs to be specified that the goal of this alternative synthetic route was to obtain the modified glycosyl donor in high quantity. Therefore, tedious chromatographic purifications were avoided whenever possible, even if that meant carrying impurities along the steps, and only the final glycosyl donor **GC74** was subjected to chromatography. In this procedure, which involves 5 steps instead of 7 for the reported procedure, the functionalization of the primary hydroxyl as tosyl group proceeded with a higher yield. This was most likely due to the higher purity of the tosyl chloride since in this case, the reagent was recrystallized immediately before use. An old batch of tosyl chloride can indeed contain impurities of *p*-toluenesulfonic acid and hydrochloric acid, which can eventually affect the outcome of the reaction. Unexpectedly, however, the introduction of the azido group did not proceed as expected, since the glycosyl donor **GC74** was obtained only with a 24 % yield. Perhaps, chromatographic purification of the intermediate could lead to an improved yield, however, at the expense of synthetic practicality.

In the final step, the glycosyl donor **GC74** was reacted with acceptor **GC03** for completing the synthesis of glycomimetics. However, this reaction is associated with various problems, from the α - or β -stereoselectivity to the formation of byproducts. The combination of thiotolyl as leaving group, **NIS/TfOH** as promoters, acetonitrile as solvent, and low temperature favours the formation of the α -stereoisomer. This selectivity is due to the formation of a kinetically favoured β -nitrilium ion after displacement of the leaving group, which eventually promotes α -product. Additionally, a glycal byproduct is generally formed in a competing elimination reaction, which diminishes the glycosylation efficiency (Scheme 6).²⁴

To avoid the formation of the undesired β -sialoside, it is important to perform the reaction at low

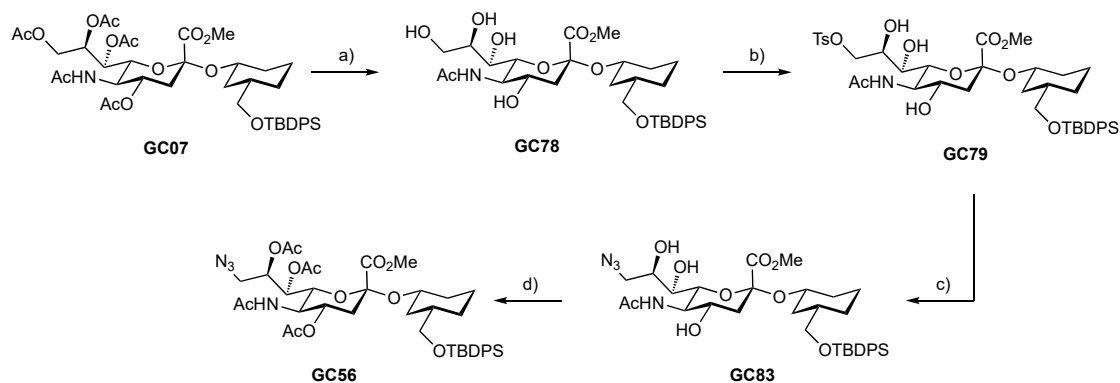


Scheme 6. Mechanism of sialylation in the presence of acetonitrile. After activation of the thiotolyl group as sulfonium iodide, the elimination of the leaving group forms a positively charged intermediate, which is attacked by acetonitrile. The kinetically favoured β -nitrilium ion is the predominant species at low temperature, therefore making the α -sialoside the major product of the reaction. Alternatively, the oxocarbenium intermediate can undergo H-elimination to form the sialyl glycal byproduct.

temperature and with acetonitrile as solvent. However, when performing the glycosylation between donor **GC74** and acceptor **GC03**, the solubility profile of the mixture was not compatible with the optimized experimental conditions (solvent, temperature and concentration) used before for the synthesis of glycomimetic **GC10**, as in this case, the mixture froze before reaching $-40\text{ }^{\circ}\text{C}$. While higher temperature promotes the β -product, a lower concentration of the reagents could detrimentally favour the competing elimination reaction. Therefore, a combination of acetonitrile and DCM was used as solvent to allow the formation of the nitrilium species while increasing the solubility of the mixture to reach $-40\text{ }^{\circ}\text{C}$. However, by change in the solvent composition alpha selectivity was still achieved, but for the price of reduced chemical yield.

Since the formation of glycal byproduct anyway represented the major issue of the sialylation, we decided to introduce the azido group after the glycosylation with the C-9 unmodified sialyl donor (Scheme 7).

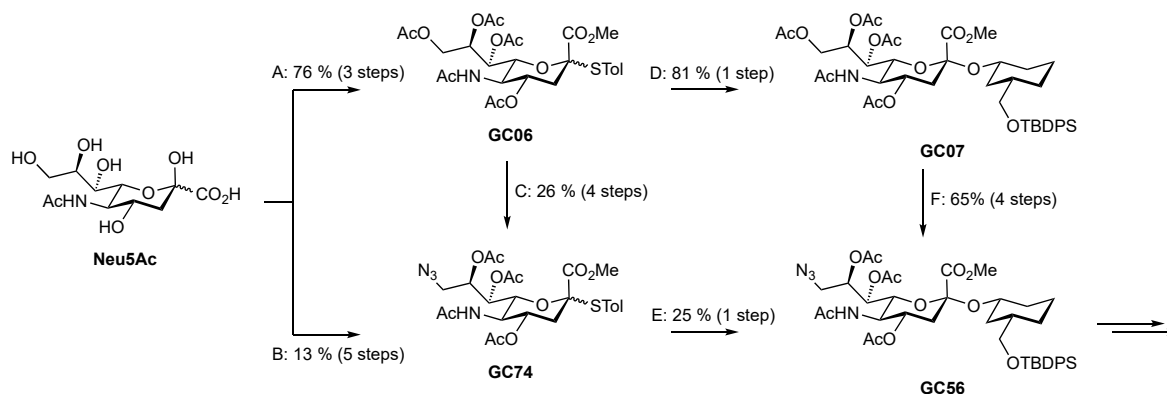
In this procedure, **GC07**¹⁷ was deacetylated using Zemlén conditions to afford the glycomimetic **GC78**, which was then treated with freshly purified tosyl chloride to selectively activate only the



Scheme 7. Alternative synthesis of compound GC56. a) MeONa, MeOH, rt, 24 h (quant.); b) TsCl, pyridine, 0 °C to rt, overnight (71 %); c) NaN₃, DMF, 70 °C, 24 h; d) Ac₂O, pyridine, 0 °C to rt, 24 h (91 % from **GC79**).

primary alcohol at the 9-position (\rightarrow **GC79**) in 71 % yield. Subsequently, the insertion of the azide moiety (\rightarrow **GC83**), followed by peracetylation proceeded smoothly to afford compound **GC56**.

Overall, three different strategies to synthesise glycomimetic **GC56** were explored (Scheme 8).

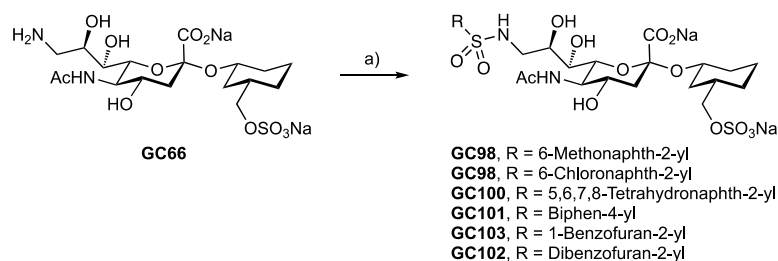


Scheme 8. Overview of the different synthetic routes for the formation of compound GC56.

The published procedure involved the synthesis of the glycosyl donor **GC74** from compound **GC06**, and subsequent glycosylation (A + C + E). This route involved a total of 8 steps, with an overall yield of 5 %. The first alternative that was investigated here was to reduce the number of reactions to obtain the same glycosyl donor **GC74** (B + E). In total, this alternative gave no yield improvement (5 %), but allowed to reduce the steps to 6. Finally, introducing the azide moiety after the glycosylation (A + D + F) proved to be the best alternative, with an overall yield of 40 % over 8 steps. In summary, despite additional improvements for each synthetic pathway could be obtained, it appears that the best option is to perform the glycosylation reaction on the unmodified sialyl donor **GC06**, and introduce the azide moiety at later stages. Indeed, the glycosylation reaction, with the undesired β -glycoside and glycan byproducts, represents the major challenge in these routes, and it seems more convenient to employ the rather non-precious donor **GC06**, which can be easily obtained in large quantities. In this way, the glycosylation can be performed with an excess of **GC06**, allowing

to completely react the glycosyl acceptor **GC03**, even if a higher amount of glycan byproduct is formed. Additionally, the more hydrophobic character of compound **GC07** entails easier handling of the compounds during workup and purification steps.

The benefits of having a sulfonamide moiety at the C-9 position of sialic acid for Siglec-8 ligands were previously demonstrated.^{17,23} Indeed, the presence of a naphthalenesulfonamide made compound **GC35** the most potent ligand in our first generation of Siglec-8 ligands, with a K_D of 15 μM . Obviously, a different binding pose between **GC35** and Siglec-8 must be expected, since in the available NMR solution structure there is no space to allocate the naphthalene modification. Presumably, a protein conformational rearrangement opens a new pocket where the naphthalene moiety can establish new interactions. This means, however, that the available structural information is not suitable to perform computational studies aimed to choose the optimal sulfonamide substituents. Therefore, for our second generation of sulfonamide analogues, variations of the naphthalene moiety were selected to assess the influence of the electronic properties of the aromatic rings, a few different aromatic scaffolds were chosen (Scheme 9), and the ligands were tested with ITC (Figure 4 and Table 3).



Scheme 9. Synthesis of C-9 modified sulfonamide Siglec-8 ligands. a) RSO_2Cl , NaHCO_3 , DMF, H_2O , rt, (29 – 62 %).

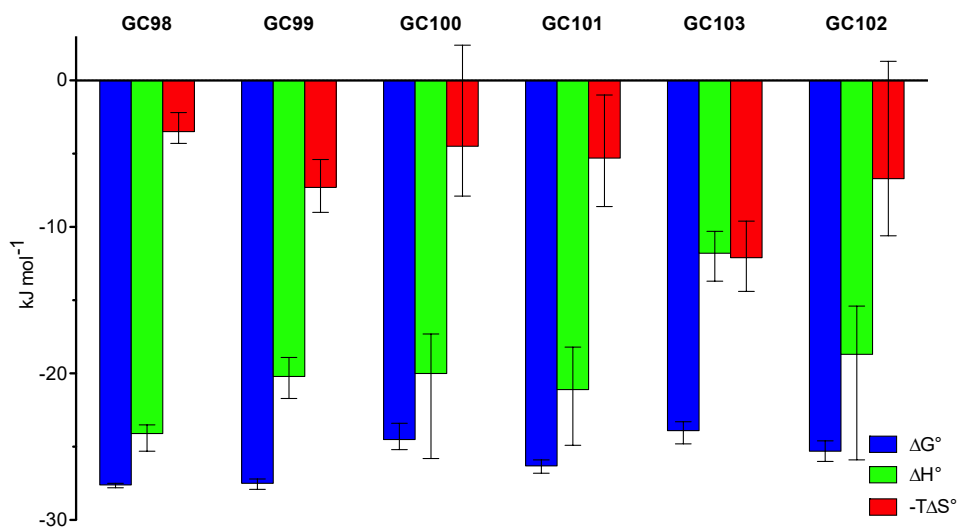


Figure 4. Thermodynamic fingerprints of 2nd generation of C-9 sulfonamides. Error estimates resemble the 68 % confidence interval from global fitting of two independent experiments (for details see Experimental Part).

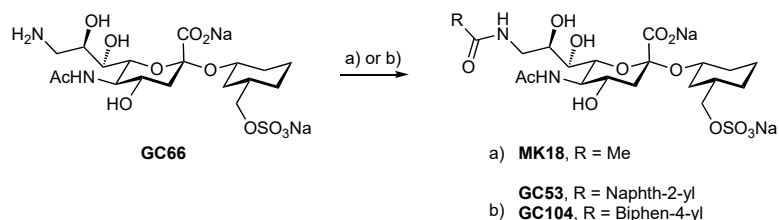
Table 3. Thermodynamic parameters of 2nd generation of C-9 sulfonamides. Error estimates resemble the 68 % confidence interval from global fitting of two independent experiments (for details see Experimental Part).

Compound	Structure	K_D [μM]	ΔG° [$\text{kJ}\cdot\text{mol}^{-1}$]	ΔH° [$\text{kJ}\cdot\text{mol}^{-1}$]	$-T\Delta S^\circ$ [$\text{kJ}\cdot\text{mol}^{-1}$]	N
GC98		14.4	-27.6	-24.1	-3.5	1.0
GC99		15.1	-27.5	-20.2	-7.3	1.1
GC100		50.9	-24.5	-20.0	-4.5	1.0
GC101		24.4	-26.3	-21.1	-5.3	1.1
GC103		64.2	-23.9	-11.8	-12.1	1.0
GC102		36.8	-25.3	-18.7	-6.7	1.1

The introduction of an OMe electron donating group (\rightarrow **GC98**), or a Cl electron withdrawing group (\rightarrow **GC99**) at the 6-position of the naphthalene moiety did not induce any significant differences compared to reference compound **GC35** (14.4 and 15.1 μM vs. 15 μM). However, it is important to have an extended conjugated aromatic system, since when the terminal ring is replaced by a tetrahydronaphthalene (\rightarrow **GC100**), the affinity suffered a 3.4-fold loss. When the naphthalene moiety was substituted by a biphenyl system (\rightarrow **GC101**), the affinity dropped to 24.4 μM . Two different heteroaromatic scaffolds, benzofuran (\rightarrow **GC103**) or dibenzofuran structures (\rightarrow **GC102**)

were synthesized. The former showed a K_D of 64.2 μM , indicating a 4.3-fold loss of activity compared to the naphthalene derivative, while the affinity for the latter was 36.8 μM .

To further confirm the importance of having the sulfonamide functionality for developing high-affinity Siglec-8 ligands, the azido and amino precursors, as well as a small series of amides (Scheme 10) were tested (Table 4).

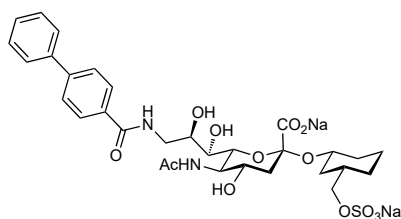


Scheme 10. Synthesis of C-9 amide Siglec-8 ligands. a) Pd(OH)₂/C, H₂ (1 atm), H₂O, rt, 16 h; then NaOH (aq.), rt, 6 h (43 %); b) RCO₂H, HATU, DIPEA, DMF, rt, (49 – 88 %).

Table 4. Biological evaluation of C-9 modified derivatives of GC10. Dissociation constants were measured via MST and ITC (for details see Experimental Part). n.d.: not detected. ^[a] Data for **GC10** and **GC33** reported from Ref. [17].

Compound	Structure	K_D [mM] (MST)	K_D [mM] (ITC)
GC10		256	259 ^[a]
GC65		10.4	-
GC66		1.0	0.840
MK18		1.3	n.d.
GC33 ^[a]		-	n.d.
GC53		-	n.d.

GC104



- n.d.

The presence of only the azido group at the 9-position (\rightarrow **GC65**) led to a complete loss of activity, since only a K_D of 10.4 mM was detected in MST. When the azide was converted to primary amine (\rightarrow **GC66**), a binding of 1.0 mM in MST and 840 μ M in ITC was detected. In the case of the small acetamide (\rightarrow **MK18**), only weak binding was detected in MST, but not in ITC. In accordance with previous findings from Nycholat and coworkers, amide analogues are not active against Siglec-8, and this was exemplified by the benzylamide derivatives of **GC10** (\rightarrow **GC33**).^{17,23} However, to exclude any potential influences of the amide substituent on this loss, the amide analogues of sulfonamides **GC35** (\rightarrow **GC53**) and **GC101** (\rightarrow **GC104**) were synthesised and tested. Not surprisingly, both compounds showed no activity in ITC experiments, confirming the crucial importance of the sulfonamide structure to achieve high affinity towards Siglec-8.

Overall, the naphthalenesulfonamide moiety still represents the most convenient substitution, leading to compounds with an affinity of around 15 μ M. However, other aromatic functionalities provided ligands with good activities, extending the variety of scaffolds that can be employed for the development of new Siglec-8 ligands. However, for an appropriate investigation of substitutions in the 9-position, new structural data are crucial, either by NMR experiment or X-ray. Information on the binding mode of these sulfonamides could allow proper computational studies allowing the identification of promising substituents.

Conclusion

The use of glycomimetics represents a valuable strategy for developing high-affinity ligands for lectins, among which Siglec-8. Here we present an extensive study starting from lead glycomimetic **GC10** to identify favourable modifications in the 4- and 9-position. While the carboxylic acid and sulfate play a crucial role in binding and can not be replaced, modification of the hydroxyl group at C-4 of the sialic acid proved to be a suitable site for modifications. Additionally, we proved the importance of the sulfonamide moiety, by showing that amide analogues with the same aromatic substitution completely lost activity. Furthermore, different aromatic sulfonamides were synthesized and tested, widening the options for the design of new ligands. Future studies should focus on

obtaining new structural information regarding the binding mode of the sulfonamides, from which new generations of ligands could be designed with the help of computational studies.

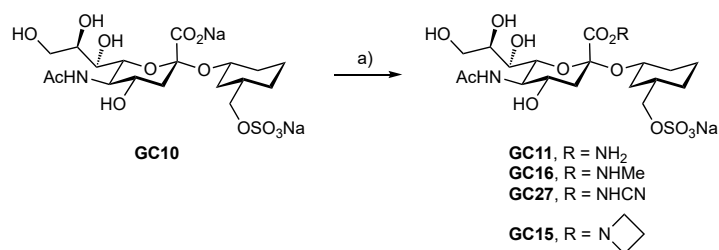
Experimental part

Synthesis of Siglec-8 inhibitors

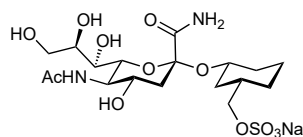
General methods

NMR spectra were recorded on Bruker Avance III 500 MHz, Bruker Ultrashield 600 MHz or Varian Mercury 400 MHz. Assignment of ¹H and ¹³C NMR spectra was achieved using 2D methods (COSY, HSQC, HMBC). Chemical shifts are expressed in ppm using residual solvent signals (CHCl₃, CHD₂OD, HDO) as reference. Optical rotations were measured with a PerkinElmer polarimeter 341. Electrospray ionization mass spectrometry (ESI-MS) data were obtained on a Waters Micromass ZQ instrument. High resolution mass (HR-MS) analyses were done on an Agilent 1100 LC, equipped with a photodiode array detector and a Bruker QTOF I, equipped with a 4 GHz digital-time converter. Reactions were monitored by TLC using glass plates coated with silica gel 60 F254 (Merck) and visualized by using UV light and/or by charring with a molybdate solution (a 0.02 M solution of ammonium cerium sulfate dihydrate and ammonium molybdate tetrahydrate in 10 % aq. H₂SO₄). Flash chromatography was done on a CombiFlash Rf from Teledyne Isco (Lincoln, NE, USA) equipped with RediSep normal phase or RP-18 reversed-phase flash columns. Size exclusion chromatography was performed on Biogel P-2 (Bio-Rad Laboratories, Inc.). Commercially available reagents and dry solvents were purchased as reagent grade from Sigma-Aldrich, Alfa Aesar and Acros and used without further purification. Molecular sieves (3Å, 4Å) were activated under vacuum at 500 °C for 0.5 h immediately before use. Compounds **GC10**, **GC08**, **GC03**, **GC07**, **GC66** and **MK10** were prepared according to [17].

Synthesis of amide bioisosteres

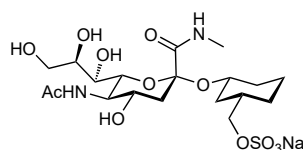


Scheme E1. a) RH, HATU, DIPEA, DMF, rt, (33 – 63 %).

(1S,3R)-3-(Sulfonatooxymethyl)cyclohexyl (5-acetamido-3,5-dideoxy-D-glycero- α -D-galacto-2-nonulopyranosylonamide) sodium salt (GC11)

Compound **GC10** (29.9 mg, 0.055 mmol) and HATU (34.5 mg, 0.091 mmol) were dissolved in dry DMF (200 μ L) under argon. DIPEA (29 μ L, 0.166 mmol) and NH_3 (0.5 M in THF, 0.2 mL, 0.100 mmol) were added and the mixture was stirred at rt overnight. The solvent was evaporated and the residue purified with RP-flash chromatography (RP-18, $\text{H}_2\text{O}/\text{MeCN}$, 1:0 to 0:1) and size-exclusion chromatography (P-2 gel, H_2O) to afford **GC11** (14.7 mg, 33 %).

$[\alpha]_D^{20} = +6.7$ ($c = 1.0$, H_2O); $^1\text{H NMR}$ (500 MHz, D_2O): δ 3.84 – 3.64 (m, 6H, H-1, CH_2O , H-5', H-7', H-9'a), 3.61 (d, $J = 10.5$ Hz, 1H, H-6'), 3.58 – 3.49 (m, 3H, H-4', H-8', H-9'b), 2.64 – 2.57 (m, 1H, H-3'e), 1.93 – 1.84 (m, 4H, H-6e, NHAc), 1.81 (d, $J = 11.7$ Hz, 1H, H-2e), 1.71 – 1.57 (m, 3H, H-3, H-5e, H-3'a), 1.53 (d, $J = 12.5$ Hz, 1H, H-4e), 1.27 – 1.07 (m, 2H, H-5a, H-6a), 0.91 (q, $J = 11.8$ Hz, 1H, H-2a), 0.77 (q, $J = 12.2$ Hz, 1H, H-6a); $^{13}\text{C NMR}$ (126 MHz, D_2O): δ 175.8 (C=O), 173.0 (C=O), 100.6 (C-2'), 75.1 (C-1), 74.24 (C-6'), 74.15 (CH_2O), 72.0 (C-7'), 68.1 (C-4'/C-8'), 67.9 (C-4'/C-8'), 63.4 (C-9'), 52.4 (C-5'), 39.8 (C-3'), 36.8 (C-3), 36.6 (C-2), 34.9 (C-6), 28.1 (C-4), 23.9 (C-5), 22.8 (NHAc); HR-MS (ESI): m/z calcd for $\text{C}_{18}\text{H}_{31}\text{N}_2\text{NaO}_{12}\text{S}$: 545.1388 $[\text{M}+\text{Na}]^+$, found 545.1389; HPLC purity: 89 %.

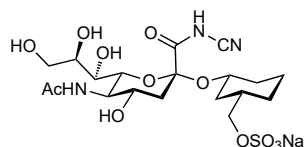
(1S,3R)-3-(Sulfonatooxymethyl)cyclohexyl (5-acetamido-3,5-dideoxy-N-methyl-D-glycero- α -D-galacto-2-nonulopyranosylonamide) sodium salt (GC16)

Compound **GC10** (29.0 mg, 0.053 mmol) and HATU (30.8 mg, 0.081 mmol) were dissolved in dry DMF (200 μ L) under argon. DIPEA (29 μ L, 0.166 mmol) and MeNH_2 (2 M in THF, 33 μ L, 0.066 mmol) were added and the mixture was stirred at rt overnight. The solvent was evaporated and the residue purified with RP-flash chromatography (RP-18, $\text{H}_2\text{O}/\text{MeCN}$, 1:0 to 0:1) and size-exclusion chromatography (P-2 gel, H_2O) to afford **GC16** (17.9 mg, 63 %).

$[\alpha]_D^{20} = +13.7$ ($c = 1.0$, H_2O); $^1\text{H NMR}$ (500 MHz, D_2O): δ 3.96 – 3.80 (m, 6H, H-1, CH_2O , H-5', H-7', H-9'a), 3.74 – 3.63 (m, 4H, H-4', H-6', H-8', H-9'b), 2.84 (s, 3H, NHMe), 2.79 (dd, $J = 12.8$,

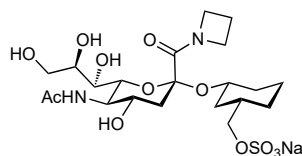
4.5 Hz, 1H, H-3'e), 2.06 (s, 3H, NHAc), 1.99 (d, $J = 12.3$ Hz, 1H, H-6e), 1.90 – 1.73 (m, 4H, H-2e, H-3, H-5e, H-3'a), 1.67 (d, $J = 12.3$ Hz, 1H, H-4e), 1.40 – 1.22 (m, 2H, H-5a, H-6a), 1.05 (q, $J = 11.9$ Hz, 1H, H-2a), 0.92 (qd, $J = 12.6, 3.6$ Hz, 1H, H-4a); ¹³C NMR (126 MHz, D₂O): δ 175.1 (C=O), 170.0 (C=O), 99.9 (C-2'), 74.0 (C-1), 73.45 (C-6'), 73.36 (CH₂O), 71.3 (C-7'), 67.4 (C-4'/C-8'), 67.1 (C-4'/C-8'), 62.9 (C-9'), 51.7 (C-5'), 39.1 (C-3'), 36.1 (C-3), 35.9 (C-2), 34.0 (C-6), 27.3 (C-4), 25.6 (NHMe), 23.1 (C-5), 22.0 (NHAc); HR-MS (ESI): m/z calcd for C₁₉H₃₃N₂NaO₁₂S: 559.1544 [M+Na]⁺, found 559.1544; HPLC purity: 99 %.

(1S,3R)-3-(Sulfonatoxymethyl)cyclohexyl (5-acetamido-N-ciano-3,5-dideoxy-D-glycero- α -D-galacto-2-nonulopyranosylonamide) sodium salt (GC27)



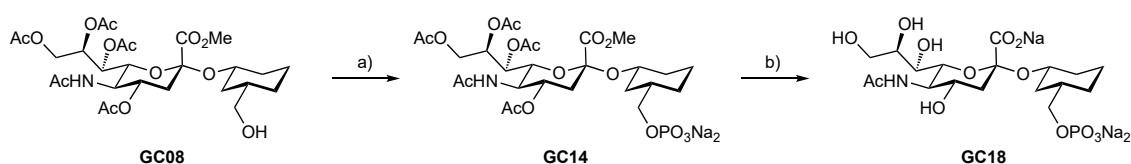
Compound **GC10** (28.2 mg, 0.052 mmol) and HATU (36.1 mg, 0.095 mmol) were dissolved in dry DMF (200 μ L) under argon. DIPEA (38 μ L, 0.218 mmol) and NH₂CN (4.4 mg, 0.105 mmol) were added and the mixture was stirred at rt overnight. The solvent was evaporated and the residue purified with RP-flash chromatography (RP-18, H₂O/MeCN, 1:0 to 0:1) and size-exclusion chromatography (P-2 gel, H₂O) to afford **GC27** (14.6 mg, 63 %).

$[\alpha]_D^{20} = +11.3$ (c = 1.0, H₂O); ¹H NMR (500 MHz, D₂O): δ 3.98 – 3.78 (m, 6H, H-1, CH₂O, H-5', H-7', H-9'a), 3.72 – 3.62 (m, 3H, H-4', H-6', H-9'b), 3.59 (dd, $J = 8.8, 1.9$ Hz, 1H, H-8'), 2.75 (dd, $J = 12.5, 4.6$ Hz, 1H, H-3'e), 2.05 – 1.98 (m, 4H, H-6e, NHAc), 1.85 (d, $J = 12.0$ Hz, 1H, H-2e), 1.82 – 1.72 (m, 2H, H-3, H-5e), 1.71 – 1.63 (m, 2H, H-4e, H-3'a), 1.37 – 1.17 (m, 2H, H-5a, H-6a), 1.04 (q, $J = 11.9$ Hz, 1H, H-2a), 0.91 (qd, $J = 12.6, 3.6$ Hz, 1H, H-4a); ¹³C NMR (126 MHz, D₂O): δ 181.4 (C=O), 176.0 (C=O), 101.3 (C-2'), 75.3 (C-1), 74.4 (CH₂O), 73.9 (C-6'), 73.0 (C-7'), 69.0 (C-8'), 68.8 (C-4'), 63.4 (C-9'), 52.7 (C-5'), 41.6 (C-3'), 37.2 (C-3), 36.7 (C-2), 35.2 (C-6), 28.5 (C-4), 24.2 (C-5), 23.0 (NHAc); HR-MS (ESI): m/z calcd for C₁₉H₃₀N₃NaO₁₂S: 570.1340 [M+Na]⁺, found 570.1341; HPLC purity: 85 %.

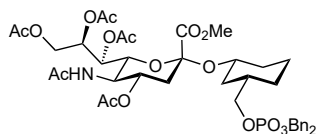
(1S,3R)-3-(Sulfonatoxymethyl)cyclohexyl (5-acetamido-N-azetidino-3,5-dideoxy-D-glycero- α -D-galacto-2-nonulopyranosylonamide) sodium salt (GC15)

Compound **GC10** (30.1 mg, 0.055 mmol) and HATU (32.4 mg, 0.085 mmol) were dissolved in dry DMF (200 μ L) under argon. DIPEA (29 μ L, 0.166 mmol) and azetidine (4 μ L, 0.059 mmol) were added and the mixture was stirred at rt overnight. The solvent was evaporated and the residue purified with flash chromatography (DCM/(MeOH/H₂O, 10:1), 1:0 to 1:1) and size-exclusion chromatography (P-2 gel, H₂O) to afford **GC15** (19.3 mg, 61 %).

$[\alpha]_D^{20} = -8.1$ ($c = 1.0$, H₂O); ¹H NMR (500 MHz, D₂O): δ 4.60 – 4.46 (m, 2H, *N*-Az-a), 4.15 – 4.03 (m, 2H, *N*-Az-b), 4.00 – 3.89 (m, 2H, H-1, CH₂Oa), 3.91 – 3.78 (m, 5H, CH₂Ob, H-4', H-5', H-7', H-9'a), 3.71 – 3.63 (m, 2H, H-6', H-9'b), 3.58 (dd, $J = 9.1, 1.6$ Hz, 1H, H-8'), 2.57 – 2.50 (m, 1H, H-3'e), 2.46 – 2.26 (m, 2H, Az), 2.06 – 1.99 (m, 4H, H-2e, NHAc), 1.96 (d, $J = 11.4$ Hz, 1H, H-6e), 1.88 – 1.76 (m, 3H, H-3, H-5e, H-3'a), 1.66 (d, $J = 12.0$ Hz, 1H, H-4e), 1.41 – 1.22 (m, 2H, H-5a, H-6a), 1.16 (q, $J = 11.9$ Hz, 1H, H-2a), 0.93 (qd, $J = 12.5, 3.6$ Hz, 1H, H-4a); ¹³C NMR (126 MHz, D₂O): δ 175.0 (C=O), 168.6 (C=O), 99.6 (C-2'), 73.7 (C-1), 73.4 (CH₂O), 72.8 (C-6'), 71.0 (C-7'), 68.0 (C-8'), 67.6 (C-4'), 62.9 (C-9'), 53.7 (*N*-Az-a), 51.8 (C-5'), 49.9 (*N*-Az-b), 38.3 (C-3'), 36.2 (C-2), 36.1 (C-3), 33.8 (C-6), 27.2 (C-4), 23.1 (C-5), 22.0 (NHAc), 15.7 (Az); HR-MS (ESI): m/z calcd for C₂₁H₃₅N₂NaO₁₂S: 585.1701 [M+Na]⁺, found 585.1701; HPLC purity: 100 %.

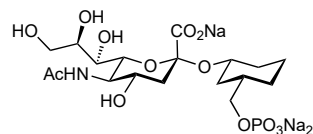
Synthesis of phosphate bioisostere

Scheme E2. a) Dibenzyl *N,N*-diisopropylphosphoramidite, 1,2,4-triazole, MeCN, 0 °C to rt, overnight; then *t*BuOOH, rt, 1 h (29 %); b) Pd/C, H₂ (1 atm), MeOH, rt, overnight; then NaOH (aq.), rt, 5 h (92 %).

(1S,3R)-3-(bis(phenylmethoxy)phosphinyl)oxymethyl)cyclohexyl (methyl 5-acetamido-4,7,8,9-tetra-O-acetyl-3,5-dideoxy-D-glycero- α -D-galacto-2-nonulopyranosylonate) (GC14)

To an ice-cooled solution of **GC08** (127.0 mg, 0.210 mmol) and 1,2,4-triazole (60.0 mg, 0.869 mmol) in dry MeCN (2.1 mL), dibenzyl *N,N*-diisopropylphosphoramidite (160 μ L, 0.428 mmol) was added, and the mixture was stirred for 30 min at 0 °C and then overnight at rt. Then, *tert*-butylhydroperoxide (120 μ L, 0.867 mmol) was added and the solution was stirred for 1 h. The reaction was quenched with 1 M aq. Na₂S₂O₃ and 1 M aq. NaHCO₃, and the mixture was extracted with DCM (3 x 20 mL), dried over Na₂SO₄, and filtered. The solvents were removed *with vacuo* and the crude product was purified by flash column chromatography (toluene/acetone, 1:0 to 1:3) to afford **GC14** (52.1 mg, 29 %).

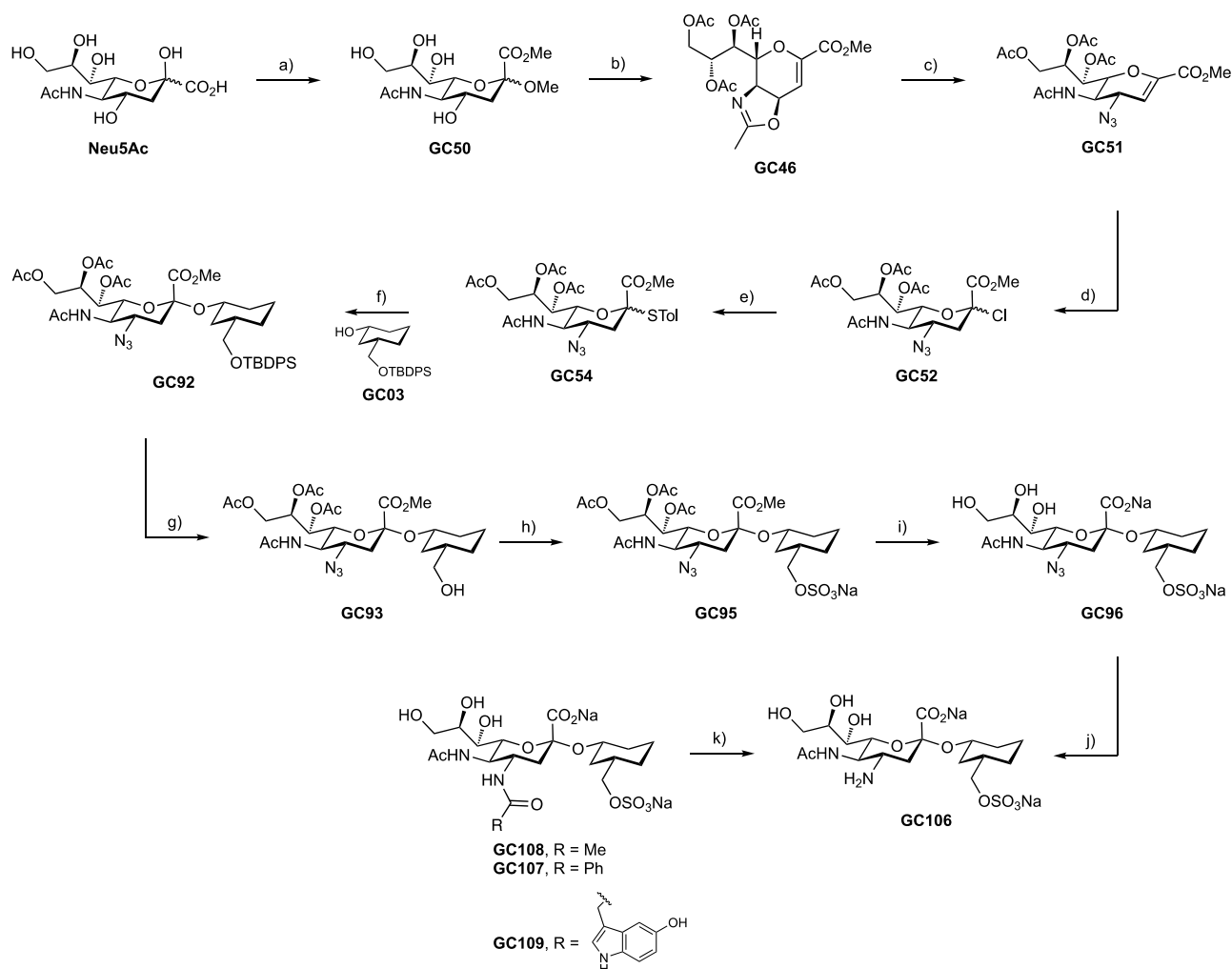
$[\alpha]_D^{20} = +18.3$ (c = 0.2, DCM); ¹H NMR (500 MHz, CDCl₃): δ 7.38 – 7.30 (m, 10H, Ph), 5.35 (ddd, *J* = 8.2, 5.6, 2.6 Hz, 1H, H-8'), 5.30 (dd, *J* = 8.5, 2.1 Hz, 1H, H-7'), 5.27 (d, *J* = 9.8 Hz, 1H, NH), 5.07 – 4.96 (m, 4H, CH₂Ph), 4.81 (ddd, *J* = 12.4, 9.8, 4.7 Hz, 1H, H-4'), 4.29 (dd, *J* = 12.5, 2.6 Hz, 1H, H-9'a), 4.10 – 4.00 (m, 3H, H-5', H-6', H-9'b), 3.79 – 3.74 (m, 2H, CH₂O), 3.71 (s, 3H, OMe), 3.70 – 3.63 (m, 1H, H-1), 2.57 (dd, *J* = 12.7, 4.7 Hz, 1H, H-3'e), 2.13 (s, 3H, OAc), 2.12 (s, 3H, OAc), 2.04 – 1.99 (m, 7H, H-6e, 2 x OAc), 1.91 – 1.84 (m, 4H, H-3'a, NHAc), 1.78 – 1.70 (m, 1H, H-5e), 1.67 – 1.54 (m, 3H, H-2e, H-3, H-4e), 1.35 (qt, *J* = 13.4, 3.5 Hz, 1H, H-5a), 1.19 (tdd, *J* = 12.8, 10.6, 3.8 Hz, 1H, H-6a), 0.93 (td, *J* = 12.7, 10.9 Hz, 1H, H-2a), 0.78 (qd, *J* = 12.7, 3.8 Hz, 1H, H-4a); ¹³C NMR (126 MHz, CDCl₃): δ 171.1 (C=O), 170.7 (C=O), 170.4 (C=O), 170.3 (C=O), 170.0 (C=O), 168.9 (C=O), 136.02 (*i*-Ph-a), 135.97 (*i*-Ph-b), 128.7 (Ph), 128.6 (Ph), 128.0 (Ph), 98.7 (C-2'), 73.8 (C-1), 72.5 (C-6'), 72.1 (d, *J* = 6.2 Hz, CH₂O), 69.33 (CH₂Ph-a), 69.28 (CH₂Ph-b), 69.26 (C-4'), 68.6 (C-8'), 67.4 (C-7'), 62.6 (C-9'), 52.7 (OMe), 49.5 (C-5'), 38.6 (C-3'), 37.3 (d, *J* = 7.6 Hz, C-3), 35.7 (C-2), 34.8 (C-6), 28.0 (C-4), 23.29 (NHAc), 23.23 (C-5), 21.2 (OAc), 20.97 (OAc), 20.96 (OAc), 20.9 (OAc); MS (ESI): *m/z* calcd for C₄₁H₅₄NO₁₇P: 886.3 [M+Na]⁺, found 886.3.

(1S,3R)-3-(disodium phosphinyl)oxymethyl)cyclohexyl (sodium 5-acetamido-3,5-dideoxy-D-glycero- α -D-galacto-2-nonulopyranosylonate) (GC18)

To a solution of **GC14** (52.1 mg, 0.60 mmol) in MeOH (3.0 mL) Pd/C (10 %, 11.5 mg) was added. The reaction was stirred under H₂ atmosphere overnight. Then, the suspension was filtered over celite and concentrated *in vacuo*. The residue was dissolved in 0.1 M NaOH (3 mL) and stirred for 5 h. Then, the solution was neutralized by addition of Amberlite IR 120, filtered and concentrated *in vacuo*. The crude product was purified by size-exclusion chromatography (P-2 gel, H₂O) to yield **GC18** (31.5 mg, 92 %).

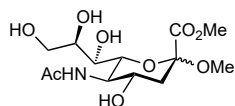
$[\alpha]_D^{20} = +7.5$ (c = 1.0, H₂O); ¹H NMR (500 MHz, D₂O): δ 3.95 – 3.77 (m, 4H, H-1, H-5', H-7', H-9'a), 3.73 – 3.58 (m, 6H, CH₂O, H-4', H-6', H-8', H-9'b), 2.76 (dd, $J = 12.4, 4.7$ Hz, 1H, H-3'e), 2.08 – 2.00 (m, 4H, H-6e, NHAc), 1.92 (d, $J = 10.4$ Hz, 1H, H-2e), 1.79 (dt, $J = 12.9, 3.1$ Hz, 1H, H-5e), 1.75 – 1.60 (m, 3H, H-3, H-4e, H-3'a), 1.36 – 1.17 (m, 2H, H-5a, H-6a), 0.99 (q, $J = 11.8$ Hz, 1H, H-2a), 0.86 (qd, $J = 13.0, 3.7$ Hz, 1H, H-4a); ¹³C NMR (126 MHz, D₂O): δ 176.0 (C=O), 174.7 (C=O), 101.9 (C-2'), 75.8 (C-1), 73.7 (C-6'), 73.1 (C-7'), 71.2 (CH₂O), 69.3 (C4', C-8'), 63.5 (C-9'), 53.0 (C-5'), 42.3 (C-3'), 38.3 (C-3), 36.9 (C-2), 35.4 (C-6), 28.7 (C-4), 24.4 (C-5), 22.9 (NHAc); HR-MS (ESI): m/z calcd for C₁₈H₂₉NNa₃O₁₃P: 590.0962 [M+Na]⁺, found 590.0964; HPLC purity: 100 %.

Synthesis of C-4 modified Siglec-8 ligands



Scheme E3. a) Dowex 50W X8, MeOH, 60 °C, 90 h (74 %); b) Ac₂O, H₂SO₄, rt, 70 h (70 %); c) TMSN₃, *t*BuOH, 80 °C, 16 h (95 %); d) HCl (g), LiCl, MS 3 Å, -30 °C to rt, 120 h (54 %); e) *p*-thiocresol, DIPEA, DCM, 0 °C to rt, 24 h (66 %); f) NIS, TfOH, MeCN, DCM, MS 3 Å, -40 °C, 24 h (16 %); g) HF·py, pyridine, 0 °C, 24 h (81 %); h) SO₃·py, DMF, rt, 24 h (85 %); i) NaOH (aq.), rt, 120 h (80 %); j) Pd(OH)₂/C, H₂ (1 atm), H₂O, rt, 24 h (97 %); k) RCO₂H, HATU, DIPEA, DMF, rt, (37 – 63 %).

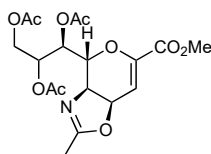
Methyl (methyl 5-acetamido-3,5-dideoxy-D-glycero-α-D-galacto-2-nonulopyranosylonate) (GC50)



To a solution of Neu5Ac (5.6898 g, 18.4 mmol) in MeOH (200 mL), Dowex 50W X8 (10.0454 g) was added. The reaction was stirred at 60 °C for 90 h. Then, the suspension was filtered over celite and concentrated *in vacuo*, affording **GC50** (4.5810 g, 74 %).

$[\alpha]_D^{20} = -6.5$ ($c = 0.4$, MeOH); $^1\text{H NMR}$ (600 MHz, CD_3OD): δ 4.08 – 4.03 (m, 1H, H-4), 4.01 (d, $J = 10.5$ Hz, 1H, H-6), 3.85 – 3.75 (m, 5H, H-5, H-9a, CO_2Me), 3.73 – 3.68 (m, 1H, H-8), 3.67 – 3.61 (m, 1H, H-9b), 3.49 (d, $J = 8.9$ Hz, 1H, H-7), 3.35 (s, 3H, OMe), 2.23 (dd, $J = 12.9, 4.7$ Hz, 1H, H-3e), 2.03 (s, 3H, NHAc), 1.88 (t, $J = 12.1$ Hz, 1H, H-3a); $^{13}\text{C NMR}$ (151 MHz, CD_3OD): δ 175.1 (C=O), 171.9 (C-1), 96.6 (C-2), 72.0 (C-6), 71.6 (C-8), 70.1 (C-7), 67.8 (C-4), 64.8 (C-4), 54.2 (C-9), 53.2 (CO_2Me), 49.8 (OMe), 40.7 (C-3), 22.7 (NHAc); MS (ESI): m/z calcd for $\text{C}_{13}\text{H}_{23}\text{NO}_9$: 360.1 $[\text{M}+\text{Na}]^+$, found 360.1.

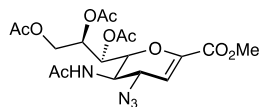
Methyl 7,8,9-tri-*O*-acetyl-2,3-didehydro-2,3,5-trideoxy-4',5'-dihydro-2'-methyloxazolo[5,4-d]-*D*-glycero-*D*-talo-2-nonulopyranosylonate (GC46)



To a solution of **GC50** (4.5810 g, 13.6 mmol) in Ac_2O (50 mL), H_2SO_4 (2.4 mL, 45.0 mmol) was added and the reaction was stirred at rt for 70 h. Then, the solution was added dropwise to a mixture of Na_2CO_3 (137.9 g of $\text{Na}_2\text{CO}_3 \cdot 10\text{H}_2\text{O}$), H_2O (280 mL) and EtOAc (14 mL) at 0 °C. After 1.5 h, the mixture was extracted with EtOAc (2 x 300 mL). The combined organics were washed with satd. aq. NaHCO_3 (200 mL), brine (200 mL), dried over Na_2SO_4 , filtered and concentrated *in vacuo*, yielding **GC46** (3.9710 g, 70 %).

$[\alpha]_D^{20} = -13.5$ ($c = 1.1$, CHCl_3); $^1\text{H NMR}$ (600 MHz, CDCl_3): δ 6.38 (d, $J = 4.0$ Hz, 1H, H-3), 5.63 (dd, $J = 6.0, 2.6$ Hz, 1H, H-7), 5.44 (td, $J = 6.2, 2.6$ Hz, 1H, H-8), 4.82 (dd, $J = 8.6, 4.0$ Hz, 1H, H-4), 4.59 (dd, $J = 12.5, 2.6$ Hz, 1H, H-9a), 4.22 (dd, $J = 12.5, 6.4$ Hz, 1H, H-9b), 3.97 – 3.93 (m, 1H, H-5), 3.81 (s, 3H, OMe), 3.42 (dd, $J = 10.1, 2.6$ Hz, 1H, H-6), 2.15 (s, 3H, OAc), 2.05 (s, 3H, OAc), 2.05 (s, 3H, OAc), 2.00 (s, 3H, Me); $^{13}\text{C NMR}$ (151 MHz, CDCl_3): δ 170.8 (C=O), 170.0 (C=O), 169.8 (C=O), 167.4 (C-1), 162.0 (C-2), 147.3 (C=N), 107.7 (C-3), 77.0 (C-6), 72.4 (C-4), 70.4 (C-8), 69.0 (C-7), 62.2 (C-5), 62.1 (C-9), 52.7 (OMe), 21.0 (OAc), 20.9 (OAc), 20.8 (OAc), 14.3 (Me); MS (ESI): m/z calcd for $\text{C}_{18}\text{H}_{23}\text{NO}_{10}$: 436.1 $[\text{M}+\text{Na}]^+$, found 436.1.

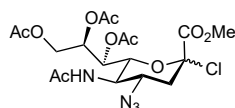
Methyl 5-acetamido-7,8,9-tri-*O*-acetyl-4-azido-2,3-didehydro-2,3,4,5-tetra-deoxy-D-glycero-D-galacto-2-nonulopyranosylonate (GC51)



To a solution of **GC46** (3.6920 g, 8.93 mmol) in *t*BuOH (30 mL), TMSN₃ (2.0 mL, 15.2 mmol) was added, and the reaction was stirred at 80 °C for 16 h. Then, the solution cooled at rt and diluted with EtOAc (100mL). Next, NaNO₂ (1.19 g in 25 mL H₂O) was added, and aq. HCl was added until pH 2. The two phases were separated, and the aqueous phase was extracted with EtOAc (50 mL). The combined organics were washed with H₂O (2 x 25 mL), satd. aq. NaHCO₃ (25 mL), H₂O (25 mL), dried over Na₂SO₄, filtered and concentrated *in vacuo*, affording **GC51** (3.9010 g, 95 %).

$[\alpha]_D^{20} = +109$ (c = 0.9, CHCl₃); ¹H NMR (600 MHz, CDCl₃): δ 5.96 (d, *J* = 2.8 Hz, 1H, H-3), 5.45 (dd, *J* = 5.3, 2.5 Hz, 1H, H-7), 5.31 (ddd, *J* = 6.7, 5.3, 2.8 Hz, 1H, H-8), 4.62 (dd, *J* = 12.4, 2.8 Hz, 1H, H-9a), 4.49 (dd, *J* = 9.9, 2.5 Hz, 1H, H-6), 4.44 (dd, *J* = 8.8, 2.8 Hz, 1H, H-4), 4.18 (dd, *J* = 12.4, 6.7 Hz, 1H, H-9b), 3.86 (dt, *J* = 9.8, 8.8 Hz, 1H, H-5), 3.80 (s, 3H, OMe), 2.12 (s, 3H, OAc), 2.06 (s, 3H, OAc), 2.04 (s, 3H, OAc), 1.99 (s, 3H, NHAc); ¹³C NMR (151 MHz, CDCl₃): δ 170.8 (2 x C=O), 170.5 (C=O), 170.3 (C-1), 161.6 (C-2), 145.3 (NHC=O), 107.7 (C-3), 75.9 (C-6), 70.9 (C-8), 67.8 (C-7), 62.1 (C-9), 57.7 (C-4), 52.7 (OMe), 48.7 (C-5), 23.5 (NHAc), 21.0 (OAc), 20.90 (OAc), 20.87 (OAc); MS (ESI): *m/z* calcd for C₁₈H₂₄N₄O₁₀: 479.1 [M+Na]⁺, found 479.1.

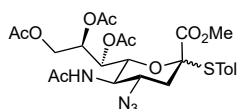
Methyl 5-acetamido-7,8,9-tri-*O*-acetyl-4-azido-2-chloro-2,3,4,5-tetra-deoxy-D-glycero-D-galacto-2-nonulopyranosylonate (GC52)



To a solution of **GC51** (3.9010 g, 8.55 mmol), LiCl (1.9422 g, 45.8 mmol), and MS 3 Å (9.4877 g) in dry degassed MeCN (100 mL), HCl (g) was bubbled for 20 min while keeping the temperature below -30 °C. Then, the reaction was stirred for 120 h at rt. Next, the mixture was filtered through celite and the filter washed with DCM. The solvents were removed with *vacuo* and the crude dissolved in DCM (200 mL). The organic phase was washed with ice-cold H₂O (120 mL), ice-cold satd. aq. NaHCO₃ (2 x 120 mL), and brine (100 mL), dried over Na₂SO₄, filtered and concentrated *in vacuo*, yielding **GC52** (3.252 g, 54 %).

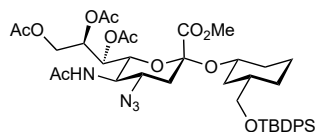
$[\alpha]_D^{20} = -10$ ($c = 1.0$, CHCl_3); $^1\text{H NMR}$ (600 MHz, CDCl_3): δ 5.45 (dd, $J = 7.1, 2.3$ Hz, 1H, H-7), 5.17 (ddd, $J = 7.0, 5.8, 2.7$ Hz, 1H, H-8), 4.50 – 4.46 (m, 1H, H-6), 4.40 (dd, $J = 12.6, 2.7$ Hz, 1H, H-9a), 4.23 – 4.14 (m, 1H, H-4), 4.08 (dd, $J = 12.5, 5.8$ Hz, 1H, H-9b), 3.86 (s, 3H, OMe), 3.82 – 3.79 (m, 1H, H-5), 2.77 (dd, $J = 14.2, 4.6$ Hz, 1H, H-3e), 2.11 (s, 3H, OAc), 2.10 – 2.06 (m, 1H, H-3a), 2.05 (s, 3H, OAc), 2.04 (s, 3H, OAc), 1.99 (s, 3H, NHAc); $^{13}\text{C NMR}$ (151 MHz, CDCl_3): δ 170.9 (C=O), 170.7 (C=O), 170.3 (C=O), 169.7 (C=O), 165.8 (C=O), 96.6 (C-2), 73.2 (C-6), 69.9 (C-8), 67.2 (C-7), 62.2 (C-9), 57.7 (C-4), 53.9 (OMe), 50.0 (C-5), 40.9 (C-3), 23.4 (NHAc), 21.0 (OAc), 20.89 (OAc), 20.87 (OAc); MS (ESI): m/z calcd for $\text{C}_{18}\text{H}_{25}\text{ClN}_4\text{O}_{10}$: 515.1 $[\text{M}+\text{Na}]^+$, found 515.1.

***p*-Tolyl (methyl 5-acetamido-7,8,9-tri-*O*-acetyl-4-azido-2,3,4,5-tetra-deoxy-2-thio-*D*-glycero-*D*-galacto-2-nonulopyranosylonate) (GC54)**



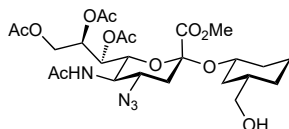
To a solution of **GC51** (3.2520 mg, 6.60 mmol) in DCM (33 mL), *p*-thiocresol (0.9014 mg, 7.26 mmol) and DIPEA (1.35 mL, 7.92 mmol) were added at 0 °C. The solution was stirred for 24 h, allowing to reach rt. The solvent was evaporated and the residue purified with flash chromatography (DCM/MeOH, 1:0 to 95:5) to afford **GC54** (2.0029 g, 66 %).

$[\alpha]_D^{20} = 12.3$ ($c = 0.4$, CHCl_3); $^1\text{H NMR}$ (600 MHz, CDCl_3): δ 7.35 (d, $J = 8.1$ Hz, 2H, Ph), 7.11 (d, $J = 7.5$ Hz, 2H, Ph), 5.26 (dd, $J = 7.0, 1.8$ Hz, 1H, H-7), 5.22 (ddd, $J = 7.1, 5.5, 2.5$ Hz, 1H, H-8), 4.38 (dd, $J = 12.6, 2.6$ Hz, 1H, H-9a), 4.23 (dd, $J = 12.5, 5.5$ Hz, 1H, H-9b), 4.07 – 4.02 (m, 1H, H-6), 3.84 – 3.79 (m, 1H, H-4), 3.78 (s, 3H, OMe), 3.36 (br s, 1H, H-5), 2.80 (dd, $J = 13.2, 4.5$ Hz, 1H, Me), 2.34 (s, 3H, OAc), 2.13 (s, 3H, OAc), 2.03 (s, 3H, OAc), 2.02 (s, 3H, OAc), 1.94 (s, 3H, NHAc), 1.75 (t, $J = 12.6$ Hz, 1H, H-3a); $^{13}\text{C NMR}$ (151 MHz, CDCl_3): δ 170.81 (C=O), 170.77 (C=O), 170.7 (C=O), 170.1 (C=O), 168.1 (C=O), 140.4 (Ph), 136.6 (Ph), 129.7 (Ph), 125.1 (Ph), 87.4 (C-2), 73.7 (C-6), 70.0 (C-8), 68.2 (C-7), 62.0 (C-9), 58.3 (C-4), 52.8 (OMe), 51.4 (C-5), 38.3 (C-3), 23.5 (NHAc), 21.4 (Me), 21.0 (OAc), 20.93 (OAc), 20.87 (OAc); MS (ESI): m/z calcd for $\text{C}_{25}\text{H}_{32}\text{N}_4\text{O}_{10}\text{S}$: 603.2 $[\text{M}+\text{Na}]^+$, found 603.0.

(1S,3R)-3-(tert-butylidiphenylsilyloxymethyl)cyclohexyl (methyl 5-acetamido-7,8,9-tri-O-acetyl-4-azido-3,4,5-trideoxy-D-glycero- α -D-galacto-2-nonulopyranosylonate) (GC92)

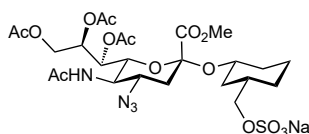
To a suspension of **GC54** (483.6 mg, 0.833 mmol), **GC06** (480.4 mg, 1.303 mmol) and MS 3Å (1.7235 g) in dry MeCN/DCM (3:1, 8 mL), *N*-iodosuccinimide (65.0 mg, 0.289 mmol) was added, followed by dropwise addition of TfOH (37 μ L, 0.289 mmol) at -40 °C under argon. The reaction mixture was stirred for 8 h and -40 °C, during which additional amounts of NIS (134.2 mg, 187.1 and 386.5 mg) were added, and then allowed to reach rt over 16 h. The suspension was neutralized with Et₃N, then filtered over a pad of celite. The solvent was evaporated, and the residue was dissolved in DCM (30 mL), washed with satd. aq. Na₂S₂O₃ (2 x 20 mL) and H₂O (20 mL), dried over Na₂SO₄, filtered and evaporated. The crude product was purified by flash column chromatography (toluene/acetone, 85:15 to 2:1) to give **GC92** (172.1 mg, 16 %).

$[\alpha]_D^{20} = -11.3$ ($c = 0.6$, DCM); ¹H NMR (500 MHz, CDCl₃): δ 7.68 – 7.62 (m, 4H, Ph), 7.44 – 7.33 (m, 6H, Ph), 5.62 (d, $J = 8.9$ Hz, 1H, NH), 5.38 (ddd, $J = 7.8, 5.1, 2.5$ Hz, 1H, H-7'), 5.31 (dd, $J = 8.5, 2.1$ Hz, 1H, H-8'), 4.30 (dd, $J = 12.5, 2.4$ Hz, 1H, H-9'a), 4.23 (dd, $J = 10.7, 2.1$ Hz, 1H, H-6'), 4.18 (dd, $J = 12.5, 5.2$ Hz, 1H, H-9'b), 3.81 – 3.68 (m, 5H, H-1, H-4', OMe), 3.54 – 3.44 (m, 2H, CH₂Oa, H-5'), 3.41 (dd, $J = 9.8, 6.3$ Hz, 1H, CH₂Ob), 2.67 (dd, $J = 13.0, 4.3$ Hz, 1H, H-3'e), 2.17 (s, 3H, OAc), 2.15 (s, 3H, OAc), 2.10 – 2.01 (m, 4H, H-6e, OAc), 1.97 (s, 3H, NHAc), 1.86 – 1.70 (m, 3H, H-2e, H-5e, H-3'a), 1.60 (dt, $J = 9.8, 4.6$ Hz, 2H, H-3, H-4e), 1.39 (qt, $J = 13.3, 3.3$ Hz, 1H, H-5a), 1.28 – 1.15 (m, 1H, H-6a), 1.09 – 0.94 (m, 10H, H-2a, *t*Bu), 0.82 (qd, $J = 13.0, 3.6$ Hz, 1H, H-4a); ¹³C NMR (126 MHz, CDCl₃): δ 170.82 (C=O), 170.79 (C=O), 170.7 (C=O), 170.0 (NHC=O), 168.7 (C-1'), 135.7 (Ph), 133.98 (*i*-Ph-a), 133.95 (*i*-Ph-b), 129.6 (Ph), 127.7 (Ph), 98.5 (C-2'), 74.6 (C-1), 71.6 (C-6'), 68.8 (CH₂O), 68.6 (C-7'), 67.9 (C-8'), 62.4 (C-9'), 57.5 (C-4'), 52.6 (OMe), 51.4 (C-5'), 39.6 (C-3), 38.7 (C-3'), 36.6 (C-2), 35.2 (C-6), 28.4 (C-4), 27.0 (*t*Bu), 23.7 (C-5), 23.6 (NHAc), 21.2 (OAc), 21.0 (OAc), 20.8 (OAc), 19.4 (q-*t*Bu); MS (ESI): m/z calcd for C₄₁H₅₆N₄O₁₁Si: 847.3 [M+Na]⁺, found 847.1.

(1S,3R)-3-(hydroxymethyl)cyclohexyl (methyl 5-acetamido-7,8,9-tri-*O*-acetyl-4-azido-3,4,5-trideoxy-*D*-glycero- α -*D*-galacto-2-nonulopyranosylonate) (GC93)

To a solution of **GC92** (504.3 mg, 0.611 mmol) in dry pyridine (17 mL) in a Teflon container, HF·py (2.3 mL) was added dropwise at 0 °C under argon. The reaction mixture was stirred for 24 h, then satd. aq. NaHCO₃ (25 mL) was added to neutralize the reaction. The aqueous phase was extracted with DCM (4 x 25 mL), and the combined organic layers were dried over Na₂SO₄, filtered and evaporated. The crude product was purified by flash column chromatography (toluene/acetone, 3:1 to 1:1) to afford **GC93** (293.0 mg, 81 %).

$[\alpha]_D^{20} = 0.0$ (c = 0.1, DCM); ¹H NMR (500 MHz, CDCl₃): δ 5.97 (d, *J* = 8.9 Hz, 1H, NH), 5.35 (ddd, *J* = 8.1, 5.5, 2.5 Hz, 1H, H-8'), 5.31 (dd, *J* = 8.2, 2.1 Hz, 1H, H-7'), 4.32 (dd, *J* = 12.4, 2.5 Hz, 1H, H-9'a), 4.18 (d, *J* = 10.4 Hz, 1H, H-6'), 4.14 (dd, *J* = 12.4, 5.5 Hz, 1H, H-9'b), 3.79 (s, 3H, OMe), 3.78 – 3.71 (m, 1H, H-1), 3.70 – 3.54 (m, 2H, H-4', H-5'), 3.46 (dd, *J* = 10.7, 6.1 Hz, 1H, CH₂Oa), 3.39 (dd, *J* = 10.7, 6.6 Hz, 1H, CH₂Ob), 2.63 (dd, *J* = 13.0, 4.2 Hz, 1H, H-3'e), 2.15 (s, 6H, 2 x OAc), 2.04 (s, 3H, OAc), 2.02 – 1.98 (m, 1H, H-6e), 1.97 (s, 3H, NHAc), 1.81 – 1.70 (m, 3H, H-2e, H-5e, H-3'a), 1.65 (d, *J* = 12.2 Hz, 1H, H-4e), 1.53 (ttq, *J* = 9.5, 6.4, 3.3 Hz, 1H, H-3), 1.38 (dddd, *J* = 16.8, 13.3, 8.4, 3.5 Hz, 1H, H-5a), 1.28 – 1.18 (m, 1H, H-6a), 0.93 (q, *J* = 12.0 Hz, 1H, H-2a), 0.80 (qd, *J* = 12.7, 3.9 Hz, 1H, H-4a); ¹³C NMR (126 MHz, CDCl₃): δ 170.9 (C=O), 170.8 (C=O), 170.6 (C=O), 170.2 (NHC=O), 168.8 (C-1'), 98.4 (C-2'), 74.0 (C-1), 71.9 (C-6'), 68.8 (C-8'), 67.9 (CH₂O), 67.8 (C-7'), 62.4 (C-9'), 57.8 (C-4'), 52.7 (OMe), 51.0 (C-5'), 39.5 (C-3), 38.4 (C-3'), 36.3 (C-2), 34.9 (C-6), 28.3 (C-4), 23.6 (C-5), 23.4 (NHAc), 21.2 (OAc), 20.9 (OAc), 20.8 (OAc); MS (ESI): *m/z* calcd for C₂₅H₃₈N₄O₁₂: 609.2 [M+Na]⁺, found 609.3.

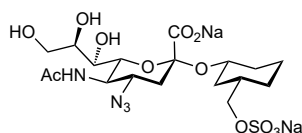
(1S,3R)-3-(sulfonatooxymethyl)cyclohexyl (methyl 5-acetamido-7,8,9-tri-*O*-acetyl-4-azido-3,4,5-trideoxy-*D*-glycero- α -*D*-galacto-2-nonulopyranosylonate) sodium salt (GC95)

To a solution of **GC92** (293.0 mg, 0.499 mmol) in dry DMF (30 mL), SO₃·py (840.4 mg, 5.28 mmol) was added at 0 °C under argon. The reaction mixture was stirred for 24 h at rt and was then quenched with powdered NaHCO₃. The suspension was stirred vigorously for 15 min, then

filtered and concentrated *in vacuo*, and the crude product was purified by flash column chromatography (DCM/MeOH, 9:1 to 8:2) to give **GC95** (293.8 g, 85 %).

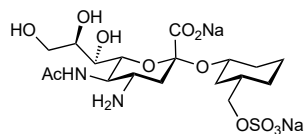
$[\alpha]_D^{20} = 0.0$ (c = 0.1, DCM); ¹H NMR (500 MHz, CD₃OD): δ 5.37 (ddd, *J* = 8.2, 5.5, 2.7 Hz, 1H, H-8), 5.32 (dd, *J* = 9.0, 2.3 Hz, 1H, H-7), 4.30 (dd, *J* = 12.4, 2.7 Hz, 1H, H-9'a), 4.07 (dd, *J* = 10.7, 2.3 Hz, 1H, H-6'), 4.03 (dd, *J* = 12.4, 5.5 Hz, 1H, H-9'b), 3.87 (t, *J* = 10.5 Hz, 1H, H-5'), 3.85 – 3.74 (m, 6H, H-1, CH₂O, OMe), 3.40 (ddd, *J* = 12.8, 10.4, 4.3 Hz, 1H, H-4'), 2.58 (dd, *J* = 13.0, 4.4 Hz, 1H, H-3'e), 2.14 (s, 3H, OAc), 2.10 (s, 3H, OAc), 2.04 – 1.97 (m, 4H, H-6e, OAc), 1.91 (s, 3H, NHAc), 1.78 – 1.71 (m, 2H, H-2e, H-5e), 1.71 – 1.64 (m, 2H, H-3, H-4e), 1.60 (t, *J* = 13.0 Hz, 1H, H-3'a), 1.45 (qt, *J* = 13.4, 3.6 Hz, 1H, H-5a), 1.25 – 1.13 (m, 1H, H-6a), 1.00 – 0.83 (m, 2H, H-2a, H-4a); ¹³C NMR (126 MHz, CD₃OD): δ 173.7 (C=O), 172.4 (C=O), 171.63 (C=O), 171.56 (C=O), 169.9 (C-1'), 99.7 (C-2'), 74.8 (C-1), 73.51 (CH₂O), 73.46 (C-6'), 69.4 (C-8'), 68.6 (C-7'), 63.5 (C-9'), 60.1 (C-4'), 53.3 (OMe), 50.8 (C-5'), 39.4 (C-3'), 37.9 (C-3), 37.3 (C-2), 36.0 (C-6), 29.4 (C-4), 24.4 (C-5), 22.8 (NHAc), 21.3 (OAc), 20.9 (OAc), 20.7 (OAc); MS (ESI): *m/z* calcd for C₂₅H₃₇N₄NaO₁₅S: 711.2 [M+Na]⁺, found 711.1.

(1S,3R)-3-(sulfonatooxymethyl)cyclohexyl (sodium 5-acetamido-4-azido-3,4,5-trideoxy-D-glycero-α-D-galacto-2-nonulopyranosylonate) sodium salt (GC96)



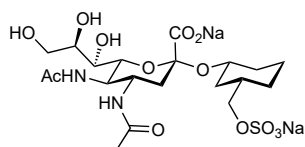
Compound **GC95** (89.1 mg, 0.129 mmol) was dissolved in 0.1 M NaOH (8 mL) and stirred for 120 h. The solution was neutralized by addition of Amberlite IR 120, filtered and concentrated *in vacuo*. The crude product was purified by flash column chromatography (DCM/(MeOH/H₂O, 10:1), 8:2 to 1:1) to yield **GC96** (59.7 mg, 80 %).

$[\alpha]_D^{20} = -81.9$ (c = 0.7, H₂O); ¹H NMR (500 MHz, D₂O): δ 3.98 – 3.83 (m, 6H, H-1, CH₂O, H-5', H-8', H-9'a), 3.80 (dd, *J* = 10.4, 2.1 Hz, 1H, H-6'), 3.71 – 3.62 (m, 2H, H-7', H-9'b), 3.58 (ddd, *J* = 12.5, 10.3, 4.6 Hz, 1H, H-4'), 2.78 (dd, *J* = 12.6, 4.5 Hz, 1H, H-3'e), 2.09 – 2.03 (m, 4H, H-6e, NHAc), 1.94 (dd, *J* = 9.5, 6.3 Hz, 1H, H-2e), 1.86 – 1.74 (m, 2H, H-3, H-5e), 1.73 – 1.62 (m, 2H, H-4e, H-3'a), 1.39 – 1.19 (m, 2H, H-5a, H-6a), 1.05 (q, *J* = 12.0 Hz, 1H, H-2a), 0.93 (qd, *J* = 12.7, 3.8 Hz, 1H, H-4a); ¹³C NMR (126 MHz, D₂O): δ 175.4 (NHC=O), 174.0 (C-1'), 101.3 (C-2'), 75.4 (C-1), 74.1 (CH₂O), 73.6 (C-8'), 72.6 (C-6'), 68.6 (C-7'), 63.1 (C-9'), 60.1 (C-4'), 50.5 (C-5'), 38.5 (C-3'), 36.8 (C-3), 36.2 (C-2), 34.8 (C-6), 28.1 (C-4), 23.8 (C-5), 22.6 (NHAc).; HR-MS (ESI): *m/z* calcd for C₁₈H₂₈N₄Na₂O₁₂S: 593.1112 [M+Na]⁺, found 593.1113; HPLC purity: 89 %.

(1S,3R)-3-(sulfonatoxymethyl)cyclohexyl (sodium 5-acetamido-4-amino-3,4,5-trideoxy-D-glycero- α -D-galacto-2-nonulopyranosylonate) sodium salt (GC106)

Compound **GC96** (119.2 mg, 0.209 mmol) and Pd(OH)₂/C (20 %, 63.3 mg) were suspended in H₂O (2.5 mL). The mixture was hydrogenated and stirred at rt for 24 h (1 atm H₂). Then, the suspension was filtered over a pad of celite, and the celite was washed with water. The solvent was removed with *vacuo*, and the residue purified with size-exclusion chromatography (P-2 gel, H₂O) to afford compound **GC106** (107.3 mg, 97 %).

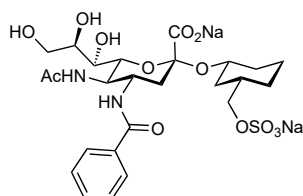
$[\alpha]_D^{20} = -1.7$ (c = 0.8, H₂O); ¹H NMR (500 MHz, D₂O): δ 3.98 – 3.87 (m, 5H, H-1, CH₂O, H-6', H-9'a), 3.85 (t, *J* = 10.2 Hz, 1H, H-5'), 3.77 (dd, *J* = 10.4, 2.0 Hz, 1H, H-8'), 3.71 – 3.63 (m, 2H, H-7', H-9'b), 2.99 (ddd, *J* = 12.4, 10.0, 4.3 Hz, 1H, H-4'), 2.73 (dd, *J* = 12.7, 4.3 Hz, 1H, H-3'e), 2.11 – 2.06 (m, 4H, H-6e, NHAc), 1.97 – 1.90 (m, 1H, H-2e), 1.86 – 1.75 (m, 2H, H-3, H-5e), 1.70 (d, *J* = 13.1 Hz, 1H, H-4e), 1.65 (t, *J* = 12.5 Hz, 1H, H-3'a), 1.40 – 1.19 (m, 2H, H-5a, H-6a), 1.06 (q, *J* = 11.9 Hz, 1H, H-2a), 0.94 (qd, *J* = 12.7, 3.8 Hz, 1H, H-4a); ¹³C NMR (126 MHz, D₂O): δ 176.0 (NHC=O), 174.5 (C-1'), 101.8 (C-2'), 75.7 (C-1), 74.4 (CH₂O), 74.3 (C-6'), 73.0 (C-8'), 69.0 (C-7'), 63.4 (C-9'), 51.6 (C-5'), 50.8 (C-4'), 40.4 (C-3'), 37.1 (C-3), 36.6 (C-2), 35.2 (C-6), 28.5 (C-4), 24.1 (C-5), 23.0 (NHAc); HR-MS (ESI): *m/z* calcd for C₁₈H₃₀N₂Na₂O₁₂S: 567.1207 [M+Na]⁺, found 567.1209; HPLC purity: 91 %.

(1S,3R)-3-(sulfonatoxymethyl)cyclohexyl (sodium 4,5-diacetamido-3,4,5-trideoxy-D-glycero- α -D-galacto-2-nonulopyranosylonate) sodium salt (GC108)

A solution of acetic acid (2.4 μ L, 0.042 mmol), HATU (21.3 mg, 0.056 mmol) and DIPEA (14 μ L, 0.080 mmol) in DMF (0.5 mL) was stirred for 10 min and then added to a solution of compound **GC106** (15.5 mg, 0.028 mmol) in DMF (0.5 mL). The reaction was stirred for 15 h at rt. Then, the solvent was evaporated and the residue purified with flash chromatography (DCM/(MeOH/H₂O, 10:1), 1:0 to 1:1) and size-exclusion chromatography (P-2 gel, H₂O) to yield **GC108** (6.2 mg, 37 %).

$[\alpha]_D^{20} = -17.6$ ($c = 1.2$, H₂O); ¹H NMR (500 MHz, D₂O): δ 3.96 – 3.80 (m, 8H, H-1, CH₂O, H-4', H-5', H-6', H-8', H-9'a), 3.69 – 3.62 (m, 2H, H-7', H-9'b), 2.62 (dd, $J = 12.7, 4.1$ Hz, 1H, H-3'e), 2.10 – 2.03 (m, 1H, H-6e), 1.98 (s, 3H, NHAc), 1.97 (s, 3H, NHAc), 1.91 (d, $J = 12.1$ Hz, 1H, H-2e), 1.84 – 1.74 (m, 2H, H-3, H-5e), 1.74 – 1.62 (m, 2H, H-4e, H-3'a), 1.38 – 1.16 (m, 2H, H-5a, H-6a), 1.04 (q, $J = 12.1$ Hz, 1H, H-2a), 0.92 (qd, $J = 12.7, 3.7$ Hz, 1H, H-4a); ¹³C NMR (126 MHz, D₂O): δ 174.6 (2 x NHC=O), 173.5 (C-1'), 100.8 (C-2'), 74.8 (C-1), 73.5 (CH₂O), 73.4 (C-6'), 72.1 (C-8'), 68.1 (C-7'), 62.4 (C-9'), 49.8 (C-5'), 48.5 (C-4'), 38.4 (C-3'), 36.2 (C-3), 35.6 (C-2), 34.2 (C-6), 27.6 (C-4), 23.2 (C-5), 21.88 (NHAc), 21.87 (NHAc); HR-MS (ESI): m/z calcd for C₂₀H₃₂N₂Na₂O₁₃S: 609.1313 [M+Na]⁺, found 609.1314; HPLC purity: 92 %.

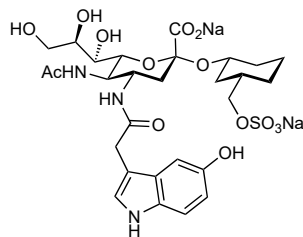
(1S,3R)-3-(sulfonatooxymethyl)cyclohexyl (sodium 5-acetamido-4-bezamido-3,4,5-trideoxy-D-glycero- α -D-galacto-2-nonulopyranosylonate) sodium salt (GC107)



A solution of benzoic acid (6.9 mg, 0.057 mmol), HATU (22.9 mg, 0.060 mmol) and DIPEA (14 μ L, 0.080 mmol) in DMF (0.5 mL) was stirred for 10 min and then added to a solution of compound **GC106** (15.0 mg, 0.028 mmol) in DMF (0.5 mL). The reaction was stirred for 14 h at rt. Then, the solvent was evaporated and the residue purified with flash chromatography (DCM/(MeOH/H₂O, 10:1), 1:0 to 1:1) and size-exclusion chromatography (P-2 gel, H₂O) to yield **GC107** (11.2 mg, 63 %).

$[\alpha]_D^{20} = -5.8$ ($c = 2.2$, H₂O); ¹H NMR (500 MHz, D₂O): δ 7.73 – 7.67 (m, 2H, *o*-Ph), 7.66 – 7.59 (m, 1H, *p*-Ph), 7.56 – 7.50 (m, 2H, *m*-Ph), 4.19 (ddd, $J = 12.7, 10.5, 4.3$ Hz, 1H, H-4'), 4.07 (t, $J = 10.5$ Hz, 1H, H-5'), 3.99 – 3.86 (m, 6H, H-1, CH₂O, H-6', H-8', H-9'a), 3.72 – 3.65 (m, 2H, H-7', H-9'b), 2.73 (dd, $J = 12.7, 4.3$ Hz, 1H, H-3'e), 2.12 – 2.05 (m, 1H, H-6e), 1.97 – 1.88 (m, 4H, H-2e, NHAc), 1.88 – 1.74 (m, 3H, H-3, H-5e, H-3'a), 1.69 (d, $J = 10.8$ Hz, 1H, H-4e), 1.38 – 1.18 (m, 2H, H-5a, H-6a), 1.05 (q, $J = 12.1$ Hz, 1H, H-2a), 0.92 (qd, $J = 12.7, 3.7$ Hz, 1H, H-4a); ¹³C NMR (126 MHz, D₂O): δ 174.4 (NHC=O), 170.8 (PhC=O), 167.6 (C-1'), 133.6 (*i*-Ph), 132.2 (*p*-Ph), 128.8 (*m*-Ph), 127.0 (*o*-Ph), 101.2 (C-2'), 74.8 (C-1), 73.5 (CH₂O), 73.4 (C-6'), 72.2 (C-8'), 68.1 (C-7'), 62.5 (C-9'), 49.8 (C-5'), 49.4 (C-4'), 38.3 (C-3'), 36.2 (C-3), 35.6 (C-2), 34.3 (C-6), 27.6 (C-4), 23.2 (C-5), 21.8 (NHAc); HR-MS (ESI): m/z calcd for C₂₅H₃₄N₂Na₂O₁₃S: 671.1469 [M+Na]⁺, found 671.1469; HPLC purity: 86 %.

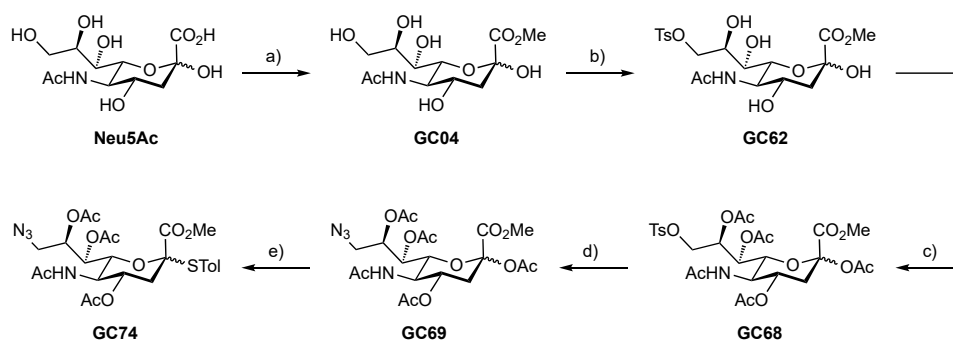
(1S,3R)-3-(sulfonatooxymethyl)cyclohexyl (sodium 5-acetamido-3,4,5-trideoxy-4-(5-hydroxyindole-3-acetamido)-D-glycero- α -D-galacto-2-nonulopyranosylonate) sodium salt (GC109)



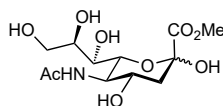
A solution of 5-hydroxyindole-3-acetic acid (8.4 mg, 0.044 mmol), HATU (22.5 mg, 0.059 mmol) and DIPEA (14 μ L, 0.080 mmol) in DMF (0.5 mL) was stirred for 10 min and then added to a solution of compound **GC106** (15.0 mg, 0.028 mmol) in DMF (0.5 mL). The reaction was stirred for 15 h at rt. Then, the solvent was evaporated and the residue purified with flash chromatography (DCM/(MeOH/H₂O, 10:1), 1:0 to 1:1) and size-exclusion chromatography (P-2 gel, H₂O) to yield **GC109** (11.0 mg, 56 %).

$[\alpha]_D^{20} = -9.1$ ($c = 2.2$, H₂O); ¹H NMR (500 MHz, D₂O): δ 7.38 (d, $J = 8.9$ Hz, 1H, H-7-In), 7.25 (s, 1H, H-2-In), 6.98 (d, $J = 2.3$ Hz, 1H, H-4-In), 6.83 (dd, $J = 8.8, 2.4$ Hz, 1H, H-6-In), 3.98 – 3.72 (m, 8H, H-1, CH₂O, H-4', H-5', H-6', H-8', H-9'a), 3.71 – 3.59 (m, 3H, H-9'b, CH₂-In), 3.56 – 3.50 (m, 1H, H-7'), 2.64 (dd, $J = 12.8, 4.4$ Hz, 1H, H-3'e), 2.06 – 1.99 (m, 1H, H-6e), 1.83 – 1.69 (m, 3H, H-2e, H-3, H-5e), 1.69 – 1.62 (m, 2H, H-4e, H-3'a), 1.52 (s, 3H, NHAc), 1.35 – 1.11 (m, 2H, H-5a, H-6a), 1.05 – 0.95 (m, 1H, H-2a), 0.95 – 0.83 (m, 1H, H-4a); ¹³C NMR (126 MHz, D₂O): δ 174.9 (C=O-In), 174.1 (NHC=O), 173.7 (C-1'), 148.9 (C-5-In), 131.5 (C-7a-In), 127.2 (C-3a-In), 125.8 (C-2-In), 112.7 (C-7-In), 111.8 (C-6-In), 107.0 (C-3-In), 102.5 (C-4-In), 100.6 (C-2'), 74.8 (C-1), 73.52 (C-6'), 73.50 (CH₂O), 72.0 (C-8'), 68.1 (C-7'), 62.4 (C-9'), 49.4 (C-5'), 48.4 (C-4'), 38.3 (C-3'), 36.1 (C-3), 35.6 (C-2), 34.2 (C-6), 32.6 (CH₂-In), 27.5 (C-4), 23.2 (C-5), 21.2 (NHAc); HR-MS (ESI): m/z calcd for C₂₈H₃₇N₃Na₂O₁₄S: 740.1684 [M+Na]⁺, found 740.1684; HPLC purity: 93 %.

Alternative synthesis of C-9 modified glycosyl donor GC74

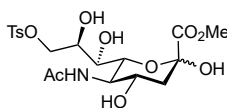


Scheme E4. a) Amberlyst-15, MeOH, rt, 120 h (98 %); b) TsCl, pyridine, 0 °C to rt, overnight; c) Ac₂O, pyridine, 0 °C to rt, 96 h (≈ 73 % from **GC04**); d) NaN₃, DMF, 60 °C, overnight; e) *p*-thiocresol, BF₃·Et₂O, DCM, 0 °C to rt, 24 h (18 % from **GC68**).

Methyl 5-acetamido-3,5-dideoxy-D-glycero-α-D-galacto-2-nonulopyranosylonate (**GC04**)

To a solution of Neu5Ac (50.02 g, 161.7 mmol) in MeOH (1000 mL), Amberlyst-15 (26.16 g) was added. The reaction was stirred at rt for 120 h. Then, the suspension was filtered over celite and concentrated *in vacuo*, affording **GC04** (50.98 g, 98 %).

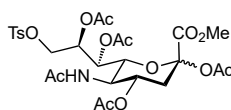
$[\alpha]_D^{20} = -22.4$ ($c = 2.0$, H₂O); ¹H NMR (500 MHz, CD₃OD): δ 4.07 – 4.02 (m, 1H, H-4), 4.00 (dd, $J = 10.5, 1.5$ Hz, 1H, H-6), 3.85 – 3.78 (m, 2H, H-5, H-9a), 3.78 (s, 3H, OMe), 3.70 (ddd, $J = 8.9, 5.6, 2.9$ Hz, 1H, H-8), 3.62 (dd, $J = 11.3, 5.8$ Hz, 1H, H-9b), 3.48 (dd, $J = 9.2, 1.5$ Hz, 1H, H-7), 2.22 (dd, $J = 13.0, 4.9$ Hz, 1H, H-3e), 2.02 (s, 3H, NHAc), 1.89 (dd, $J = 12.9, 11.4$ Hz, 1H, H-3a); ¹³C NMR (126 MHz, CD₃OD): δ 175.2 (NHC=O), 171.8 (C-1), 96.6 (C-2), 72.0 (C-6), 71.6 (C-8), 70.0 (C-7), 67.8 (C-4), 64.7 (C-9), 54.2 (C-5), 53.2 (OMe), 40.6 (C-3), 22.6 (NHAc); MS (ESI): m/z calcd for C₁₂H₂₁NO₉: 346.1 [M+Na]⁺, found 346.0.

Methyl 5-acetamido-3,5-dideoxy-9-O-tosyl-D-glycero-α-D-galacto-2-nonulopyranosylonate (**GC62**)

To a solution of **GC04** (50.98 g, 157.7 mmol) in pyridine (750 mL), tosyl chloride (31.22 g, 163.8 mmol) was added at 0 °C. The reaction was stirred at rt overnight, then directly subjected to the next step.

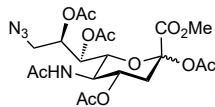
¹H NMR (500 MHz, CD₃OD): δ 7.79 (d, J = 8.4 Hz, 2H, Ph), 7.44 (d, J = 8.4 Hz, 2H, Ph), 4.28 (dd, J = 10.0, 2.2 Hz, 1H, H-9a), 4.07 – 3.98 (m, 2H, H-4, H-9b), 3.93 (dd, J = 10.5, 1.5 Hz, 1H, H-7), 3.90 – 3.82 (m, 2H, H-5, H-8), 3.77 (s, 3H, OMe), 3.43 (dd, J = 9.2, 1.5 Hz, 1H, H-6), 2.46 (s, 3H, Me), 2.20 (dd, J = 13.0, 4.9 Hz, 1H, H-3e), 2.01 (s, 3H, NHAc), 1.86 (dd, J = 13.0, 11.3 Hz, 1H, H-3a).

Acetyl (methyl 5-acetamido-4,7,8-tri-*O*-acetyl-3,5-dideoxy-9-*O*-tosyl-D-glycero- α -D-galacto-2-nonulopyranosylonate) (GC68)



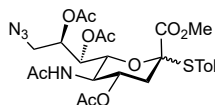
To the reaction solution of **GC62** in pyridine, Ac₂O (150 mL, 1.574 mol) was added at 0 °C. The reaction was stirred for 96 h, during which additional amounts of Ac₂O (2 x 50 mL) were added. Then, MeOH (100 mL) was added at 0 °C and the reaction stirred for 30 min, after which the solvent was evaporated. The residue was dissolved in DCM (500 mL), washed with 1 M HCl (500 mL), satd. aq. Na₂S₂O₃ (500 mL) and brine (500 mL), dried over Na₂SO₄, filtered and evaporated, affording crude **GC68** (73.89 g, 73 % over two steps from **GC04**).

$[\alpha]_D^{20}$ = -24.9 (c = 1.0, DCM); ¹H NMR (500 MHz, CDCl₃): δ 7.75 (d, J = 8.4 Hz, 2H, *o*-Ph), 7.31 (d, J = 8.5 Hz, 2H, *m*-Ph), 5.66 (d, J = 9.6 Hz, 1H, NH), 5.37 (dd, J = 4.7, 2.2 Hz, 1H, H-7), 5.22 (ddd, J = 11.4, 9.9, 4.9 Hz, 1H, H-4), 5.02 – 4.97 (m, 1H, H-8), 4.51 (dd, J = 11.2, 2.8 Hz, 1H, H-9b), 4.13 – 4.01 (m, 3H, H-5, H-6, H-9a), 3.73 (s, 3H, OMe), 2.50 (dd, J = 13.4, 5.1 Hz, 1H, H-3e), 2.41 (s, 3H, Me), 2.10 (s, 3H, OAc), 2.06 (s, 3H, OAc), 2.00 (s, 3H, OAc), 1.99 – 1.97 (m, 1H, H-3a), 1.96 (s, 3H, OAc), 1.85 (s, 3H, NHAc); ¹³C NMR (126 MHz, CDCl₃): δ 170.9 (C=O), 170.5 (C=O), 170.3 (C=O), 170.1 (C=O), 168.3 (C=O), 166.4 (C-1), 144.8 (*i*-Ph), 133.1 (*p*-Ph), 129.9 (*o*-Ph), 128.0 (*m*-Ph), 97.4 (C-2), 72.8 (C-6), 71.0 (C-8), 68.3 (C-4), 67.7 (C-7), 67.6 (C-9), 53.2 (OMe), 49.2 (C-5), 36.0 (C-3), 23.2 (NHAc), 21.7 (Me), 20.9 (OAc), 20.8 (OAc), 20.77 (OAc), 20.75 (OAc); MS (ESI): m/z calcd for C₂₇H₃₅NO₁₅S: 668.2 [M+Na]⁺, found 668.1.

Acetyl (methyl 5-acetamido-4,7,8-tri-*O*-acetyl-9-azido-3,5,9-trideoxy-*D*-glycero- α -*D*-galacto-2-nonulopyranosylonate) (GC69)

To a solution of **GC68** (14.60 g, 22.61 mmol) in DMF (220 mL), NaN₃ (2.4421 g, 37.56 mmol) was added. The reaction mixture was stirred overnight at 70 °C. Then, the suspension was filtered through celite and the filter was washed with MeOH. The solvent was removed with *vacuo*, then the residue was dissolved in H₂O (100 mL) and extracted with EtOAc (4 x 100 mL). The combined organics were dried over Na₂SO₄, filtered and evaporated, affording crude **GC69**, which was used in the next step without purification.

¹H NMR (500 MHz, CDCl₃): δ 5.72 (d, J = 9.5 Hz, 1H, NH), 5.37 (dt, J = 4.0, 2.0 Hz, 1H, H-7), 5.22 (ddd, J = 11.4, 10.2, 5.0 Hz, 1H, H-4), 4.88 (dt, J = 7.9, 2.8 Hz, 1H, H-8), 4.18 – 4.04 (m, 2H, H-5, H-6), 3.82 – 3.79 (m, 1H, H-9a), 3.78 (s, 3H, OMe), 3.36 (dd, J = 13.6, 7.9 Hz, 1H, H-9b), 2.50 (dd, J = 13.4, 5.0 Hz, 1H, H-3a), 2.13 (s, 3H, OAc), 2.12 (s, 3H, OAc), 2.06 (s, 3H, OAc), 2.01 (s, 3H, OAc), 1.86 (s, 3H, NHAc); ¹³C NMR (126 MHz, CDCl₃): δ 171.1 (C=O), 170.8 (C=O), 170.6 (C=O), 170.4 (C=O), 168.5 (C=O), 166.5 (C-1), 97.3 (C-2), 73.7 (C-8), 73.3 (C-6), 68.5 (C-4), 68.4 (C-7), 50.2 (C-9), 49.1 (C-5), 36.3 (C-3), 23.2 (NHAc), 21.0 (OAc), 20.93 (OAc), 20.87 (OAc), 20.8 (OAc); MS (ESI): m/z calcd for C₂₀H₂₈N₄O₁₂: 539.2 [M+Na]⁺, found 539.0.

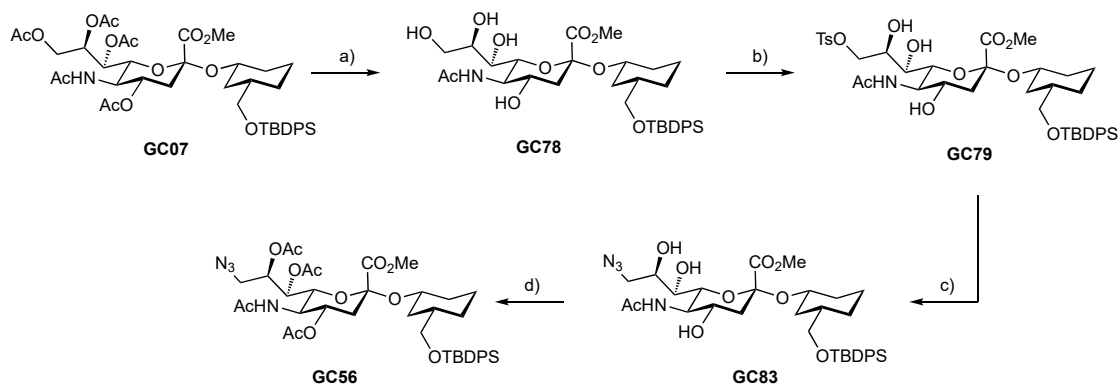
***p*-Tolyl (methyl 5-acetamido-4,7,8-tri-*O*-acetyl-9-azido-2,3,5,9-tetradeoxy-2-thio-*D*-glycero- α -*D*-galacto-2-nonulopyranosylonate) (GC74)**

To a solution of crude **GC69** in DCM (55 mL), *p*-thiocresol (5034.1 mg, 40.53 mmol) was added, followed by dropwise BF₃·Et₂O (8 mL, 64.82 mmol) at 0 °C. The solution was stirred for 24 h, allowing to reach rt. The solution was filtered over celite, and the filter washed with DCM (100 mL). Then, satd. aq. NaHCO₃ (100 mL) was added, and the mixture was stirred for 30 min. Next, the organic phase was separated and washed with satd. aq. NaHCO₃ (150 mL) and brine (150 mL), dried over Na₂SO₄, filtered and evaporated. The residue was purified with flash chromatography (PE:acetone, 1:0 to 0:1) to afford **GC74** (2.6700 g, 18 % over two steps from **GC68**).

$[\alpha]_D^{20}$ = -89.4 (c = 0.2, DCM); ¹H NMR (500 MHz, CDCl₃): δ 7.30 (d, J = 8.1 Hz, 2H, Ph), 7.19 (d, J = 7.9 Hz, 2H, Ph), 5.49 (d, J = 10.2 Hz, 1H, NH), 5.43 (m, 1H, H-7), 5.37 (m, 1H, H-4), 4.76

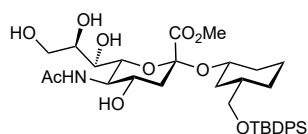
(m, 1H, H-8), 4.58 (dd, $J = 10.5, 2.4$ Hz, 1H, H-6), 4.12 (m, 1H, H-5), 3.68 (s, 3H, OMe), 3.63 (dd, $J = 13.4, 2.4$ Hz, 1H, H-9a), 3.31 (dd, $J = 13.4, 9.4$ Hz, 1H, H-9b), 2.67 (dd, $J = 13.8, 4.8$ Hz, 1H, H-3e), 2.35 (s, 3H, Me), 2.15 – 2.10 (m, 4H, H-3a, OAc), 2.09 (s, 3H, OAc), 2.04 (s, 3H, OAc), 1.90 (s, 3H, NHAc); ¹³C NMR (126 MHz, CDCl₃): δ 171.5 (C=O), 171.3 (C=O), 170.7 (C=O), 170.6 (C=O), 168.6 (C=O), 141.2 (Ph), 136.3 (Ph), 130.5 (Ph), 124.8 (Ph), 88.8 (C-2), 74.9 (C-8), 73.3 (C-6), 69.2 (C-4), 69.1 (C-7), 53.1 (OMe), 50.0 (C-9), 49.6 (C-5), 37.5 (H-3), 23.5 (NHAc), 21.6 (Me), 21.4 (OAc), 21.2 (OAc), 21.1 (OAc); MS (ESI): m/z calcd for C₂₅H₃₂N₄O₁₀S: 603.2 [M+Na]⁺ found: 603.0

Alternative synthesis of C-9 modified GC56



Scheme E5. a) MeONa, MeOH, rt, 24 h (quant.); b) TsCl, pyridine, 0 °C to rt, overnight (71 %); c) NaN₃, DMF, 70 °C, 24 h; d) Ac₂O, pyridine, 0 °C to rt, 24 h (91 % from GC79).

(1S,3R)-3-(*tert*-butyldiphenylsilyloxymethyl)cyclohexyl (methyl 5-acetamido-3,5-dideoxy-D-glycero- α -D-galacto-2-nonulopyranosylonate) (GC78)

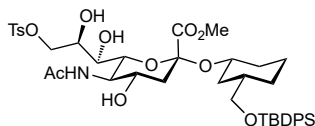


To a solution of GC07 (4547.1 mg, 5.40 mmol) in MeOH (50 mL), NaOMe (25 % w/V in MeOH, 0.5 mL, 2.18 mmol) was added, and the solution was stirred for 24 h. The solution was neutralized by addition of Amberlyst-15, filtered and concentrated with *vacuo*. The crude product was purified by flash column chromatography (DCM/MeOH, 1:0 to 9:1) to yield GC78 (3735.6 mg, quant.).

¹H NMR (500 MHz, CDCl₃): δ 7.63 – 7.54 (m, 4H, Ph), 7.41 – 7.29 (m, 6H, Ph), 3.88 – 3.79 (m, 2H, H-6', H-9'a), 3.76 – 3.67 (m, 6H, H-1, H-5', H-8', OMe), 3.53 – 3.41 (m, 3H, CH₂Oa, H-4', H-9'b), 3.41 – 3.35 (m, 1H, CH₂Ob), 3.32 (dt, $J = 10.4, 2.1$ Hz, 1H, H-7'), 2.72 (dd, $J = 13.0, 4.7$ Hz, 1H, H-3'e), 2.00 – 1.94 (m, 4H, H-6e, NHAc), 1.83 – 1.75 (m, 1H, H-3'a), 1.75 – 1.67 (m, 2H, H-2e,

H-5e), 1.62 – 1.48 (m, 2H, H-3, H-4e), 1.27 – 1.13 (m, 2H, H-5a, H-6a), 1.03 – 0.92 (m, 10H, H-2a, *t*Bu), 0.78 (qd, $J = 12.6, 4.7$ Hz, 1H, H-4a); MS (ESI): m/z calcd for C₃₅H₅₁NO₁₀Si: 696.3 [M+Na]⁺, found 696.3.

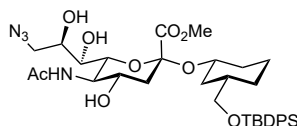
(1S,3R)-3-(*tert*-butyldiphenylsilyloxymethyl)cyclohexyl (methyl 5-acetamido-3,5-dideoxy-9-*O*-tosyl-D-glycero- α -D-galacto-2-nonulopyranosylonate) (GC79)



To a solution of **GC78** (1128.6 mg, 1.67 mmol) in pyridine (20 mL), tosyl chloride (324.2 mg, 1.70 mmol) was added at 0 °C. The reaction was stirred at rt overnight. Then, the solvents were evaporated under reduced pressure and the crude product was purified by flash column chromatography (DCM/MeOH, 1:0 to 9:1) to give **GC79** (989.9 mg, 71 %).

¹H NMR (500 MHz, CDCl₃): δ 7.79 (d, $J = 8.4$ Hz, 2H, Tol), 7.64 – 7.61 (m, 4H, Ph), 7.43 – 7.33 (m, 8H, Ph, Tol), 6.22 (d, $J = 7.9$ Hz, 1H, NH), 4.32 (dd, $J = 10.1, 2.4$ Hz, 1H, H-9'a), 4.21 (dd, $J = 10.1, 5.1$ Hz, 1H, H-9'b), 4.01 (ddd, $J = 7.6, 5.1, 2.5$ Hz, 1H, H-8'), 3.81 – 3.68 (m, 5H, H-1, H-5', OMe), 3.67 – 3.60 (m, 1H, H-4'), 3.51 (d, $J = 9.0$ Hz, 1H, H-7'), 3.48 – 3.44 (m, 1H, CH₂Oa), 3.42 – 3.36 (m, 2H, CH₂Ob, H-6'), 2.77 (dd, $J = 13.0, 4.7$ Hz, 1H, H-3'e), 2.44 (s, 3H, Me), 2.06 (s, 3H, NHAc), 1.97 – 1.91 (m, 1H, H-6e), 1.82 (dd, $J = 13.0, 11.7$ Hz, 1H, H-3'a), 1.77 – 1.69 (m, 2H, H-2e, H-5e), 1.64 – 1.49 (m, 2H, H-3, H-4e), 1.27 – 1.14 (m, 2H, H-5a, H-6a), 1.05 – 0.94 (m, 10H, H-2a, *t*Bu), 0.80 (tt, $J = 16.2, 8.1$ Hz, 1H, H-4a); MS (ESI): m/z calcd for C₄₂H₅₇NO₁₂SSi: 850.3 [M+Na]⁺, found 850.2.

(1S,3R)-3-(*tert*-butyldiphenylsilyloxymethyl)cyclohexyl (methyl 5-acetamido-9-azido-3,5,9-trideoxy-D-glycero- α -D-galacto-2-nonulopyranosylonate) (GC83)

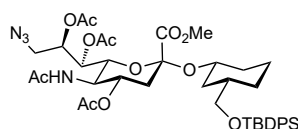


To a solution of **GC79** (989.9 mg, 1.20 mmol) in DMF (20 mL), NaN₃ (419.8 mg, 6.46 mmol) was added. The reaction mixture was stirred for 24 h at 70 °C. Then, the suspension was filtered through celite and the filter was washed with MeOH. The solvents were removed with *vacuo*, then the residue was dissolved in H₂O (200 mL) and extracted with EtOAc (4 x 200 mL). The combined

organics were dried over Na₂SO₄, filtered and evaporated, affording **GC83**, which was used in the next step without purification.

¹H NMR (500 MHz, CDCl₃): δ 7.68 – 7.58 (m, 4H, Ph), 7.45 – 7.32 (m, 6H, Ph), 4.00 (tt, *J* = 6.4, 3.3 Hz, 1H, H-8'), 3.94 – 3.78 (m, 1H, H-5'), 3.78 – 3.69 (m, 4H, H-1, OMe), 3.65 (dd, *J* = 13.2, 2.2 Hz, 1H, H-9'a), 3.61 – 3.53 (m, 1H, H-4'), 3.53 – 3.35 (m, 5H, CH₂O, H-6', H-7', H-9'b), 2.80 (dd, *J* = 12.7, 4.6 Hz, 1H, H-3'e), 2.06 (s, 3H, NHAc), 2.03 – 1.93 (m, 1H, H-6e), 1.90 – 1.69 (m, 3H, H-2e, H-5e, H-3'a), 1.65 – 1.52 (m, 2H, H-3, H-4e), 1.31 – 1.19 (m, 2H, H-5a, H-6a), 1.09 – 0.96 (m, 10H, H-2a, *t*Bu), 0.92 – 0.73 (m, 1H, H-4a); MS (ESI): *m/z* calcd for C₃₅H₅₀N₄O₉Si: 721.3 [M+Na]⁺, found 721.2.

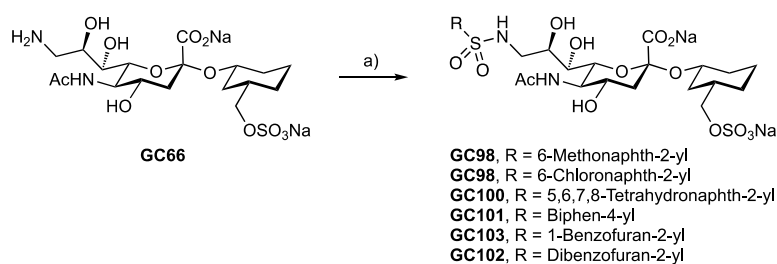
(1S,3R)-3-(tert-butylidiphenylsilyloxymethyl)cyclohexyl (methyl 5-acetamido-4,7,8-tri-O-acetyl-9-azido-3,5,9-trideoxy-D-glycero-α-D-galacto-2-nonulopyranosylonate) (GC56)



To a solution of crude **GC83** in pyridine (13 mL), Ac₂O (1.3 mL, 13.75 mmol) was added at 0 °C. The reaction was stirred for 24 h allowing to reach rt. Then, the solvent was evaporated affording **GC56** (1003.9 mg, 91 % over two steps from **GC79**).

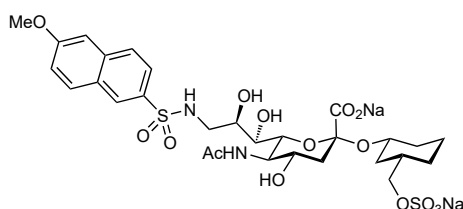
[α]_D²⁰ = -1.2 (c = 0.3, DCM); ¹H NMR (500 MHz, CDCl₃): δ 7.66 – 7.60 (m, 4H, Ph), 7.42 – 7.35 (m, 6H, Ph), 5.33 – 5.26 (m, 2H, H-6', H-8'), 5.21 (d, *J* = 10.1 Hz, 1H, NH), 4.81 (m, 1H, H-4'), 4.11 (m, 1H, H-5'), 4.01 (m, 1H, H-7'), 3.75 (s, 3H, OMe), 3.71 (m, 1H, H-1), 3.61 (dd, *J* = 13.5, 2.9 Hz, 1H, H-9'a), 3.45 – 3.39 (m, 2H, CH₂O), 3.28 (dd, *J* = 13.5, 6.4 Hz, 1H, H-9'b), 2.62 (dd, *J* = 12.7, 4.6 Hz, 1H, H-3'e), 2.18 (OAc), 2.16 (OAc), 2.02 (OAc), 2.00 (m, 1H, H-6e), 1.93 (t, *J* = 12.5 Hz, 1H, H-3'a), 1.87 (s, 3H, NHAc), 1.81 – 1.74 (m, 2H, H-2e, H-5e), 1.62 – 1.56 (m, 2H, H-3, H-4e), 1.40 (m, 1H, H-5a), 1.25 (m, 1H, H-6a), 1.04 (s, 9H, *t*Bu), 0.99 (m, 1H, H-2a), 0.82 ppm (m, 1H, H-4a); ¹³C NMR (126 MHz, CDCl₃): δ 171.5 (C=O), 170.67 (C=O), 170.66 (C=O), 170.5 (C=O), 169.1 (C-1'), 135.8 (Ph), 134.0 (Ph), 129.8 (Ph), 127.9 (Ph), 98.9 (C-2'), 74.7 (C-1), 73.1 (C-7'), 70.5 (C-6'), 69.3 (C-4'), 68.8 (CH₂O), 68.3 (C-8'), 53.0 (OMe), 51.0 (C-9'), 49.5 (C-5'), 39.7 (C-3), 38.7 (C-3'), 36.7 (C-2), 35.4 (C-6), 28.5 (C-4), 27.1 (*t*Bu), 23.5 (C-5), 23.5 (NHAc), 21.4 (OAc), 21.24 (OAc), 21.22 (OAc), 19.6 (q-*t*Bu); MS (ESI): *m/z* calcd for C₄₁H₅₆N₄O₁₂Si: 847.4 [M+Na]⁺; found: 847.2.

Synthesis of C-9 modified sulfonamide Siglec-8 ligands



Scheme E6. a) RSO_2Cl , NaHCO_3 , DMF, H_2O , rt, (29 – 62 %).

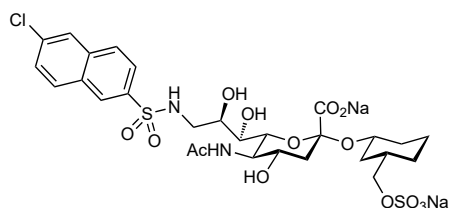
(1S,3R)-3-(Sulfonatoxymethyl)cyclohexyl (sodium 5-acetamido-3,5,9-trideoxy-9-(6-methoxynaphthalene-2-sulfonamido)-D-glycero- α -D-galacto-2-nonulopyranosylonate) sodium salt (GC98)



Compound **GC66** (12.7 mg, 0.023 mmol), NaHCO_3 (9.5 mg, 0.113 mmol) and 6-methoxynaphthalene-2-sulfonyl chloride (9.8 mg, 0.038 mmol) were dissolved in DMF/ H_2O (2:1, 1.5 mL) and the solution was stirred at rt overnight. The solution was evaporated to dryness. The residue was purified by flash chromatography on silica (DCM/(MeOH/ H_2O , 10:1), 8:2 to 1:1) and size-exclusion chromatography (P-2 gel, H_2O) to afford **GC98** (7.1 mg, 40 %).

$[\alpha]_D^{20} = +10.3$ (c = 1.0, H_2O); ^1H NMR (500 MHz, D_2O): δ 8.43 (d, $J = 2.1$ Hz, 1H, H-1-Np), 8.02 – 7.98 (d, 2H, H-4-Np, H-8-Np), 7.83 (dd, $J = 8.7, 2.0$ Hz, 1H, H-3-Np), 7.43 (d, $J = 2.6$ Hz, 1H, H-5-Np), 7.32 (dd, $J = 9.1, 2.5$ Hz, 1H, H-7-Np), 3.99 (s, 3H, OMe), 3.79 – 3.75 (m, 2H, CH_2O), 3.75 – 3.68 (m, 2H, H-5', H-8'), 3.65 – 3.56 (m, 3H, H-1, H-4', H-6'), 3.53 – 3.46 (m, 2H, H-7', H-9'a), 3.12 (dd, $J = 14.3, 8.2$ Hz, 1H, H-9'b), 2.68 (dd, $J = 12.4, 4.7$ Hz, 1H, H-3'e), 2.01 (s, 3H, NHAc), 1.74 (m, 2H, H-2e, H-6e), 1.56 (t, $J = 12.1$ Hz, 1H, H-3'a), 1.42 – 1.30 (m, 3H, H-3, H-4e, H-5e), 0.95 – 0.82 (m, 2H, H-2a, H-6a), 0.78 – 0.62 (m, 2H, H-4a, H-5a); ^{13}C NMR (126 MHz, D_2O): δ 176.0 (NHC=O), 174.5 (C-1'), 160.4 (C-6-Np), 137.5 (C-4-Np), 134.9 (C-2-Np), 132.0 (C-8-Np), 129.5 (C-4-Np), 128.7 (C-1-Np), 128.4 (C-8a-Np), 123.2 (C-3-Np), 121.1 (C-7-Np), 107.4 (C-5-Np), 102.0 (C-2'), 75.7 (C-1), 74.3 (CH_2O), 73.5 (C-6'), 71.9 (C-8'), 70.5 (C-7'), 69.2 (C-4'), 56.5 (OMe), 52.8 (C-5'), 46.4 (C-9'), 42.1 (C-3'), 36.8 (C-3), 36.4 (C-2), 35.0 (C-6), 28.4 (C-4), 23.8 (C-5), 22.9 (NHAc); HR-MS (ESI): m/z calcd for $\text{C}_{29}\text{H}_{38}\text{N}_2\text{Na}_2\text{O}_{15}\text{S}_2$: 787.1401 $[\text{M}+\text{Na}]^+$; found: 787.1402; HPLC purity: 94 %.

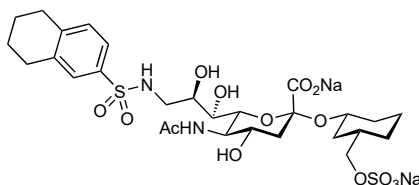
(1S,3R)-3-(Sulfonatoxymethyl)cyclohexyl (sodium 5-acetamido-9-(6-chloronaphthalene-2-sulfonamido)-3,5,9-trideoxy-D-glycero- α -D-galacto-2-nonulopyranosylate) sodium salt (GC99)



Compound **GC66** (12.5 mg, 0.023 mmol), NaHCO₃ (10.6 mg, 0.126 mmol) and 6-chloronaphthalene-2-sulfonyl chloride (12.0 mg, 0.046 mmol) were dissolved in DMF/H₂O (2:1, 1.5 mL) and the solution was stirred at rt overnight. The solution was evaporated to dryness. The residue was purified by flash chromatography on silica (DCM/(MeOH/H₂O, 10:1), 8:2 to 1:1) and size-exclusion chromatography (P-2 gel, H₂O) to afford **GC99** (10.2 mg, 58 %).

$[\alpha]_D^{20} = +2.4$ (c = 0.9, H₂O); ¹H NMR (500 MHz, D₂O): δ 8.51 (d, $J = 2.3$ Hz, 1H, H-1-Np), 8.10 – 8.01 (m, 3H, H-4-Np, H-5-Np, H-8-Np), 7.91 (dd, $J = 8.9, 2.0$ Hz, 1H, H-3-Np), 7.66 (dd, $J = 8.7, 2.1$ Hz, 1H, H-7-Np), 3.82 – 3.76 (m, 2H, CH₂O), 3.75 – 3.66 (m, 2H, H-5', H-8'), 3.65 – 3.55 (m, 3H, H-1, H-4', H-6'), 3.53 – 3.45 (m, 2H, H-7', H-9'a), 3.13 (dd, $J = 14.3, 8.2$ Hz, 1H, H-9'b), 2.68 (dd, $J = 12.4, 4.7$ Hz, 1H, H-3'e), 2.01 (s, 3H, NHac), 1.79 – 1.69 (m, 2H, H-2e, H-6e), 1.56 (t, $J = 12.1$ Hz, 1H, H-3'a), 1.43 – 1.28 (m, 3H, H-3, H-4e, H-5e), 0.97 – 0.81 (m, 2H, H-2a, H-6a), 0.77 – 0.65 (m, 2H, H-4a, H-5a); ¹³C NMR (126 MHz, D₂O): δ 176.0 (NHC=O), 174.5 (C-1'), 137.6 (C-2-Np), 136.3 (C-8a-Np), 135.5 (C-4a-Np), 132.0 (C-8-Np), 131.3 (C-6-Np), 130.0 (C-4-Np), 129.5 (C-7-Np), 128.8 (C-1-Np), 127.6 (C-5-Np), 123.6 (C-3-Np), 101.9 (C-2'), 75.6 (C-1), 74.3 (CH₂O), 73.5 (C-6'), 71.9 (C-8'), 70.4 (C-7'), 69.2 (C-4'), 52.8 (C-5'), 46.4 (C-9'), 42.1 (C-3'), 36.9 (C-3), 36.4 (C-2), 35.0 (C-6), 28.3 (C-4), 23.9 (C-5), 22.9 (NHAc); HR-MS (ESI): m/z calcd for C₂₈H₃₅ClN₂Na₂O₁₄S₂: 791.0906 [M+Na]⁺; found: 791.0907; HPLC purity: 95 %.

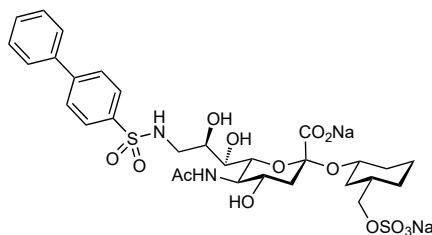
(1S,3R)-3-(Sulfonatoxymethyl)cyclohexyl (sodium 5-acetamido-3,5,9-trideoxy-9-(5,6,7,8-tetrahydronaphthalene-2-sulfonamido)-D-glycero- α -D-galacto-2-nonulopyranosylonate) sodium salt (GC100)



Compound **GC66** (12.6 mg, 0.023 mmol), NaHCO₃ (10.6 mg, 0.126 mmol) and 5,6,7,8-tetrahydronaphthalene-2-sulfonyl chloride (11.2 mg, 0.048 mmol) were dissolved in DMF/H₂O (2:1, 1.5 mL) and the solution was stirred at rt overnight. The solution was evaporated to dryness. The residue was purified by flash chromatography on silica (DCM/(MeOH/H₂O, 10:1), 8:2 to 1:1) and size-exclusion chromatography (P-2 gel, H₂O) to afford **GC100** (7.2 mg, 42 %).

$[\alpha]_D^{20} = +1.1$ (c = 0.3, H₂O); ¹H NMR (500 MHz, D₂O): δ 7.62 (d, $J = 2.1$ Hz, 1H, H-1-Np), 7.59 (dd, $J = 8.1, 2.1$ Hz, 1H, H-3-Np), 7.35 (d, $J = 8.1$ Hz, 1H, H-4-Np), 3.91 – 3.84 (m, 2H, CH₂O), 3.82 – 3.73 (m, 3H, H-1, H-5', H-8'), 3.67 – 3.59 (m, 2H, H-4', H-6'), 3.50 (dd, $J = 8.5, 2.0$ Hz, 1H, H-7'), 3.34 (dd, $J = 13.8, 2.7$ Hz, 1H, H-9'a), 3.04 (dd, $J = 14.0, 7.7$ Hz, 1H, H-9'b), 2.85 (dt, $J = 6.7, 4.0$ Hz, 4H, H-5-Np, H-8-Np), 2.75 – 2.70 (m, 1H, H-3'e), 2.03 (s, 3H, NHAc), 1.96 – 1.90 (m, 1H, H-6e), 1.87 (d, $J = 11.7$ Hz, 1H, H-2e), 1.81 (dq, $J = 6.9, 3.3$ Hz, 4H, H-6-Np, H-7-Np), 1.73 – 1.63 (m, 3H, H-3, H-4e, H-5e), 1.61 (t, $J = 12.1$ Hz, 1H, H-3'a), 1.19 – 1.07 (m, 2H, H-5a, H-6a), 0.99 (q, $J = 12.0$ Hz, 1H, H-2a), 0.93 – 0.83 (m, 1H, H-4a); ¹³C NMR (126 MHz, D₂O): δ 176.0 (NHC=O), 174.6 (C-1'), 144.9 (C-4a-Np), 140.1 (C-8a-Np), 136.4 (C-2-Np), 131.2 (C-4-Np), 128.1 (C-1-Np), 124.2 (C-3-Np), 102.0 (C-2'), 75.8 (C-1), 74.4 (CH₂O), 73.5 (C-6'), 71.7 (C-8'), 70.3 (C-7'), 69.2 (C-4'), 52.8 (C-5'), 46.1 (C-9'), 42.1 (C-3'), 37.1 (C-3), 36.5 (C-2), 35.2 (C-6), 30.0 (C-5-Np/C-8-Np), 29.8 (C-5-Np/C-8-Np), 28.6 (C-4), 24.1 (C-5), 23.2 (C-6-Np/C-7-Np), 23.1 (C-6-Np/C-7-Np), 23.0 (NHAc); HR-MS (ESI): m/z calcd for C₂₈H₄₀N₂Na₂O₁₄S₂: 761.1609 [M+Na]⁺; found: 761.1608; HPLC purity: 93 %.

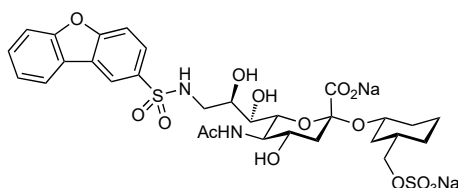
(1S,3R)-3-(Sulfonatoxymethyl)cyclohexyl (sodium 5-acetamido-9-(biphenyl-4-sulfonamido)-3,5,9-trideoxy-D-glycero- α -D-galacto-2-nonulopyranosylonate) sodium salt (GC101)



Compound **GC66** (12.8 mg, 0.024 mmol), NaHCO₃ (12.2 mg, 0.145 mmol) and 4-biphenylsulfonyl chloride (12.9 mg, 0.051 mmol) were dissolved in DMF/H₂O (2:1, 1.5 mL) and the solution was stirred at rt overnight. The solution was evaporated to dryness. The residue was purified by flash chromatography on silica (DCM/(MeOH/H₂O, 10:1), 8:2 to 1:1) and size-exclusion chromatography (P-2 gel, H₂O) to afford **GC101** (5.8 mg, 32 %).

$[\alpha]_D^{20} = +7.8$ (c = 0.3, H₂O); ¹H NMR (500 MHz, D₂O): δ 7.99 (d, $J = 8.7$ Hz, 2H, H-3-Bp, H-5-Bp), 7.93 (d, $J = 8.7$ Hz, 2H, H-2-Bp, H-6-Bp), 7.83 – 7.78 (m, 2H, H-2'-Bp, H-6'-Bp), 7.61 – 7.56 (m, 2H, H-3'-Bp, H-5'-Bp), 7.53 – 7.49 (m, 1H, H-4'-Bp), 3.77 – 3.57 (m, 7H, H-1, CH₂O, H-4', H-5', H-6', H-8'), 3.52 – 3.44 (m, 2H, H-7', H-9'a), 3.12 (dd, $J = 14.2, 8.1$ Hz, 1H, H-9'b), 2.70 (dd, $J = 12.4, 4.7$ Hz, 1H, H-3'e), 2.02 (s, 3H, NHAc), 1.83 – 1.75 (m, 2H, H-3e, H-6e), 1.62 – 1.51 (m, 3H, H-3, H-5e, H-3'a), 1.47 (d, $J = 11.7$ Hz, 1H, H-4e), 1.07 – 0.91 (m, 2H, H-5a, H-6a), 0.87 (q, $J = 12.2$ Hz, 1H, H-2a), 0.67 – 0.57 (m, 1H, H-4a); ¹³C NMR (126 MHz, D₂O): δ 176.0 (NHC=O), 174.4 (C-1'), 146.3 (C-1-Bp), 139.8 (C-1'-Bp), 138.9 (C-4-Bp), 130.2 (C-3'-Bp, C-5'-Bp), 129.8 (C-4'-Bp), 128.8 (C-3-Bp, C-5-Bp), 128.3 (C-2'-Bp, C-6'-Bp), 128.1 (C-2-Bp, C-6-Bp), 102.1 (C-2'), 75.9 (C-1), 74.3 (CH₂O), 73.5 (C-6'), 71.8 (C-8'), 70.4 (C-7'), 69.2 (C-4'), 52.7 (C-5'), 46.5 (C-9'), 42.2 (C-3'), 36.9 (C-3), 36.4 (C-2), 35.0 (C-6), 28.2 (C-4), 24.0 (C-5), 23.0 (NHAc); HR-MS (ESI): m/z calcd for C₃₀H₃₈N₂Na₂O₁₄S₂: 783.1452 [M+Na]⁺; found: 783.1452; HPLC purity: 94 %.

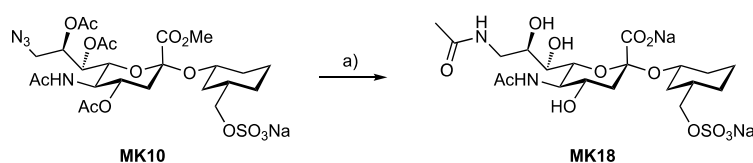
(1S,3R)-3-(Sulfonatoxymethyl)cyclohexyl (sodium 5-acetamido-9-(dibenzofuran-2-sulfonamido)-3,5,9-trideoxy-D-glycero- α -D-galacto-2-nonulopyranosylonate) sodium salt (GC102)



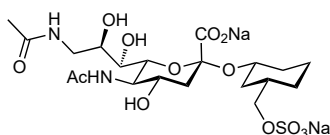
Compound **GC66** (13.8 mg, 0.025 mmol), NaHCO₃ (9.8 mg, 0.117 mmol) and dibenzofuran-2-sulfonyl chloride (14.3 mg, 0.054 mmol) were dissolved in DMF/H₂O (2:1, 1.5 mL) and the solution was stirred at rt overnight. The solution was evaporated to dryness. The residue was purified by flash chromatography on silica (DCM/(MeOH/H₂O, 10:1), 8:2 to 1:1) and size-exclusion chromatography (P-2 gel, H₂O) to afford **GC102** (12.1 mg, 62 %).

$[\alpha]_D^{20} = +2.0$ (c = 0.4, H₂O); ¹H NMR (500 MHz, D₂O): δ 8.51 (d, $J = 2.0$ Hz, 1H, H-1-Db), 8.03 (dt, $J = 7.8, 1.1$ Hz, 1H, H-9-Db), 7.97 (dd, $J = 8.7, 2.0$ Hz, 1H, H-3-Db), 7.72 (d, $J = 8.7$ Hz, 1H, H-4-Db), 7.64 (dt, $J = 8.2, 0.9$ Hz, 1H, H-6-Db), 7.59 (ddd, $J = 8.4, 7.2, 1.3$ Hz, 1H, H-7-Db), 7.45 (td, $J = 7.3, 1.1$ Hz, 1H, H-8-Db), 3.77 – 3.68 (m, 4H, CH₂O, H-5', H-6'), 3.67 – 3.56 (m, 3H, H-1, H-4', H-8'), 3.52 – 3.44 (m, 2H, H-7', H-9'a), 3.13 (dd, $J = 14.1, 8.0$ Hz, 1H, H-9'b), 2.68 (dd, $J = 12.4, 4.6$ Hz, 1H, H-3'e), 2.00 (s, 3H, NHAc), 1.79 – 1.71 (m, 2H, H-2e, H-6e), 1.55 (t, $J = 12.1$ Hz, 1H, H-3'a), 1.45 – 1.32 (m, 2H, H-3, H-5e), 1.29 (d, $J = 12.4$ Hz, 1H, H-4e), 0.98 – 0.74 (m, 3H, H-2a, H-5a, H-6a), 0.59 (qd, $J = 12.7, 3.7$ Hz, 1H, H-4a); ¹³C NMR (126 MHz, D₂O): δ 176.0 (NHC=O), 174.5 (C-1'), 158.8 (C-4a-Db), 157.5 (C-5a-Db), 134.8 (C-2-Db), 129.7 (C-7-Db), 126.8 (C-3-Db), 125.6 (C-9b-Db), 124.7 (C-8-Db), 123.6 (C-9a-Db), 122.3 (C-9-Db), 121.1 (C-1-Db), 113.4 (C-4-Db), 112.9 (C-6-Db), 102.0 (C-2'), 75.6 (C-1), 74.2 (CH₂O), 73.5 (C-6'), 71.8 (C-8'), 70.4 (C-7'), 69.2 (C-4'), 52.8 (C-5'), 46.4 (C-9'), 42.1 (C-3'), 36.7 (C-3), 36.4 (C-2), 35.0 (C-6), 28.2 (C-4), 23.9 (C-5), 22.9 (NHAc); HR-MS (ESI): m/z calcd for C₃₀H₃₆N₂Na₂O₁₅S₂: 797.1245 [M+Na]⁺; found: 797.1245; HPLC purity: 94 %.

Synthesis of aliphatic C-9 modified amide Siglec-8 ligand

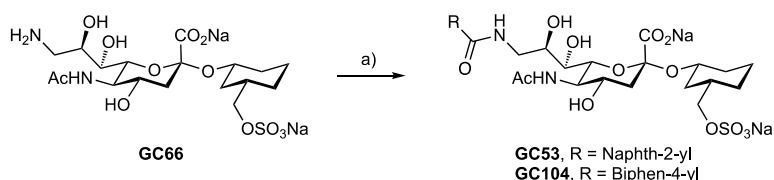


Scheme E7. a) Pd(OH)₂/C, H₂ (1 atm), H₂O, rt, 16 h; then NaOH (aq.), rt, 6 h (43 %).

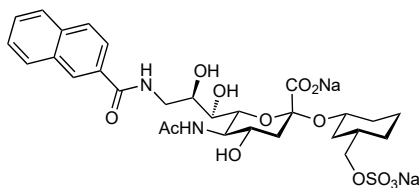
(1S,3R)-3-(Sulfonatoxymethyl)cyclohexyl (sodium 5,9-diacetamido-3,5,9-trideoxy-D-glycero- α -D-galacto-2-nonulopyranosylonate) sodium salt (MK18)

Compound **MK10** (30.0 mg, 0.044 mmol) and Pd(OH)₂/C (20 %, 13.1 mg) were suspended in H₂O (1.1 mL). The mixture was hydrogenated and stirred at rt for 16 h (1 atm H₂). Then, the suspension was filtered over a pad of celite, and the celite was washed with water. The solvent was removed with *vacuo*, and the residue purified by flash chromatography on silica (DCM/MeOH, 1:0 to 4:1). Then, the solid was dissolved in 0.1 M NaOH (3 mL) and stirred for 6 h. The solution was neutralized by addition of Amberlite IR 120, filtered and concentrated with *vacuo*. The crude product was purified by flash column chromatography (DCM/(MeOH/H₂O, 10:1), 1:0 to 1:1) and size-exclusion chromatography (P-2 gel, H₂O) to give **MK18** (11.0 mg, 43 %).

$[\alpha]_D^{20} = +75.6$ (c = 1.0, H₂O); ¹H NMR (500 MHz, D₂O): δ 3.95 – 3.85 (m, 4H, H-1, CH₂O, H-8'), 3.81 (t, *J* = 10.1 Hz, 1H, H-5'), 3.75 – 3.62 (m, 2H, H-4', H-6'), 3.59 (dd, *J* = 14.1, 3.0 Hz, 1H, H-9'a), 3.50 (dd, *J* = 8.9, 2.1 Hz, 1H, H-7'), 3.30 (dd, *J* = 14.1, 7.7 Hz, 1H, H-9'b), 2.75 (dd, *J* = 12.3, 4.6 Hz, 1H, H-3'e), 2.09 – 1.99 (m, 7H, H-6e, 2 x NHAc), 1.93 – 1.86 (m, 1H, H-2e), 1.84 – 1.72 (m, 2H, H-3, H-5e), 1.72 – 1.60 (m, 2H, H-6e, H-3'a), 1.38 – 1.13 (m, 2H, H-5a, H-6a), 1.04 (q, *J* = 11.9 Hz, 1H, H-2a), 0.92 (qd, *J* = 12.9, 4.0 Hz, 1H, H-4a); ¹³C NMR (126 MHz, D₂O): δ 176.2 (NHC=O), 175.6 (NHC=O), 175.0 (C-1'), 102.2 (C-2'), 76.0 (C-1), 74.7 (CH₂O), 73.8 (C-6'), 71.5 (C-8'), 71.0 (C-7'), 69.5 (C-4'), 53.0 (C-5'), 43.3 (C-9'), 42.3 (C-3'), 37.4 (C-3), 36.8 (C-2), 35.5 (C-6), 28.8 (C-4), 24.5 (C-5), 23.2 (NHAc), 23.0 (NHAc); HR-MS (ESI): *m/z* calcd for C₂₀H₃₂N₂Na₂O₁₃S: 609.1313 [M+Na]⁺; found: 609.1317; HPLC purity: 95 %.

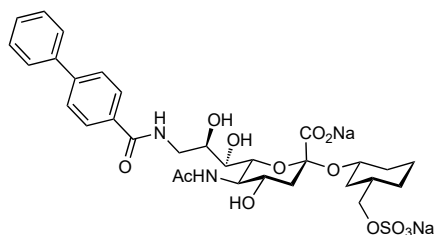
Synthesis of aromatic C-9 amide Siglec-8 ligands

Scheme E8. a) RCO₂H, HATU, DIPEA, DMF, rt, (49 – 88 %).

(1S,3R)-3-(Sulfonatoxymethyl)cyclohexyl (sodium 5-acetamido-3,5,9-trideoxy-9-(naphthalene-2-amido)-D-glycero- α -D-galacto-2-nonulopyranosylonate) sodium salt (GC53)

A solution of 2-naphthoic acid (13.7 mg, 0.080 mmol), HATU (21.3 mg, 0.056 mmol) and DIPEA (20 μ L, 0.115 mmol) in DMF (0.5 mL) was stirred for 10 min and then added to a solution of compound **GC66** (20.2 mg, 0.037 mmol) in DMF (0.5 mL). The reaction was stirred overnight at rt. Then, the solvent was evaporated and the residue purified with flash chromatography (DCM/(MeOH/H₂O, 10:1), 1:0 to 1:1) and size-exclusion chromatography (P-2 gel, H₂O) to yield **GC53** (22.8 mg, 88 %).

$[\alpha]_D^{20} = -19.0$ ($c = 0.7$, H₂O); ¹H NMR (600 MHz, D₂O): δ 8.22 (s, 1H, Np), 7.96 – 7.91 (m, 3H, Np), 7.73 (d, $J = 8.4$ Hz, 1H, Np), 7.65 – 7.57 (m, 2H, Np), 4.06 (td, $J = 8.2, 2.9$ Hz, 1H, H-8'), 3.92 – 3.86 (m, 1H, H-1), 3.86 – 3.78 (m, 4H, CH₂O, H-5', H-9'a), 3.77 – 3.72 (m, 1H, H-6'), 3.66 (ddd, $J = 11.5, 9.7, 4.6$ Hz, 1H, H-4'), 3.61 – 3.56 (m, 2H, H-7', H-9'b), 2.75 (dd, $J = 12.3, 4.6$ Hz, 1H, H-3'e), 2.04 (d, $J = 10.6$ Hz, 1H, H-6e), 1.99 (s, 3H, NHAc), 1.87 (d, $J = 12.4$ Hz, 1Hm H-2e), 1.70 – 1.61 (m, 3H, H-3, H-5e, H-3'a), 1.53 (d, $J = 12.9$ Hz, 1H, H-4e), 1.25 – 1.12 (m, 2H, H-5a, H-6a), 1.00 (q, $J = 11.9$ Hz, 1H, H-2a), 0.83 (qd, $J = 12.5, 3.8$ Hz, 1H, H-4a); ¹³C NMR (151 MHz, D₂O): δ 176.0 (C=O), 174.7 (C=O), 171.9 (C=O), 135.5 (Np), 133.1 (Np), 131.9 (Np), 129.8 (Np), 129.4 (Np), 129.1 (Np), 128.7 (Np), 128.6 (Np), 128.0 (Np), 124.4 (Np), 101.9 (Np), 75.7 (C-1), 74.4 (CH₂O), 73.6 (C-6'), 71.7 (C-8'), 70.8 (C-7'), 69.2 (C-4'), 52.8 (C-5'), 43.6 (C-9'), 42.1 (C-3'), 37.1 (C-3), 36.5 (C-2), 35.3 (C-6), 28.4 (C-4), 24.2 (C-5), 22.9 (NHAc); HR-MS (ESI): m/z calcd for C₂₉H₃₆N₂Na₂O₁₃S: 721.1626 [M+Na]⁺, found 721.1627; HPLC purity: 98 %.

(1S,3R)-3-(Sulfonatooxymethyl)cyclohexyl (sodium 5-acetamido-9-(biphenyl-4-amido)-3,5,9-trideoxy-D-glycero- α -D-galacto-2-nonulopyranosylonate) sodium salt (GC104)

A solution of biphenyl-4-carboxylic acid (9.6 mg, 0.048 mmol), HATU (13.1 mg, 0.034 mmol) and DIPEA (12 μ L, 0.069 mmol) in DMF (0.5 mL) was stirred for 10 min and then added to a solution of compound **GC66** (12.7 mg, 0.023 mmol) in DMF (0.5 mL). The reaction was stirred overnight at rt. Then, the solvent was evaporated and the residue purified with flash chromatography (DCM/(MeOH/H₂O, 10:1), 1:0 to 1:1) and size-exclusion chromatography (P-2 gel, H₂O) to yield **GC104** (8.3 mg, 49 %).

$[\alpha]_D^{20} = 3.1$ (c = 0.2, H₂O); ¹H NMR (500 MHz, D₂O): δ 7.59 (d, $J = 7.8$ Hz, 2H, H-3-Bp, H-5-Bp), 7.48 (d, $J = 8.1$ Hz, 2H, H-2-Bp, H-6-Bp), 7.43 (d, $J = 7.6$ Hz, 2H, H-2'-Bp, H-6'-Bp), 7.33 – 7.27 (m, 2H, H-3'-Bp, H-5'-Bp), 7.28 – 7.21 (m, 1H, H-4'-Bp), 3.86 (t, $J = 8.3$ Hz, 1H, H-8'), 3.72 – 3.58 (m, 5H, H-1, CH₂O, H-5', H-9'a), 3.56 (d, $J = 10.4$ Hz, 1H, H-6'), 3.46 (td, $J = 11.9, 10.8, 4.5$ Hz, 1H, H-4'), 3.42 – 3.31 (m, 2H, H-7', H-9'b), 2.55 (dd, $J = 12.3, 4.3$ Hz, 1H, H-3'e), 1.89 – 1.78 (m, 4H, H-6e, NHAc), 1.68 (d, $J = 11.6$ Hz, 1H, H-2e), 1.54 – 1.37 (m, 3H, H-3, H-5e, H-3'a), 1.34 (d, $J = 13.4$ Hz, 1H, H-4e), 1.07 – 0.90 (m, 2H, H-5a, H-6a), 0.81 (q, $J = 11.7$ Hz, 1H, H-2a), 0.64 (q, $J = 11.9$ Hz, 1H, H-4a); ¹³C NMR (126 MHz, D₂O): δ 176.0 (NHC=O), 174.8 (C-1'), 171.7 (BpC=O), 145.1 (C-1-Bp), 140.4 (C-1'-Bp), 133.3 (C-4-Bp), 130.2 (C-3'-Bp, C-5'-Bp), 129.4 (C-4'-Bp), 128.8 (C-3-Bp, C-5-Bp), 128.1 (C-2-Bp, C-6-Bp, C-2'-Bp, C-6'-Bp), 101.9 (C-2'), 75.8 (C-1), 74.4 (CH₂O), 73.7 (C-6'), 71.7 (C-8'), 70.9 (C-7'), 69.3 (C-4'), 52.8 (C-5'), 43.6 (C-9'), 42.1 (C-3'), 37.1 (C-3), 36.6 (C-2), 35.3 (C-6), 28.5 (C-4), 24.3 (C-5), 23.0 (NHAc); HR-MS (ESI): m/z calcd for C₃₁H₃₈N₂Na₂O₁₃S: 747.1782 [M+Na]⁺, found 747.1782; HPLC purity: 94 %.

Protein expression and purification

Protein expression was performed in *Escherichia coli* strain Rosetta-gami B (DE3), which were transfected as previously described.¹⁷ Cells were initially cultivated overnight in 15 mL Terrific Broth medium substituted with 0.1 mg/mL ampicillin at 37 °C and then transferred into 1 L Terrific Broth medium substituted with 0.1 mg/mL ampicillin. Cells were incubated for 5 h at 37 °C and 160 rpm, then Siglec-8 expression was induced by addition of 1.0 mM IPTG. After 16 h, cells were harvested

by centrifugation (5000 rpm, 30 min, 4 °C), resuspended in 20 mL lysis buffer (50 mM Tris·HCl, 10 mM MgCl₂, 0.1 % Triton X100, pH 7.5), and lysed by addition of 1.0 mg/mL lysozyme, incubating on ice for 4 h. The cell lysate was centrifuged (11000 rpm, 15 min, 4 °C), the supernatant discarded, and the precipitated material was washed three times with 25 mL washing buffer (50 mM Tris·HCl, 4 M urea, 500 mM NaCl, pH 8.0). The purified inclusion bodies were dissolved in 20 mL of denaturation buffer (6 M guanidine hydrochloride, 100 mM Tris·HCl, 1 mM DTT, pH 8.0) for 1 h at 37 °C. After ultracentrifugation (22000 rpm, 30 min, 4 °C), the denatured protein was refolded by slow dilution into 100 mL refolding buffer (100 mM Tris·HCl, 1 M L-arginine, 150 mM NaCl, 120 mM sucrose, pH 8.0). The mixture was stirred for 2 d at 4 °C and dialyzed against binding buffer (50 mM NaH₂PO₄, 20 mM Imidazole, 300 mM NaCl, pH 8.0). Precipitated protein was removed by ultracentrifugation (22000 rpm, 30 min, 4 °C) and the refolded soluble protein was purified by affinity chromatography on a Ni-NTA column (50 mM NaH₂PO₄, 250 mM Imidazole, 300 mM NaCl, pH 8.0). The fractions containing 6His-Siglec-8-CRD were pooled and dialyzed against assay buffer (100 mM HEPES, 150 mM NaCl, pH 7.4). The purity of the protein was verified by non-reducing SDS-PAGE.

Differential scanning fluorimetry

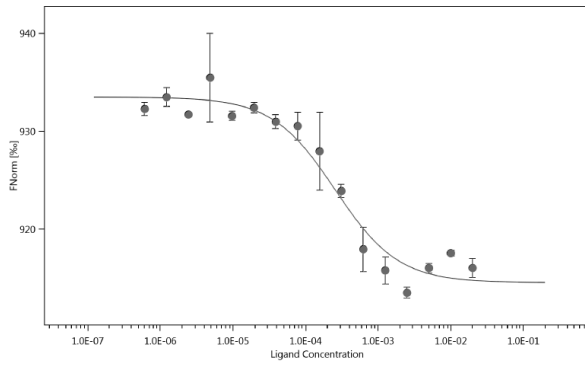
Differential scanning fluorimetry assays were performed using a Prometheus NT.48 (Nanotemper, Munich, Germany) instrument set to 50 % excitation power and 1.0 °C/min temperature slope. The Nanotemper Pr.ThermControl software suite was employed for analysis of experimental data. In a typical experiment, a 20 µM solution of Siglec-8-CRD was incubated alone or with 1 mM solution of ligand and measured over a temperature range from 20 to 80 °C.

Microscale thermophoresis

Microscale thermophoresis experiments were performed using a Monolith NT.115 (Nanotemper, Munich, Germany) instrument set to 25 °C, 50 – 70 % excitation power, and 40 % MST power. The Nanotemper MO. Affinity Analysis software suite was employed for analysis and nonlinear fitting of experimental data. In a typical experiment, a serial ligand dilution starting at 10 – 50 mM was incubated with an equal volume of 200 nM FITC labelled Siglec-8 and measured directly using the green channel of the instrument.

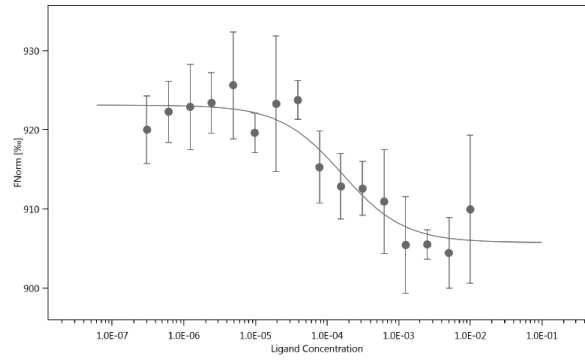
2nd Generation of Siglec-8 ligands

Compound GC10



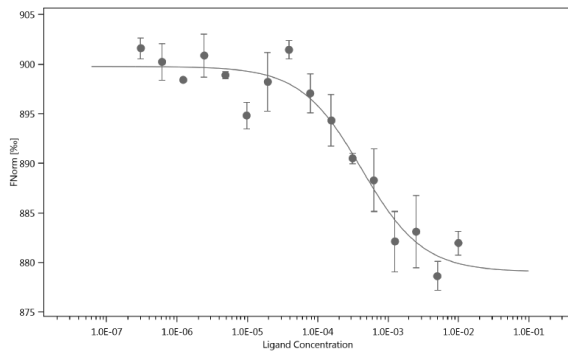
Name:	GC-10 Exp. 1 (#01)
Graph Color:	●
Target Name:	Siglec-8
Target Concentration:	80 nM
Ligand Name:	MyLigand
Ligand Concentration:	2E+07 nM to 610 nM
n:	2
Comments:	
Excitation Power:	50%
MST Power:	40%
Temperature:	25.0°C
Kd:	0.00025629
Kd Confidence:	± 7.2818E-05
Response Amplitude:	18.958575
TargetConc:	8E-08[Fixed]
Unbound:	933.46
Bound:	914.5
Std. Error of Regression:	1.7765495
Reduced χ^2 :	16.57733
Signal to Noise:	11.463107

Compound GC96



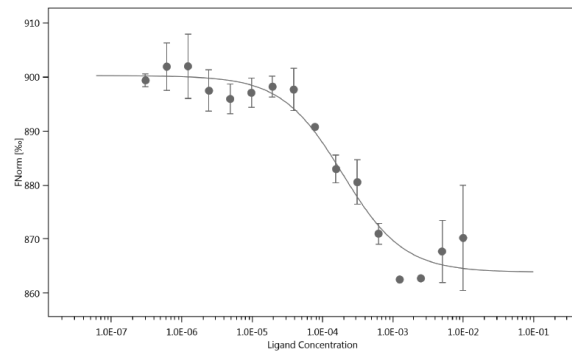
Name:	GC96 a (#20)
Graph Color:	●
Target Name:	Siglec-8
Target Concentration:	100 nM
Ligand Name:	GC96
Ligand Concentration:	1E+07 nM to 305 nM
n:	4
Comments:	
Excitation Power:	60%
MST Power:	40%
Temperature:	25.0°C
Kd:	0.00016183
Kd Confidence:	± 7.206E-05
Response Amplitude:	17.380093
TargetConc:	1E-07[Fixed]
Unbound:	923.11
Bound:	905.73
Std. Error of Regression:	2.5255213
Reduced χ^2 :	0.46697713
Signal to Noise:	7.3922222

Compound GC106



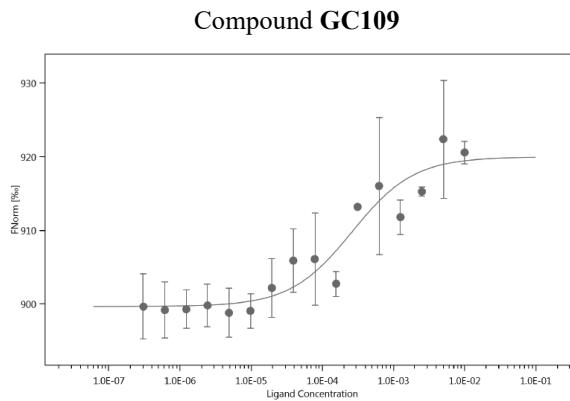
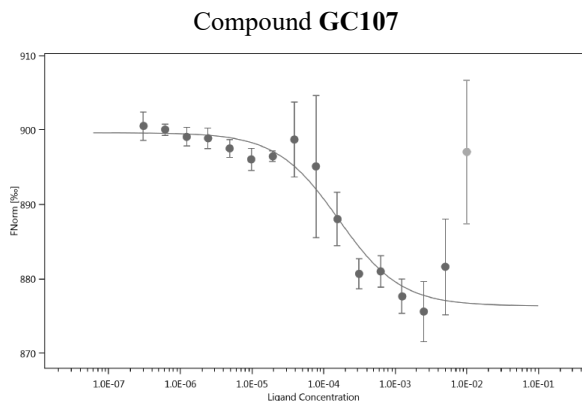
Name:	GC106 a (#24)
Graph Color:	●
Target Name:	Siglec-8
Target Concentration:	100 nM
Ligand Name:	GC106
Ligand Concentration:	1E+07 nM to 305 nM
n:	3
Comments:	
Excitation Power:	60%
MST Power:	40%
Temperature:	25.0°C
Kd:	0.00042096
Kd Confidence:	± 0.00013882
Response Amplitude:	20.704423
TargetConc:	1E-07[Fixed]
Unbound:	899.75
Bound:	879.05
Std. Error of Regression:	2.0593724
Reduced χ^2 :	7.5251627
Signal to Noise:	10.799464

Compound GC108



Name:	GC108 a (#30)
Graph Color:	●
Target Name:	Siglec-8
Target Concentration:	100 nM
Ligand Name:	GC108
Ligand Concentration:	1E+07 nM to 305 nM
n:	3
Comments:	
Excitation Power:	60%
MST Power:	40%
Temperature:	25.0°C
Kd:	0.00019314
Kd Confidence:	± 5.4694E-05
Response Amplitude:	36.317436
TargetConc:	1E-07[Fixed]
Unbound:	900.2
Bound:	863.89
Std. Error of Regression:	3.323045
Reduced χ^2 :	
Signal to Noise:	11.739589

2nd Generation of Siglec-8 ligands



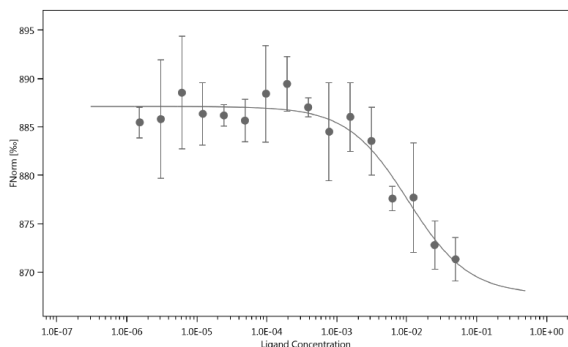
Name:	GC107 a (#27)
Graph Color:	●
Target Name:	Siglec-8
Target Concentration:	100 nM
Ligand Name:	GC107
Ligand Concentration:	5E+06 nM to 305 nM
n:	3
Comments:	
Excitation Power:	60%
MST Power:	40%
Temperature:	25.0°C
Kd:	0.00016141
Kd Confidence:	± 5.5614E-05
Response Amplitude:	23.29543
TargetConc:	1E-07[Fixed]
Unbound:	899.65
Bound:	876.35
Std. Error of Regression:	2.4463658
Reduced χ^2 :	0.89105993
Signal to Noise:	10.285436

Name:	GC109 a (#30)
Graph Color:	●
Target Name:	Siglec-8
Target Concentration:	100 nM
Ligand Name:	GC109
Ligand Concentration:	1E+07 nM to 305 nM
n:	3
Comments:	
Excitation Power:	60%
MST Power:	40%
Temperature:	25.0°C
Kd:	0.00026191
Kd Confidence:	± 0.00010982
Response Amplitude:	20.306511
TargetConc:	1E-07[Fixed]
Unbound:	899.65
Bound:	919.96
Std. Error of Regression:	2.6924092
Reduced χ^2 :	
Signal to Noise:	8.1015513

Figure E1. MST results for C-4 derivatives. Results and errors are given from the global fitting of two or more independent experiments.

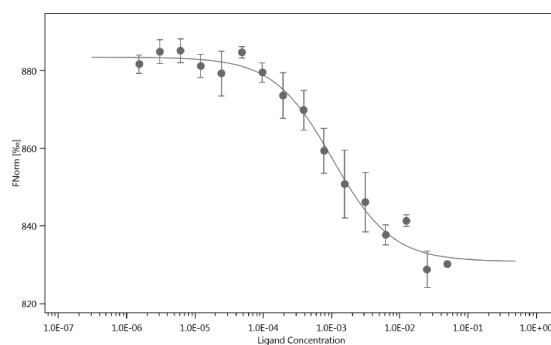
2nd Generation of Siglec-8 ligands

Compound GC65



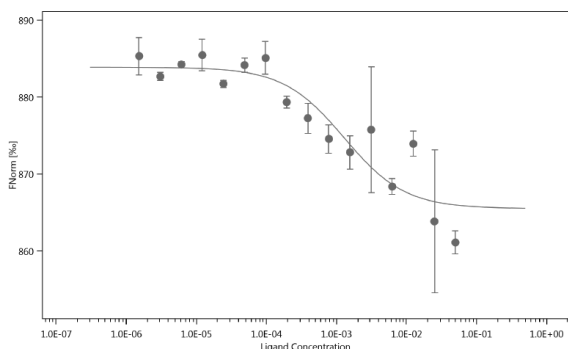
Name:	MK17_60%_b (#02)
Graph Color:	●
Target Name:	Siglec-8
Target Concentration:	100 nM
Ligand Name:	MK17
Ligand Concentration:	5E+07 nM to 1.53E+03 nM
n:	3
Comments:	
Excitation Power:	60%
MST Power:	40%
Temperature:	25.0°C
Kd:	0.010443
Kd Confidence:	± 0.0039644
Response Amplitude:	19.439964
TargetConc:	1E-07[Fixed]
Unbound:	887.13
Bound:	867.69
Std. Error of Regression:	1.5415101
Reduced χ^2 :	0.56564599
Signal to Noise:	13.546373

Compound GC66



Name:	MK19_70%_a (#02)
Graph Color:	●
Target Name:	Siglec8
Target Concentration:	100 nM
Ligand Name:	MK19
Ligand Concentration:	5E+07 nM to 1.53E+03 nM
n:	3
Comments:	
Excitation Power:	70%
MST Power:	40%
Temperature:	25.0°C
Kd:	0.0010412
Kd Confidence:	± 0.00017703
Response Amplitude:	52.638259
TargetConc:	1E-07[Fixed]
Unbound:	883.49
Bound:	830.85
Std. Error of Regression:	2.8782771
Reduced χ^2 :	2.6090338
Signal to Noise:	19.644585

Compound MK18



Name:	MK18_a (#01)
Graph Color:	●
Target Name:	Siglec-8
Target Concentration:	100 nM
Ligand Name:	MK18
Ligand Concentration:	5E+07 nM to 1.53E+03 nM
n:	3
Comments:	
Excitation Power:	50%
MST Power:	40%
Temperature:	25.0°C
Kd:	0.0012898
Kd Confidence:	± 0.00070884
Response Amplitude:	18.387202
TargetConc:	1E-07[Fixed]
Unbound:	883.9
Bound:	865.51
Std. Error of Regression:	3.1994423
Reduced χ^2 :	4.9774686
Signal to Noise:	6.1732707

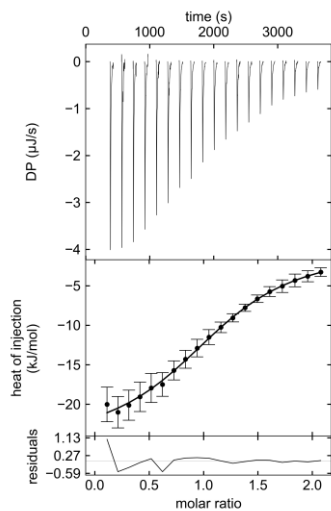
Figure E2. MST results for C-9 derivatives. Results and errors are given from the global fitting of two or more independent experiments.

Isothermal Titration Calorimetry

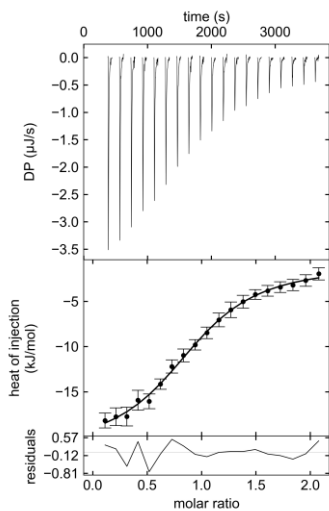
Isothermal titration calorimetry experiments were performed at 25 °C on an ITC200 (MicroCal, Northampton, USA) instrument set to 6 $\mu\text{cal}\cdot\text{s}^{-1}$ reference power, 750 rpm stirring speed, feedback mode high, 2 s filter period). Protein solutions were dialyzed against ITC buffer (100 mM HEPES, 150 mM NaCl, pH 7.4) prior to the experiments and all samples were prepared using the dialysate buffer to minimize dilution effects. Protein concentrations were determined spectrophotometrically with the specific absorbance at 280 nm employing an extinction coefficient of $33240\text{ mol}^{-1}\cdot\text{cm}^{-1}$. In a typical experiment, a 1 – 50 mM ligand solution was titrated to a solution containing 35 – 100 μM Siglec-8 to ensure more than 80 % saturation. For low c experiment, the stoichiometry parameter was constrained to 1. Baseline correction, peak integration, and non-linear regression analysis of experimental data were performed using the NITPIC (version 1.2.2.)²⁵ and SEDPHAT (version 12.1b)²⁶ software packages. Replicates were analysed using global fitting, and the 68 % confidence intervals were calculated as an estimate of experimental error.

Table E1. ITC results for C-9 derivatives. Error estimates resemble the 68 % confidence interval from global fitting of two independent experiments. ^[a] Result corresponding to a single experiment.

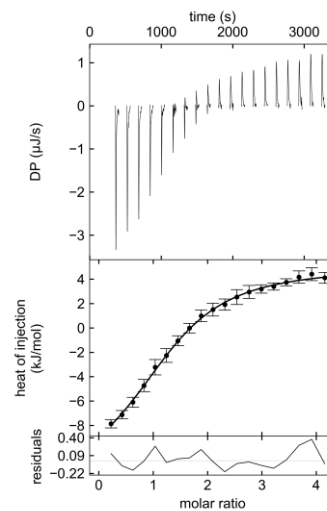
Compound	K_D [μM]	ΔG° [$\text{kJ}\cdot\text{mol}^{-1}$]	ΔH° [$\text{kJ}\cdot\text{mol}^{-1}$]	$-\Delta S^\circ$ [$\text{kJ}\cdot\text{mol}^{-1}$]	N
GC98	14.4 (13.5 – 15.5)	-27.6 (-27.8 – -27.5)	-24.1 (-25.3 – -23.5)	-3.5 (-4.3 – -2.2)	1.0 (1.0 – 1.0)
GC99	15.1 (13.0 – 17.5)	-27.5 (-27.9 – -27.2)	-20.2 (-21.7 – -18.9)	-7.3 (-9.0 – -5.4)	1.1 (1.1 – 1.2)
GC100	50.9 (38.6 – 79.3)	-24.5 (-25.2 – -23.4)	-20.0 (-25.8 – -17.3)	-4.5 (-7.9 – 2.4)	1.0 (1.0 – 1.2)
GC101	24.4 (20.1 – 29.3)	-26.3 (-26.8 – -25.9)	-21.1 (-24.9 – -18.2)	-5.3 (-8.6 – -1.0)	1.1 (1.0 – 1.3)
GC103	36.8 (28.0 – 48.9)	-25.3 (-26.0 – -24.6)	-18.7 (-25.9 – -15.4)	-6.7 (-10.6 – 1.3)	1.1 (1.0 – 1.4)
GC102	64.2 (46.0 – 83.8)	-23.9 (-24.8 – -23.3)	-11.8 (-13.7 – -10.3)	-12.1 (-14.4 – -9.6)	1.0 (1.0 – 1.1)
GC66^[a]	840 (772 – 914)	-17.6 (-17.8 – -17.3)	-21.9 (-22.8 – -21.0)	4.3 (3.2 – 5.5)	1 (fixed)



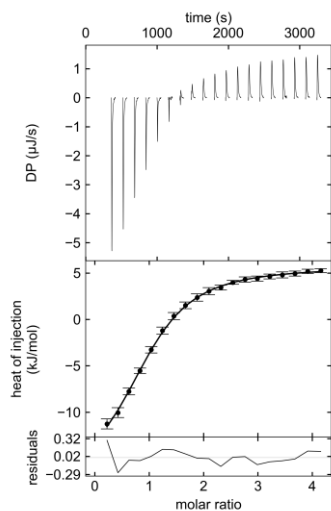
Compound GC98



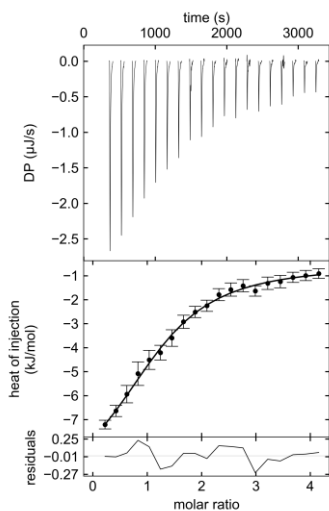
Compound GC99



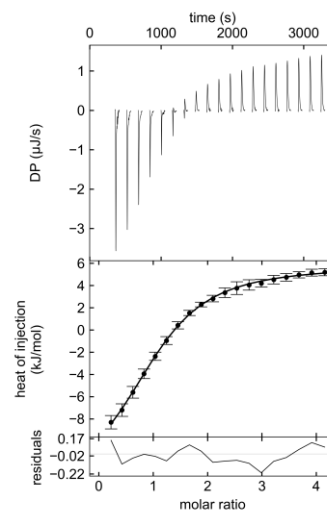
Compound GC100



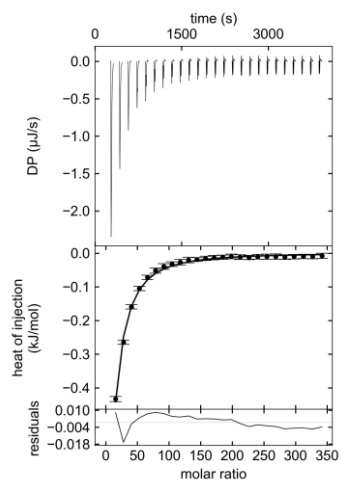
Compound GC101



Compound GC103



Compound GC102



Compound GC66

Figure E2. Exemplifying ITC analyses. Thermograms and binding isotherms for analysed C-9 analogues.

References

- 1 P. R. Crocker, J. C. Paulson, A. Varki, Siglecs and their roles in the immune system, *Nat. Rev. Immunol.* **2007**, *7*, 255–266.
- 2 S. Pillai, I. A. Netravali, A. Cariappa, H. Mattoo, Siglecs and Immune Regulation, *Annu. Rev. Immunol.* **2012**, *30*, 357–392.
- 3 M. S. Macauley, P. R. Crocker, J. C. Paulson, Siglec-mediated regulation of immune cell function in disease, *Nat. Rev. Immunol.* **2014**, *14*, 653–666.
- 4 T. Angata, C. M. Nycholat, M. S. Macauley, Therapeutic Targeting of Siglecs using Antibody- and Glycan-Based Approaches, *Trends Pharmacol. Sci.* **2015**, *36*, 645–660.
- 5 B. S. Bochner, N. Zimmermann, Role of siglecs and related glycan-binding proteins in immune responses and immunoregulation, *J. Allergy Clin. Immunol.* **2015**, *135*, 598–608.
- 6 S. Duan, J. C. Paulson, Siglecs as Immune Cell Checkpoints in Disease, *Annu. Rev. Immunol.* **2020**, *38*, 365–395.
- 7 H. Floyd, J. Ni, A. L. Cornish, Z. Zeng, D. Liu, K. C. Carter, J. Steel, P. R. Crocker, Siglec-8. A novel eosinophil-specific member of the immunoglobulin superfamily, *J. Biol. Chem.* **2000**, *275*, 861–866.
- 8 G. Foussias, G. M. Yoused, E. P. Diamandis, Molecular Characterization of a Siglec8 Variant Containing Cytoplasmic Tyrosine-Based Motifs, and Mapping of the Siglec8 Gene, *Biochem. Biophys. Res. Commun.* **2000**, *260*, 775–781.
- 9 H. Aizawa, J. Plitt, B. S. Bochner, Human eosinophils express two Siglec-8 splice variants, *J. Allergy Clin. Immunol.* **2002**, *109*, 176.
- 10 J. A. O’Sullivan, A. T. Chang, B. A. Youngblood, B. S. Bochner, Eosinophil and mast cell Siglecs: From biology to drug target, *J. Leukoc. Biol.* **2020**, 1–9.
- 11 E. Nutku, H. Aizawa, S. A. Hudson, B. S. Bochner, Ligation of Siglec-8: a selective mechanism for induction of human eosinophil apoptosis, *Blood* **2003**, *101*, 5014–5020.
- 12 E. Nutku, S. A. Hudson, B. S. Bochner, Mechanism of Siglec-8-induced human eosinophil apoptosis: Role of caspases and mitochondrial injury, *Biochem. Biophys. Res. Commun.* **2005**, *336*, 918–924.
- 13 S. A. Hudson, N. V. Bovin, R. L. Schnaar, P. R. Crocker, B. S. Bochner, Eosinophil-selective binding and proapoptotic effect in vitro of a synthetic siglec-8 ligand, polymeric 6’-

- sulfated sialyl lewis X, *J. Pharmacol. Exp. Ther.* **2009**, *330*, 608–612.
- 14 D. J. Carroll, J. A. O’Sullivan, D. B. Nix, Y. Cao, M. Tiemeyer, B. S. Bochner, Sialic acid-binding immunoglobulin-like lectin 8 (Siglec-8) is an activating receptor mediating β 2-integrin-dependent function in human eosinophils, *J. Allergy Clin. Immunol.* **2018**, *141*, 2196–2207.
- 15 P. J. Barnes, Immunology of asthma and chronic obstructive pulmonary disease, *Nat. Rev. Immunol.* **2008**, *8*, 183–192.
- 16 Y. Feng, H. Mao, Specific regulator of eosinophil apoptosis: Siglec-8 - new hope for bronchial asthma treatment, *Chin. Med. J. (Engl.)* **2012**, *125*, 2048–2052.
- 17 B. S. Kroezen, G. Conti, B. Girardi, J. Cramer, X. Jiang, S. Rabbani, J. Müller, M. Kokot, E. Luisoni, D. Ricklin, O. Schwardt, B. Ernst, A Potent Mimetic of the Siglec-8 Ligand 6'-Sulfo-Sialyl Lewis^x, *ChemMedChem* **2020**, *15*, 1706–1719.
- 18 C. Büll, T. Heise, G. J. Adema, T. J. Boltje, Sialic Acid Mimetics to Target the Sialic Acid-Siglec Axis, *Trends Biochem. Sci.* **2016**, 519–531.
- 19 J. M. Pröpster, F. Yang, S. Rabbani, B. Ernst, F. H. T. Allain, M. Schubert, Structural basis for sulfation-dependent self-glycan recognition by the human immune-inhibitory receptor Siglec-8, *Proc. Natl. Acad. Sci. U. S. A.* **2016**, *113*, E4170–E4179.
- 20 Schrödinger Release 2016–4: Maestro Schrödinger LLC. New York, NY(USA), **2016**.
- 21 The PyMOL Molecular Graphics System, Version 1.8 Schrödinger, LLC, **n.d.**
- 22 H. Ogura, K. Furuhata, M. Itoh, Y. Shitori, Syntheses of 2-O-glycosyl derivatives of N-acetyl-d-neuraminic acid, *Carbohydr. Res.* **1986**, *158*, 37–51.
- 23 C. M. Nycholat, S. Duan, E. Knuplez, C. Worth, M. Elich, A. Yao, J. O’Sullivan, R. McBride, Y. Wei, S. M. Fernandes, Z. Zhu, R. L. Schnaar, B. S. Bochner, J. C. Paulson, A Sulfonamide Sialoside Analogue for Targeting Siglec-8 and-F on Immune Cells, *J. Am. Chem. Soc.* **2019**, *141*, 14032–14037.
- 24 G.-J. Boons, A. V. Demchenko, Recent Advances in O-Sialylation, *Chem. Rev.* **2000**, *100*, 4539–4566.
- 25 T. H. Scheuermann, C. A. Brautigam, High-precision, automated integration of multiple isothermal titration calorimetric thermograms: New features of NITPIC, *Methods* **2015**, *76*, 87–98.

- 26 H. Zhao, G. Piszczek, P. Schuck, SEDPHAT – A platform for global ITC analysis and global multi-method analysis of molecular interactions, *Methods* **2015**, *76*, 137–148.

Summary and outlook

Siglec-8 is an inhibitory immunoreceptor expressed on eosinophils and mast cells, which can effectively promote apoptosis of the former and inhibition of degranulation for the latter, upon binding with antibodies or synthetic glycopolymer. Therefore, it represents a promising pharmacological target for dealing with eosinophil- and mast cell-associated disorders.

This thesis describes a medicinal chemistry approach for the development of small molecules to target Siglec-8. Starting from the preferred tetrasaccharide 6'-sulfo-sLe^x, a glycomimetic structure was synthesized, while the introduction of a sulfonamide moiety at its C-9 position provided additional binding benefits. Further exploration of the different functionalities of Neu5Ac showed that amides in the C-4 position enhance affinity. Additionally, substituted aromatic sulphonamides at C-9 will allow in the future to generate new compounds libraries. It would be interesting to combine the best modifications at C-4 and C-9, as well as changes at the C-5 which are under investigation in our group, to see if additive effects will lead to further affinity improvements. However, structural information from co-crystallizing the best ligands with Siglec-8 could guide the proper selection of promising extensions leading to new, high-affinity compounds.

Additionally, the effects of multivalent presentation of Siglec-8 ligands were studied. The thermodynamic fingerprints of their binding were analysed and dissected in the various components, providing insight into the enthalpy-entropy compensation observed with multivalent ligands. Further studies on these compounds, as well as additional structures with the same valency but much different central scaffolds, could lead to a better understanding of how the multivalent scaffold influence binding affinities. Finally, one glycomimetic was also attached to a polymer, providing a compound able to bind Siglec-8 with nanomolar affinity and to trigger an intracellular response in a surrogate cellular model. Additional studies with natively expressing cells could provide more accurate information on the biological effects of Siglec-8 binding with polymer structures or with small molecules.

To conclude, this thesis provides the first evidence that our glycomimetic structures can effectively bind Siglec-8 on cells and trigger a biological response, confirming the potential use of such molecules as future pharmacological treatments for eosinophil- and mast cell-related diseases.

Acknowledgements

It has been a long journey since I started this PhD in March 2018, with a lot of ups and downs, but that allowed me to meet fantastic people along the way, for which I am really grateful. First and foremost, I want to thank **Prof. Beat Ernst** for the incredible support you gave me during these years. Your endless scientific curiosity was inspiring, and all the discussions we had made me a better scientist. You always showed big enthusiasm for this project and confidence in me, which were really helpful to stop me from doubting myself. I definitely could not have expected a better supervisor, vielen Danke für Alles!

I also need to thank **Prof. Daniel Ricklin**, for welcoming me to the Molecular Pharmacy group and being my co-supervisor. I really enjoyed my time here, and I am sure you played a big factor for the nice atmosphere within the group.

I would also like to thank **Prof. Roland Pieters**, for having me in your lab in Utrecht, for all the suggestions and inputs you gave me, especially on multivalency. It was a great opportunity for me to get experience in a new lab, with new colleagues and in a new country. A little bit too much rain for my taste, though.

A special thanks goes to **Dr. Martin Smiesko**, for agreeing to be my second supervisor, but mostly for all the ideas and advices that you always provided me. You are definitely one of the best computational scientists I came across.

Thanks to **Prof. Karl-Heinz Altmann** and **Prof. Geert-Jan Boons**, for accepting to be the co-referees of my thesis.

Furthermore, I want to thank **Dr. Said Rabbani**, for patiently teaching me how to perform protein expression, something that I had never done before, and **Dr. Oliver Schwardt**, for your availability whenever I needed some chemistry suggestions.

Special thanks also go to **Maja** and **Aline**, the two students who were brave enough to have me as supervisor during their internships. I hope I was as helpful for you as you were for me and my project.

I am really pleased I have been part of the fantastic family of **PhD4GlycoDrug**. Thank you to **Prof. Marko Anderluh** and all supervisors, for making this network possible and for all that you have done for us. All the meetings we had were just fabulous, in all respects, and I will really miss them. But most of all, thank you for bringing us ESRs together. It is incredible how rapidly and strongly we bound, despite we only spent few days all together. I will always remember the time, laughs, drinks, complaints about PhD and life we had together. Thank you all!

Among the PhD4GlycoDrug fellows, I want to especially thank the ones I had the pleasure to work with in Utrecht. To **Cyril**, for all the fun from teasing each other. After all, what else can you expect by putting a French and an Italian guy together? To **Margherita**, who I successfully avoided during our Master's studies in Milan, but no, fate had different plans for us and put us next to each other in the lab in Utrecht (thank you fate). Among everything, I will always remember when you, so surprised, said to me: "you know, I thought you were such a serious and smart person, instead you are really an idiot". To **Dania**, one of the best people I met, not only a great scientist, but also a true friend. You were always there cheering us when nothing was working. Not to mention your great cooking skills, I loved tacos al pastor. To **Rodrigo**, the adopted ESR 13. To **Elena**, the perfect labmate for complaining together about the PhD life (I bet we will both end up doing a PostDoc). To **Nives**, for keeping me posted on the news from Milan and for the time we shared together. Also, to all the other people from Roland's group: **Reshmi, Diksha, Pouya, Xuan, Nishant**, and the whole CBDD people, especially **Vito, Gael, Roosmarijn, Luca, Francesco, Helena**. If I had a nice time in Utrecht, it was mainly because of you, thanks!

Coming back to Basel, I would like to thank first the Lab 4020. Endless thanks to **Jonathan**, the most knowledgeable, willing and kind young scientist I know. It is because of you if now I know much more about biophysics and bioassays. Thank you for always being available for all the stupid questions I had, even when you were no longer in the lab. I wish you the best of luck for your new adventure in Düsseldorf. Thanks to **Philipp**, who first introduced me to the PADMET field and taught me how to take care of cells. Finally, thank you to **Butrint, Adem, Nicole, Lijuan, Horst, Edvin**, for the friendly environment you created here.

Such atmosphere was so nice on the rest of the 4th floor too, and for this, I want to thank the other member of the group: **Aleksandra, Carla, Christina, Clément, Katia, Kevin, Rachel, Richard, Riccardo, Sateesh, Tiago, Xiaohua**, and all the other people that were around. A particular thanks to **Bea** and **Claudia**, for their incredible support for technical and bureaucratic problems.

I also want to specifically mention **Elisa** and **Ivan**, who were extremely helpful during my hardest times. It would have been much different without you!

Benedetta. What can I say? What I have found in you is definitely much much more than a colleague working on the same project. You are the only one that really knows the efforts and sacrifices we made during these years. I will (kind of) miss the evenings and the weekends in the lab, when we were trying to get some results, and the times when you were coming to me with your desperate "Gaaaaaaaabriiii" because something was not working or you needed someone to listen

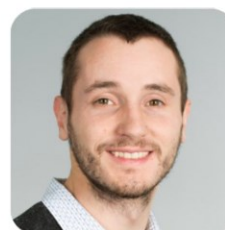
to you. What I will definitely miss are all the laughs and nice moments we had together, and the sfogliatelle (I am still waiting for them!). I can not explain how glad I am that we met.

If I was able to face this adventure and be the person I am, it is thanks to **Gloria**. You have been the most important person in my life, and I will always be grateful for this.

Finally, I want to thank my family and friends in Italy. You were rooting for me all along, even if we barely saw each other. I can not wait to spend more time back home with you all.

Curriculum Vitae

Gabriele Conti, PhD



Profile

I currently work as BPI in the context of (pre-)clinical studies for the investigation of small and large molecules. With more than 5 years in medicinal chemistry and bioanalysis, with a PhD in Pharmaceutical Sciences and MSc and BSc in Chemistry, I have experience in almost all drug discovery and development phases.

Experience

- Bioanalytical Principal Investigator**
Celerion Switzerland AG | 11/2022 - Present
 - Leading and managing GxP bioanalysis of clinical studies and method validations (PK, PD and immunogenicity).
 - Acting as primary study contact for clients.
 - Responsible person for issues of study plans and reports, and for management of project and project teams.
- R&D Scientist**
Celerion Switzerland AG | 02/2022 – 11/2022
 - Development of bioanalytical methods to support PK, PD and immunogenicity assessment in preclinical and clinical studies.
- Postdoctoral Research Scientist**
Universität Basel | 11/2022 - 02/2022
 - Synthesis and biological evaluation of lectin ligand.
- Marie Skłodowska-Curie Early-Stage Researcher**
Universität Basel - Universiteit Utrecht | 03/2018 - 10/2021
 - Leading discovery, development and preclinical characterization of new lectin ligands.
 - Presentation of research findings at international scientific conferences and regular team meetings.
 - Oversight of analytical HPLC and HPLC-MS instruments.
 - Student supervision and teaching.
- Intern in Computer-Aided Drug Design**
Idorsia Pharmaceuticals Ltd | 05/2021 - 06/2021
 - Computational studies to support drug discovery programs.

Education

- European Joint PhD in Pharmaceutical Sciences (Summa cum Laude)**
Universität Basel - Universiteit Utrecht | 03/2018 - 09/2021
Thesis: "Synthesis of glycomimetics of the natural Siglec-8 ligand and their pharmacodynamic characterization."
- MSc in Chemical Sciences (110/110 cum Laude)**
Università degli Studi di Milano | 10/2015 - 10/2017
Thesis: "Synthesis of small molecules against infectious diseases."
- BSc in Chemistry (108/110)**
Università degli Studi di Milano | 10/2012 - 07/2015
Thesis: "Synthesis of polyamide macrocycles and attempts of isomer separation."

Contact

🏠 Rümelbachstrasse 54, 8153 Rümlang
☎ +41 77 909 95 94
✉ gabriele.conti92@outlook.com
🌐 [https://www.linkedin.com/in/gabriele conti/](https://www.linkedin.com/in/gabriele%20conti/)

Competences

- ✓ Project management
- ✓ Medicinal chemistry
- ✓ PK, PD and immunogenicity bioanalytics
- ✓ GxP and SOP writing

Achievements

- 📄 **Publications**
2 papers and 1 front cover.
- 🗣 **Scientific contributions**
3 talks and 4 poster presentations.
- 🏆 **Awards**
Best Poster Awards at CHAINS2019.

Languages

Italian ██████████
English ██████████
German ██████████